A STUDY ON MONSOON FLOOD HAZARD AND VULNERABILITY ASSESSMENT OF OLD-BRAHMAPUTRA RIVER FLOODPLAIN UNDER CLIMATE CHANGE SCENARIO

A Thesis Submitted

By

Afeefa Rahman

1015162001(P)

In Partial Fulfillment of the requirement for the degree of

MASTER OF SCIENCE IN WATER RESOURCES ENGINEERING

Department of Water Resources Engineering

BANGLADESH UNIVERSITY OF ENGINEERING AND TECHNOLOGY

DHAKA-1000

March 24, 2019

Dedicated to my loving parents

AUTHOR'S CONTACT

_____

Afeefa Rahman
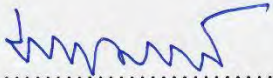
Lecturer
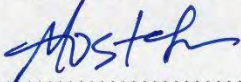
Department of Water Resources Engineering

Bangladesh University of Engineering and Technology (BUET)

Email: afeefa@wre.buet.ac.bd

DEPARTMENT OF WATER RESOURCES ENGINEERING

BANGLADESH UNIVERSITY OF ENGINEERING AND TECHNOLOGY

The thesis titled **"A Study on Monsoon Flood Hazard and Vulnerability Assessment of Old-Brahmaputra River Floodplain under Climate Change Scenario"** submitted by Afeefa Rahman, Roll No. 1015162001(P), Session October, 2015, to the Department of Water Resources Engineering, Bangladesh University of Engineering and Technology, has been accepted as satisfactory in partial fulfillment of the requirement for the degree of M. Sc. in Water Resources Engineering on 24 March, 2019.

BOARD OF EXAMINERS

....
Dr. Md. Sabbir Mostafa Khan
Professor
Department of Water Resources Engineering
Bangladesh University of Engineering and Technology, Dhaka

Chairman
(Supervisor)

....
Dr. Md. Mostafa Ali
Professor and Head
Department of Water Resources Engineering
Bangladesh University of Engineering and Technology, Dhaka

Member
(Ex Officio)

....
Dr. Umme Kulsum Navera
Professor
Department of Water Resources Engineering
Bangladesh University of Engineering and Technology, Dhaka

Member

....
Abu Saleh Khan
Deputy Executive Director (Operation)
Institute of Water Modelling (IWM)
Mohakhali, Dhaka - 1206, Bangladesh

Member
(External)

CANDIDATE'S DECLARATION

This is hereby declared that this thesis entitled as **"A Study on Monsoon Flood Hazard and Vulnerability Assessment of Old-Brahmaputra River Floodplain under Climate Change Scenario"** is the outcome of research carried out by me under the supervision of Dr. Md. Sabbir Mostafa Khan, Professor, Department of Water Resources Engineering, Bangladesh University of Engineering and Technology, Dhaka. I do hereby declare that this thesis or any part of it has not been submitted elsewhere for the award of any degree or diploma from any other institution.

....

Afeefa Rahman

(Candidate)

ACKNOWLEDGEMENT

ABSTRACT

This study is formulated to assess the monsoon flood hazard, vulnerability and risk of Old-Brahmaputra River and its surrounding floodplain for future climate change scenario of RCP 8.5 using numerical modeling approach. Firstly, a calibrated and validated hydrologic model of Brahmaputra river basin in HEC-HMS has been used to obtain the future flow magnitude for early (2020s), mid (2050s) and late century (2080s) for predicted climate data of RCP 8.5 scenario. Then the future flow at the Mymensingh of Old-Brahmaputra River has been obtained by conducting linear regression analysis considering the historical flow at Bahadurabad transit of Brahmaputra-Jamuna River as independent variable and the flow at Mymensingh of Old-Brahmaputra River as dependent variable. Then the study presents the simulation of flood flow of old Brahmaputra River and surrounding floodplain using HEC-RAS 1D-2D coupled hydrodynamic model. The 1D flow simulation was applied for the Old-Brahmaputra river channel and then integrated into 2D flow simulation incorporating the contribution of major tributaries and distributaries in the floodplain area using RAS Mapper. The developed hydrodynamic model is then calibrated and validated for Manning's roughness coefficient, n=0.014-0.017 for the year 2017 and 2016 respectively. To calibrate the inundation extent, flood inundation map obtained from simulation has been compared with the Sentinel-1 satellite image and flood map produced by FFWC on 16th August of 2017. Mean flood depth obtained in each upazilla under the study area has also been compared with the mean flood depth for the upazilla within the study area recommended by FFWC for 16th August of 2017 that provided satisfactory matching.

Calibrated model was then simulated to obtain flood depth, flood flow velocity and inundation area of the years 1988, 1998, 2004, 2007, 2010, 2013, 2016 and 2017. Analysis results depicted that among the historical flood years, flood event of 1988 and 1998 were of devastating consequences comparing with others. Then the synthetic inflow hydrographs of Old Brahmaputra river generated for baseline, 2020s, 2050s and 2080s of RCP 8.5 scenario were fed into validated HEC-RAS model of Old Brahmaputra to generate the flood inundation depth, velocity and inundation area maps in the study area. The analysis results show an increasing trend of flood variables from baseline to 2080s. From baseline to 2080s, the total inundation area extended from 1975 km^2 to 3923 km^2 which is almost half of the study extent. Additionally, the mean flood depth and mean flood flow velocity are found to be increased as well. Thereafter, flood depth, velocity and inundation area have been incorporated with weightage obtained from PCA to calculate the flood hazard. The percentage area under different hazard zones for RCP 8.5

Scenario has been analyzed which shows that from baseline to 2080s the very low, low, medium and high and very high hazard zone changed from 25%, 36%, 36%, 3% and 0% to 5%, 36%, 40%, 14% and 5% highlighting significant increase of high to very high hazard zone.

Thereafter, sensitivity, adaptive capacity, vulnerability and exposure have been estimated for the present and future socio-economic condition. Future population of each Upazilla was estimated using the logistic growth method. Selected indicators have been predicted for 2020s, 2050s and 2080s by trend analysis of the indicators of previous decades obtained from Population and Agricultural Census. Analysis on vulnerability maps highlights significant increase of moderate and high vulnerability zone from present to 2080s. Similarly, assessment of exposure for present and future highlights significant shift of few of the upazillas from high to very high exposure zones from present to 2080s. Thereafter, the flood risk is calculated for baseline and future multiplying flood hazard of each of the upazilla with the exposure and vulnerability of that particular unit. Risk assessment shows that all the upazillas are in the low to medium risk zone except Gaffargaon. Major part of the total study area may exist under the low to medium risk zone throughout the century. Thus, it can be interpreted that future climate change is going to have moderate impact on the flood situation of major portion of the old Brahmaputra River floodplain even if the wettest climate change scenario of RCP 8.5 is considered but there is an increasing trend of the flood from baseline to 2080s and the increment is significant after 2020s. It is hoped that the results would help floodplain management authorities in minimizing flood damage and loss of lives through technical approach.

LIST OF ABBREVIATION

ACRONYM	ELABORATION
2020s	2010-2039
2050s	2040-2069
2080s	2070-2099
ArcGIS	Arc Geographic Information System
AHP	Analytical Hierarchy Process
Baseline	1976-2010
BBS	Bangladesh Bureau of Statistics
BRB	Brahmaputra River Basin
BTM	Bangladesh Transverse Mercator
BWDB	Bangladesh Water Development Board
CORDEX	Coordinated Regional Climate Downscaling Experiment
DEM	Digital Elevation Model
FGD	Focus Group Discussion
GBM	Ganges Brahmaputra Meghna
GCM	General Circulation Model
RCM	Regional Climate Model
HEC-RAS	Hydrologic Engineering Center River Analysis System
IPCC	Intergovernmental Panel on Climate Change
PWD	Public Works Department
RCP	Representative Concentration Pathways
TIN	Triangular Irregular Networks
USGS	U.S. Geological Survey
WARPO	Water Resources Planning Organization
NSE	Nash- Sutcliffe efficiency
PBIAS	Percent Bias
PCA	Principal Component Analysis
PRA	Participatory Rural Appraisal
RSR	RMSE-Observations standard deviation ratio

TABLE OF CONTENTS

LIST OF FIGURES

LIST OF TABLES

CHAPTER 1

INTRODUCTION

1.1   Background of the Study

River flood, triggered by heavy rainfall and release of surplus runoff from upstream is recognized as one of the major causes of economic damages to infrastructures and loss of human lives (Dottori, 2016; Malik and Ahmad, 2014, Bronstert, 2003). Future projections of the meteorological triggers, including heavy precipitation and snowmelt, may alter the characteristics of the flood events (Hall et al., 2014). Climate change is very likely to increase the level of rainfall during the monsoon season (IPCC 2014) and such an increase will undoubtedly lead to more frequent and severe flooding in monsoon (Ahmed, A.U. 2006). Change to the timing of rainfall events due to climate change are also predicted to significantly alter the flooding experience around the world leading to the increased uncertainty of future flood risk (Ashley et al., 2005; Wheater and Evans, 2009). Frequent flooding might aggravate already existing drainage problem, including the diminution of river gradients as more and more sediments are brought down. Consequently, the conveyance capacity of these rivers will decrease significantly; this in turn will increase the duration of flooding.

Bangladesh, a tropical monsoon country of South Asia is an active delta of the Ganges, Brahmaputra and Meghna (GBM) (Basak et.al, 2015). Indeed, the majority of Bangladesh is made up of low-lying floodplains, and the country is crossed by more than 230 waterways which bring water from the Himalayas in the north to the Bay of Bengal in the south (Basak et.al, 2015). Geophysical position of the country forces itself to drain out huge cross-border monsoon runoff together with its own runoff through the river networks to the Bay of Bengal (Rouf, 2015). Besides, stronger-than-usual backwater effect due to sea level rise results into retardation of discharge of flow from upstream. As a consequence, the risk of riverine and rainfall-induced intense floods with prolonged duration, as in the case of flood 1998, will increase significantly making Bangladesh an "Impact Hotspot" and threatening the infrastructure, livelihoods and food production of the country (IDMC 2015; PIK 2013). This is how flood stands as the most common and major natural hazard affecting Bangladesh (Alauddin, 2010), with about 20 million people present in zones subject to flooding (Gemenne et al. 2011). On average, at least one fifth of Bangladesh's territory is flooded every year, and this proportion may increase to almost three quarters in the event of catastrophic

floods (Disaster Management Bureau, 2010, Mirza, 2002). The country is particularly much more vulnerable to disaster shocks comparing with others due to high density of population, higher poverty rate, greater dependence on climate-sensitive resources, lack of awareness of climate risks, and unplanned urbanization coupled with poor infrastructures (Islam et al., 2010).

1.2   Justification and Significance of the Study

Flood impacts may increase in future due to social and economic developments of ever-growing population in the watershed and climate change induced by natural and anthropogenic issues resulting in threats to enhancement of vulnerability of the communities residing in floodplains (Nur and Shrestha, 2016; Toda et.al., 2017). The fact justifies an increasing number of studies on modelling the impact of climate change on floods, with the focus on changing magnitude & frequency of the flood events (Booij, 2005; Gain et al., 2013; Raff et al., 2009). To reduce the flood induced damages, estimation of the flood depth, accurate prediction of the inundation area and dissemination of information to emergency managers, planners and the general public is necessary (Mujiburrehman, 2015). Flood hazard, vulnerability and risk assessment for future climate change scenario is therefore a basis for decision-making in flood management at international, national, regional and local levels (*ISRBC*, 2014).

Flood hazard assessment is the estimation of adverse effects of flooding depending on hazard parameters such as depth of flooding, duration of flooding, flood wave velocity and rate of rise of water level (Samarasinghea, 2010). Socio-economic vulnerability analyzes the relative level of vulnerability of different elements at risk thus serves as a necessary pre-requisite for comprehensive flood mitigation programs (Bankoff et al., 2004; Bhuiyan, 2014). Therefore, flood hazard mapping and vulnerability assessment forms the foundation of risk assessment and management by providing information like rapidly-accessible charts and maps essential to understand the nature and characteristics of the community's vulnerability and risk to flooding thus facilitating the administrators and planners to prioritize the mitigation measures (Bhuiyan, 2014).

Old Brahmaputra River, the main left-bank distributary of the Brahmaputra-Jamuna is a high flow spill river contributing largely to flood (FFWC, 2014). The river is famous for its rich reserve of aquatic life. A large number of rural people live in the east of the riverbank, whose livelihoods are adapted to its aquatic environment and agriculture on its flood plain (Afrose, 2016). The recurrent flood in Old Brahmaputra River floodplain causes great damage to cultivable lands, irrigation projects and valuable infrastructures situated on the bank of this river (Rakib et.al., 2017). Hereafter, the potential consequence of the historical

and plausible future flood events in this area make the study on the flood hazard, vulnerability and risk mapping in the Old Brahmaputra River immensely important. Few studies have been accomplished so far on potential flood hazard and risk assessment considering climate change impact for the major rivers and floodplains of Bangladesh (Tingsanchali & Karim, 2005; Nishat, 2017). However, no comprehensive study on the flood hazard and risk of the Old Brahmaputra River has been conducted yet. Considering the facts, this study is formulated to analyze the monsoon flood inundation pattern, hazard mapping, vulnerability and risk assessment of Old-Brahmaputra river flood plain for present and predicted climate change scenario using mathematical modeling approach.

Apart from the remote sensing approach, numerical model application can also be used for developing flood inundation maps that apparently plays an important role in flood hazard assessment being the only way that could provide the information of future changes in flood variables and consequent vulnerability under changing climate (Anh et.al, 2016). Hence the catastrophic impacts of river floods can be reduced using mathematical models for predicting flood hazard, vulnerability and risk (Dottori et.al., 2016; European Commission, 2007). Among available commercial and open source mathematical models for hydrodynamic and flood flow assessment, HEC-RAS (Hydrologic Engineering Center River's Analysis System) has been chosen to carry out this study due to its accuracy in analysis of river system and special feature of 1D-2D river-floodplain coupling simulation (HEC-RAS, 2016). The flood depth, flow velocity and inundation area have been considered as hazard parameters. Among the available categories of vulnerabilities such as "natural vulnerability", "socio-economic vulnerability" and "institutional vulnerability" (Elisabeth Angel, 2014; Geoscience, 2014), only the socio-economic vulnerability has been assessed in this study. Sequentially, monsoon flood induced risk for present and future plausible flood flow scenario have been generated by aggregation of Hazard, Exposure and vulnerability indicators into a number of steps. Produced maps were then analyzed for identification of spatial differences and management plans and prioritization of resources.

1.3   Scope of the Study

This study is focused on the assessment of flood inundation, hazard, vulnerability and risk assessment of Old Brahmaputra river floodplain. The present study is confined primarily to three specific indicators obtained from the hydrodynamic modeling for assessing Hazard. The study includes hydrologic and hydrodynamic aspects of surface runoff only and does not incorporate the hydraulics of channel flow and damage assessment of flooding which are extensive subject on their own merit beyond the scope of this study. The study is however limited to pluvial flooding (surface runoff) estimation and flood hazard in the

study area. To identify the vulnerability to flood, only the socio-economic aspect of vulnerability has been considered to obtain a holistic view and the vulnerability of specific agricultural crop or infrastructure are beyond the study scope. Remote Sensing and GIS has been used as a tool to identify flood prone areas within the study area and derive relativity of hazard, vulnerability and risk.

1.4   Objectives of the Study

The research aims at the following objectives:

   i.   To use a calibrated and validated hydrologic model of Brahmaputra river basin in estimating future flow at Bahadurabad transit of Brahmaputra-Jamuna river in HEC-HMS

   ii.   To establish the relationship of the flow at Bahadurabad transit of Brahmaputra-Jamuna river and at Mymensingh of Old-Brahmaputra river by statistical approach.

   iii. To develop a calibrated and validated HEC-RAS 1D/2D coupled model of Old-Brahmaputra River and its floodplain.

   iv.   To assess flood hazard, vulnerability and risk of Old Brahmaputra river floodplain for base and future flood flow scenario.

The expected outcomes of the research are as follows:

   i.   A validated hydrodynamic model of Old-Brahmaputra River to be used in designing flood mitigation measures.

   ii.   Flood hazard, Vulnerability and Risk maps for future flood flow scenarios providing information on the plausible future extent of flood induced impact.

1.5   Organization of the Thesis

The full thesis is organized as follows:

Chapter 1 presents a brief overview of the background of the study and objectives of the thesis.

Chapter 2 starts with an overview on types and causes of the flood with mitigation strategies in Bangladesh, hydro-morphological status of the Old Brahmaputra River, flood statistics in Bangladesh and in study area and the impact of climate change on future flood scenario of Bangladesh. Thereafter, the conceptual framework of flood hazard, vulnerability, exposure and risk has been discussed. The chapter also includes findings from few previous studies on flood hazard, vulnerability and risk assessment around the world as well as in Bangladesh.

Chapter 3 discusses about the salient features of models used in this study including the user interfaces, data storage & management, reporting capability and the theoretical background of simulation. The chapter also highlights the applicability of HEC-RAS 1D-2D coupled model in flood inundation assessment.

Chapter 4 describes the methodology employed to carry out the research work in detail with the elaboration of different steps required for flood hazard, vulnerability and risk mapping. It initiates from data collection, selection of study area, choice of RCP scenario, generation of future flood hydrographs & establishing the relationship between the flows using statistical approach. Then the methodology focuses on the development of hydrodynamic model of Old Brahmaputra River in HEC-RAS 1D-2D coupled model. The chapter ends up with the selection of the hazard, exposure and vulnerability indicators with justification of the selection of the indicators including the approaches followed to project the exposure and vulnerability indicators for future socio-economic condition and the technique of assessing hazard, vulnerability and risk induced by monsoon flood in the study area.

Chapter 5 is on the results and discussions relating to the flood hazard, vulnerability and risk mapping. It contains calibration and validation of developed hydrodynamic model, analysis of historical flood events and simulation of future floods and hazard assessment for the future climate change scenario. It also discusses the assessment of vulnerability of the study area for current and future socio-economic condition by explaining how different vulnerability domains and indicators are contributing in overall socio-economic vulnerability assessment. It also combined the results obtained from hazard, vulnerability and exposure assessment to evaluate the risk by monsoon flood for the present and future climate change scenario.

Chapter 6 provides with the conclusions and recommendations of the study with a summary of the results obtained and suggestions for advanced study relevant to this study concept.

CHAPTER 2

THEORY AND SALIENT FEATURES OF MODEL

2.1 General

This chapter presents the literature review that provides the basic information regarding concept of flooding – definition and types, factors contributing to flood hazard, climate change impact on floods, flood risk management in Bangladesh, hydro-morphological status of the Old Brahmaputra River, flood statistics in Bangladesh and in Old Brahmaputra flood plain in particular, general and specific conceptualization of flood hazard, vulnerability and risk, review on the notable previous studies on flood hazard vulnerability and risk, conceptualization of statistical analysis and projection of socio-economic indicators for vulnerability assessment.

2.2 Flood and Its Types

Flooding is defined as a general temporal condition of partial or complete inundation of normally dry areas from overflow of inland or tidal waters or from unusual and rapid accumulation of runoff (Jeb and Aggarwal, 2008). By spilling the banks of the rivers and channels, when water inundates the flood plains and adjoining high lands to some extent the situation is termed as flood (Rahman, et al., 2007). There are several kinds of flood and each one bears a different impact in terms of how it occurs, the damage it causes, and how it is forecasted (Tazin, 2018). Bangladesh generally experiences four main types of floods: flash floods, riverine floods, rain floods and storm-surge floods (Rouf, 2015, Hossain, 2013, Brammer, et al., 1993).The types of floods in Bangladesh are explained below.

2.2.1 Flash Flood from Hilly Areas

Excessive rainfall with high intensity is the main source of flash flood in the hilly area and associates with landslide in the area composed of unconsolidated rocks (Sarker and Rashid, 2013). In Bangladesh, flash floods is characterized by a sharp rise in water level and high flow velocity as a result of exceptionally heavy precipitation occurring over neighboring hills and mountains in India along the borders of Bangladesh (Rouf, 2015). Most of the agricultural crops are sown in December-January period and harvested in April-May. Flash floods at the time of harvesting period cause devastating damage to crops of the northeast Haor area of Bangladesh (Hossain, 2013).

2.2.2 Rain floods by heavy rains and drainage congestion

Rain floods are caused by high intensity local rainfall of long duration associated with disturbed natural drainage systems. When intense rainfall takes place and the natural drainage system cannot carry the run-off generated by the storm, rain flood occurs (Hasan, 2015). From year to year, the extent and depth of rain water flooding varies with monsoon, depending on the amount and intensity of local precipitation and current water levels in the major rivers that control drainage from the land (Rouf, 2015).

2.2.3 Monsoon floods

Monsoon floods also defined as Riverine floods, generating from the spilling of river banks by climatological events such as heavy and prolonged rainfall (Smith and Ward, 1998) commonly rise and fall slowly over 10–20 days or more (Rouf, 2015). Of the total riverine flow, around 80% occurs from June to October during monsoon (WARPO, 2004) following a similar pattern of the rainfall (Hasan, 2015). As a consequence of the skewed temporal distribution of river flow and rainfall, Bangladesh suffers from abundance of water in monsoon, frequently resulting into floods. Moreover, climatologically the discharge into Bangladesh, from upper catchments, occurs at different time of the monsoon. In the Brahmaputra, maximum discharge occurs in early monsoon in June and July whereas in the Ganga maximum discharge occurs in August and September (Rouf, 2015). Synchronization of the peaks of these rivers results in devastating floods in Bangladesh.

2.2.4 Coastal floods caused by storm surge

Coastal floods occur in low-lying coastal areas like estuaries and deltas, extensive tidal flats and low-lying islands, when the land is inundated by brackish or saline water (Eigege, 2011). Brackish-water floods result when river water overspills embankments in coastal reaches and can be intensified when high-tide levels in the sea are increased by storm-surge or when large freshwater flood flows are moving down an estuary (Eigege, 2011). Saline water coastal floods may occur when extremely large wind-generated waves are driven into semi-enclosed bays during severe storm (Smith and Ward, 1998). The severity of a coastal flood is determined by factors including the strength, size, speed, direction of the storm and the onshore and offshore topography (Tazin, 2018). Coastal flood mostly occurs along the coastline of about 800 km at the southern part of Bangladesh. Continental shelves in this part are shallow and coastline in the eastern portion is funnel like in shape. Due to the factors, storm surge generated by cyclonic storm is higher in Bangladesh compared to the same storm in other parts of the world (Hasan, 2015). Figure 2.1

shows the types of flood occurs in Bangladesh highlighting the fact that the old Brahmaputra river floodplain experiences the river and rainfall induced flood. Flood in Bangladesh has also been classified in terms of extent of inundation and respective return periods as shown in Table 2.1.

Figure 2.1: Types of flood in Bangladesh (Source: Google)

Table 2.1: Types of flood in terms of inundated area & chances of occurrence in Bangladesh*

Type of Flood	Parameters		
	Flooded Area(Sq. Km)	% Inundation	Probability of occurrence**
Normal Flood	<31000	21	0.5
Moderate Flood	31000-38000	21-26	0.3
Severe Flood	38000-50000	26-34	0.1
Catastrophic Flood	50000-57000	34-38.5	0.05
Exceptional Flood	>57000	>38.5	0.05

*Source: Mirza et.al, 1997

**Probability of occurrence was calculated based on area flooded during 1954–1999

2.3   Causes of flooding in General and Bangladesh in particular

The general factors causing flood are listed in Table 2.2. In case of flooding in Bangladesh, the main causes are excessive precipitation, low topography and flat slope of the country (Tazin, 2018). Few of the other associated triggering factors include the followings-

i.   Tectonic uplift of the Himalayas means that erosion rates of sediment increase as the rivers have more potential for erosion. This mass of sediment is dumped in Bangladesh that choke the river channels and make them more inefficient by reducing hydraulic radius which ultimately increases flooding in dry lands.

ii.   Some parts of the GBM basin receive very high rainfall in a day during monsoon leading flood.

iii.   Deforestation of the Himalaya reduces interception rate which means shorter lag time and higher peak discharges causing flash flood.

iv.   Three massive rivers converge in Bangladesh – the Ganges, Brahmaputra and Meghna massively swells discharges during high flow season.

v.   Cyclones from the Bay of Bengal cause and contribute to coastal flooding.

vi.   Snowmelt affects the rivers and causes flood as ice and snow melting from glaciers and mountain peaks in the Himalaya works its way into rivers.

Table 2.2: Factors Contributing Flooding*

Meteorological Factors	Hydrological Factors	Human Factors Aggravating Flood Hazard
Rainfall	Soil Moisture	Land Use Change e.g. Surface Dealing Due to (urbanization, deforestation) Increase Runoff Sedimentation.
Cyclonic Storm	Ground Water Level Prior to Storm	Occupation of Flood Plain Flow.
Small Storm generate by Wind and Earthquake	Natural Surface Infiltration	Inefficiency or Non Maintenance of Infrastructure.
Abrupt Change in Temperature	Presence of Impervious Cover	Too Efficient Drainage of Area Increases Flood Peaks.
Snow Fall and Upstream Snow Melt	Channel Cross section Shape and Channel Roughness	Climate Change Effect Magnitude and Frequency of Precipitation of Floods.
	Presence or Absence of Overbank Flow, Channel Network	Urban Microclimate May Enforce Precipitation.
	Synchronize of Runoff from Various Part of the Watershed.	
	High Tide Impeding Drainage.	

*Source: Associated Programme on Flood Management, 2012

2.4   Flooding in Bangladesh

Flood is a natural phenomenon in Bangladesh and occurs on an annual basis. In the 19th century, for Bangladesh six major floods were recorded in 1842, 1858, 1871, 1875, 1885 and 1892 (Rouf, 2015). Eighteen major floods occurred in the 20th century. Those of 1987 and 1988, 1998, 2004, 2007 and 2010 were of catastrophic consequence and significant ones.

The catastrophic flood of 1987, estimated as once in 30-70 year flood event occurred throughout the monsoon and affected 57,300 km^2 of land, which is about 40% of the total country area. The main cause of flood was the creation of erranticophrus (top soil wash away reaction) from the inhabitants of the Himalayas irrigating their mountains vertically (Rouf, 2015). These seriously affected regions were on the western side of the Brahmaputra, the area below the confluence of the Ganges and the Brahmaputra and north of Khulna. The flood of 1988 was also of catastrophic consequence occurring throughout the month of August and September. This flood inundated about 82,000 km^2 of land (about 60% of the area) and its return period was estimated as 50–100 years. Rainfall together with synchronization of very high flows of all the three major rivers of the country in only three days aggravated the flood and lasted for 15 to 20 days. Dhaka, the capital of Bangladesh, got severely affected in the flood event. In 1998, over 75% of the total area of the country was flooded. It was similar to the catastrophic flood of 1988 in terms of the extent of the flooding. A combination of heavy rainfall within and outside the country and synchronization of peak flows of the major rivers caused the flood (Mirza, 2002).

The 2004 flood was very similar to the 1988 and 1998 floods with two thirds of the country under water. This flood lasted from July to September covering 50% of the country. In the month of July of 2004, 40% of the Dhaka city got under water. 600 deaths were reported and 30 million people became homeless. Bridges were destroyed, the death toll rose to 750 and the airport and major roads were flooded. The damage to infrastructures was estimated as $7 billion. The rice and cash crops such as jute and sugar got affected.

In 2007, more than half of Bangladesh was severely affected by monsoon flooding caused by excessive rainfall in catchment of GBM in Nepal, Bhutan and Northern India. It affected 13.3 million people of 46 districts. The flood of 2010 affected 49 districts and ten millions of the country people. More than 12000 Bangladeshi were homeless as hundreds of houses were destroyed. Due to the floodwater, crops were damaged and roads became inaccessible leaving food and drinking water in short of supply (Alauddin, 2010). Flood of 2017 was also a severe one. The rise of water levels in the various rivers in the northern

part of the country due to heavy rainfall as well as water flow from the upstream hills in India have led to the inundation of the river basin areas in the northern parts of Bangladesh. Almost 42% of the country got flood affected which corresponded to 35 districts of the country.

Flooding primarily takes place during the monsoon season as the GBM Rivers dispel enormous discharge that converges in an area with low gradient and flat terrain (Nandargi, 2010). Based on the historic records, it is observed that the frequency, magnitude, and duration of floods have increased substantially during the last few decades. Analysis on 20 years of floods of the GBM basin under climate scenarios concluded that the probability of flooding in this basin will increase (Mirza, 2003). Studies on the Brahmaputra River in India have found that flood on this river in recent years has already become more severe, due to occurrence of extreme weather events and newly emerged interventions and destruction of wetlands (Jamil, et. al., 2008). Percent of the total affected area of Bangladesh in flood since 1954 is presented in Table 2.3 which shows that the flood of 1955, 1974, 1987, 1988, 1998, 2004, 2007 and 2017 inundated more than 50000 sq. km of the area causing enormous damages to properties and loss of life.

Table 2.3: Year-wise flood affected area in Bangladesh

Year	Flood Affected Area(sq km)	Flood Affected Area (%)	Year	Flood Affected Area(sq km)	Flood Affected Area (%)	Year	Flood Affected Area(sq km)	Flood Affected Area (%)
1954	36800	25	1977	12500	8	2000	35700	24
1955	50500	34	1978	10800	7	2001	4000	2.8
1956	35400	24	1980	33000	22	2002	15000	10
1960	28400	19	1982	3140	2	2003	21500	14
1961	28800	20	1983	11100	7.5	2004	55000	38
1962	37200	25	1984	28200	19	2005	17850	12
1963	43100	29	1985	11400	8	2006	16175	11
1964	31000	21	1986	6600	4	2007	62300	42
1965	28400	19	1987	57300	39	2008	33655	23
1966	33400	23	1988	89970	61	2009	28593	19
1967	25700	17	1989	6100	4	2010	26530	18
1968	37200	25	1990	3500	2.4	2011	29800	20
1969	41400	28	1991	28600	19	2012	17700	12
1970	42400	29	1992	2000	1.4	2013	15650	10.6
1971	36300	25	1993	28742	20	2014	36895	25
1972	20800	14	1994	419	.2	2015	47200	32
1973	29800	20	1995	32000	22	2016	48675	33
1974	52600	36	1996	35800	24	2017	61979	42
1975	16600	11	1998	100250	68			
1976	28300	19	1999	32000	22			

* Source: FFWC, 2017

2.5   Flood Statistics of Old Brahmaputra River

Old Brahmaputra River is one of the major distributary of the Brahmaputra-Jamuna river of Bangladesh carrying a small but significant amount of the Brahmaputra-Jamuna flow to the Upper Meghna River (Ahmed, 2018). Flood along the Old Brahmaputra frequently occurs during the rainy season (BWDB, 2010). Mymensingh, Kishoreganj and surrounding districts are notable among the flood affected districts of Bangladesh. The danger level at Jamalpur (SW 225) and Mymensingh (SW 228.5) of Old Brahmaputra River is 17 m and 12.5m respectively. Locations of the water level measuring stations in Jamalpur and Mymensingh Sadar are shown in Figure 2.2.

Figure 2.2: Locations of the water level measuring stations in Old Brahmaputra River

It has been recorded that during the historical flood event in Bangladesh, the water level in Old Brahmaputra River was above the danger level and caused flooding on the nearby floodplain. During the devastating floods of 1998 and 1988 in Bangladesh, the water level in Old Brahmaputra at Jamalpur (SW 225) was 17.47 m and 17.83m respectively exceeding the danger level. At Mymensingh (SW 228.5) the water levels were recorded as 13.04m and 13.69m during the devastating floods of 1998 and 1988 respectively both exceeding the danger level of the water level at Mymensingh. Figure 2.3(a) and (b) showing the water level at Jamalpur (SW 225) and Mymensingh (SW 228.5) of Old Brahmaputra River for the flood year 1987,

1988, 1998, 2004, 2007, 2010, 2015 and 2017 depict that the water level of 1987, 1988, 1998, and 2004 was above the danger level.

The peak water levels of the Old Brahmaputra River during monsoon are documented in different Annual Flood Reports of FFWC. In 2011, the WL of Old Brahmaputra River at Jamalpur showed rise and fall during the monsoon, one peak of 15.30 m, one of 15.25 at the 2nd week of August and the last and the highest one at 3rd week of August was recorded 15.41m. At Mymensingh the WL of the river followed the similar trend; the recorded peak was 10.72m at 19th August.
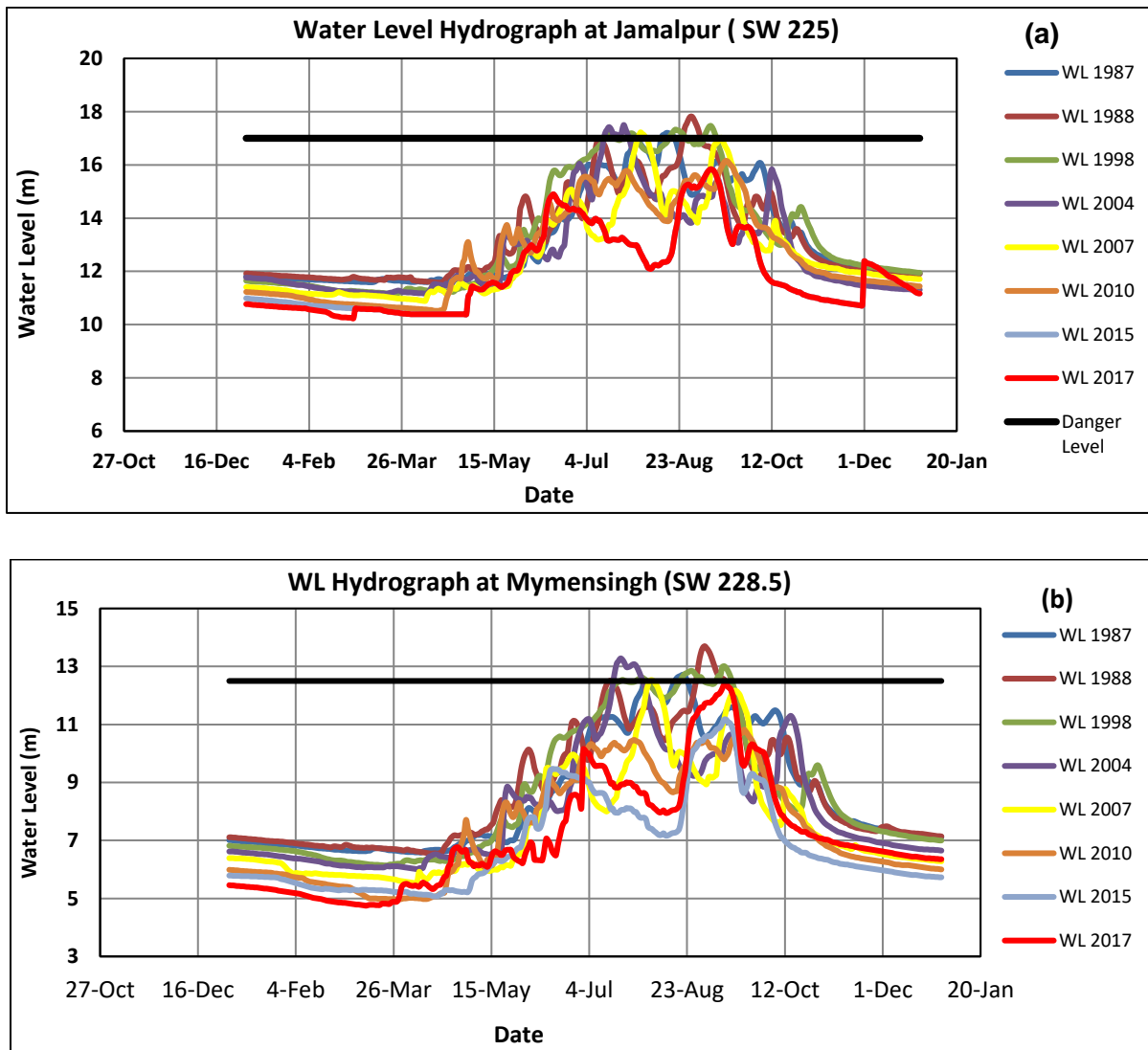
Figure 2.3: Comparison of flood hydrographs of Old Brahmaputra River (a) Jamalpur (b) Mymensingh

In 2012, The WL of the Old Brahmaputra River at Jamalpur and Mymensingh showed rise and fall during the monsoon, but remained below the respective DLs at both the stations. At Jamalpur the peak WL recorded of 16.70mPWD on 30th September which is 30cm below the DL at this point (DL 17.0m). At Mymensingh the peak WL recorded was 10.70mPWD on 27th July, which was180cm below the DL (12.5m) at this point. In 2013, The WL of the Old Brahmaputra River at Jamalpur and Mymensingh showed rise and fall during the monsoon, but remained below the respective DLs at both the stations. At Jamalpur the peak WL recorded of15.80mPWDon12th September which is 120cm below the DL at this point (DL 17.0m). At Mymensingh the peak WL recorded was 10.12mPWD on 16th September, which was 238cm below the DL (12.5m) at this point.

In 2014, The WL of the Old Brahmaputra River at Jamalpur and Mymensingh showed rise and fall during the monsoon, but remained below the respective DL at both the stations. At Jamalpur the peak WL recorded of16.33 mPWD on 1st September which is 67cm below the DL at this point (DL 17.0m). At Mymensingh the peak WL recorded was 11.25 mPWD on 6th September, which was 125cm below the DL (12.5m) at this point. In 2015, The WL of the Old Brahmaputra River at Jamalpur and Mymensingh showed rise and fall during the monsoon, but remained below the respective DLs at both the stations. At Jamalpur the peak WL recorded of 15.84 mPWD on 9th September which is 116 cm below the DL at this point (DL 17.0m). At Mymensingh the peak WL recorded was 11.19 mPWD on 11th September, which was 131cm below the DL (12.5m) at this point.

In 2016, The WL of the Old Brahmaputra River at Jamalpur and Mymensingh showed rise and fall during the monsoon, but remained below the respective DLs at both the stations. At Jamalpur, the peak WL recorded of 16.76 mPWD on 1st August which is 24cm below the DL at this point (DL 17.0m). At Mymensingh the peak WL recorded was 11.66 mPWD on 4th August, which was 84cm below the DL (12.5m) at this point.

In 2017, The WL of the Old Brahmaputra River at Jamalpur and Mymensingh showed rise and fall during the monsoon. At Jamalpur, the water level crossed the DL (17.00m) on 18th August for 1 day with the recorded peak WL of 17.01 mPWD which is 1cm above the DL at this point (DL 17.0m). At Mymensingh, the WL remained below the DL (12.50m) during the whole monsoon. The peak WL recorded was 12.03 mPWD on 21st August, which was 47cm below the DL (12.5m) at this point. In 2018, The WL of the Old Brahmaputra River at Jamalpur and Mymensingh showed rise and fall during the monsoon. At Jamalpur, the water level reached the DL (17.00m) on 20th September. At Mymensingh, the peak WL recorded as 12.01 mPWD on 22nd September, which was 1cm above the DL (12.5m) at this point. Analysis on the

historical water level of Old Brahmaputra River supports the occurrence of flood during monsoon on the floodplain.

2.6   Impact of Climate Change on Flood Situation of Bangladesh

Climate change refers to any change in climate over time, whether due to natural variability or as a result of human activity (IPCC, 2001). The major factor that influences flood is the climatic condition of a particular geographic location and it manifests in the form of amount, duration and intensity of precipitation (rainfall) and temperature. One of the consequences of global warming in humid environment is increase and alteration of rainfall patterns (O‟Hare, 2002). According to the IPCC synthesis report (Tirpak et.al., 2007) hot extremes, heat waves and heavy precipitation events will become more frequent all over the world and future tropical cyclones will become more intense with larger peak wind speeds and heavy precipitation associated with ongoing increase of tropical sea surface temperatures (Silva et.al., 2016) thus flood risk will progressively increase over time around the world (Bates *et al.,* 2008). Particularly low lying coastal areas & deltas will be under increased risk as sea level rise occurs along with intense rainfall induced surface runoff and overwhelmed drainage congestions.

Climate change and its impact is a significant concern of the twenty-first century. Global warming induced changes in temperature, rainfall and sea level are already evident worldwide as well as in Bangladesh (Ahmed & Alam, 1999; Stocker, et al., 2013). According to the fifth assessment report (AR5) of IPCC (International Panel on Climate Change), the global mean surface temperature may increase between 0.3°C to 4.8°C for low (RCP 2.6) to high (RCP 8.5) emission scenarios from its baseline (1985-2005) by the end of 21st century (IPCC, 2014). Increase in global temperature and precipitation will significantly increase the monsoon flows of the major rivers of Ganges-Brahmaputra-Meghna (GBM) basin causing significant frequent flood in Bangladeshi territory.

2.7   Flood Mitigation Strategies

The issues of flood management should be considered from different angles of improvement of quality of life, impact on physical environment, socio-economic condition and environmental preservation etc (Uddin, 2017). It is usually found that different methods or techniques are practiced in different parts of the world to tackle the flood hazard and associated risk. Bangladesh Practices two type of flood management that are structural and non-structural flood management techniques. The structural measures are mainly engineering structure build for protecting the floodplain such as Flood Embankment, Channel

Improvement, River Training measures etc. The non-structural option consists of the Flood Plain Zoning & Management; Policies for infrastructure Planning and Development in the flood plains; Flood Proofing; Disaster Preparedness & Response Planning and Flood Forecasting and Warning.

2.7.1   Structural Measures adopted in Bangladesh

After the devastating flood in 1950's, a national scale Flood Control and Drainage (FCD) project for building coastal embankments has been taken and this FCD project continued till creation of Flood Action Programme (FAP). Considering the issues of securing peoples' life and property, livelihood, food etc. the Govt. put emphasis on protecting Medium High and Low Lands from floods through construction of embankments. Since 1960s Bangladesh has implemented about 628 numbers of large, medium and small-scale FCDI projects (Tazin, 2018). Total investment was around US$ 4.0 billion (Hossain, 2003). It provided flood protection to 5.37 million ha of land, which is about 35% of the country area.

2.7.2   Non-Structural Measures in Bangladesh

The structural method of flood management was not sustainable for Bangladesh as we experienced devastating flood even after the existence of embankments. In spite of all the structural activities, it was found that the people living in the Medium High and Medium Low Lands are immune to flooding during moderate to extreme flood events. Government realized that to minimize flood loss non-structural means like early warning is very important and can save life and property. With this end in view, Flood Forecasting and Warning Centre (FFWC) got established in 1972 with 10 Flood Monitoring Stations on the major river systems. After disastrous floods of 1987 & 1988 the Government realized the importance of FFWC and took steps to modernize the system. New FFWC model was developed on the basis of Mike-11 hydrodynamic model and flood-monitoring stations were increased to 30 in 1996. In 1998 flood FFWC was found to be very useful providing the early warning on the flood. With the experience of 1998 flood the Government attempted to cover all the flood prone areas of the country under real time flood monitoring. A project was undertaken from year 2000 to improve the FFWC further. It now covers the entire country with 85 Flood Monitoring Stations and provides real time flood information with early warning with lead-time of 24 and 48 hours. FFWC currently is helping the Government, the disaster mangers and the communities living in the flood prone areas in flood preparedness, preparation of emergency mitigation plan, agricultural planning and rehabilitation processes.

2.8　　　General Conceptualization of Hazard Assessment

Hazard can be defined as the occurrence of a potentially damaging natural or man-made phenomenon in a given area within a specific period of time (Hossain, 2013). Flood Hazard can be divided into primary hazards that occur due to direct contact with water, secondary effects that occur because of the flooding, such as disruption of facilities, services and health impacts, and tertiary effects such as changes in the position of river channels and migration of people (Tazin, 2018). Flood hazard is the most common natural disasters around the world as one-third of the world's land area is flood prone affecting 82 percent of the world's population (Tazin, 2018). The geographical location, flat topography, numerous river networks, skewed temporal and spatial pattern of rainfall and river flow with coastal hydrodynamic processes render Bangladesh highly vulnerable to flood hazard (Jahan, 2018).

Hazard assessment is concerned with the characterization of the nature, magnitude and timing including frequency and duration of hazard events (Hossain, 2013) and can be categorized based on the level of consequences to daily life and damage to properties. In general, flood hazard is classified as low, medium and high (UNDRO, 1991; Tingsanchali & Karim, 2005) expressing the intensity by relative scale and represented by maps showing relative comparison of hazard within the area. For the inclusive assessment of flood hazard, it is necessary to determine the most important parameters of the flooding event under consideration. There are different parameters of a flooding event which can have an important impact on the hazard such as depth of flooding, flood flow velocity, time of occurrence of flood, inundation area and duration of flooding (Hossain, 2013). Flood hazard assessment is a vital component in flood prone areas as it creates comprehensive charts and maps which facilitate the administrators to identity areas of risk and prioritize their mitigation efforts (Bhuiyan, 2014).

2.9　　　General Conceptualization of Vulnerability Assessment

In spite of some divergence over the meaning of vulnerability, understanding vulnerability requires more than analyzing the direct impact of a hazard including socio-environmental conditions that limit communities to cope with the impact of hazard (Jahan, 2018, Birkmann, 2006). No universal concrete definition of vulnerability exists (Birkmann 2006b). According to the United Nations International Strategy for Disaster Reduction (UNISDR 2009), vulnerability can be defined as 'the characteristics and circumstances of a community, system or asset that make it susceptible to the damaging effects of a hazard'. The United Nations Development Programme (UNDP) defines vulnerability as a human condition resulting from physical, social, economic and environmental factors, which determine the

likelihood and scale of damage from the impact of a given hazard' (UNDP 2004). Depending on the connection to the triggers and factors, vulnerability can be of 4 types (Roy, 2015; UNISDR, 2013) as discussed below.

Physical Vulnerability

Physical vulnerability is related to the susceptibility of physical structures and related components. It is mainly concerned with the impacts of a hazard event and is viewed as the amount of damage experienced by a system as a result of a hazard (Aulong and Kast, 2011; Brooks, 2003). Physical vulnerability assessment makes use of vulnerability functions or damage functions constructed by correlating the magnitude of the hazard event (for example: flood depth, duration, velocity of flood and inundation) and the degree of damage. Poor design and construction of buildings, earthen embankments, unregulated land use planning etc enhances the physical vulnerability of an existing physical element.

Social Vulnerability

Social vulnerability concentrates on determining the sensitivity and adaptive capacity of the society putting the human system on the central stage influenced by indicators such as social status, health and sanitation facilities, access to insurance, housing quality, exclusion and discrimination by gender, disability and age, psychological factors etc.

Economic Vulnerability

Economic vulnerability concentrates on determining the sensitivity and adaptive capacity of the society, determined by the factors including the livelihoods, dependence on single industries, globalization of business and supply chain, poverty rate, literacy and schooling of the community people, agricultural production etc.

Environmental Vulnerability

Natural resource depletion and resource degradation are key aspects of environmental vulnerability (ODPM, 2017). Environmental vulnerability focuses on the environmental factors like overused land, percentage of eroded area, forest area, and percentage of agricultural land depicting poor environmental management and over consumption. For example, wetlands, such as the Caroni Swamp, are sensitive to increasing salinity from sea water, and pollution from storm water runoff containing agricultural chemicals, eroded soils, etc.

Comparison with the physical and environmental vulnerability with the social and economic vulnerability shows that the physical and environmental vulnerability change depending on the type and intensity of the hazard and become applicable for particular type of hazard whereas the assessment of social and economic vulnerability is not hazard-specific. In this study an attempt has been made to assess the social and economic vulnerability measured by different indexes based on sets of socio-economic indicators.

2.10   General Conceptualization of Exposure Assessment

Similar to flood vulnerability, flood exposure indicates susceptibility of a region to flood damages. Exposure is defined as the degree, duration and extent to which a system is in contact with, or subject to, perturbation (Kasperson et al. 2005; Kasperson & Dow 2005). Exposure is location and variable dependent (Brenkert and Malone, 2005). For example, population and household characteristics is a descriptor of flood exposure. Land use pattern focusing on agricultural land area has direct relationship with flood impact as well. In the present study, flood exposure is assessed from population and land use characteristics.

2.11   IPCC conceptualization of Vulnerability, Exposure and Risk

Recently, IPCC has introduced the latest concept of risk in the Fifth Assessment Report (AR5) which includes hazard, exposure and vulnerability to assess the risk of a hazard as shown in Figure 2.4 (Cardona et al., 2012).
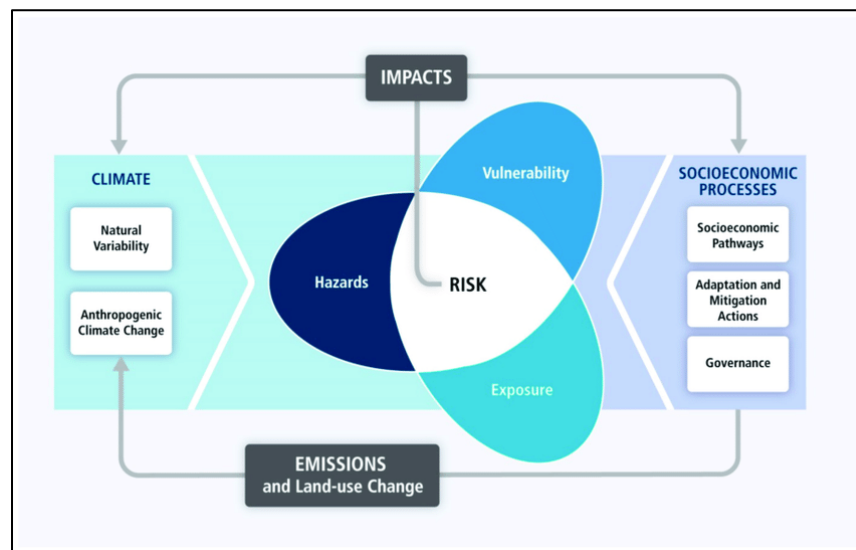
Figure 2.4: IPCC AR5 concept of risk (*Source:* IPCC, 2014)

IPCC AR5 defines risk as "the potential for consequences where something of value is at stake and where the outcome is uncertain, recognizing the diversity of values." Risk results from the interaction of hazard, vulnerability and exposure" (Agard and Schipper, 2015). IPCC defined Hazard as the potential occurrence of a natural or human-induced physical event that may cause loss of life, injury, or other health impacts, as well as damage and loss to property, infrastructure, livelihoods, service provision, and environmental resources. It defines vulnerability as "the propensity or predisposition to be adversely affected". Vulnerability encompasses a variety of concepts including sensitivity or susceptibility to harm and lack of capacity to cope and adapt (Agard & Schipper, 2015). On the other hand, exposure is defined as "the presence of people, livelihoods, species or ecosystems, environmental services and resources, infrastructure, or economic, social, or cultural assets in places that could be adversely affected" (Agard and Schipper, 2015). By this definition exposure is often assessed using population and infrastructural objects' location in a zone potentially affected by a natural hazard.

Vulnerability and exposure are the result of socio-economic pathways and societal conditions, including adaptation and mitigation actions. Changes in both the climate system and socio-economic processes are central drivers of the different core components (vulnerability, exposure, and hazards) that constitute risk (Satta et al., 2015). This study defines flood risk as a combination of flood exposure, hazard and vulnerability as suggested by IPCC, 2015, Peck et.al, 2007 and Jahan, 2018. Mathematically this translates into the following expression:

Flood Risk = (Hazard) × (Exposure) × (Vulnerability)   (2.1)

2.12   Conceptualization of Projection of Future Socio-Economic Parameters

To obtain the future condition of socio economic indicators and assessing the future sensitivity, adaptive capacity and vulnerability parameters of population, household and related domain need to be projected on some logical ground. To project the population and household related indicators, suitable of the available projection methods has been used in this study. The methods available for the forecasting population and household related indicator are discussed below

Arithmetic increase method

Average rate of increase in the population considered is assumed to be constant from decade to decade in this method. Average increase per decade is found out from the previously available census data. The

product of this amount obtained and number of decades for which the population is to be worked out is added to the present population of the subjected area to get the approximate population after n decades (Gawatre et.al., 2016). Equation (2.2) represents the formula of Arithmetic increase method.

$$P_n = P + nd \qquad (2.2)$$

Where, P_n = future population after n decades; P = present population; n = number of decades and d = average increase per decade

Geometric increase method

Average percentage increase in population is assumed to be constant from decade to decade in this method. Average percentage increase per decade is found out from the previously available census data. By using the formula given in Equation (2.3) the future population is worked out (Gawatre et.al., 2016).

$$P_n = P \left(1 + \frac{r}{100}\right)^n \qquad (2.3)$$

Where, P_n=future population after n decades; P= present population; n= number of decades and r = average percentage increase per decade

Incremental increase method

The advantages of both arithmetic increase method and geometrical increase method are included in this method. Average increase per decade is found out first of all and average percentage increase per decade is worked out as in arithmetic increase method and geometric increase method respectively. Future population is worked out from the equation (2.4) (Gawatre et.al., 2016).

$$Pn = P + nd + \frac{n(n+1)}{2} t \qquad (2.4)$$

Where, Pn= future population after n decades; P = present population; n = number of decades; t = average incremental increase per decade and d = average increase per decade

Exponential Increase Method

The exponential increase approach is closely related to the geometric, but it views change as occurring continuously rather than at discrete intervals (George et.al., 2004). The exponential rate of population change during the base period can be computed as:

$$r = [\ln (P_l / P_b)] / (y) \qquad (2.5)$$

Where, r is the average annual exponential rate of change, ln represents the natural logarithm, P_l is the population in the recent year, P_b is the population in the previous year, and y is the number of years within the recent and previous year. A population projection using this method can be computed as:

$$P_t = (P_l)(e^{rz})$$ (2.6)

Where, P_t is the population in the target year, P_l is the population in the recent year, e is the base of the system of natural logarithms (approximately 2.71828), r is the average exponential rate of change computed for the base period, and z is the number of years in the projection horizon (George et.al., 2004).

Simple graphical method

Graph between the population and the corresponding year is plotted based on the available census data. The obtained curve is extended in the same manner to get the population of required year. It is the approximate method as the accuracy is dependent on the skill and experience of the person dragging the curve (Gawatre et.al., 2016)

The logistic curve method

The growth is assumed to be a function of the time and follows some logical mathematical relationship. According to the logistic curve, population tends to increase at low rate followed by high rate and then at lower rate towards the saturation limit (Gawatre et.al., 2016). As long as there are enough resources available, there will be positive growth rate and as the limited resources begin to decrease, increasing rate of the population slows down. Logistic model illustrates how a population may increase until it reaches the carrying capacity of its environment. When a population reaches the carrying capacity, growth slows down or stops altogether. The Logistic method is useful in case of limited space and economic opportunity under the assumption that population growth occurs under normal situation and is not affected by extraordinary changes like epidemic, war or natural disaster (Jain et.al, 2013-2015). If P_0, P_1 and P_2 are the population of an area at time t_0, t_1 and t_2, the saturation population equivalent to the carrying capacity of the area can be calculated by using following equations.

Saturation population, $P_S = \dfrac{2P_0P_1P_1P_2-[P_1 \times P_1(P_0+P_2)]}{(P_0P_2-P_1P_1)}$ (2.7)

And projected population for the time t

$$P = \dfrac{Ps \times P0}{P0+(Ps-P0)e(-rt)}$$ (2.8)

Where, $r = \dfrac{2.3 \times \log 10\{P0(Ps-P1)/P1(Ps-P0)\}}{t1}$ (2.9)

Cohort-Component method

In Cohort-Component method, initial populations for countries are grouped into cohorts defined by age and sex, and the projection proceeds by updating the population of each age and sex-specific group according to assumptions about three components of population change: fertility, mortality, and migration (BIDS, 2014). Based on past information, assumptions are made about future trends in these components of change. Each cohort survives forward to the next age group according to assumed age-specific mortality rates. Five-year age groups (and five year time steps) are commonly used (although not strictly necessary) for long-range projections.

Ratio Method

Ratio method adjusts a population distribution to an assigned total in proportion to the frequencies in this distribution. Ratio method is applied mainly for projecting the population of small areas within a country for which all inputs required by the component method are not always readily available. The method is also useful in the projection of urban and rural populations. This method is used where an area containing the population to be projected (say district) is part of a larger ("parent") area for which projections are available. The main drawback of this method is that it assumes that all the smaller areas will grow at the same rate as the parent area. After the ratio of the district to national population is obtained, assumptions are made on the future values of these ratios. Once the future values of ratios are fixed, the population of the district can be obtained by applying those ratios to the projected national population in respective years.

2.13   Concept of Simple Linear Regression Analysis

Simple linear regression analysis predict the values of a dependent (response) variable based on values of at least one independent (explanatory) variable explaining the effect of the independent variables on the dependent variable. According to the concept, relationship between variables is described by a linear function representing the equation of a straight line. The change of one variable causes the other variable to change showing a degree of inter-dependency. Simple linear regression model can be expressed as Equation 2.10.

$$Y_i = \beta_0 + \beta_1 X_i + \varepsilon_i$$ (2.10)

Where, Y_i =Dependent (Response) Variable; X_i =Independent (Explanatory) Variable; β_1 =Population Slope Coefficient; β_0 =Population Y Intercept and ε_i =Random Error.

2.14   Salient Features of the Model used in the Study

The major tools used in this study are one and two dimensional numerical model HEC-RAS 5.0.3, Arc GIS for spatial data processing and HEC-GeoRAS for interfacing between HEC-RAS and Arc GIS. General overview on the used software tools are presented below.

2.14.1   HEC-RAS

HEC-RAS is a computer program that models the hydraulics of water flow through Natural River and constructed channels. The program was developed by the US Department of Defense, Army Corps of Engineers to manage the rivers, harbors and public works under their jurisdiction. Prior to the recent updated version, the program was one dimensional, but release of version 5.0 introduced two-dimensional modeling of flow including hydraulic effect of cross section shape changes, bends as well as sediment transfer in a river or channel network.

2.14.1.1   Capabilities of HEC-RAS

Major capabilities of HEC-RAS include: User Interface, Hydraulic Analysis Components, Data Storage and Management, Graphing and Reporting and RAS Mapper. The following is a description of the major capabilities of HEC-RAS.

User Interface

The user interacts with HEC-RAS through a graphical user interface (GUI) which focuses to make the use of the software easy maintaining a high level of efficiency. The interface provides with functions of File Management, Data Entry and Editing, Hydraulic Analyses, Tabulation and Graphical Displays of Input and Outputs, Inundation mapping and animations of water propagation and so on.

Hydraulic Analysis Components

The HEC-RAS system contains several river analysis components for: (i) steady flow water surface profile computations; (ii) one- and two-dimensional unsteady flow simulation; (iii) movable boundary sediment transport computations; and (iv) water quality analysis. A key element is that all four components use a common geometric data representation and common geometric and hydraulic computation routines.

- Steady Flow Surface Profile

This steady flow component is intended for calculating water surface profiles for steady gradually varied flow with handling capability of channel network or a single reach. The component is proficient for modeling subcritical, supercritical, and mixed flow regimes. The basic computation bases on the solution of 1D energy equation. Energy losses are evaluated by friction and contraction/expansion coefficients. The momentum equation may be used in rapidly varied water surface profiles including mixed flow regime (i.e., hydraulic jumps), hydraulics of bridges, and evaluating profiles at river confluences.

- One and Two Dimensional Unsteady Flow Simulation

This component of the HEC-RAS modeling system is capable of simulating 1D, 2D, and combined 1D-2D unsteady flow through network of open channels, floodplains, and alluvial fans. The unsteady flow component can be used to perform subcritical, supercritical, and mixed flow regime calculations in unsteady flow. Few of the special features of the unsteady flow component include: Dam break analysis; levee breaching and overtopping; navigation dam operations; automated calibration features; and combined one and two-dimensional unsteady flow modeling.

- Sediment Transport/ Movable Boundary Computations

This component of the modeling system is intended for the simulation of 1D sediment transport/movable boundary calculations resulting from scour and deposition over moderate time periods. The sediment transport potential is computed by grain size fraction, thereby allowing the simulation of hydraulic sorting. Major features include the ability to model a full network of streams, channel dredging, various levee and encroachment alternatives, and the use of several different equations for the computation of sediment transport. This system can be used to evaluate deposition in reservoirs and predict the influence of dredging on the rate of deposition, estimate maximum possible scour during large flood events, and evaluate sedimentation in fixed channels.

- Water Quality Analysis

This component of the modeling system is intended to allow the user to perform riverine water quality analyses. An advection-dispersion module is included with this version of HEC–RAS, adding the capability to model water temperature. This new module uses the QUICKEST-ULTIMATE explicit numerical scheme to solve the 1D advection-dispersion equation using a control volume approach with a fully implemented heat energy budget. Transport and Fate of a limited set of water quality constituents is now also available in HEC-RAS. The currently available water quality constituents are: Dissolved

Nitrogen and Phosphorus; Algae; Dissolved Oxygen (DO); and Carbonaceous Biological Oxygen Demand (CBOD).

Data Storage and Management

Data storage is accomplished through the use of "flat" files (ASCII and binary), the HECDSS (Data Storage System), and HDF5 (Hierarchical Data Format, Version 5). User input data are stored in flat files under separate categories of project, plan, geometry, steady flow, unsteady flow, quasi-steady flow, sediment data, and water quality information. Output data is predominantly stored in separate binary files (HEC and HDF5). Data can be transferred between HEC-RAS and other programs by utilizing the HEC-DSS. Data management is accomplished through the user interface. The user is requested to enter a single filename for the project and once the project filename is entered, all other files are automatically created and named by the interface.

Graphics and Reporting

Graphics include X-Y plots of the river system schematic, cross-sections, profiles, rating curves, hydrographs and inundation mapping. A three-dimensional plot of multiple cross sections is also provided. Inundation mapping is accomplished in the HEC-RAS Mapper portion of the software. Inundation maps can also be animated, and contain multiple background layers (terrain, aerial photography etc.). All graphical and tabular output can be displayed on the screen, sent directly to a printer (or plotter), or passed through the Windows Clipboard to other software, such as a word-processor or spreadsheet. Reporting facilities allow for printed output of input data as well as output data. Reports can be customized as to the amount and type of information desired.

RAS-Mapper

HEC-RAS has the capability to perform inundation mapping of water surface profile results directly from HEC-RAS. Using the HEC-RAS geometry and computed water surface profiles, inundation depth and floodplain boundary datasets are created through the RAS Mapper. Additional geospatial data can be generated for analysis of velocity, shear stress, stream power, ice thickness and floodway encroachment data. In order to use the RAS Mapper for analysis, it is necessary to have a terrain model in the binary raster floating-point format (.flt). The resultant depth grid is stored in the .flt format while the boundary dataset is stored in ESRI's Shapefile format for use with geospatial software.

2.14.1.2 Theoretical Basis for Hydrodynamic Modeling in HEC-RAS

2.14.1.2.1 Computation of 1D Steady Flow Water Surface Elevation

HEC-RAS is currently capable of performing 1D water surface profile for subcritical, supercritical, and mixed flow regime of steady gradually varied flow in natural or constructed channels. Water surface profiles are computed from one cross section to the next by solving the Energy equation with an iterative procedure called the standard step method. The Energy equation is written as follows

$$z_2 + y_2 + \frac{\alpha_2 v_2^2}{2g} = z_1 + y_1 + \frac{\alpha_1 v_1^2}{zg} + h_e \tag{2.11}$$
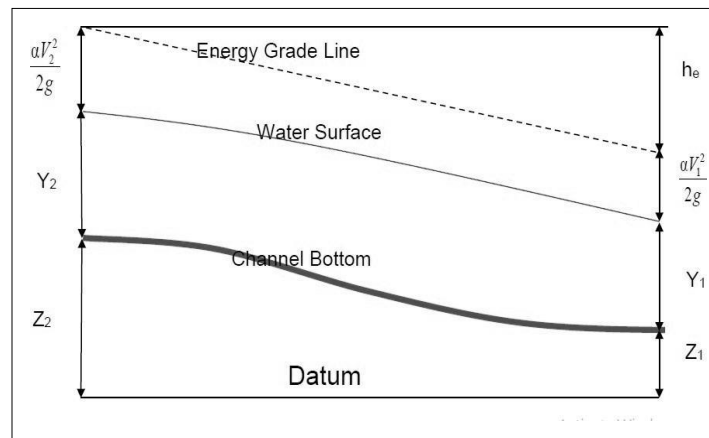
Figure 2.5: Representation of terms in the energy equation

Where, Z_1, Z_2 = elevation of the main channel inverts; Y_1, Y_2 = depth of water at cross sections

V_1, V_2 = average velocities (total discharge/ total flow area); α_1, α_2 = velocity weighting coefficients;

g = gravitational acceleration; he = energy head loss. A diagram showing the terms of the energy equation is shown in Figure 2.5.

The energy head loss (he) is expressed as

$$h_e = L\bar{S}_f + C \left| \frac{a_2 v_2^2}{2g} - \frac{a_1 v_1^2}{2g} \right| \tag{2.12}$$

Where, L = discharge-weighted reach length; $\bar{S}_f$ =Representative friction slope between two sections

C=expansion or contraction loss coefficient. The distance weighted reach length, L, is calculated as:

$$L = \frac{L_{lob}Q_{lob} + L_{ch}Q_{ch} + L_{rob}Q_{rob}}{Q_{lob} + Q_{ch} + Q_{rob}} \tag{2.13}$$

Where, *Llob, Lch, Lrob*= x-section reach length specified for flow in the left overbank, main channel and right overbank respectively and *Qlob + Qch + Qrob* = arithmetic average of the flows between sections for the left overbank, main channel and right overbank respectively.

Application of Momentum Equation

Whenever the water surface passes through critical depth, the energy equation is not considered to be applicable. The energy equation is only applicable to gradually varied flow situations. There are several instances when rapidly varying flow situation occurs including significant changes in channel slope, bridge constrictions, drop structures and weirs and stream junctions. In some of these instances it is necessary to apply the momentum equation to obtain an answer. The momentum equation is derived from Newton's second law of motion:

$$F_x = ma \qquad (2.14)$$

Where, F_x=force, m=mass and a= acceleration (change in momentum)
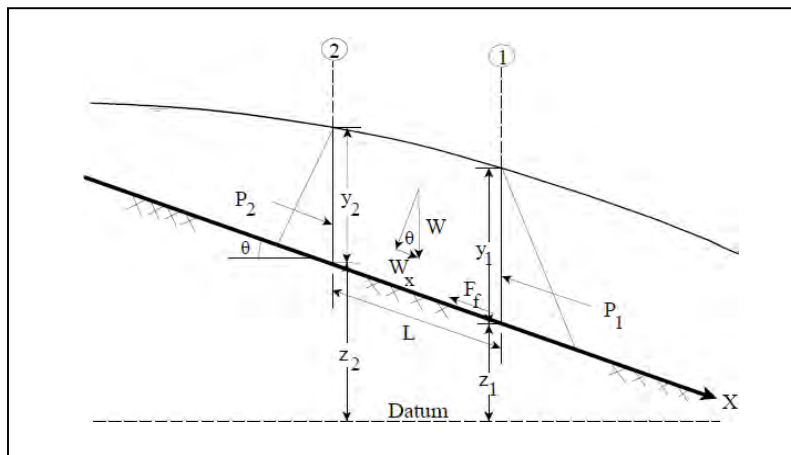
Figure 2.6: Application of momentum principle

Applying Newton's second law of motion to a body of water enclosed by two cross sections at location 1 and 2 (Figure 2.6), the following expression for the change in momentum over a unit time can be written:

$$P_2-P_1+W_X-F_f=Q_P\Delta V_X \qquad (2.15)$$

Where, P= hydrologic pressure force at location 1 and 2, W_x=Force due to the weight of water in the X direction, F_f =Force due to the weight of water in the X direction, Q_p= discharge, $_P$ = Density of Water and ΔV_X= Change on velocity from 2 to 1, in the X direction

Hydrostatic Pressure Force

The force in the X direction due to hydrostatic pressure is:

$$P = \gamma A\bar{Y} \cos \theta \qquad (2.16)$$

28

The assumption of hydrostatic pressure distribution is only valid for slopes less than 1:10. The $\cos\theta$ for a slope of 1:10 (approximately 6 degrees) is equal to 0.995. Because the slope of ordinary channels is far less than 1:10, the $\cos\theta$ correction for depth can be set equal to 1.0. Therefore, the equations for the hydrostatic pressure force at section 1 and 2 are as follows:

$$P_1 = \gamma A_1 Y_1 \tag{2.17}$$

$$P_2 = \gamma A_2 Y_2 \tag{2.18}$$

Where,

γ = unit weight of water

A_i = wetted area of the cross section at location 1 and 2

Y_i = depth measured from water surface to the centroid of the cross sectional area at location 1 and 2.

The Weight of Water Force

Weight of water = (unit weight of water) x (volume of water)

$$W = \gamma \left(\frac{A_1 + A_2}{2}\right) L \tag{2.19}$$

$$W_x = W \sin\theta \tag{2.20}$$

$$\sin\theta = \frac{z_2 - z_1}{L} = S_0 \tag{2.21}$$

$$W_x = \gamma \left(\frac{A_1 + A_2}{2}\right) L S_0 \tag{2.22}$$

Where,

L = Distance between sections 1 and 2 along the X axis; S_0 = Slope of the channel, based on mean bed elevations and Z_i = Mean bed elevation at locations 1 and 2

Force to External Friction

$$F_f = \tau P L \tag{2.23}$$

Where,

τ = shear stress and P = Average wetted perimeter between section 1 and 2

$$\tau = \gamma \bar{R} \bar{S}_f \tag{2.24}$$

Where, $\bar{R}$ = Average Hydraulic Radius (R=A/P), $\bar{S}_f$ = representative friction slope between two sections,

$$F_f = \tau \frac{A}{P} S_f L \tag{2.25}$$

$$F_f = \gamma \left(\frac{A_1 + A_2}{2}\right) S_f L \tag{2.26}$$

Mass time acceleration

$$\text{ma=}Q\rho\Delta V_X \tag{2.27}$$

$$\rho = \frac{\gamma}{g} \text{ and } \Delta V_X = (\beta_1 V_1 - \beta_2 V_2) \tag{2.28}$$

$$\text{ma=}\frac{Q\gamma(\beta_1 V_1 - \beta_2 V_2)}{g} \tag{2.29}$$

Where, B = momentum coefficient that accounts for a varying velocity distribution in irregular channels

Substituting back into equation 3-4 and assuming Q can vary from 2 to 1

$$\gamma A_2 Y_2 - \gamma A_1 Y_1 + \gamma \left(\frac{A_1+A_2}{2}\right)LS_0 - \gamma \left(\frac{A_1+A_2}{2}\right)LS_f = \frac{Q_1\gamma}{g}\beta_1 V_1 - \frac{Q_2\gamma}{g}\beta_2 V_2 \tag{2.30}$$

$$\frac{Q_2\beta_2 V_2}{g} + A_2 Y_2 + \left(\frac{A_1+A_2}{2}\right)LS_0 - \gamma \left(\frac{A_1+A_2}{2}\right)LS_f = \frac{Q_1\beta_1 V_1}{g} + A_1 Y_1 \tag{3.21}$$

$$\frac{Q_2^2\beta_2}{gA_2} + A_2 Y_2 + \left(\frac{A_1+A_2}{2}\right)LS_0 - \gamma \left(\frac{A_1+A_2}{2}\right)LS_f = \frac{Q_1^2\beta_1}{gA_1} + A_1 Y_1 \tag{3.22}$$

This is the functional form of the momentum equation that is used in HEC-RAS. All applications of the momentum equation within HEC-RAS are derived from this equation.

2.14.1.2.2   Theoretical Basis for One - Two Dimensional Hydrodynamic Calculation

This study is focused on the development of 1D-2D coupled hydrodynamic modeling for the Arial Khan River floodplain through HEC-RAS 5.0.3 published by USACE. The equations for 1D-2D coupled modeling have been stated in (Patel, et al., 2017). The HECRAS 5.0.3 is fully solved using the 2D Saint-Venant equation (Brunner, 2016; Brunner, 2016b; HEC-RAS, 2016; Quiroga, et al., 2016):

$$\frac{\delta\zeta}{\delta t} + \frac{\delta\rho}{\delta t} + \frac{\delta q}{\delta t} = 0 \tag{3.23}$$

$$\frac{\delta p}{\delta t} + \frac{\delta}{\delta x}\left(\frac{p^2}{h}\right) + \frac{\delta}{\delta x}\left(\frac{pq}{h}\right) = -\frac{n^2pg\sqrt{p^2+q^2}}{h^2} - gh\frac{\delta\varepsilon}{\delta t} + pf + \frac{\delta}{P\delta x}(h\tau_{xx}) + \frac{\delta}{P\delta y}\left(h\tau_{xy}\right) \tag{3.24}$$

$$\frac{\delta q}{\delta t} + \frac{\delta}{\delta y}\left(\frac{q^2}{h}\right) + \frac{\delta}{\delta y}\left(\frac{pq}{h}\right) = -\frac{n^2qg\sqrt{p^2+q^2}}{h^2} - gh\frac{\delta\varepsilon}{\delta t} + qf + \frac{\delta}{p\delta y}\left(h\tau_{yy}\right) + \frac{\delta}{P\delta y}\left(h\tau_{xy}\right) \tag{3.25}$$

30

Where, h is the water depth (m), p and q are the specific flow in the x and y-direction (m2s-1), ε is the surface elevation (m),g is the acceleration due to gravity (ms-2), n is the Manning resistance, q is the water density (kg m-3), τ_{xx} τ_{yy} τ_{xy} are the components of the effective shear stress and f is the Coriolis (s-1) (Quiroga, et al., 2016)**.**

2.14.2   ArcGIS

GIS is defined as computer systems capable of assembling, storing, manipulating, and displaying geographically referenced information (USGS, 1998). GIS provides a setting in which to overlay data layers and perform spatial queries, and thus create new spatial data. The results can be digitally mapped and tabulated, facilitating efficient analysis and decision-making. Structurally, GIS consists of a computer environment that joins graphical elements (points, lines, polygons) associated with tabular attribute descriptions. In order to provide a conceptual framework, it is necessary first to define some basic GIS constructs.

2.14.2.1   Data Model

Geographic elements in a GIS are typically described by two data models: vector and raster. Each of these is described below:

Vector

Vector objects include three types of elements: points, lines, and polygons. A point is defined by a single set of Cartesian coordinates [easting (x), northing (y)]. A line is defined by a string of points in which the beginning and end points are called nodes, and intermediate points are called vertices (Smith, 1995). A straight line consists of two nodes and no vertices whereas a curved line consists of two nodes and a varying number of vertices. Three or more lines that connect to form an enclosed area define a polygon. Vector feature representation is typically used for linear feature modeling (roads, lakes, etc.) and cartographic base maps.

Raster

The raster data structure consists of a rectangular mesh of points joined with lines, creating a grid of uniformly sized square cells. Each cell is assigned a numerical value that defines the condition of any desired spatially varied quantity (Smith, 1995). Grids are the basis of analysis in raster GIS, and are typically used for steady-state spatial modeling and two-dimensional surface representation. A land surface representation in the raster domain is called a digital elevation model (DEM).

2.14.3 HEC-GeoRAS

HEC-GeoRAS is an ArcGIS extension specifically designed to process geospatial data for use with the HEC-RAS. The extension allows users to create an HEC-RAS import sample containing geometric attribute data from an existing digital terrain model (DTM) and complementary data sets. Water surface profile results may also be processed to visualize inundation depths and boundaries. HEC-GeoRAS extension for ArcGIS used an interface method to provide a direct link to transfer information between the ArcGIS and the HEC-RAS. Several requirements and tools of HEC-GeoRAS are described below: (HEC-GeoRAS, 2009)

2.14.3.1 Software Requirements

HEC-GeoRAS 10.2 is an extension used for ArcGIS 10.3. Both the 3D Analyst extension and the Spatial Analyst extension are required. The full functionality of HEC-GeoRAS 10.3 requires HEC-RAS 5.0 beta, or later, to import and export all of the GIS data options. Older versions of HEC-RAS may be used, however, with limitations on importing roughness coefficients, ineffective flow data, blocked obstructions, levee data, hydraulic structures, and storage area data. Further, data exported from older versions of HEC-RAS should be converted to the latest XML file structure using the SDF to XML conversion tools provided.

2.14.3.2 Data Requirements

HEC-GeoRAS requires a DTM in the form of a TIN or a GRID. The DTM must be a continuous surface that includes the bottom of the river channel and the floodplain to be modeled. Because all cross-sectional data will be extracted from the DTM, only high resolution DTMs that accurately represent the ground surface should be considered for hydraulic modeling.

2.14.3.3 The HEC-GeoRAS Menu

ApUtilities menu of HEC-GeoRAS is used to manage the data layers created through GeoRAS and the Help menu provides online help information. Beyond the ApUtilities and Help, the HEC-GeoRAS menu includes threo major menu options called as RAS Geometry and RAS Mapping and *HEC-GeoRAS Tools*. The three menu options are discussed below.

RAS Geometry

The RAS Geometry menu is for pre-processing geometric data for import into HEC-RAS. Items are listed in the RAS Geometry dropdown menu in the recommended order of completion. Items available in the

RAS Geometry menu items are Create RAS Layers, Layer Set up, Stream Centerline Attributes, XS cutlines Attributes, Manning's n values, Export RAS Data, Terrain Tiles etc. This menu is also capable of incorporating Manning's n values, levees, ineffective flow areas, bridges/culverts, inline and lateral structures, Storage areas and connections.

RAS Mapping

The RAS Mapping menu is for post-processing exported HEC-RAS results. Items available from the RAS Mapping dropdown menu are layer setup, import RAS data, inundation mapping, velocity mapping, Ice mapping, shear stress mapping, stream power mapping, visualization, post-processing utilities.

HEC-GeoRAS Tools

There are several tools such as assigning river and reach code, station code, assign flow path XS cutlines etc. are provided in the toolbar. A tool waits for user action after being activated and will either invoke a dialog or change the mouse pointer, indicating the need for further action.

CHAPTER 3

LITERATURE REVIEW

3.1   General

A number of studies have been carried out in the past, particularly concerning the floodplain inundation mapping, flood hazard, flood forecasting and risk assessment. This chapter focuses on the literature review on few of the notable studies on flood hazard, vulnerability and risk around the world and in Bangladesh in particular.

3.2   Studies on Flood Hazard, Vulnerability and Risk Assessment around the World

Notable studies have been conducted on flood hazard, vulnerability and risk assessment for historical, recent and future flood scenario corresponding to climate change scenario and extreme flood events so far. A few relevant literatures pertaining to hazard, vulnerability and risk assessment carried out worldwide has reviewed below.

Flax et al. (2002) developed a risk and vulnerability assessment methodology named as Community Vulnerability Assessment Tool (CVAT), which assists to reduce hazard vulnerabilities through hazard mitigation, comprehensive land use, and development planning. The model considered storm surge, wind, flood and tornado as hazard and gives a methodology to identify and prioritize the hazards.

Shrestha, et al. (2004) assessed flood risk and vulnerability combining the hydrologic analysis with socioeconomic resources and constraints with the help of HEC-RAS for flood elevation estimate and GIS for vulnerability and risk. Primary data on socio-economic condition, susceptibility, response capability was collected to develop vulnerability map using house, built-up area, land cover and road infrastructure as vulnerability parameters and risk was obtained by the multiplication of vulnerability and hazard.

Singh et al. (2009) developed a remote sensing based approach for urban floodplain mapping for the Tapi catchment of India in which GIS has been utilized to prepare urban flood hazard and risk maps for various water-level condition only. Later, Tu et.al (2009) studied on flood inundation, damage and risk assessment in Hoang Long basin of Vietnam in which rainfall runoff model MIKE-NAM has been used to predict the flood hydrograph for extreme rainfall events of 5, 10, 20, 50, 100,200 year return period obtained from

rainfall frequency analysis. Results obtained from the hydrological modeling were used as inputs of MIKE 11 for simulation of flood. Flood depth and duration obtained from simulation were used as hazard indicators to be used for flood risk assessment using damage curve prepared for the residential, agricultural and road damages.

Tu and Tingsanchali, (2010) studied the flood hazard and risk assessment of Hoang Long River basin of Vietnam. In this study, design flow hydrograph for different return period are found from rainfall-runoff model MIKE-NAM that are fed to hydrodynamic model MIKE 11 to simulate flood flow in Hoang Long Basin. Then the risk map has been prepared multiplying the hazard considering flood depth and duration as hazard indicators with population density as vulnerability unit. Later, Samarasinghea (2010) prepared flood hazard maps of Kalu-Ganga River using HEC-HMS and HEC-RAS for different return periods (10, 20, 50 and 100 years). Population and physical vulnerability of the lowest administrative division subjected to floods have also been assessed, and using above results flood risk analysis of the study area has been conducted.

Forkuo et.al., (2011) developed an additive model to create flood hazard maps of the study area in Ghana. Using available topographical, land cover and demographic data, the study created a district level map indicating flood hazard prone areas. A composite flood hazard index was developed incorporating variables of near distance to the White Volta River, population density, no. of towns in each district, area of cultivated crops and availability of high ground.

Lorraine and Maksym, (2014) focused on analysis of the magnitude, frequency and severity of the historical, current and future flood and drought risks in Manyame catchment of Zimbabwe. It involved the analysis of historical and future precipitation trends, frequencies and severities using several climatological and standardized indices and numerical models. The historical damages of floods and droughts were correlated to the rainfall anomalies by use of Standardized indices (SPI, SPEI, and SOI). Mani et al. (2014) studied on flood hazard assessment with multi parameter approach derived from coupled 1D-2D hydrodynamic model. Flood depth, cross product of flood depth and velocity and flood duration was used for assessing the flood hazard and proposal of a flood hazard classification scheme.

Nugraha et.al., (2015) intended to develop tidal flood risk map of Semarang in Java Island. In order to develop the flood risk map, the validation and prediction of the tidal flood were done to produce a hazard map on the tidal water level and topographic map. Subsequently, the maps of vulnerability and adaptive capacity of the study area were produced based upon VCA (Vulnerability Capacity Analysis) by using

fuzzy logic and weighted method approaches. Combining the hazard and vulnerability, risk has been assessed. Later, Roy and Blaschke, (2015) developed a methodology for the spatial vulnerability assessment of flood in the coastal regions of Bangladesh. For a 706 km² area in the Sundarbans Reserve Forest and its surroundings 12 vulnerability domains are defined and 44 indicators are developed. These indicators are ranked by 20 local experts through an analytic hierarchy process (AHP). All data-sets are transformed into 100 m resolution raster (grid) data-sets in a geographic information system (GIS). This grid approach surmounts the problems of data availability and different data scales, and allows the inclusion of indicators for the social dimension. A spatial vulnerability assessment is carried out using GIS weighted overlay. The resulting maps and figures reveal both the extents and levels of vulnerabilities.

Silva, et al., (2016) analyzed the potential extreme rainfalls and resulting flood inundation for Lower Kelani River Basin of Sri Lanka under A2 (high emission) and B2 (low emission) climate change scenarios in which HEC-HMS has been used to generate future flood discharge under the climate change scenarios and flood inundation along the Kelani River has been analyzed by the application of flood simulation model-FLO-2D. As result, areas vulnerable to inundation under the climatic change scenarios have been presented in this study.

Shrestha and Lohpaisankrit, (2016) studied the flood induced hazard of Yang River Basin of Thailand for climate change scenarios of RCP 4.5 and RCP 8.5 using a physically-based distributed hydrological model, TOPMODEL and a hydraulic model, HEC-RAS. The study results suggested that the annual flood intensity expects an increase for both RCP 4.5 and 8.5 scenarios with increased inundation area for the event of return period of 100 years comparing with the baseline period.

Azmeri et.al., (2016) aimed to obtain flash flood hazard zones at the Krueng Teungku watershed. The method used in this study was weighted overlay technique through Geographic Information System (GIS). This paper also provided the review of factors that affect the incidence of flash flooding, including the factors of peak discharge, slope, watershed shape, stream gradient, damming, drainage density, erosion, slope stability and reservoir volume.

Anh et.al., (2016) aims to present the assessment of flood and inundation risk in downstream of river basins in North Central Vietnam in which the river systems are modelled using MIKE FLOOD with rainfall-runoff model (NAM), MIKE 11 and MIKE 2. Maximum flood depth, inundation duration and flood peak velocity used as hazard indicators. To estimate susceptibility and resilience indices of the local communities, series of surveys were conducted for 32 selected indicators. The index maps of hazard,

susceptibility and resilience were then overlapped with exposure maps by GIS tools to establish the vulnerability and risk.

Ibrahim et.al., (2017) Flood vulnerability indices for the Kelantan River sub-basins were developed from various flood related variables. The vulnerability indices of the Kelantan River sub-basins involved flood depth-inundation area, soil erosion potential, and potential of soil for agricultural use, population vulnerability, road infrastructure vulnerability and market infrastructure vulnerability using of Geographic Information System (GIS).

Ntajal et.al., (2017) focused on assessment and mapping of social flood risk in the Lower Mono River Basin, West Africa. The study combined GIS, Remote Sensing and indicator-based flood risk assessment techniques in mapping flood risk. This section considered hydrological analysis of the topography and the physical characteristics of the Lower Mono River Basin. In order to create the risk map, each of the components of flood risk (Hazard, Exposure, and Vulnerability and Capacity measures) were given weight according to their relative importance in causing flood and based on literature review, expert knowledge and the authors' knowledge of the study area.

3.3   Studies on Flood Hazard and Risk Assessment of Bangladesh

Chowdhury and Karim (1996) developed risk-based zoning maps considering only cyclonic storm surge floods of 45 land units in the Ganges tidal flood prone area. Hazard factors were based on the simulated spatial distribution of 100-year flood depths while the vulnerability factors were based on the distribution of population densities. The land units grouped into low, moderate, high and severe risk zones. Islam and Sado (2000) studied flood hazard in Bangladesh using NOAA AVHRR data with GIS. In that study, hazard assessment was made considering the depth and duration of flooding as hazard parameters where Satellite images were used for the prediction of the two parameters. For the generation of flood hazard map physiographic divisions, geological divisions, land cover categories and drainage network data were used as GIS components with the depth and duration of flooding.

Tingsanchali and Karim (2005) developed methodology for hazard and risk mapping in south west region. Flood hazard assessment was done considering flooding depth and duration for 1988 flood scenario and hazard index considered similar to that of Chowdhury and Karim (1996). After that, Masood (2006) studied flood hazard and risk assessment in mid-eastern part of Dhaka. In this study, DEM data were collected from Shuttle Radar Topography Mission (SRTM) and the observed flood data for 32 years (1972-2004) were used. The inundation simulation was conducted using HEC-RAS program for 100 year

flood. Hasan (2006) applied geoinformatics to assess flood hazard vulnerability in Tarapur union of Bangladesh. Flood hazard vulnerability of agriculture is assessed for different flood magnitudes through development of flood inundation and depth maps and vulnerability function.

Dewan et al. (2007) illustrated the development of flood hazard and risk maps in Greater Dhaka of Bangladesh using geoinformatics. Multi-temporal RADARSAT SAR and GIS data were employed to delineate flood hazard and risk areas for the 1998 historical flood. Flood affected frequency and flood depth were estimated from multi-date SAR data and considered as hydrologic parameters for the evaluation of flood hazard using land-cover, geomorphic units and elevation data as thematic components. Flood hazard maps were created by considering the interactive effect of flood frequency and flood water depth concurrently.

Comprehensive Disaster Management Programme (CDMP) with IWM (2008) carried out the Impact assessment of climate change causing increased rainfall and sea level rise on monsoon flooding based on the recommendations of the Forth Assessment Report (AR4) of the Intergovernmental Panel on Climate Change (IPCC). The study area covered seven districts of Bangladesh namely Sirajganj, Gaibandaha, Pabna, Faridpur, Sunamganj, Satkhira and Barishal. The study depicts the impact of climate change are different in Jamuna, Ganges and Meghna basins and in the coastal area due to different flooding pattern in these basins.

Hossain, (2013) developed flood damage and risk assessment model in the haor basin of Bangladesh. The primary objective of this study was to assess flood damage and risk of agricultural Boro crop due to pre-monsoon flash flood. The inundation information has been extracted from a 2D hydrodynamic flood model MIKE 21 for 2, 10, 20 and 100 recurrence intervals. Then, flood hazard map has been developed considering two combinations of hazard parameter. In the first combination, flood depth and flooding duration were considered whereas in the second combination, flood depth and flood velocity were considered. Later, Haque et al, (2013) developed flood hazard and risk maps with the effect of climate change scenario in three different types of floods such as river flood, flash flood and cyclone storm surge flood in three hydrologic regions namely Sirajganj, Baniachang and Barguna. Satellite images for land cover mapping, DEM data for developing inundation maps in different location and crops and settlement data have been used as elements for vulnerability and risk mapping.

Islam (2014) assessed flood risks of the Brahmaputra-Jamuna Floodplain. The model involved the analysis of the hydrologic, topographic and the local resident's coping capacity variables. Combining the weight

of the above variables throughout the study area the model was able to demarcate flood risk zones of various intensities. Flood intensity and duration of the area is controlled mainly by the hydrological and topographical characteristics of the catchment area. Coping strategies and options of the local residents were found to be poor and inadequate and are mainly based on indigenous knowledge. A Hazard Intensity Surface Index has been prepared for the area combining all the variables that contribute to the overall hazard potential of the study area.

Mondal et.al., (2017) studied on the simulation of flood risk due to climate change in major rivers of Bangladesh using a Hydrodynamic Model. They setup a one-dimensional hydrodynamic model HEC-RAS for the major rivers of Bangladesh and simulated the model for flood hydrographs under base condition and changed climate at model boundaries (Bahadurabad on the Brahmaputra, Hardinge Bridge on the Ganges and Bhairab Bazar on the Meghna). The results revealed that the peak flood level in the Ganges-Brahmaputra would increase by 24-31cm due to changes in rainfall in the upstream areas.

3.4   Previous Studies on Old Brahmaputra River

Though extensive flood hazard and risk related studies have been conducted on the rivers around the world and few remarkable hazard and risk analysis have done on the major river flood plain of Bangladesh , no comprehensive study on the flood hazard, vulnerability and risk of Old Brahmaputra River has been conducted yet. Few studies on the morphological assessment of Old Brahmaputra river has been obtained from literature review. For example, Noor (2013) performed morphological Study of Old Brahmaputra Offtake using two dimensional mathematical model MIKE 21' where the impact of dredging and guide bund at the offtake on the flow condition and siltation at offtake were focused. Ahmed and Navera (2018) carried out a study to observe the planform changes of Old Brahmaputra River offtake over the period of 1973 to 2017 by different Landsat image composite.

Uddin et.al.,(2017) studied on the physicochemical analysis of Mymensingh municipality sewage water and Old Brahmaputra river water in which water samples were analyzed to determine water quality indices for finding the usability in agriculture and household. Afrose and Ahmed (2016) studied on assessment of fish biodiversity and fishing practices of the Old Brahmaputra River where the authors identified a total of 39 species of fish belonging to 17 common groups in the catches of the river.

Few attempts have been undertaken to assess the inundation and flood induced vulnerability for Old Brahmaputra River. For instance, Rakib et.al., (2017) studied the flood vulnerability mapping of the Old Brahmaputra River for Mymensingh Sadar upazilla. Flood vulnerability mapping of 14 unions of

Mymensingh Sadar has been made by using satellite images, a structured questionnaire, observation and secondary data for the historical flood event of 1998 and 2007 using GIS. No hazard, vulnerability and risk assessment has been done for future specific climate change scenario. Moreover other upazilla through which the river Old Brahmaputra flows were not included in this study. The study calculated vulnerability index using the parametric thematic maps of geomorphology, slopes, elevations, distances, water height and inundation range. No specific social and economic vulnerability has been estimated here. Biswas et.al., 2018 introduces hydro-morphometric modeling to assess flood hazard vulnerability in old Brahmaputra River in which basin, flow accumulation, flow direction, stream order, stream length, stream density and drainage density were combined for the estimation of flood hazard vulnerability by subdividing area into five sub-basin.

But hazard, vulnerability and risk assessment on the Old Brahmaputra floodplain due to climate change scenarios has not been done yet. Hence, the flood hazard, vulnerability and risk assessment of Old Brahmaputra River considering new concepts of climate change scenarios along with different exposure and vulnerability indices are very required. That's why, this study is designed for the hazard, vulnerability and risk assessment of Old Brahmaputra River and its floodplain for predicted climate change scenarios using open source numerical model.

CHAPTER 4

METHODOLOGY

4.1   General

The most conjoint methodology to define flood risk consists of calculating the hazard, that is, the physical and statistical aspects of the actual flood like the depth, extent & flow velocity of flood, the level of vulnerability depicting susceptibility of the elements at risk due to flood and the exposure of people & things to the flood. Flood hazard and vulnerability assessment forms the foundation of risk assessment and management by providing information essential to understand the nature and characteristics of the community's vulnerability to flooding. This chapter describes a brief discussion about the methodology and model setup to achieve the study goals.

4.2   Outline of the Methodology at a Glance

The definite objective of this study is to assess flood hazard, vulnerability and risk for the selected river reach of the Old Brahmaputra River under the impact of future climate change scenario. Figure 4.1 shows the outline of the study methodology at a glance.
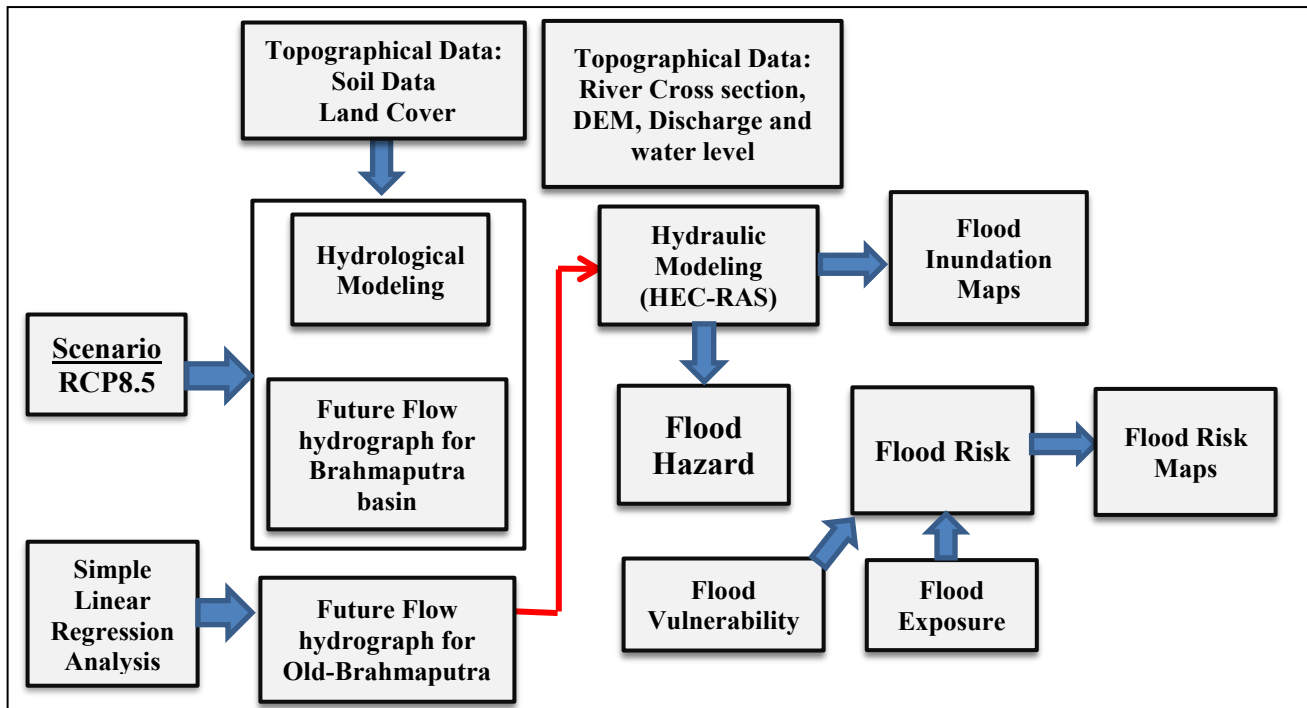
Figure 4.1: Outline of Methodology of the study

To achieve the goals, the future flood flow hydrographs of the Old Brahmaputra River have been generated from the simulation of hydrological model in HEC HMS and using the concept of linear regression analysis. Sequentially, a HEC-RAS 1D-2D coupled model has been developed and simulated for different flood flow scenarios to get the values of the flood hazard parameters under changing climate. The qualitative risk assessment has been performed combining the hazard indicators with vulnerability and exposure indices adopting the latest integrated risk framework of IPCC.

4.3   Introduction to Old Brahmaputra River

The Old Brahmaputra is one of the major distributaries of the Brahmaputra-Jamuna River that discharges part of the flow of the mighty Jamuna River over a large area of North Central region of Bangladesh. Old Brahmaputra River takes off from the left-bank of Brahmaputra River which is approximately 10km upstream from Bahadurabad and flowing towards the south-eastern region of Bangladesh over Jamalpur, Sreepur, Netrokona, Mymensingh, Kishoreganj, Narsingdi and Gazipur district the river falls into the Meghna River near Bhairab Bazar (Ahmed, 2018; BWDB, 2010). The river got reduced to a left bank spill channel of the Brahmaputra River and now only active during the high stage of the Brahmaputra River having limited capacity for passing flood discharge. In the lower areas of the Old Brahmaputra river basin flooding situation aggravates due to the tendency of channels to overflow towards the floodplains during the flood period (Noor, 2013).

Table 4.1: The Prominent characteristic features of the Old Brahmaputra

Offtake	Kholabarichar of Brahmaputra-Jamuna River
Outfall	Bhairab Bazar of Upper Meghna River
District	Gaibandha, Jamalpur, Sherpur, Mymensigh, Kishoreganj, Narsingdi, Gazipur
Tributary	Jinjirum and Mora Jinjirum
Distributary	Jhinai, Lakhya, Sutia, Banar, Arial Khan, Aiman-Akhila
Length from offtake to outfall	225 km
Width	200 m (at Mymensingh)
Type	Meandering
Flow	$12\sim4,890\text{m}^3$/s
Channel sinuosity(Avg.)	1.24
Average Bed slope (upto Jamalpur)	6 cm/km (8.4 cm/km near Jamalpur and 5.8cm/km near Toke
Average grain diameter (d50)	0.005mm to 0.348mm
Average sinuosity	1.24

*Source: BWDB, 2011; FAP24, 1996

The tributaries, Jinjirum and Mora Jinjirum, coming from across the Indo-Bangladesh border joins the Old Brahmaputra River very close to its off-take and act as a source of dry season flow of the river Old Brahmaputra as well (Noor, 2013). Table 4.1 highlights the prominent characteristic features of the Old Brahmaputra River.

4.4   Hydro-Morphological Characteristics of Old-Brahmaputra River

To obtain an idea on the hydro-morphological condition of the old Brahmaputra River, historical data on discharge and water level of selected locations along the river have been analyzed. Locations considered for this assessment are shown in Figure 4.2.
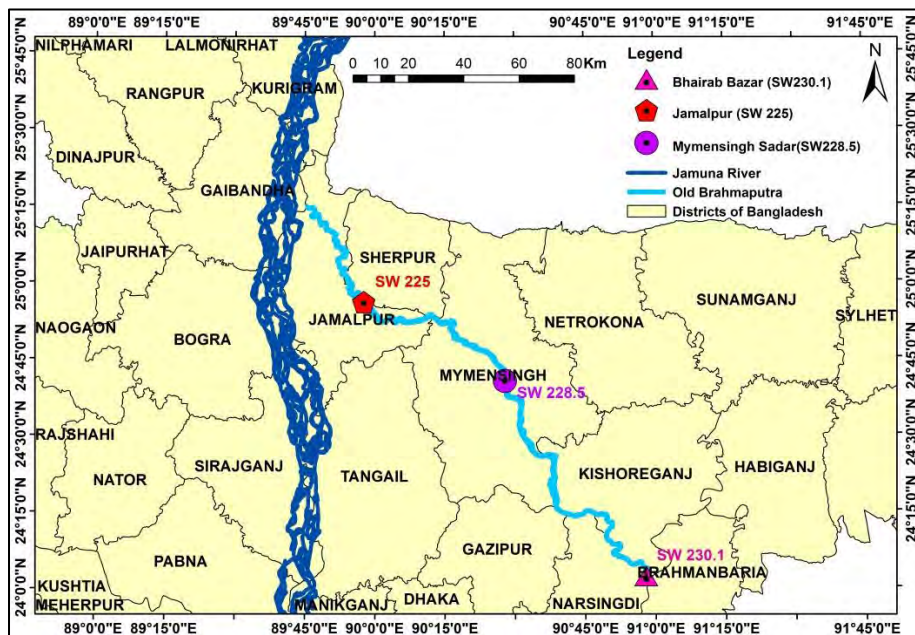
Figure 4.2: Location of hydrologic stations in Old Brahmaputra River

4.4.1   Hydrological Characteristics

Discharge

The hydro-morphological condition of the river depends on the position of off-take and the deviation of flow direction to the off-take from the parent river, the Brahmaputra-Jamuna. Analysis of annual maximum flow of Old Brahmaputra at Mymensingh (SW 228.5) from 1966 to 2017 as shown in Figure 4.3 demonstrates that the flow trend is decreasing over the year. The declining pattern indicates to some extent that the flow from the offtake of the Old Brahmaputra has been declining due to siltation thus the carrying capacity of the river throuout the reach is also decreasing which in turn increases the tendency of flood in dry land during momsoon.

Maximum Discharge of Old Brahmaputra at SW 228.5
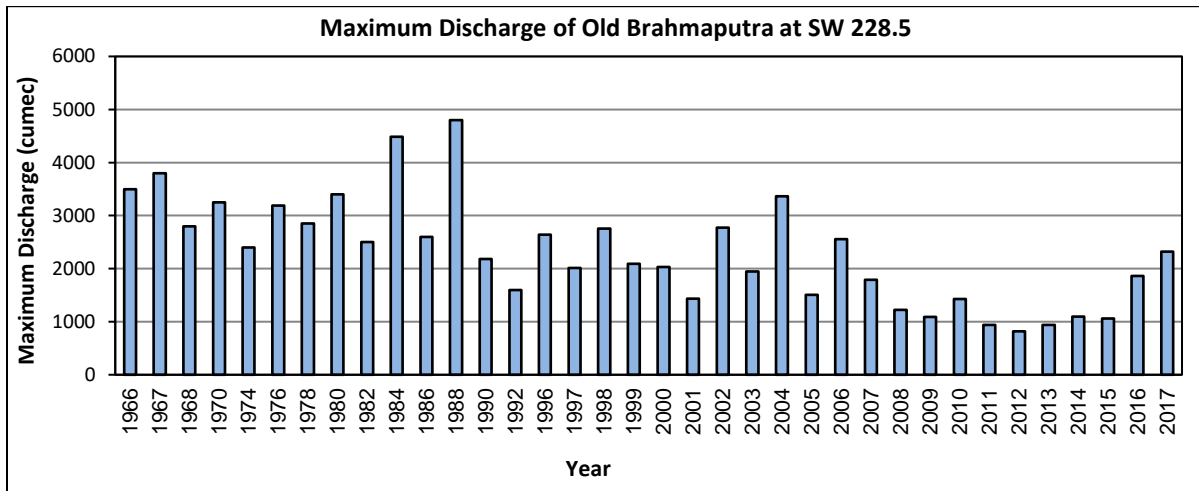
Figure 4.3: Peak annual discharge of Old Brahmaputra at Mymensingh Sadar (SW 228.5) for past years

The annual flow of the river varies substantially as found from the data of 1966 to 2017 where the highest recorded discharge of the river at Mymensingh is 4890 m^3/s during monsoon in year of 1988 and the lowest recoded discharge was measured in 2012. Maximum discharge increases during 1979 to 1988 and then drops. Analysis on minimum flow of Old Brahmaputra River at the same station showed that during the lean flow season the discharge gets reduced to less than 100 m^3/s and has been found as low as 12m^3/s during specific dry period of a year (Noor, 2013). Rivers that experience such large fluctuation of discharge tend to be unstable and may change its morphology in medium to long-term perspective (Ali, 2010).

Water level

Old Brahmaputra River has six water level stations. Among them data of three measuring stations surround the study area collected to conduct analysis in this study. Figure 4.4 (a), (b), (c) show the maximum, minimum and average water level of Old Brahmaputra River at Mymensingh (SW 228.5), Jamalpur (SW 225) and Bhairab Bazar (SW 230.1). At Jamalpur water level is slightly in decreasing trend. The maximum water level is 17.9m happened in 1988 and the minimum water level is 10.45 m in 2017. At Mymensingh water level is in slight decreasing trend as well with maximum in 1988 and minimum in 2017. It is obviously clear that water level will decrease with slope towards downstream as a result water level at Mymensingh is lower than the water levels at Jamalpur. Similar pattern has been found in case of water level at Bhairab Bazar.

44
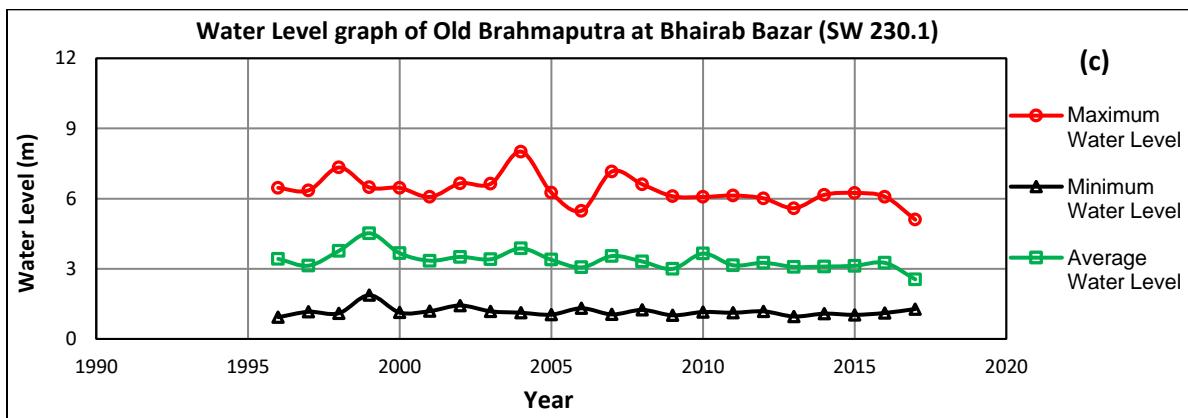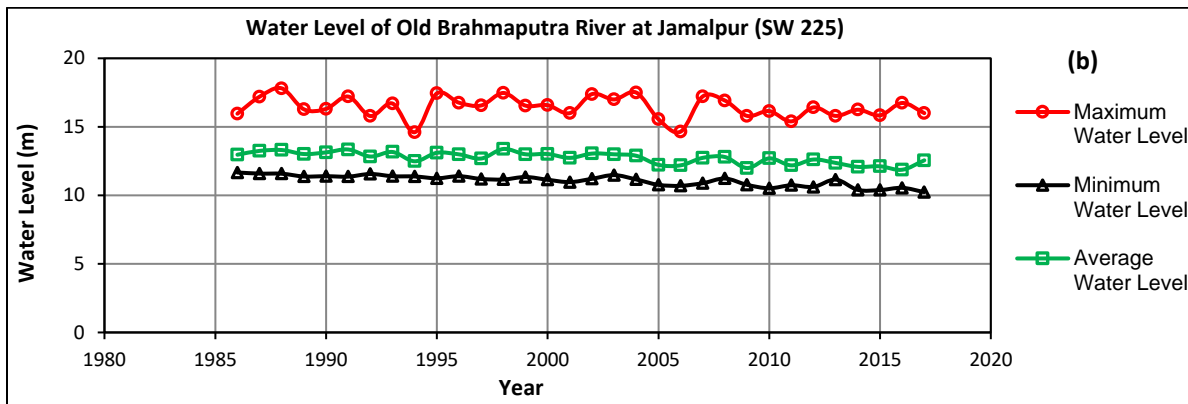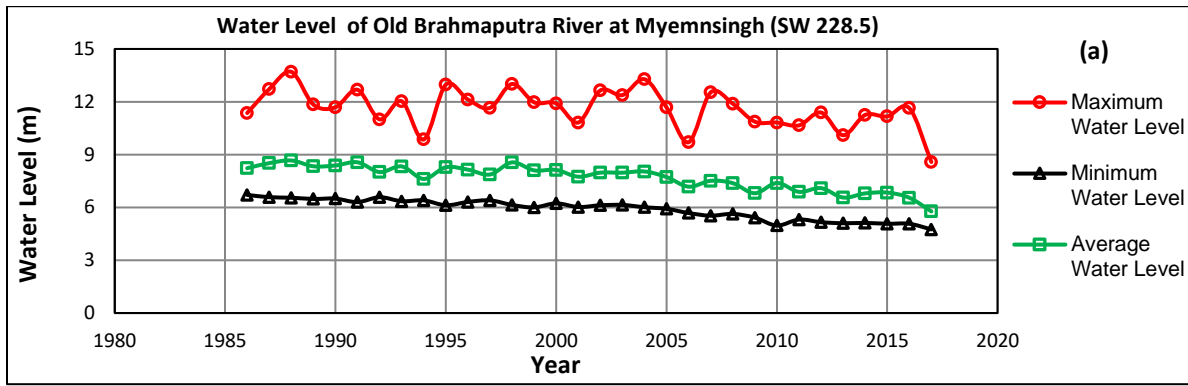
Figure 4.4: Water level of Old Brahmaputra River at (a) Mymensingh (b) Jamalpur (c) Bhairab Bazar

4.4.2 Morphological Characteristics

Old Brahmaputra River offtake is one of the four major offtakes in Bangladesh and is one of the most dynamics. The flow of Old Brahmaputra River has been decreased due to siltation at the offtake and upstream reach. Flow input at offtake from Brahmaputra River is decreasing as shown in Figure 4.5. From 1973 percentage of Jamuna river flow to the Old Brahmaputra River was 6.69% and in recent year this percentage of flow is reduced to around 3% revealing the siltation problem at the mouth (Ali, 2010).
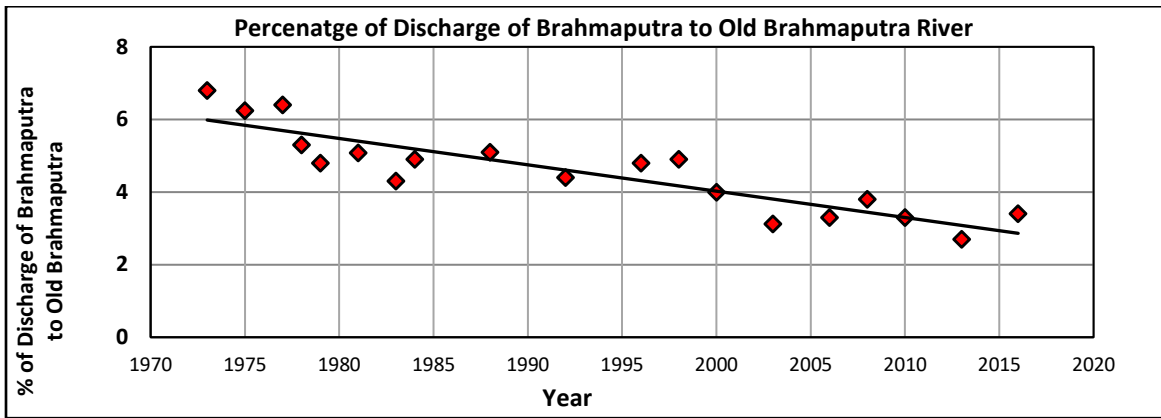
Figure 4.5: Percentage of Discharge of Brahmaputra River to Old Brahmaputra River

From the analysis on sediment transport rate in Old Brahmaputra River as shown in Figure 4.6, the maximum sediment discharge was 28080 tons/day in August of 1988 and the lowest sediment discharge was 489 tons/day in 1991 (Noor, 2013). In Old Brahmaputra, the maximum discharge was 4280 cumecs in August of 1988 and the lowest discharge was 435 cumecs in May of 1991which implies that when the river gets greater discharge, sediment discharge rate also increases.
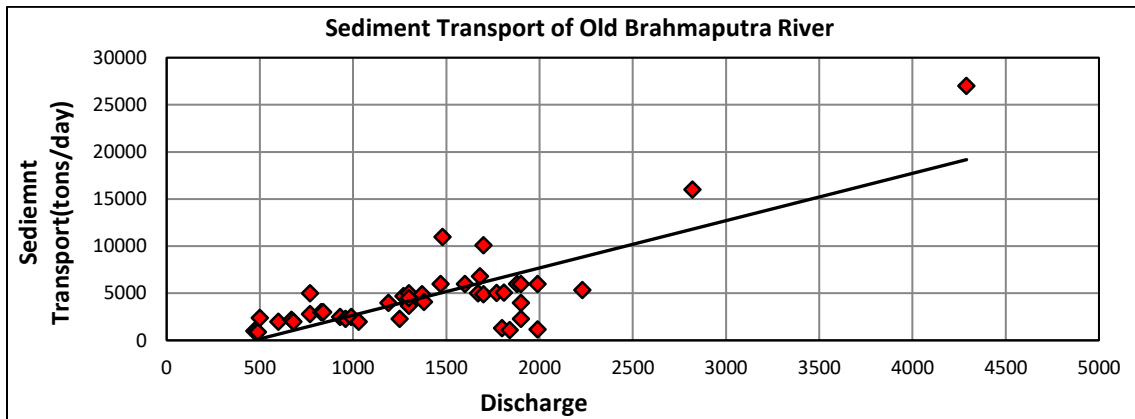
Figure 4.6: Comparison of Sediment Transport with Discharge in Brahmaputra River

In a river highly charged with sediment, the bed configuration changes drastically under different flow regimes. Deposition of sediment in one place causes erosion in another place. Thus the thalweg tends to wander continuously from one position to another within the river bank lines. Analysis on the deepest points of all available cross-sections from 1966 to 2005 showed that the thalweg of the particular river is very dynamic frequently moving left ward and right ward over the years (Noor, 2013). The plot also depicts that there is a gradual deposition of sediment in thalweg elevation of about 20.05 m during 1996 to 2005 at the upstream reach of the river.

4.4.3   Bank line Migration

Analysis of the satellite imagery for last 34 years from 1973 to 2007 shows that both the banks of the Old Brahmaputra River are dynamic and frequency of bank line movements differ reach wise due to erosion and accretion along the reaches (Noor, 2013). Analysis result shows that the maximum migration from left bank was 2149.29 m during 1973-1999 and minimum migration was 33.14 m during 1973-2002.The maximum migration from right bank was 2297.12m at during 1973-1995 and minimum was 30.55m during 1973-1995. Massive changes occurred in bank line shifting after the flood of 1988 and 1998. Study on the planform changes of Old Brahmaputra River offtake over the period of 1973 to 2017 by different Landsat image depicted that the Old Brahmaputra offtake has been silted up and de-connected with the parent river after 1990 during lean period (Ahmed, 2018). Analysis on reach wise sinuosity values varied from 0.56 to 0.71 implying larger amount of associated land erosion in the bends (Noor, 2017) as shown in Figure 4.7.
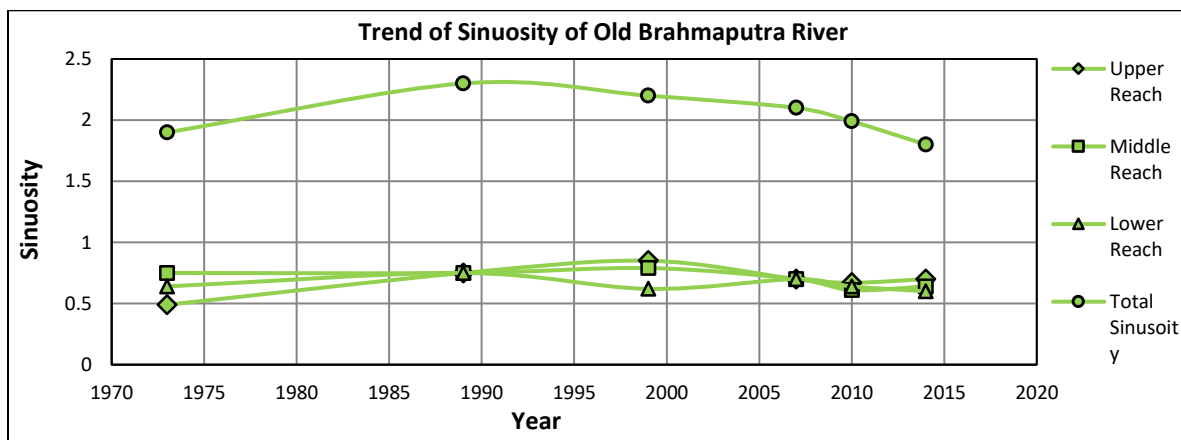
Figure 4.7: Trend of Sinuosity of the Old Brahmaputra River

4.5   Selection of Study Area

The total river length between the off-take and outfall is approximately 283 km (BWDB, 2015). Sreepur, Netrokona and Mymensingh stand on the left and Jamalpur, Kishoreganj, Narsingdi and Gazipur districts are at the right side of the river. In this study, the lower reach of Old Brahmaputra River having a length of around 130 km and its adjacent floodplains have been proposed as the study area due to the existing problem of the area with monsoon flood inundation. Figure 4.8(a) shows map of the area used for the analysis on flood variables, hazard, vulnerability and risk.
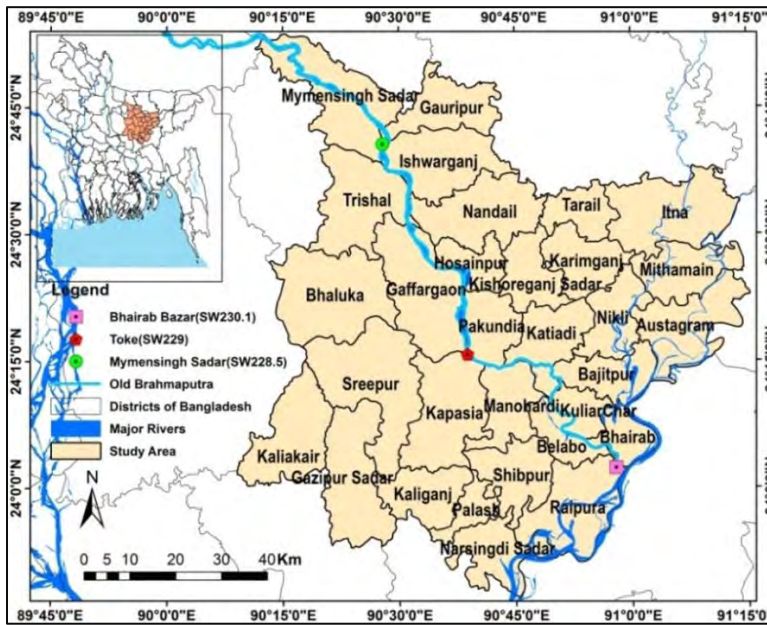
Figure 4.8 (a): Map of the Area showing extent of analyses

The goal of this study is to assess the flood hazard, vulnerability and risk of Old-Brahmaputra river floodplain for future climate change scenario of RCP 8.5. That is why after the analyses of the variables within the study area represented as in Figure 4.8(a), the flood induced hazard, vulnerability and risk have been reported for the Old Brahmaputra floodplain also that is obtained from the process of watershed delineation as shown in the Figure 4.8(b).
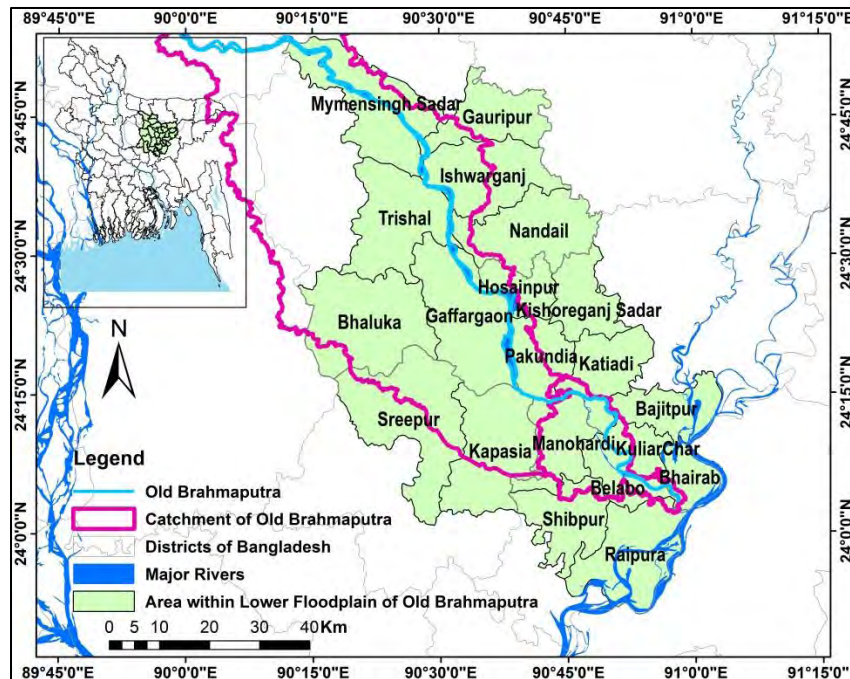
Figure 4.8 (b): Map showing area within lower segment of Old Brahmaputra floodplain

4.6   Data Collection

In order to estimate the flood induced hazard, vulnerability and risk of the old Brahmaputra river floodplain various dataset have been collected and processed. According to the requirement of the hydrodynamic and flood model, data including cross section, water level, discharge, terrain profile of the study area have been collected. To assess the socio-economic vulnerability and exposure to flood of the study area, data on notable social and economic indicators have also been collected. Table 4.2 includes the data used in this study with the source, location and time period.

Table 4.2: Summary of the Data used in the study

Data Type	Data Source	Location	Period
SRTM DEM	USGS	Bangladesh	2014
Bathymetry	BWDB, IWM	Old Brahmaputra	2015-16
Discharge	BWDB	Mymensingh Sadar(SW 228.5) Bahadurabad transit (SW 46.9L), Bhairab Bazar (SW 273), Demra (SW 179)	1986-2017
Water Level	BWDB	Jamalpur(SW 225), Mymensingh (SW 228.5), Toke (SW229), Bhairab Bazar(SW230.1), Bhairab Bazar (SW 273)	1986-2017
Socio-economic indicators	BBS	Mymensingh, Kishoreganj, Narsingdi and Gazipur districts	Population Census 2011, 2001, 1991, 1981& Agriculture Census 2008, 1998, 1986 and 1981

Bathymetry

River cross-sections of Old-Brahmaputra River are collected for the years of 2015-2016 from Bangladesh Water Development Board (BWDB). BWDB collects cross-section data at 36 different stations of Old Brahmaputra River with station id OB 1 to OB 36 measured from upstream to downstream. Collected surveyed bathymetry data from IWM included 102 cross sections with easting, northing and reduced level. In this study, 47 available cross sections of the lower reach of Old Brahmaputra River have been used for the model setup.

Discharge Data

The discharge data of Mymensingh (SW 228.5) of the old Brahmaputra River, Bahadurabad transit (SW 46.9L) of Brahmaputra-Jamuna river, Bhairab Bazar (SW 273) of Surma-Meghna river and Demra (SW

179) of Lakhya river were collected from the Bangladesh Water Development Board (BWDB) for the year 1986-2017 to be used for the boundary condition of 1D river channel and 2D floodplain of the study area. For the development of hydrodynamic model discharge hydrograph of daily interval was preferred to use to grasp the incremental change of the flood water depth in main channel and the flood plain. Rating curves were used to generate a continuous daily time series of discharges from daily observed river stages for the years where daily data were not available. The general equation of the rating curves developed by (Kennedy, 1984) is used in this study is shown in Equation (4.1),

$$Q = C[h - a]^n \tag{4.1}$$

Where, Q = discharge, C and n = constants, h = river stage and a = river stage at which discharge is zero.

Water Level Data

The water level data of Jamalpur (SW 225), Mymensingh (SW 228.5), Toke (SW229), Bhairab Bazar (SW230.1) and Bhairab Bazar (SW 273) are collected from BWDB for the year 1986-2017. These water level data are used for defining the downstream boundary of the hydrodynamic models and calibrating and validating the models as well. The collected water level data were in daily intervals.

DEM

A digital elevation model (DEM) is a digital model or 3D representation of a terrain's surface, created from terrain elevation data. A DEM can be represented as a raster (a grid of squares, also known as a height map when representing elevation) or as a vector-based triangular irregular network (TIN). This data is required to formulate computational mesh of 2D flow area. Each cell, and cell face, of the computational mesh of 2D flow area is pre-processed in order to develop detailed hydraulic property tables based on the underlying terrain used in the modeling process (Brunner, et al., 2015). In this study, the Shuttle Radar Topographic Mission (SRTM) Digital Elevation Model (DEM) of 90m resolution has been collected from USGS Earth Explorer

Satellite Image

For the purpose of comparison between model simulated flood map and observed flood map, Sentinel-1 imagery showing flood Map, flood maps prepared by FFWC (Flood forecasting and Warning Center) and the generated flood maps by FFWC through flood model simulation have been collected.Sentinel-1 is the first of the Copernicus Programme satellite constellation conducted by the European Space Agency. This

mission is composed of a constellation of two satellites, Sentinel-1A and Sentinel-1B, which share the same orbital plane. They carry a C-band synthetic-aperture radar instrument which provides a collection of data in all-weather, day or night. This instrument has a spatial resolution of down to 5m and a swath of up to 400km. The constellation is on a sun synchronous, near-polar (98.18°) orbit. The orbit has a 12 day repeat cycle and completes 175 orbits per cycle.

4.7 Assessment of Future Flow Availability of Brahmaputra River Basin for RCP 8.5 Scenario

4.7.1 Selection of RCP Scenarios

A Representative Concentration Pathway (RCP) is a greenhouse gas concentration trajectory adopted by the IPCC for its fifth Assessment Report (AR5) in 2014 that suggested four pathways for climate modeling and research describing different climate futures. The four RCPs are named: RCP2.6, RCP4.5, RCP6 and RCP8.5. They are labeled after a possible range of radiative forcing values in the year 2100 relative to pre-industrial values which are +2.6, +4.5, +6.0, and +8.5W/m^2 respectively. RCP 2.6 assumes that global annual GHG emissions measured in CO2-equivalents peaks from 2010 to 2020 with emission declining substantially thereafter. Emissions in RCP 4.5 peak around 2040 then decline. In RCP 6, emissions peak around 2080 then decline. In RCP 8.5, emissions continue to rise throughout the 21st century (Meinshausen, et al., 2011) as shown in Figure 4.9. In this study, RCP 8.5 has been selected being the pessimistic high emission scenario among the 4 scenarios adopted by the 5th assessment report of IPCC (IPCC, 2014).
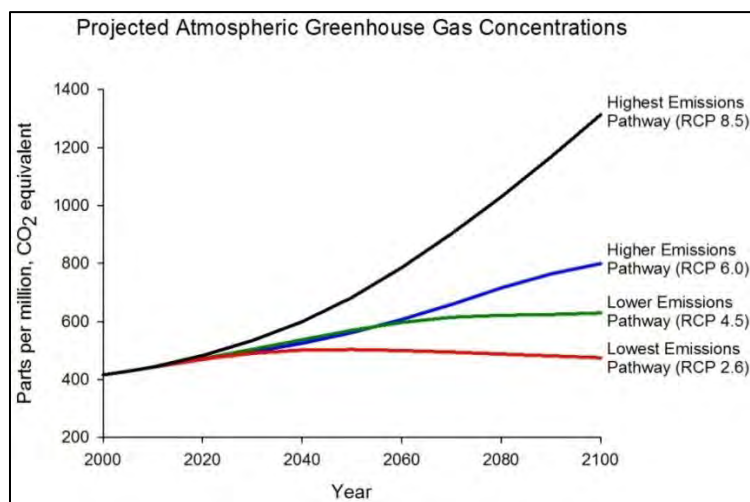
Figure 4.9: Projected Atmospheric Greenhouse Gas Emissions for the four RCP Scenarios

4.7.2   Selection of RCP Model for RCP 8.5 Scenario

From Coordinated Regional Climate Downscaling Experiment (CORDEX)-South Asia domain database, an 11 member ensemble from 3 regional climate model (RCM) forced by eight general circulation model (GCM) were collected and analyzed by IWFM, BUET. Precipitation obtained from different ensembles was then averaged for three periods such as 2010-2039 (2020s), 2040-2069 (2050s) and 2070-2099(2080s) and for the periods the changes of the precipitations from the baseline to the end of the 21st century have been assessed as shown in Table 4.3. Model giving the highest positive and negative change in precipitation were selected as the wettest and driest condition in future respectively. The model giving the nearest change in precipitation to middle value represents moderate wet scenario (Haque et al, 2018). The output of this analysis was reviewed in this study to choose the specific model for generating future flow for the study area. For RCM SMHI-RCA4 forced by GCM IPSL-CM5A-MR the percentage increase in precipitation are 11.81, 15.4 and 33.53 for 2020s, 2050s and 2080s respectively those were highest among all the models. That is why the IPSL-CM5A-MR_SMHI-RCA4 model has been selected as the wettest consideration in which highest precipitation will occur in future enhancing the probability of floods in the Brahmaputra river basin.

Table 4.3: Selection of RCM for Climate impact analysis on discharge and flood events*

Selected RCMs	Time regime			Condition
	2020s	2050s	2080s	
MPI-M-MPI-ESM-LR_MPI-CSC-REMO2009	-0.74	-0.93	-8.93	Driest
ACCESS1-0_CSIRO_CCAM_1391M	0.92	0.45	-2.40	
CNRM-CM5_CSIRO-CCAM-1391M	0.78	-2.58	-2.22	
MPI-ESM-LR_CSIRO-CCAM-1391M	-0.86	-0.15	-1.43	
CCSM4_CSIRO-CCAM-1391M	-1.26	-1.63	-0.33	
MPI-M-MPI-ESM-LR_SMHI-RCA4	0.39	6.97	12.13	Moderate Wet
NOAA-GFDL-GFDL-ESM2M_SMHI-RCA4	1.29	7.56	15.24	
CNRM-CERFACS-CNRM-CM5_SMHI-RCA4	3.47	10.19	18.9	
ICHEC-EC-EARTH_SMHI-RCA4	8.53	15.23	23.09	
MIROC-MIROC5_SMHI-RCA4	8.94	18.12	27.06	
IPSL-CM5A-MR_SMHI-RCA4	**11.81**	**15.4**	**33.53**	**Wettest**

*Source: Haque et. al (2018)

4.7.3   Assessment of Future flow of Brahmaputra River Basin

Using the precipitation data of RCM SMHI-RCA4 forced by GCM IPSL-CM5A-MR, an already calibrated and validated hydrological model of Brahmaputra River Basin in HEC-HMS by Haque et. al. (2018) has been used to obtain the future flow for 2020s, 2050s and 2080s for RCP 8.5 scenario. The selected domain for the hydrologic model is the whole Brahmaputra basin considering the Bahadurabad transit as the basin outlet as shown in Figure 4.10.
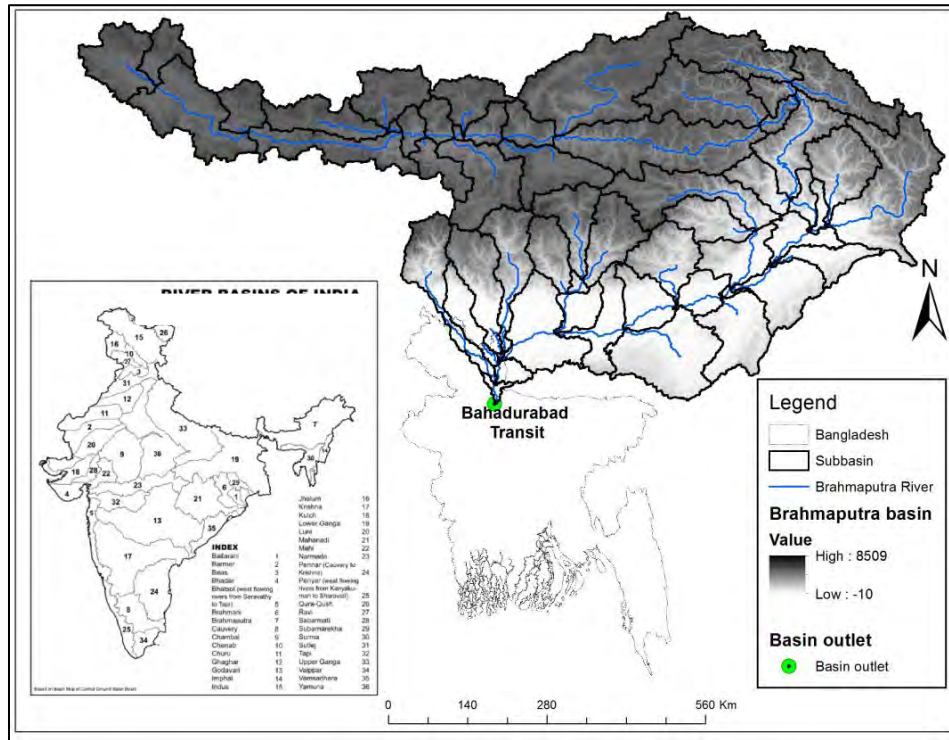
Figure 4.9: Study Area of the hydrological model of Brahmaputra River Basin in HEC-HMS

This model has been set up using 90 m resolution DEM of the year 2003 from Shuttle Radar topography Mission (SRTM) website of CGIAR-CSI GeoPortal, land cover map of 500m resolution from USGS (United State Geological Survey) which is a product of 0.50km MODIS based Global Land Cover analysis based on images of 2001 to 2010 and digital soil map of scale 1:5000000 of year 2007 from FAO. Meteorological data including precipitation, average temperature, solar radiation, relative humidity and wind speed have been used from NASA-Prediction of Worldwide Energy Resource for the climate normal period of (1983-2010). Discharge data for the calibration and validation was obtained from Bangladesh Water Development Board (BWDB). The developed hydrologic model of Brahmaputra river basin was calibrated for the time range of 1983-1996 and validated for 1997-2010. The values of NSE, PBIAS and RSR for the calibration and validation period were 0.65, -20.92, 0.59 and 0.54, -23.40, 0.68 respectively

depicting satisfactory matching of the simulated and observed data (Haque et.al., 2018). To predict the future flow at the Bahadurabad transit of Brahmaputra-Jamuna river basin, predicted data of precipitation corresponding to the wettest scenario of RCP 8.5 were fed into the validated model of Brahmaputra river basin in HEC HMS. The future flow hydrographs of Bahadurabad Transit (SW 46.9L) of Brahmaputra basin for baseline period (1976-2100), early century (2020s), mid-century (2050s) and late century (2080s) for the RCP 8.5 scenario are shown in Figure 4.11. The hydrographs show that the future flow for the 2080s of RCP 8.5 scenario is significantly higher comparing with the baseline period during the months of monsoon.
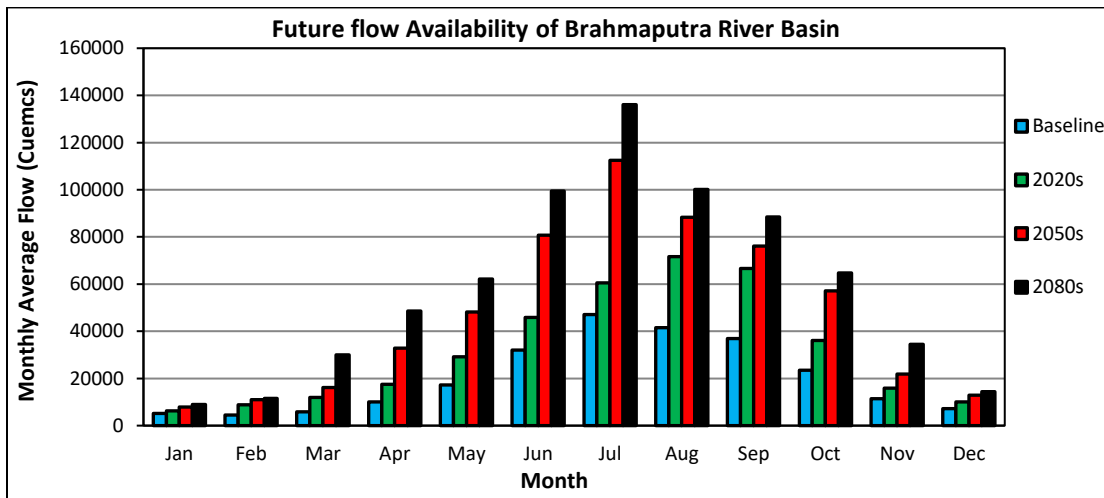
Figure 4.10: Flow availability of Brahmaputra River Basin at Bahadurabad Transit (SW 46.9L) for IPSL-CM5A-MR_SMHI-RCA4 model of RCP 8.5 scenario

4.8 Establishing Relationship between the Flow of Brahmaputra and Old Brahmaputra River

The Old Brahmaputra is one of the main distributaries of the Brahmaputra-Jamuna River that takes off from the left-bank of Brahmaputra River. Presently, though the mouth of Old Brahmaputra River is being dried up due to heavy siltation in the vicinity of the offtake (Noor, 2013), it receives significant amount of flow from Brahmaputra River during flood season causing flood in downstream reach. Thus the flow in the river Brahmaputra affects the inflow to the Old Brahmaputra from offtake following similar trend of rise and fall in the water level as well. In this study an attempt has been taken to establish a relationship between the flows at Mymensingh (SW 228.5) of Old Brahmaputra River with the flow at Bahadurabad (SW 46.9L) of mighty Brahmaputra-Jamuna River using the concept of linear regression analysis. The locations of the discharges considered are shown in Figure 4.12.
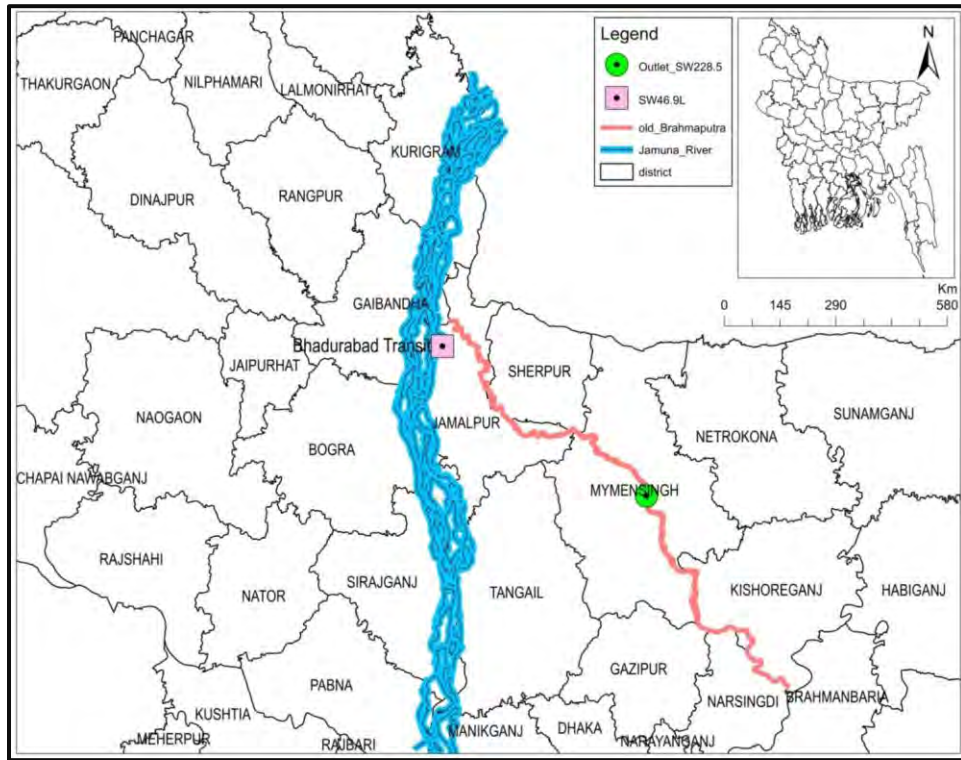
Figure 4.11: Map showing the locations of flow for linear regression analysis

For the development of regression equation, the time series discharge data of Bahadurabad transit (SW 46.9L) and Mymensingh (SW 228.5) have collected from 1966 to 2017 from Bangladesh Water Development Board. Then, a simple linear regression equation has been developed considering the flow at Mymensingh (SW228.5) of Old Brahmaputra River as the dependent variable (Y) and the flow at the Bahadurabad transit (SW46.9L) of Brahmaputra River as the independent variable (X). The equation forms an equation of the straight line looking like Equation 4.2.

$$Y_i = \beta_0 + \beta_1 X_i \tag{4.2}$$

Where Yi is the dependent variable, Xi is the independent variable, β_0, β_1 are the coefficients and the equation is termed as correlation equation. Correlation analysis is used to describe strength and direction of linear relationship between two variables represented by the Pearson's correlation coefficient, r. The extreme values of r, that is, when $r = \pm 1$, indicate that there is perfect (positive or negative) correlation between the variables and if r is 0, we say that there is no or zero correlation. The ranges of the Pearson's correlation coefficient, r and its significance in defining the type of correlation are represented in Figure 4.13 (Akoglu H., 2018). Correlation analysis on the flows of the two rivers in SPSS show that is positive

correlation between the flows of two locations which means that when the flow at Bahadurabad increases, flow at Mymensingh (SW228.5) of Old Brahmaputra River increases.
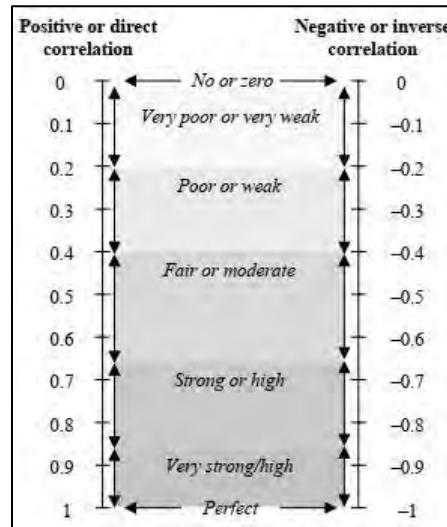
Figure 4.12: Ranges of Pearson's correlation coefficient and its significance

Bangladesh has a subtropical monsoon climate characterized by wide seasonal variation in rainfall, moderately warm temperatures with high humidity. Regional climatic differences in this flat country are minor. Four meteorological seasons are recognized as- pre-monsoon/Summer (March, April and May), monsoon (June to September), post-monsoon (October and November) and winter (December, January and February) (Khatun et.al., 2016). Generally, Pre-monsoon months are hot and humid; monsoon months are humid and rainy, post-monsoon months are quiet hot and dry but the winter months are cool and dry (Khatun et.al., 2016). To capture the variability in flow volume in establishing the regression relationship between the flows, 4 different regression equations have been developed for each of the seasons.

Figure 4.14 (a), (b),(c) and (d) shows the correlation graphs of the flow at Mymensingh (SW 228.5) of Old Brahmaputra River knowing the future flow at Bahadurabad transit (SW 46.9L) of mighty Brahmaputra-Jamuna River for the four seasons around a year and Table 4.4 represents the Pearson's correlation coefficient obtained for each season. The performance of this equation has been assessed through Pearson's correlation coefficient, r and P value in SPSS. The values of the correlation coefficient are within 0.64 to 0.78 implying fair to strong correlation. The P value is found less than 0.001 which proves statistical significance of the regression equation as well.

Statistical Relation between Brahmaputra river and Old Brahmaputra River in Monsoon

$y = 0.0366x - 531.96$
$R^2 = 0.612$

(a)

Statistical Relation between Brahmaputra river and Old Brahmaputra River in Post Monsoon

$y = 0.0233x - 195.45$
$R^2 = 0.5019$

(b)

Statistical Relation between Brahmaputra river and Old Brahmaputra River in Summer

$y = 0.0079x - 38.939$
$R^2 = 0.5297$

(c)
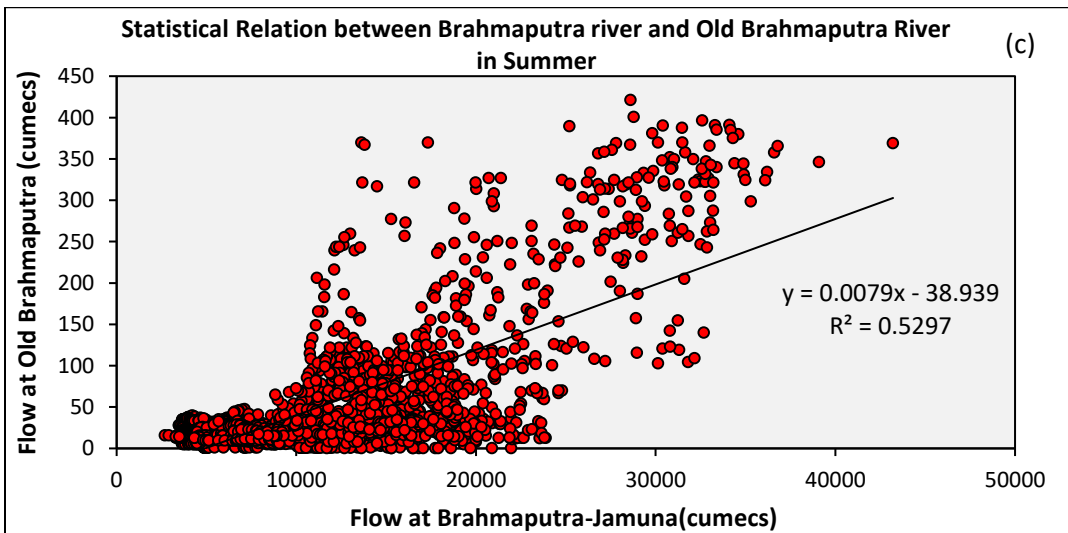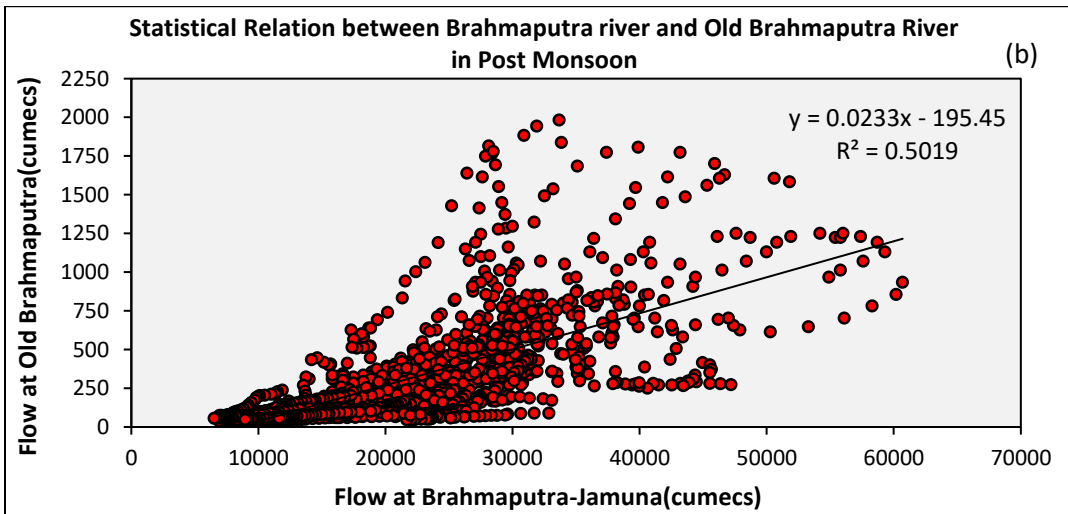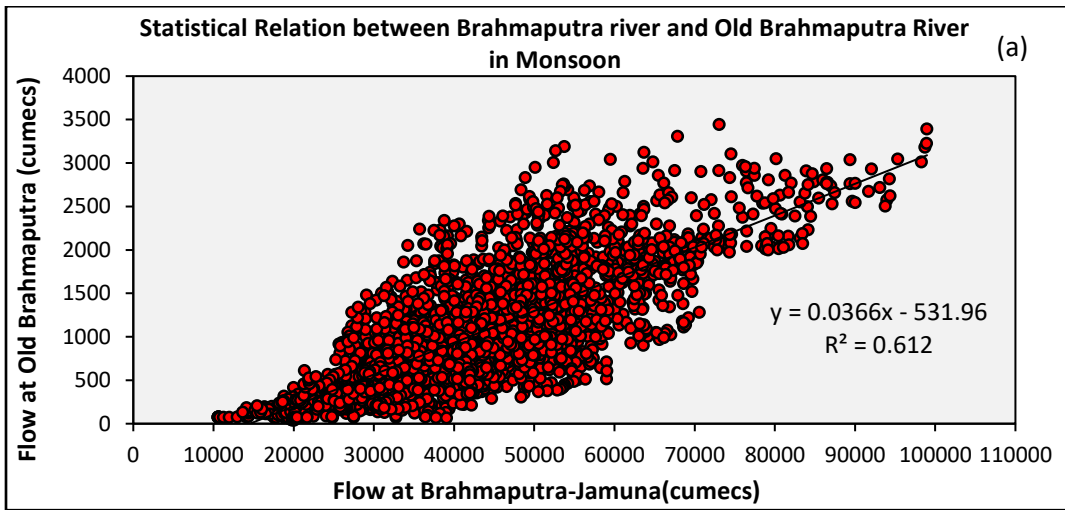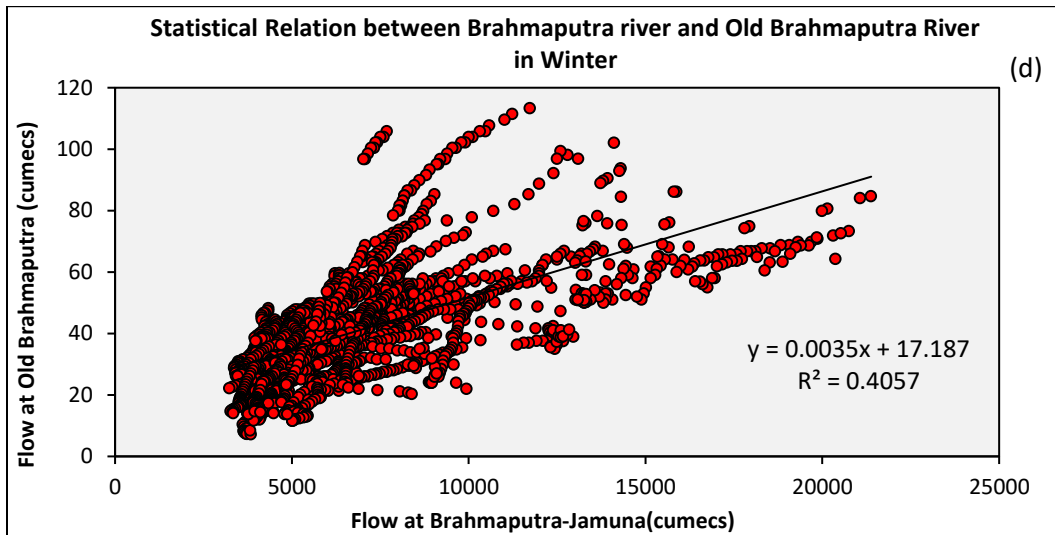
Figure 4.13: correlation graphs of the flow at Mymensingh (SW 228.5) of Old Brahmaputra River for (a) Monsoon Season, (b) Post-Monsoon Season (c) Summer season and (d) Winter season

Table 4.4: Pearson's correlation coefficients and performance rating of regression equations

Season	Regression Equation	Pearson's correlation coefficient, r	Correlation Type
Summer (March, April and May)	$Q_{Old\ Brahmaputra} = 0.0079 * Q_{Brahmaputra-Jamuna} - 38.939$	0.73	Strong/High
Monson (June to September)	$Q_{Old\ Brahmaputra} = 0.0366 * Q_{Brahmaputra-Jamuna} - 531.96$	0.78	Strong/High
Post Monsoon (October and November)	$Q_{Old\ Brahmaputra} = 0.0233 * Q_{Brahmaputra-Jamuna} - 195.45$	0.70	Strong/High
Winter (December, January and February)	$Q_{Old\ Brahmaputra} = 0.0035 * Q_{Brahmaputra-Jamuna} - 17.178$	0.64	Fair/Moderate

The developed regression equations were then used to generate the flow for baseline and future at Mymensingh (SW 228.5) of Old Brahmaputra River knowing the averaged future flow at Bahadurabad transit (SW 46.9L) of mighty Brahmaputra-Jamuna River from the hydrological modeling. It is hoped that the regression equation would produce representative future flow for the Old Brahmaputra River as there is no other tributary and distributary in this part of Brahmaputra River except the Old Brahmaputra River. The generated synthetic flow hydrographs for the base, 2020s, 2050s and 2080s are then used as the boundary condition of the calibrated and validated 1D-2D coupled model Old Brahmaputra River to simulate the flood scenario for the base, 2020s, 2050s and 2080s respectively. Figure 4.15 shows flow

availability of Old Brahmaputra River at Mymensingh Sadar (SW 228.5) for the base period, 2020s, 2050s and 2080s of IPSL-CM5A-MR_SMHI-RCA4 model of RCP 8.5 scenario.
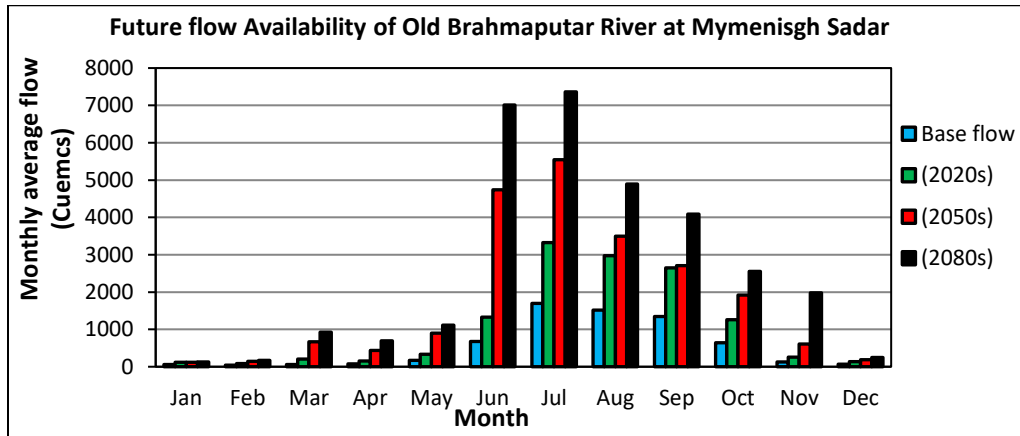
Figure 4.14: Flow availability of Old Brahmaputra River at Mymensingh Sadar (SW 228.5) for the base period, 2020s, 2050s and 2080s of IPSL-CM5A-MR_SMHI-RCA4 model of RCP 8.5 scenario

4.9   Set up of 1D-2D Coupled Hydrodynamic model of Old Brahmaputra River and Surrounding Floodplain

4.9.1   Processing of Digital Elevation Model (DEM)

To start with, the Digital Elevation Model (DEM) of Bangladesh in the geographical coordinate system (GCS_WGS_1984) was collected from the FTP server of the Shuttle Radar Topographic Mission (SRTM) of USGS Earth Explorer. Geographic coordinate system indicates location using longitude and latitude based on a sphere (or spheroid) while projected coordinate systems use easting and northing values based on a plane. The collected DEM data of Bangladesh then transformed to a projected coordinated system named as Bangladesh Transverse Mercator (BTM) which comprises of a resolution of 90m x 90m. The elevation values of the cells of collected DEM belong to the reference of mean sea level (MSL). In this study all the elevations including topography of river cross sections and water surface elevation have been measured considering the Public Work Datum (PWD) as reference. PWD is a horizontal datum that is approximately 1.5 ft. below the MSL established in India under the British Rule and brought to Bangladesh during the Great Trigonometric Survey. To adjust this difference in elevation, an elevation of 1.5ft (0.46m) is added to the collected DEM of Bangladesh.

The study area includes 31 upazilla of 4 districts surrounding the lower reach of the Old Brahmaputra River. To replicate the actual flooding scenario of the study area a wider rectangular shapefile including

the study area inside has been created to clip the area from the DEM which is going to be used as the 2D model domain. The processed and clipped DEM of the model domain including the study area is shown in Figure 4.16.
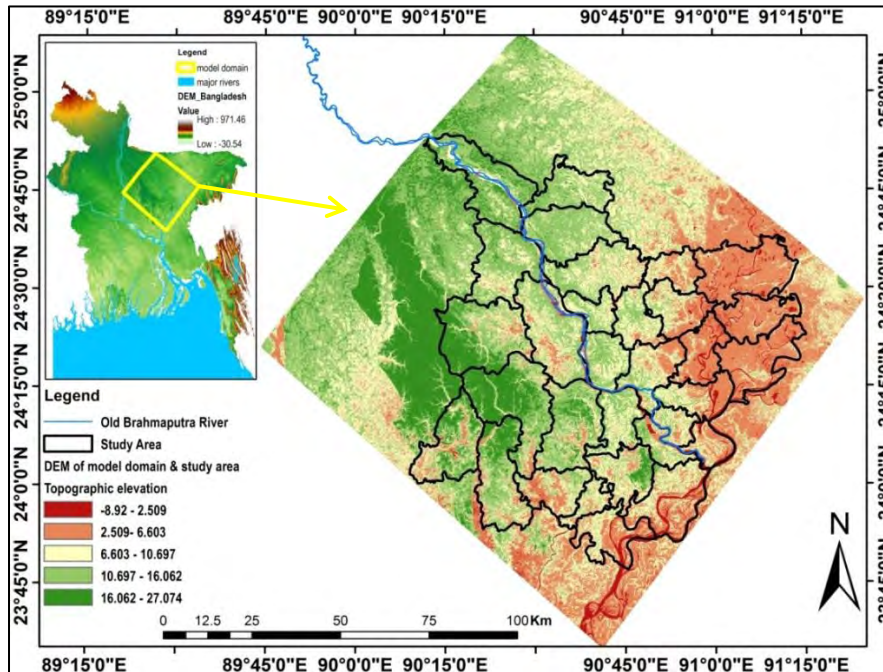
Figure 4.15: Processed and clipped DEM of the model domain and Study Area

4.9.2 Pre-processing in HEC-GeoRAS

HEC-GeoRAS, an ArcGIS extension is specifically designed as a pre-processing (preRAS) and post-processing (postRAS) tool of HEC-RAS to process geospatial data for the use in HEC-RAS. This extension allows user to create a file containing geometric attributes from an existing Digital Terrain Model (DTM) and complementary dataset. Water surface profile results may also be processed to visualize inundation depths and boundaries. However, HEC-RAS 5.0 is capable of processing the results of the 2D and 1D-2D coupling in newly added RASMapper tool of HEC-RAS. As this study is focused on 1D-2D coupling, HECGeoRAS is hereby used to process the input details of 1D bathymetry only.

At first, the lower reach Old Brahmaputra River having a length of around 130 km has been drawn by using the stream centerline layer starting from the upstream end and working downstream following the plausible thalweg of the channel. Then the riverbanks were drawn under specific layer that separate the main channel from the overbank areas when flooding occurs. There are precisely two bank lines per cross section and therefore defined them as left and right bank considering the direction of flow. Thereafter

comes the drawing of flow Path Centerlines that are used to identify the hydraulic flow path in the left overbank, main channel and right overbank. Creating the flow path centerline layer assists in setting the cross-sectional cut lines correctly. In this case, river centerline has been copied for the flow path in the main channel. All flow paths (left overbank main channel and right overbank) are drawn from upstream to downstream extending each of the cross-sections. The flow paths are used to derive downstream reach lengths in HEC-RAS. Once the digitization of the flow paths was completed, each flow path is identified as a left, right or channel flow path. The channel is the flow path along the center of the river channel and the left and right flow path are identified considering the direction of flow as well.

After that, Cross Section Cut Lines are drawn representing the location, position and expanse of the river cross sections. This theme will identify the planar location of the cross sections and the station elevation data being extracted from the DTM along each cut line for use in HECRAS. During drawing, cross-sectional cut lines must be pointed from the left overbank to the right overbank looking downstream. Cross-sectional cut lines must cross each of the three flow paths and the two banks exactly once and should be perpendicular to the direction of flow not intersecting each other. Forty seven cross-section locations were chosen for the river reach within study area and drawn according to the morphological station position of BWDB and IWM.

After digitizing centreline, bankline and flowpath, all the data such as topology, length/stations and elevations need to be extracted. For this reason, all the above mentioned features are extracted from the "Stream Centerline Attributes" menu of RAS Geometry toolbar. It is also vital to ensure that all the cross-section data are correctly extracted. To complete this, all features such as River/Reach, Stationing, Bank stations, Downstream Reach Length, Elevations are extracted from the "XS Cut Line Attributes'' of RAS Geometry toolbar. In this phase, the 2D feature class of XS Cut Lines is intersected with the TIN to create a feature class with 3D cross section. The generation of the HEC-RAS import file is the last step of the HEC-GeoRAS preprocessing. In this phase, an HEC-RAS input file is created in RAS Import format which includes the terrain elevation extracted from the TIN, the 3-D stream centerline and the 3-D cross-sections themes as z values (z value is the elevation above public work datum and, for our case, is in units of the meter). The "Extract GIS DATA" is clicked under the menu "RAS Geometry" from the HEC-GeoRAS toolbar. The default name GIS2RAS is accepted and saved in the selected folder. Figure 4.17 shows the river centerline, bank lines, flow paths and cross-section cut lines with the TIN of the model domain.
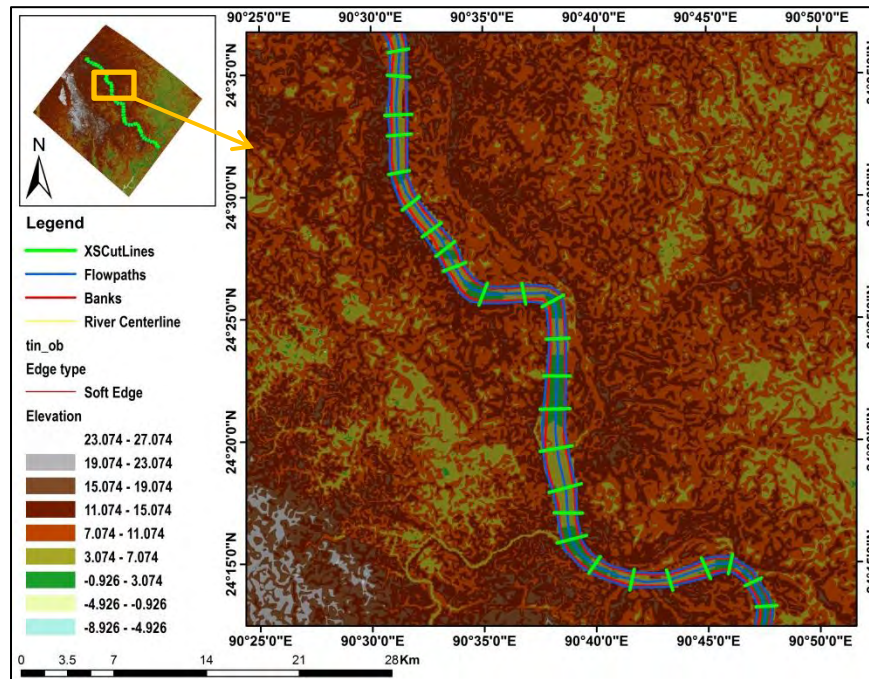
Figure 4.16: River centerline, bank line, flow paths & cross-section cutlines of TIN of model domain

4.9.3   Processing in HEC-RAS

The GIS format of the Old Brahmaputra River bathymetry processed in HECGeoRAS has been incorporated in the Geometry Data window of HEC-RAS. Initially, the geometry data includes the elevation of the TIN from which it has been processed in HEC-GeoRAS. Later, the bathymetry data of 47 available cross-sections of the Old Brahmaputra River within the study area for 2016-17 collected from BWDB and IWM has been incorporated in the cross-section data and the roughness values of the river is incorporated at each cross section manually. After preparing the 1D river bathymetry, the DEM of the model domain is added using the new terrain layer tool of RAS-Mapper which converts this DEM file into the terrain layer of GeoTIFF (*.tif) file format under the projected coordinate system of BTM. Then to replicate the surrounding floodplain of the Old Brahmaputra River, 2D Flow area is defined by laying out a polygon on both side of the main river channel following the Terrain boundary and named as left and right respectively. A mesh of 500m×500m grid resolution has been defined for each of the 2D flow areas and initially Manning's roughness, n=0.06 has been proposed for the 2D flood plains. To connect the 1D river reach to the 2D storage areas and generate lateral movement of water from the main channel to floodplain, lateral structure has been provided at the left and right overbank area spanning the whole reach.

After processing the bathymetry and flood plains of the 1D-2D coupled model of Old Brahmaputra boundary conditions are to be provided for making the model ready to simulation. In this study, data on discharge hydrograph of Mymensingh Sadar (SW 228.5) and water level hydrograph of Bhairab Bazar (SW 230.1) are being used as upstream and downstream boundary conditions. The upstream discharge boundary and downstream water level boundary condition for initial simulation of the year 2017 to be used for calibration and validation are shown in Figure 4.18.
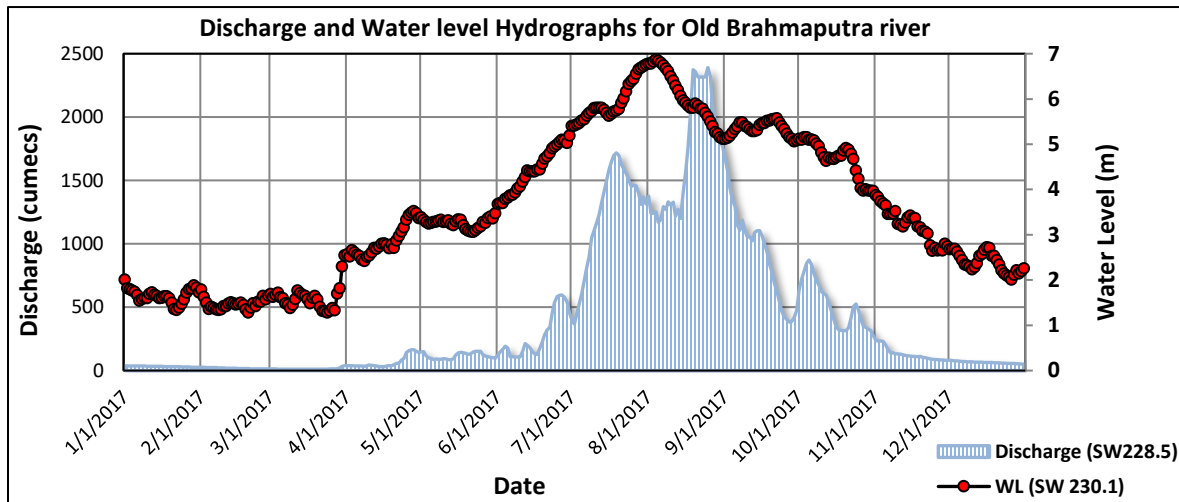
Figure 4.17: Boundary conditions for Old Brahmaputra River for year 2017

Boundary conditions have also been applied to the 2D flow areas to replicate actual life flood water flow scenario of the surrounding floodplain of the selected reach of Old Brahmaputra river. There are 5 peripheral boundaries incorporated in the model of the study area. Out of which the total 5, two inflow boundaries are provided at the upstream point just left and right of the left and right overbank to consider the inflow from mighty Brahmaputra Jamuna River and overland flood water flow from upstream. Certain percentage of the discharge data of Old Brahmaputra River has been used in this regard. At the downstream location of model domain, Surma-Meghna River meets the Old Brahmaputra at Bhairab Bazar thus sharing the floodplain. To represent the lateral spill of flow from Meghna River that causes flood to the shared floodplain, a certain percentage of the discharge of Meghna River has provided at the downstream region of the left 2D area. The above discussed boundaries are inflow boundaries. After meeting Old Brahmaputra River, Meghna river flows further downstream carrying significant volume of flood water to meet the Padma River. Thus to address the outflow of water from the Meghna river, a boundary has been provided at the downstream location of the right 2D area. Normal depth has been used as the boundary type to represent the outflow from the model domain at downstream region. Furthermore, the Lakhya River takes off from the Old Brahmaputra River at around 80km from the upstream of the

selected model domain. To represent this outflow from the floodplain, discharge data of Lakhya River has been used at the two third length of the model boundary of right 2D flow area. Boundary locations of the 2D flood plain of the model has been shown in Figure 4.19 showing the inflow and outflow boundaries.
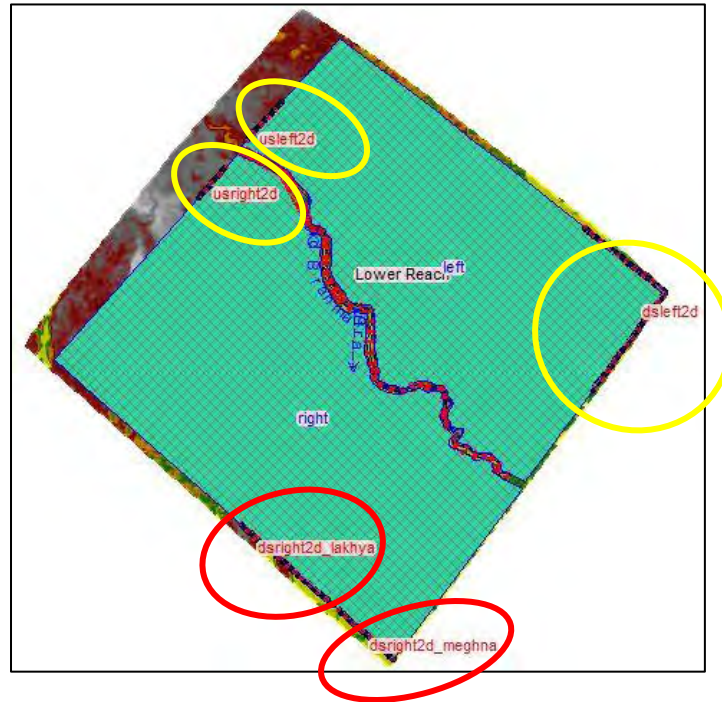
Figure 4.18: Upstream and Downstream boundary condition for 2D flow area

After the processing of geometry and providing the boundary condition the model has been simulated for the year 2017 initially. Then the simulated model has been repeatedly simulated for several times by changing the manning's roughness of the main channel and flood plain to match the simulated water level with observed water level at an intermediate location.

4.9.4   Calibration and Validation of Hydrodynamic model:

Calibration is the process whereby selected parameters and variables of the model are adjusted to make the model output match observations. In this study, simulated water level obtained from the model has been compared with the observed water level at the intermediate location named as Toke between the boundaries to calibrate and validate the developed model. To simulate the model with base and different flow conditions, it is necessary to test the model's capability to replicate the real life flow dynamics. The calibration of hydrodynamic model generally includes the finding of an appropriate value of roughness coefficient (Manning's 'n') such that simulated values from the model should be close to the observed values in the river (Timbadiya, et al., 2011). Thus manning's roughness, n has been used as the calibration parameter of the 1D channel in this study. To calibrate and validate the inundation, simulated inundation

extent obtained from simulation was compared with the inundation map of FFWC. To reproduce the closest approximation of the actual inundation depth, mean inundation depth for each upazilla within the study area obtained from the model simulation was compared with the averaged inundation depth of the upazillas obtained from the processed inundation RASTER file took from FFWC. Model validation involves testing of the calibrated model with a different set of data for both the 1D channel and 2D floodplain.

4.9.5   Performance Evaluation of the developed 1D-2D Coupled model of Old Brahmaputra River

Some of the model performance evaluation technique includes Coefficient of Determination (R^2), RMSE, MAE, MSE, NSE, RSR and PBIAS etc. In this study, to evaluate the performance of the developed 1D-2D coupled hydrodynamic model of Old Brahmaputra River, widely used quantitative statistical performance indicators named Coefficient of Determination (R2), Coefficient of Nash-Sutcliffe Efficiency (NSE), PBIAS and RSR have been used for comparison of simulated output graph with the observed data.

Coefficient of Determination (R^2)

The coefficient of determination is the proportion of the variance in the dependent variable that is predictable from the independent variable(s). It provides a measure of how well-observed outcomes are replicated by the model, based on the proportion of total variation of outcomes explained by the model. It is denoted as R^2. For a simple linear regression r^2 is used instead of R^2 where r^2 is simply the square of the sample correlation coefficient (i.e., r) between the observed outcomes and the observed predictor values and can be obtained from Equation 4.3.

$$r = \frac{n(\Sigma xy) - (\Sigma x)\Sigma y}{[n\Sigma y^2 - (\Sigma y)^2]\sqrt{[n\Sigma x^2 - (\Sigma x)^2]}}$$
(4.3)

Nash Sutcliffe Efficiency (NSE)

The Nash- Sutcliffe Efficiency (NSE) determines the relative magnitude of the residual variance compared with the measured data variance (Nash and Sutcliffe, 1970) as a normalized statistic.

$$\text{NSE} = 1 - \left[\frac{\Sigma_{i=1}^{n}\left(y_i^{obs} - y_i^{sim}\right)^2}{\Sigma_{i=1}^{n}\left(y_i^{obs} - y_i^{mean}\right)^2}\right]$$
(4.4)

Where, y_i^{sim} is the simulated value and y_i^{obs} is the observed value, y_i^{mean} is the mean value of the data set and n is the total number of observations.

Percent BIAS (PBIAS)

Percent bias measures the average tendency of the simulated data to be larger or smaller than their observed counterparts. The optimal value of PBIAS is 0 with low magnitude values indicating accurate model simulation. Positive value indicates model underestimation bias and negative value indicates model overestimation bias (Gupta et.al., 1999).

$$\text{PBIAS} = \left[\frac{\Sigma_{i=1}^n \left(y_i^{obs} - y_i^{sim}\right) * 100}{\Sigma_{i=1}^n \left(y_i^{obs}\right)} \right] \tag{4.5}$$

RMSE- observations standard deviation ratio (RSR)

RMSE is one of the commonly used error statistics that is calculated as the ratio of the root mean square error (RMSE) and standard deviation of the measured data.

$$\text{RSR} = \frac{RMSE}{STDEV_{obs}} = \frac{\left[\sqrt{\Sigma_{i=1}^n \left(y_i^{obs} - y_i^{sim}\right)^2} \right]}{\left[\sqrt{\Sigma_{i=1}^n \left(y_i^{obs} - y_i^{sim}\right)^2} \right]} \tag{4.6}$$

Table 4.5 shows the general reported rating of R, NSE, PBIAS and RSR.

Table 4.5: General reported rating of model performance evaluation technique*

Performance Rating	R	NSE	RSR	PBIAS
Very Good	$R^2 > 0.70$	$0.75 < NSE \leq 1.00$	$0.00 \leq RSR \leq 0.50$	$PBIAS < \pm 10$
Good	$0.5 < R^2 \leq 0.70$	$0.65 < NSE \leq 0.75$	$0.50 < RSR \leq 0.60$	$\pm 10 \leq PBIAS < \pm 15$
Satisfactory	$0.50 < R^2 \leq 0.3$	$0.50 < NSE \leq 0.65$	$0.60 < RSR \leq 0.70$	$\pm 15 \leq PBIAS < \pm 25$
Unsatisfactory	$R^2 \leq 0.30$	$NSE \leq 0.50$	$RSR > 0.70$	$PBIAS \geq \pm 25$

*Source: Haque et al, 2018

4.9.6   Assessment of Flood Inundation Depth, Flood Flow Velocity and Inundation Area

The inundation depth and flood flow velocity for the model domain are exported directly from RAS-Mapper as RASTER file based on the terrain. Inundation area for the model domain has been exported from RAS-Mapper as polygon type of vector feature. The raw exported files on flood inundation depth,

flood flow velocity and inundation area from RAS-Mapper includes the values of the parameters on the 2D flood plains as well as the main 1D river channel. As the depth, velocity and inundation extent of the 1D river channel do not contribute in flood induced hazard and risk the river portion need to be excluded from the RASTER and vector files of the depth, flood flow velocity and inundation boundary. This is done by clipping out the RATER and vector files with the polygon shapefile of the Old Brahmaputra River digitized from the Google earth during the lean flow season of the year 2017. Then the zone wise values of the three flood parameters were obtained using zonal statistics tool of ArcGIS.

4.10   Classification of Flood Inundation and Flood Flow Velocity

In this study flood inundation depth are classified into five classes: F0 (0-0.3 m), F1 (0.3 m- 0.9 m), F2 (0.9 m-1.8 m), F3 (1.8 m-3.6 m) and F4 (>3.6 m). This inundation classification is developed by the National Water Management Plan (NWMP) and used by numerous flood related studies of Bangladesh (Tazin, 2018; Rouf, 2015; IWM, 2014; DDM, 2016). Flood flow velocity is generally presumed to influence flood induced damage particularly of infrastructures like unpaved roads, railways and residential buildings and houses even if the magnitude seems low (Kreibich et.al., 2009). Therefore the classification of the flood flow velocity should span small incremental ranges. In this study, flood flow velocities of the study area are classified in five categories: V0 (0-0.15 m/s), V1 (0.15 m-0.3m/s), V2 (0.3 m-0.45 m/s), V3 (0.45 m-0.60 m/s) and V4 (>0.6 m/s).

4.11   Selection, Normalization and Weighing of Hazard Indicators

For the inclusive assessment of flood hazard, it is necessary to determine the most important parameters of the flooding events under consideration. There are several parameters which can have an important impact on flood hazard such as flood depth, flow velocity, time of occurrence of flood, inundation area and duration of flooding, flood return period, flow rate flood affected frequency and physical and other related statistical aspects of the actual flood. In this study, flood depth, flow velocity and inundation area represented as the percentage of an Upazilla inundated have been used as flood hazard indicators to assess the flood induced hazard for 31 Upazilla and the Old Brahmaputra river under the selected area.

Hazard assessment is concerned with the characterization of the nature, magnitude and timing of hazard. Thus the relative importance of the selected hazard indicators needs to be addressed. Weights are assigned to the flood depth, flood flow velocity and inundation area by Principal Component Analysis (PCA) and review of the available secondary literatures. Ibrahim et.al studied on the identification of vulnerable areas to floods in Kelantan River sub-basins by using flood vulnerability index in which flood depth and

67

inundation area were used as hazard indicators. Author proposed a weight of 0.7 for the flood depth and 0.3 for the inundation area (Ibrahim et.al, 2017). Amin et.al. (2017) studied on floodplain simulation for Musi River using integrated 1D/2D hydrodynamic model where flood depth and flow velocity were considered and flood depth obtained the greater weightage. In this study results on PCA using the normalized values of the flood hazard indicators supported the reviewed literatures. Flood depth received the greatest weight among three and the flood flow velocity was assigned with the smallest weight. To normalize the indicators following equation 4.5 has been utilized.

$$\text{Normalized score} = 1 + \frac{(100-1)*(\text{Actual value} - \text{Min})}{(\text{Max} - \text{Min})} \tag{4.7}$$

Using the weights and normalized value flood hazard for an Upazilla has been calculated using the equation 4.6.

$$\textbf{Flood hazard for an upazilla, } H = W_1 \times I_1 + W_2 \times I_{2+} W_3 \times I_{3+}\text{.......................}+ W_N \times I_N \tag{4.8}$$

Where W is the weight of the flood hazard indicator and I is the normalized value of the indicator.

4.12   Methodology of Vulnerability and Exposure Assessment

Bangladesh is highly vulnerable to the impact of climate change induced hazards like flood owing to its own unique geographic location, high population density & poverty rate, and overwhelming dependency on natural resources (Fung et al., 2006) causing loss of agricultural land, and ecological imbalance of the country. Owing to be a human enterprise, the socio-economic vulnerability is at the very heart of management practice strongly influencing mitigation measures of flood and related disasters (Anh et.al., 2012; McLaughlin et al., 2002). In this study, upazilla based assessment of socio-economic vulnerability and exposure for the present and future socio economic regime in the selected area have been assessed.

4.12.1   Selection of Domain for Vulnerability Assessment

Vulnerability of an area is influenced by several aspects including human condition, infrastructure and land use, social imbalances and economic pattern (Nasiri et.al., 2013). Consideration of different domains of vulnerability allows distinguishing their relative importance as well as relative contribution to the flood risk assessment (Jahan, 2018). In this study total eight domains have been considered for vulnerability assessment and exposure including population, gender, health, education, housing and infrastructure, land

use, economic and livelihood that have been used in the flood risk assessment by McLaughlin et al., 2002 and Jahan, 2018. Each domain includes few specific indicators that have been selected based on secondary literatures representing different components of exposure, sensitivity and adaptive capacity for vulnerability and risk assessment.

Population Domain and Indicators

Women, children, elderly and disabled people are more vulnerable compared to other people in times of natural hazards like flood (Flanagan et al., 2011; Cutter et al., 2003) since they are at a stage where there is greater reliance on others to get things done. In the case of children, they don't have knowledge of real world and the elderly people in spite of having knowledge become vulnerable due to physical restrictions (BBS, 2015). In this study, population domain consists of four indicators; social dependency ratio, ratio of disabled to able people, % Population aged between 10-60 year and floating population.

Gender Domain and Indicators

Women usually disproportionately suffer the impacts of disasters, severe weather events, and climate change because of cultural norms and the inequitable distribution of roles, resources, and power, especially in developing countries (BBS, 2015). The gender domain consists of one indicator named female to male ratio which is obtained from the data of sex ratio.

Education domain and indicators

Education domain focuses on the analysis of educational capacity for vulnerability assessment (Roy & Blaschke, 2015). Education and human resource development of a society is important for developing the community's adaptive capacity to face the adverse impacts of disasters. The illiterate group is more vulnerable to food insecurity due to lack of technological knowledge in farming and livelihood adaptations (BBS, 2015). The domain 'education' contains indicators such as 'adult literacy rate' and 'school attendance rate.

Housing and Infrastructure Domain and Indicators

The relationship that exists between poor housing and poor mental and physical health is well-documented (BBS, 2015). Indicators related to infrastructure include: number of total household; internal and external condition of household, cyclone and flood shelter, length of unpaved road and existence of electricity connection. Katcha and jhupri type of household structures are directly related to increased vulnerability providing minimum protection in natural hazards like storm surge, flood etc. as well as an indicator of

poor livelihood status (Laila, 2013). On the other hand cyclone and flood shelter along with providing shelter are used as school building throughout the year which is increasing literacy rate of the locality thus contributes in adaptive capacity (Jahan, 2018).

Economic Domain and Indicators

The economic condition of communities is an important determinant of how quickly communities can adapt or adjust to the effects of natural hazards (Roy & Blaschke, 2015). The indicators selected under this domain are crop productivity, poverty rate and % unemployed people. Higher cropping intensity reduces vulnerability by giving alternate cropping availability to the people after any natural disaster.

Livelihood Domain and Indicators

Livelihood domain refers to the potential of switching to alternative income-generating activities in disastrous situations. According to the local residents and stakeholders, communities with diverse economic activities are more able to adjust to the effects of natural disasters (Roy & Blaschke, 2015). The livelihood domain addresses available opportunities for vulnerable people to recover from the effects of disasters. In this study, livelihood domain consists of three indicators such as People engaged in Household Works, People engaged in Agriculture and People engaged in Industry and Service.

Land Use Domain and Indicators

In this study, livelihood domain consists of one indicator named Aman rice production area as the study area produces significant amount of Aman paddy during monsoon which is highly sensitive to the excessive and untimed flood water.

Health Domain and Indicators

Health domain is an important factor contributing towards socio-economic vulnerability. Health domain consists of four indicators: % household using tap water, % household using tube well water, % household using pond water, % household having sanitation facility, % household having no sanitation facility and number of hospitals and clinics for serving with healthcare facility.

4.12.2   Selection of Indicators for Vulnerability and Exposure Assessment

Selection of the indicators was guided by the prime considerations of what data is most appropriate to quantify the vulnerability and risk of the monsoon flood in particular and what data are available in all

previous census and statistical yearbooks at that spatial scale of interest so that using the previous census data future trend of the indicators can be estimated. The required data were collected from Household and Population Census, Agricultural Census and Statistical yearbooks for the available years from Bangladesh Bureau of Statistics (BBS). Classification of indicators into exposure and vulnerability was made based on literature review on journals, thesis papers and reports. Each 'Vulnerability' indicator falls into specific socio-economic domain. A total number of 25 indicators have been selected among which 14 are of sensitivity indicators and 11 remaining indicators contribute to the determination of adaptive capacity. The sensitivity indicators come up with the positive dependency on vulnerability assessment implying the fact that with the increase of the indicator's magnitude vulnerability gets increased whereas adaptive capacity indicators provide negative dependency on vulnerability indicating that as the indicator value increases resilience of a community towards hazard gets increased thus vulnerability of the community reduces. The categorization of the indicators in sensitivity and adaptive capacity has been done according to Cutter et al., 2008, Roy & Blaschke, 2015, Adhikary, 2015, Sarker, 2016, and Jahan, 2018. Table 4.6 represents the socio-economic indicators for vulnerability assessment across all Upazilla of the study area.

Table 4.6: List of the socio-economic indicators used for exposure and vulnerability assessment

Exposure	Vulnerability	
	Sensitivity	Adaptive Capacity
1.Population Density 2.Number of Household 3.Total Cropped Area	1.Floating population 2.Disable Population 3.Female to Male Ratio 4.Social Dependency Ratio 5.Poverty Rate 6.Unemployed people 7.People engaged in Household Works 8.People engaged in Agriculture 9. % Household (Kucca+ Jhupri) 10.Length of Unpaved Road 11.Aman Cropped Area 12.% Household of No Sanitation Facility 13.% Household using Pond Water 14.% Household using Tubewell Water	1.People engaged in Industry+ Service 2.No of Hospitals and Clinics 3.Literacy Rate 4.School Attendance Rate 5.% Household (Pucca and Semi-Pucca) 6. % Household using Tap Water 7. % Household having electricity connection 8. Cyclone and Flood Shelter 9. Crop Productivity 10.% Household having Sanitation Facility 11.% Population aged between 10-60 year

4.12.3   Normalization of indicators

The indicators for vulnerability assessment have different physical meaning. To eliminate differences in the units and dimensions of different process variables, data pretreatment is needed (Wang et.al, 2015). Four types of data pretreatment have been used in literature: (1) mean centering, (2) differentiation, (3)

normalization, and (4) auto-scaling (Amrhein et al., 1996).In this paper, to avoid the incommensurability of the units of individual indicators, normalization of data to a common comparable unit less scale (1 to 100) was performed. Normalization of individual variables provides a linear transformation preserving the ranking and correlation structure of the original data and allows the variables to be used together (Tran et al., 2010; Smith and Tran, 2003). For this study, normalization of each indicator was performed by using Equation 4.7.

4.12.4   Assigning Weights for Domains and Indicators of Vulnerability

The indicators need to assigned different weights to avoid the uncertainty of equal weighing given the diversity of indicators used (Jahan, 2018). Principal Component Analysis (PCA) has been employed to identify potential significance of the indicators of sensitivity and adaptive capacity and the eight domains for the assessment of vulnerability (Jahan, 2018). The technique of PCA has already been extensively applied in socioeconomic vulnerability assessments in regional, national and global level (Deressa et al., 2008; Abson et al., 2012, Piya et al. 2012; Borja-Vega and De la Fuente, 2013). The objective of PCA is to explain potential relations between a set of independent variables such as socio-economic indicators with a latent dependent variable which in our case is the vulnerability level of each upazilla. The indicators are tested for potential correlations with each independent variable (indicator), known as factor loadings which are equivalent to standardized regression coefficients (β weights) in multiple regressions (Beaumont, 2013). The components presenting eigenvalue higher than 1 are approved for explaining the independent indicators (Everitt and Hothorn, 2011, Abson et al., 2012). Weights are chosen to maximize the explained proportion of the variance in the original set of indicators. A potential limitation of PCA is the weighing importance in the selected variables. Some authors claim that the PCA may not reflect the higher significance that variables may possess. The introduction of experts' judgment (Kaly and Pratt, 2009), correlation with past disaster events and use of fuzzy logic (Eakin and Tapia, 2008) are some suggestions for the verification of weighing coefficient obtained from PCA. In our case, we have calculated the variances of each indicator under a specific domain with the standardized values. Each indicator within a domain and each domain have been assigned with weights as well depending on their relative importance by PCA as presented in Table 4.7. PCA of the indicators of population domain depicts that social dependency is the most dominating factor for determining population vulnerability than other indicators within the particular domain. No PCA was performed for the gender and land use domain as each of the two domains includes only one indicator. In the education domain, literacy rate got the greater weight that increases adaptive capacity of the people of a community. Within the housing and

72

infrastructure domain % pucca and semi-pucca household and % household having electricity connection received the highest and second highest weight as the housing facilities define the strength of a community. Condition of the roadways within the community is very important as it gives mobility to the people in times of emergency thus the indicator named length of unpaved road gets the third highest weight. Among the indicators of economic domain, crop productivity received maximum weight and poverty rate received the second highest weight as the indicator contributes significantly determining economic vulnerability. In livelihood domain, people involved in household works got the most weight. Within the health domain sanitation facility is the most dominant indicator as it contributes the community's strength and vice versa. PCA of the domains shows that the, livelihood, land use and economic domain received greater weightage comparing with other domains due to the fact that these indicators outline the ability of the community people to face and ease the hazardous impact of a natural disaster like monsoon flood.

Table 4.7: List of the Domain wise socio-economic indicators and their weights

Domain	Weight of Domain	Indicators	Indicator Weight
Population	0.120	Dependency Ratio	0.47
		Disable Population	0.43
		% Population aged between 10-60 year	0.02
		Floating population	0.08
Gender	0.105	Female to Male Ratio	1.000
Education	0.130	Literacy Rate	0.600
		School Attendance Rate	0.400
Housing and Infrastructure	0.110	% Household (Pucca and Semi-Pucca)	0.270
		% Household (Kucca+Jhupri)	0.100
		Cyclone and Flood Shelter	0.170
		Length of Unpaved Road	0.210
		% electricity connection	0.250
Economic	0.160	Poverty Rate	0.330
		Unemployed people	0.323
		Crop Productivity	0.347
Livelihood	0.165	People engaged in Household Works	0.358
		People engaged in Agriculture	0.328
		People engaged in Industry+ Service	0.313
Land Use	0.165	Aman Area	1
Health	0.046	% Household using Tap Water	0.200
		% Household using Pond Water	0.100
		% Household using Tubewell Water	0.115
		% Household having Sanitation Facility	0.265
		% Household of No Sanitation Facility	0.225
		No of Hospitals and Clinics	0.096

4.12.5 Assessment of Sensitivity, Adaptive Capacity and Vulnerability for present socio-economic condition

To assess the existing sensitivity, adaptive capacity and vulnerability of 31 upazillas under the selected area, data of all the indicators of sensitivity and adaptive capacity were normalized into 1–100 scale by Equation 1. In this study, vulnerability has been considered as a function of sensitivity and adaptive capacity where with the increase of sensitivity indicators vulnerability increases and with the increase of adaptive capacity vulnerability decreases and vice versa. Therefore the domain wise sensitivity value has been obtained by adding the weighted indicators under a specific domain and then the each domain has been multiplied by the assigned weight for that domain. Finally all the weighted domain wise sensitivity has been added up to obtain the total sensitivity value for each upazilla. Similar procedure has been followed for assessing the adaptive capacity value for all the upazilla and then vulnerability was obtained by deducting adaptive capacity value from the sensitivity. Formulae used for the calculation of sensitivity, adaptive capacity and vulnerability are as follows-

Domain wise Sensitivity, $Sd = WI_{S1} \times I_{S1} + WI_{S2} \times I_{S2} + WI_{S3} \times I_{S3} + \ldots\ldots\ldots + WI_{SN} \times I_{SN}$ (4.9)

Where, WI_S is the weight of the Sensitivity indicator and I_S is the Sensitivity indicator value under a specific domain.

Sensitivity for a upazilla, $S = D_1 \times Sd_1 + D_2 \times Sd_2 + D_3 \times Sd_3 + \ldots\ldots\ldots + D_N \times Sd_N$ (4.10)

Where, D is the weight of the domain and Sd is the sensitivity value of the domain.

Domain wise Adaptive Capacity, $Ad = WI_{A1} \times I_{A1} + WI_{A2} \times I_{A2} + WI_{A3} \times I_{A3} + \ldots\ldots\ldots + WI_{AN} \times I_{AN}$ (4.11)

Where WI_A is the weight of the Adaptive Capacity indicator and I_A is the Adaptive Capacity indicator value under a specific domain.

Adaptive Capacity for a upazilla, $A = D_1 \times Ad_1 + D_2 \times Ad_2 + D_3 \times Ad_3 + \ldots\ldots\ldots + D_N \times Ad_N$ (4.12)

Where D is the weight of the domain and Ad is the value of the Adaptive Capacity domain.

Vulnerability of upazilla, V = Sensitivity of upazilla, S - Adaptive Capacity of upazilla, A (4.13)

4.12.6 Assessment of Exposure for Present Socio-Economic Condition

Exposures are directly proportional to environmental risk due to climate change. Higher exposure value implies higher risk and vice versa. In this study three indicators have been selected for assessing the exposure of the study area i.e Population Density, No of Household and Total Cropped Area. PCA has also been adopted to assign weight to the indicators of exposure using the Statistical Package for the Social Sciences (SPSS) software. Among the three selected exposure indicators, Population density contributes more to risk followed by the Total cropped area and No of Household as shown in Table 4.8. All the exposure indicators of the year 2011 were then normalized into 1 – 100 scale by using Equation 4.12. After weightage determination by using PCA, exposure (Ex) was calculated by using weighted sum method as mentioned in following equation. Vulnerability is viewed as the function of positive and negative relation with selected indicators which means the higher the value, higher the vulnerability and vice-versa.

Exposure of a Upazilla, $Ex = W_1 \times I_{Ex1} + W_2 \times I_{Ex2} + W_3 \times I_{Ex3} + \ldots\ldots\ldots\ldots + W_n \times I_{Exn}$ $\qquad$ (4.14)

Where, W is the weight assigned to the indicator and I_{Ex} is the indicator.

Table 4.8: List of the socio-economic indicators and their weights used for exposure

Component	Name of the Indicator	Domain	Weight
Exposure	Population Density	Population	0.367
	No of Household	Housing and Infrastructure	0.274
	Total Cropped Area	Land Use	0.359

4.12.7 Assessment of Sensitivity, Adaptive Capacity & Vulnerability for Future Projected Socio-Economic Regime

It has long been acknowledged that socioeconomic determinants play an important role in the characterization of climate risk through vulnerability and exposure (IPCC, 2012). As a result, nearly all the assessments of climate risk consider both climatic (hazard) and socioeconomic (vulnerability and exposure) conditions (De Sherbinin, 2014). Nevertheless, when it comes to modelling of the future climate-related risk, studies have been based on projections of future climatic conditions through climate models and scenarios superimposed on current socioeconomic conditions (Ebi et.al, 2016; Preston et.al, 2011; Rohat et.al, 2018) by making the implicit assumption that drivers of risk other than climate change remain constant (Jurgilevich, 2017). Though the dynamics of vulnerability have been long recognized, future socioeconomic condition has been very rarely accounted for (Jurgilevich, 2017). This study aims to project the socio-economic indicators of sensitivity, adaptive capacity, vulnerability and exposure for

the 2020s, 2050s and 2080s to address the influence of socio economic condition in estimation of flood risk for the future.

Population of a country can be forecasted using various methods such as arithmetic increase method, geometric increase method, the logistic curve method and cohort component method each assuming various factors and assumptions (Gawatre et.al., 2016; Jain et.al, 2013-2015). Figure 4.20 shows the projection of population of Bangladesh suggested by UN population division. UN population division proposed 3 variants for projecting population in national level among which high variant provides with maximum increasing rate of population using the logarithmic distribution based on previous population census data. The medium variant stands for the increase in population up to the carrying capacity which is the concept of logistic growth method.
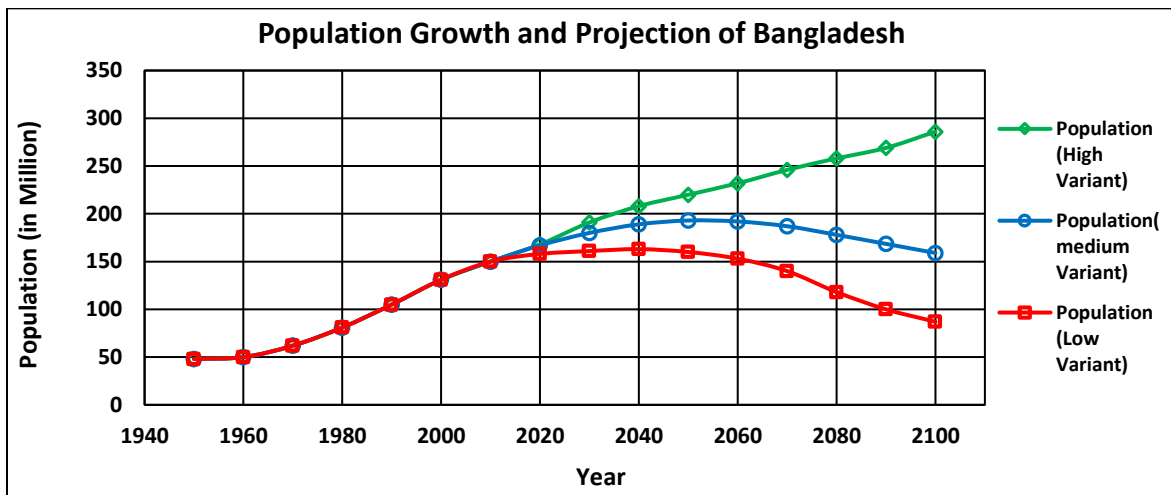
Figure 4.19: Projection of population of Bangladesh by UN population division.

Among the available methods for forecasting population, Geometric increase method and the Logistic curve method provide better approximation of the calculated population to actual population with lower percentage error (Gawatre et.al., 2016). In this study, for the projection of total population of each of the upazilla logistic growth method has been implied as followed by Akhter et al, 2018 and Zabadi.et.al, 2017. According to ideal concept of the logistic growth method as long as there are enough resources available, there will be a positive growth rate and as the limited resources begin to decrease, increasing rate of the population slows down. Logistic model illustrates how a population may increase until it reaches the carrying capacity of its environment. When a population reaches the carrying capacity, growth slows down or stops altogether. The Logistic method is useful in case of limited space and economic opportunity under the assumption that population growth occurs under normal situation and is not affected by extraordinary

changes like epidemic, war or natural disaster (Jain et.al, 2013-2015). If P_0, P_1 and P_2 are the population of an area at time t_0, t_1 and t_2, the saturation population equivalent to the carrying capacity of the area can be calculated by using following equation

$$\text{Saturation population, } Ps = \frac{2P0P1P1P2-[P1\times P1(P0+P2)]}{(P0P2-P1P1)} \qquad (4.15)$$

And projected population for the time t

$$P = \frac{Ps\times P0}{P0+(Ps-P0)e(-rt)} \qquad (4.16)$$

$$\text{Where, r} = \frac{2.3\times \log 10\{P0(Ps-P1)/P1(Ps-P0)\}}{t1} \qquad (4.17)$$

Population of each of 31 upazilla of the study area has been forecasted for the decades of the whole century using the population census data of 1981, 1991, 2001 and 2011 and Equation (4.15), (4.16) and (4.17) of logistic growth method. Decadal values from 2011 to 2040, 2040 to 2070 and 2070-2100 were then averaged to get the mean population density of early (2020s) mid (2050s) and late century (2080s) for each of the Upazilla. Figure 4.21(a) shows the forecasted population of the upazilla of Mymensingh district. Population density for each of the upazilla has been obtained by dividing the upazilla population by the area of the upazilla. The projected population of the upazilla under a particular district have been summed up and compared with the forecasted population of the district using Cohort component method by Bangladesh Institute of Development Studies (BIDS). Percentage variation in district wise population estimated by Logistic growth method and Cohort component method varied from 8.85% to 14.9% for the districts under the study area. Predicted populations of other upazillas are presented in Appendix A.
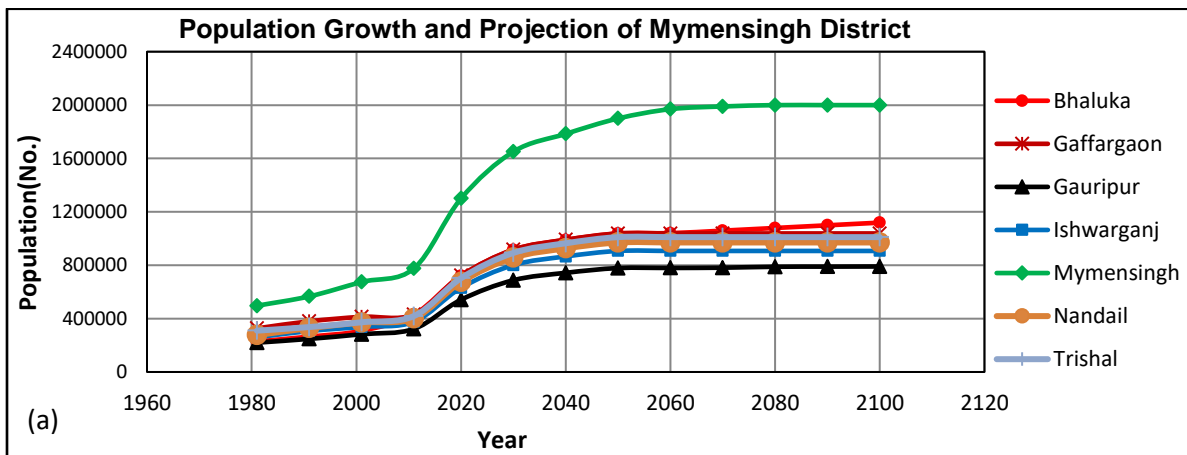

Figure 4.20 (a): Forecasted population of the upazilla of Mymensingh district

To predict the total number of household firstly raw data of the number of household for the year 1981, 1991, 2001 and 2011 have been collected. The ratio of the number of household to the total population for the year 1981, 1991, 2001 and 2011 have been obtained and the rates were then projected for future by trend analysis in which polynomial distribution fit the rates with satisfactory coefficient of determination, r^2. Using the predicted rates and predicted population of each upazilla number of total household for each of the upazillas was predicted for every decade from 2020 to 2100. Decadal values from 2011 to 2040, 2040 to 2070 and 2070-2100 were then averaged to get the mean number of household of each upazilla for early (2020s) mid (2050s) and late century (2080s). Figure 4.21(b) shows the predicted total number of household of the upazillas of Mymensingh district. Predicted total number of household for other upazilla is shown in Appendix A.
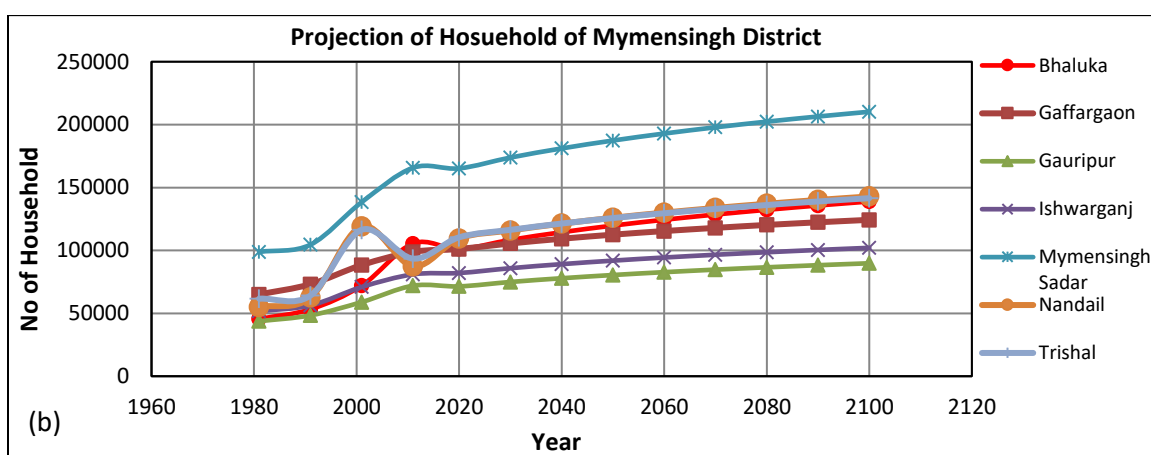
Figure 4.21 (b): Forecasted no. of household of the upazilla of Gazipur district

To forecast the indicators "Unemployed People", "Floating Population" and "School Attendance" for the future socio economic condition, firstly, the rate of unemployment, rate of floating population and school attendance rate have been obtained using the total unemployed people, total floating population, total number school attendance and total population for 1981, 1991, 2001, 2011. The unemployment rate showed a decreasing trend for all the Upazilla of Gazipur and Narsingdi district for the last 3 decades. But the upazilla of the Kishoreganj and Mymensingh district showed an increasing rate of unemployment over the last 3 decades. Similarly the rate of floating population and school attendance rate have been observed to vary upazilla wise. Then the trend of the rate of unemployment, floating population and school attendance of all the upazilla have been analyzed which came up with fair regression coefficient for logarithmic distribution. Using the future rates of unemployment, floating population, school attendance and total population of each upazilla, the number of unemployed people floating population and school attendance for each upazilla for every decade has been obtained.
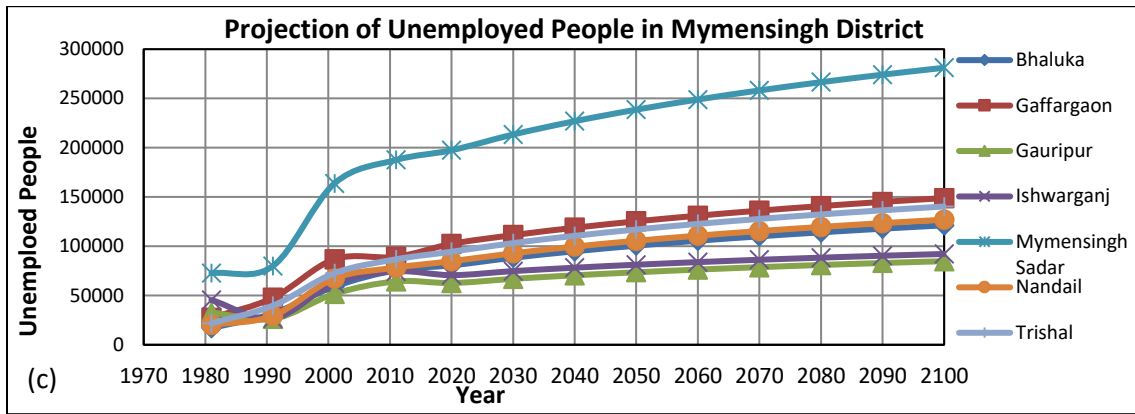
Figure 4.22 (c): Future trend of total unemployed people for all the upazilla of Mymensingh district
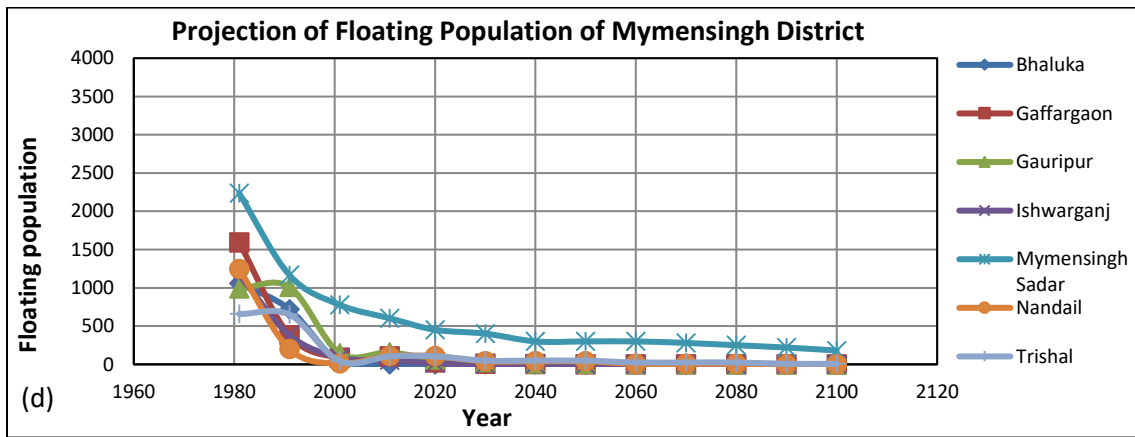
Figure 4.23 (d): Future trend of Floating Population for all the upazilla of Mymensingh district
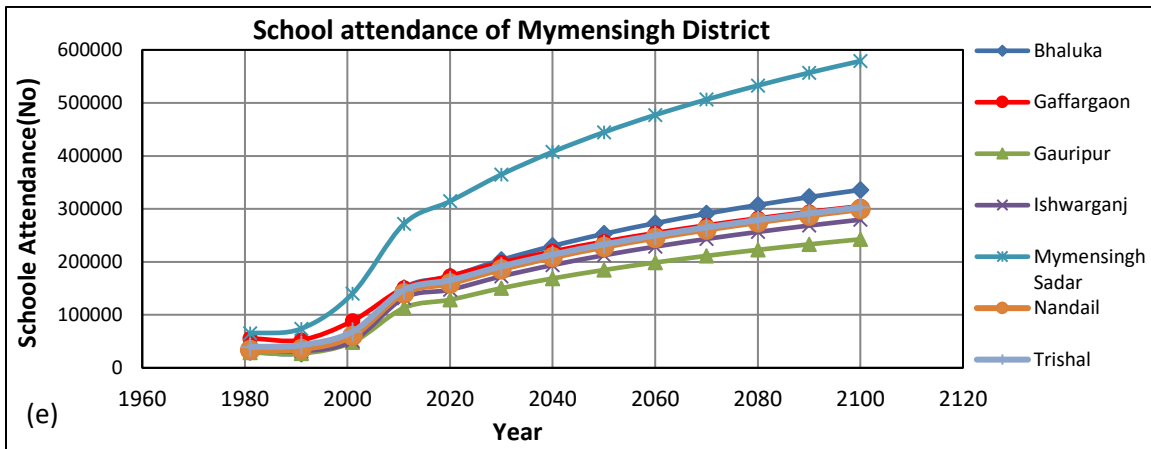
Figure 4.24 (e): Future trend of total school attendance for all the upazilla of Mymensingh district

Figure 4.21(c), (d) and (e) show the future trend of total unemployed people, floating people and the future trend of school attendance for all the upazilla of Mymensingh district. Trend for all other upazilla are presented in Appendix A.

To predict the three indicators named "People in Agriculture", "People in Industry+Service" and "People in Household Activities" firstly data of the number of people in agriculture, people in industry and service and people in household activities were collected for the year 1981, 1991, 2001 and 2011 from Population census reports. The ratio of the number of people in agriculture to total population, ratio of the number of people in industry and service to total population and ratio of the number of people in household activities to total population for the year 1981, 1991, 2001 and 2011 have been obtained and the rates were then projected for future for each indicator were obtained from trend analysis in which polynomial distribution fit the rates with satisfactory coefficient of determination, r^2.Using the predicted rates and predicted total population of each upazilla as obtained earlier, number of total number of "People in Agriculture", "People in Industry+Service" and "People in Household Activities" for each of the upazillas was predicted for every decade from 2020 to 2100. Decadal values from 2011 to 2040, 2040 to 2070 and 2070-2100 were then averaged to get the mean values of the indicators of each upazilla for early century (2020s) mid-century (2050s) and late century (2080s).
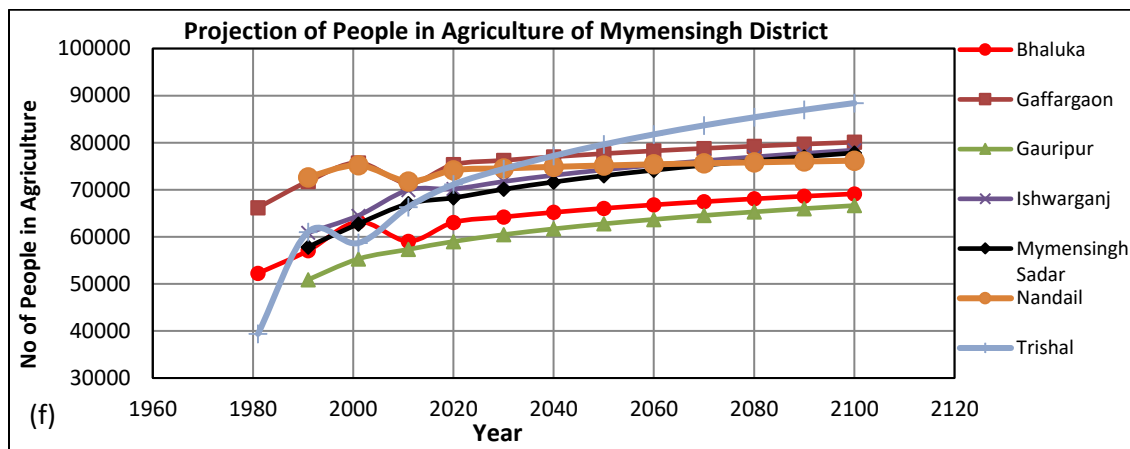
Figure 4.25 (f): Future trend of "People in Agriculture" for all the upazilla of Mymensingh district
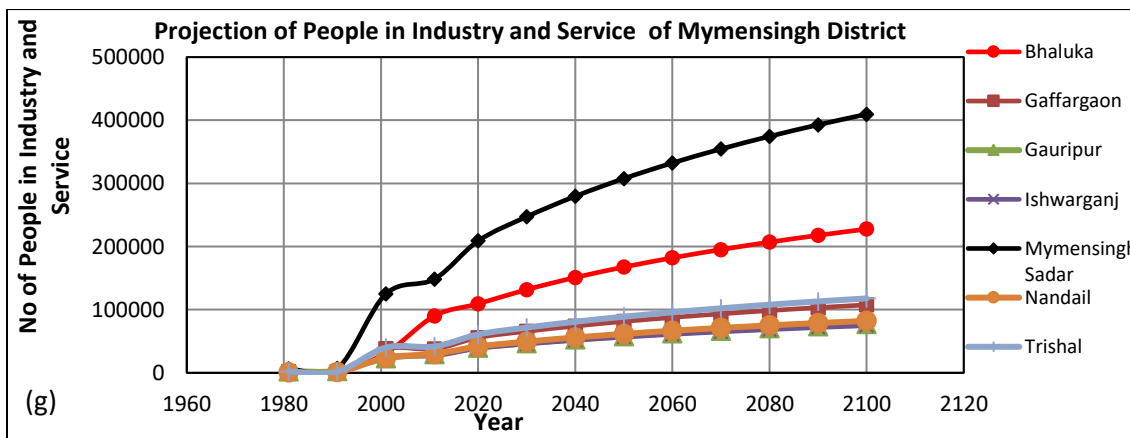
Figure 4.26 (g): Future trend of "People in Industry+Service" for all the upazilla of Mymensingh district

80
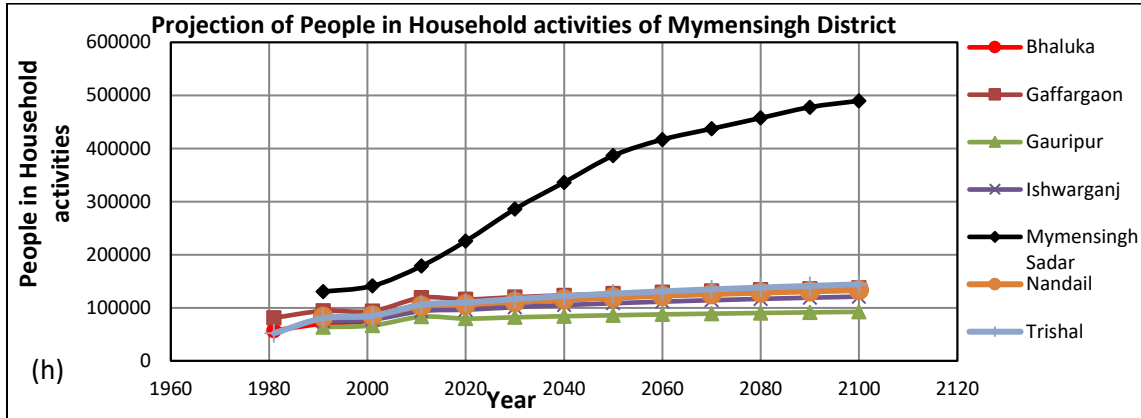
Figure 4.27 (h): Future trend of "People in Household Activities" for the upazilla of Mymensingh district

Figure 4.21(f), (g) and (h) shows the predicted "People in Agriculture", "People in Industry+Service" and "People in Household Activities" of the upazillas of Mymensingh district. Trend for all other upazilla are presented in Appendix A.
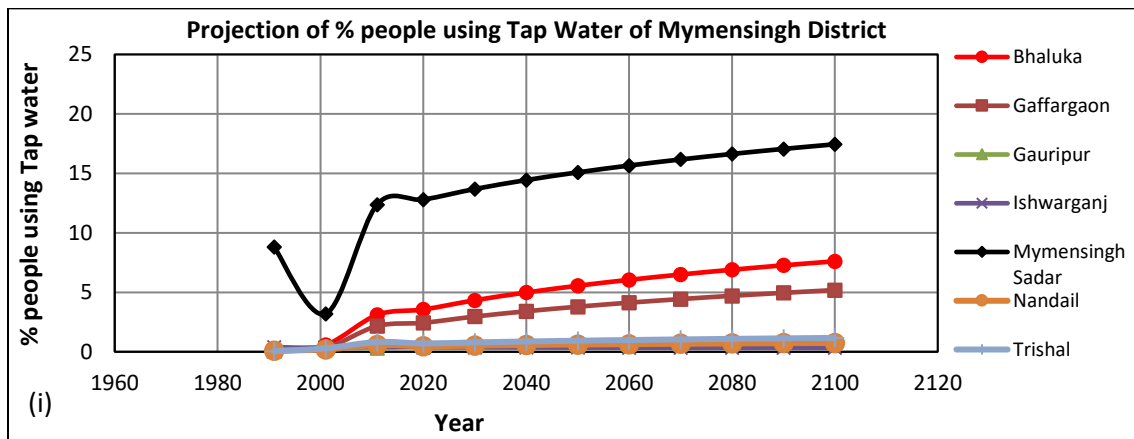
Figure 4.28 (i): Predicted "% people using Tap water" of upazillas of Mymensingh district
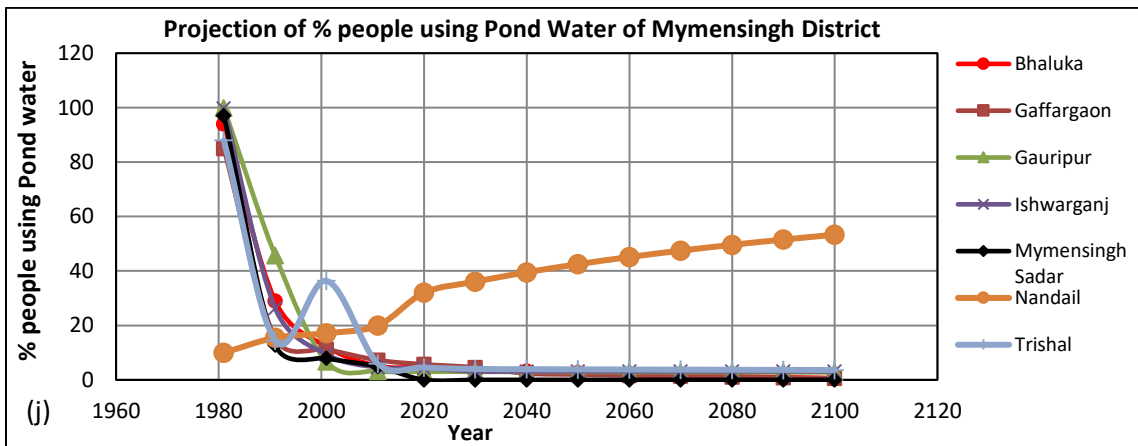
Figure 4.29 (j): Predicted "% people using Pond Water" of upazillas of Mymensingh district

81
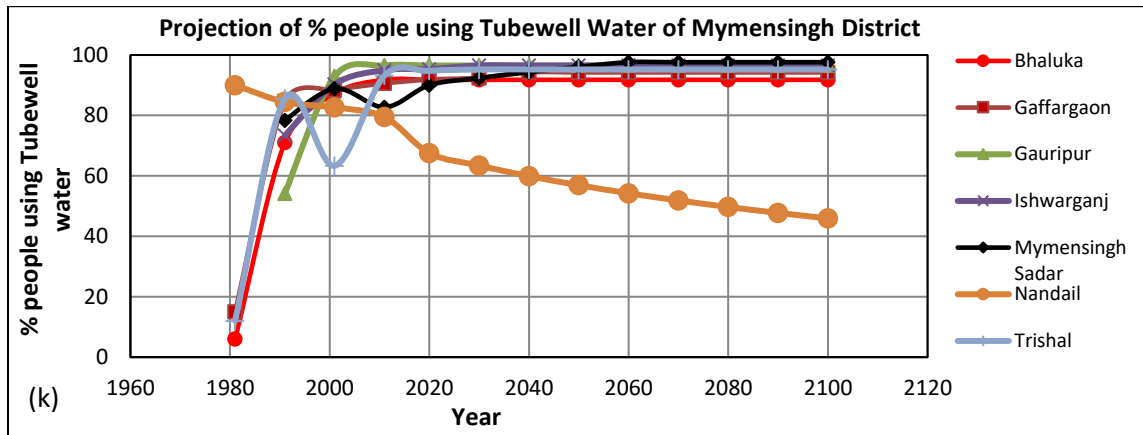
Figure 4.30 (k): Predicted "% People using Tubewell water" of upazillas of Mymensingh district

Similar approach has been utilized to forecast the % people using Tap water, % people using Pond Water and %people using Tubewell water of the upazilla under the study area. Figure 4.21 (i), (j) and (k) shows the predicted indicators for upazillas of Mymensingh District.

To predict the three indicators named "Percent Pucca+Semi-pucca Household", data of percent Pucca+Semi-pucca Household has been collected for the year 1981, 1991, 2001 and 2011 from Population census reports. Projected percenatges of Pucca+Semi-pucca Household for future for each decade were obtained from trend analysis in which polynomial distribution fit the data with satisfactory coefficient of determination, r^2. Decadal values from 2011 to 2040, 2040 to 2070 and 2070-2100 were then averaged to get the mean values of the indicators of each upazilla for early century (2020s) mid-century (2050s) and late century (2080s). Similar approach has been adopted to predict "Percent Kutcha+Jhupri Household", "Percent Household having Sanitary Facility" and "Percent Household having no Sanitary Facility".
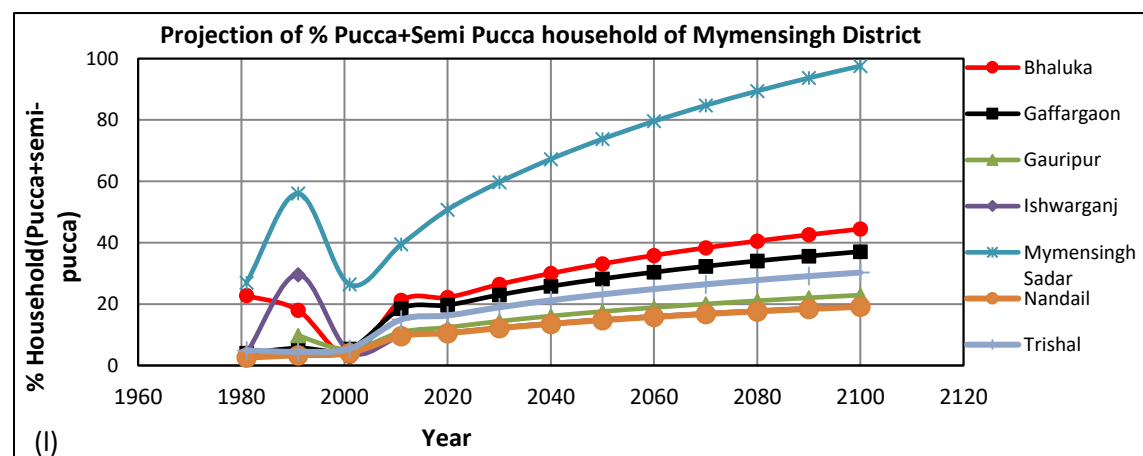
Figure 4.31 (l): Future trend of "Percent Pucca+Semi-pucca Household" for of Mymensingh District

82
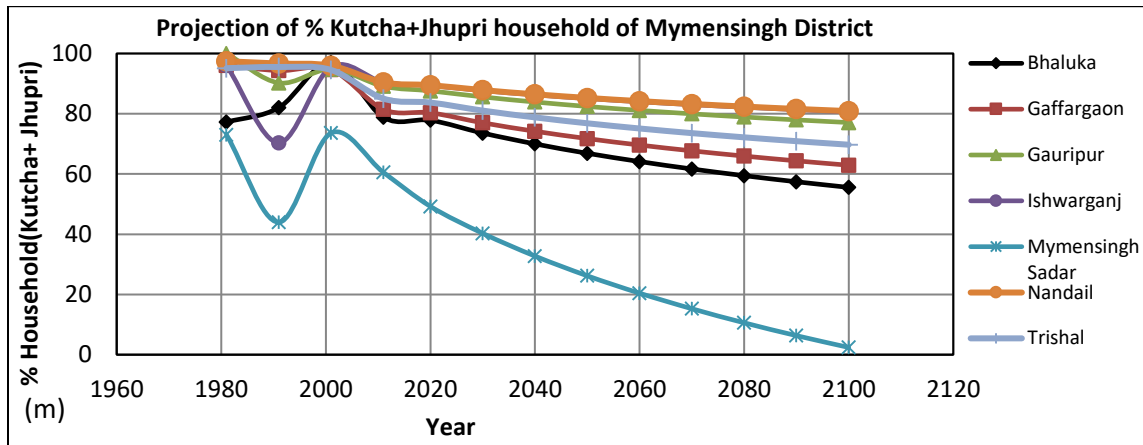
Figure 4.32 (m): Future trend of "Percent Kutcha+Jhupri Household" for Mymensingh District
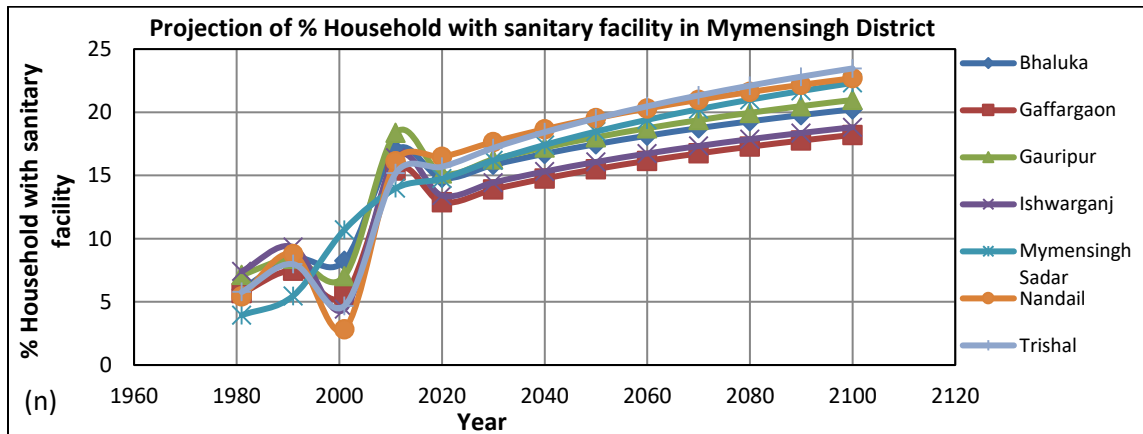
Figure 4.33 (n): Predicted "Percent Household with Sanitary Facility" of Mymensingh district
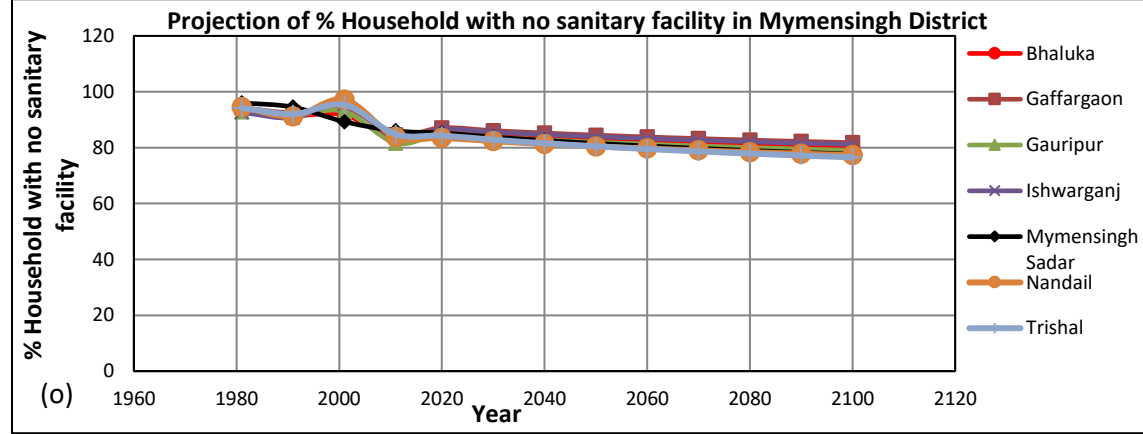
Figure 4.34 (o): Predicted "Percent Household with no Sanitary Facility" of Mymensingh district

Figure 4.21(l), (m) and (n) and (o) show the predicted "Percent Pucca+Semi-pucca Household", "Percent Kutcha+Jhupri Household", "Percent Household having Sanitary Facility" and "Percent Household having no Sanitary Facility" respectively.

To predict the variables "Aman Production Area" and "Crop Productivity" upazilla wise data of total Aman area and crop productivity for the year 1984, 1998, 1996 and 2008 have been collected from the Agricultural census reports of the districts. Using the dataset of last four decades trend analysis have been performed in which polynomial distribution fit the data in both case with acceptable correlation coefficient. The predicted decadal from 2008 to 2040, 2040 to 2070 and 2070-2100 were then averaged to get the mean Aman Area and Crop productivity of each upazilla for early century (2020s) mid-century (2050s) and late century (2080s). Figure 4.21(p) and (q) show the predicted "Aman Production Area" and "Crop Productivity" upazillas of Gazipur district.
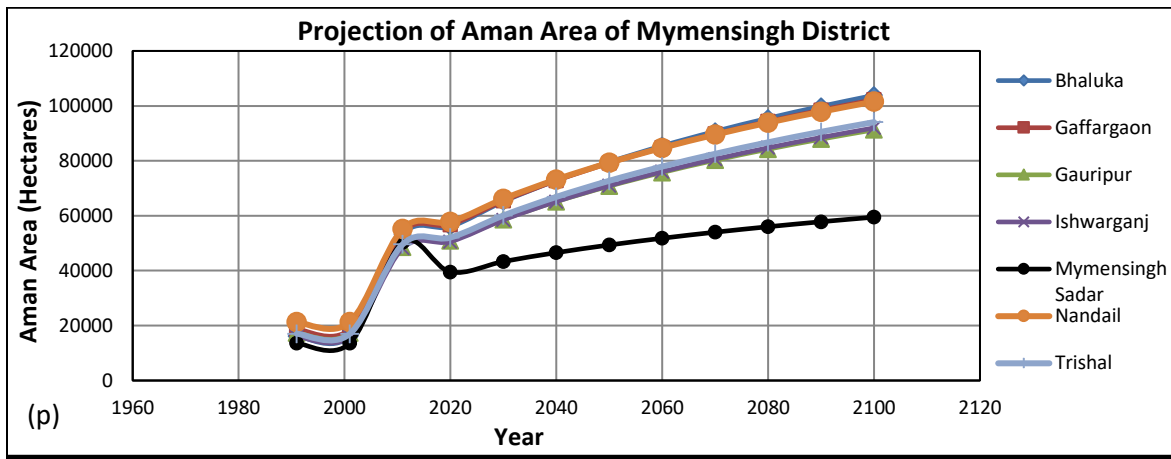
Figure 4.35 (p): Future trend of "Aman Production Area" for all the upazilla of Mymensingh district
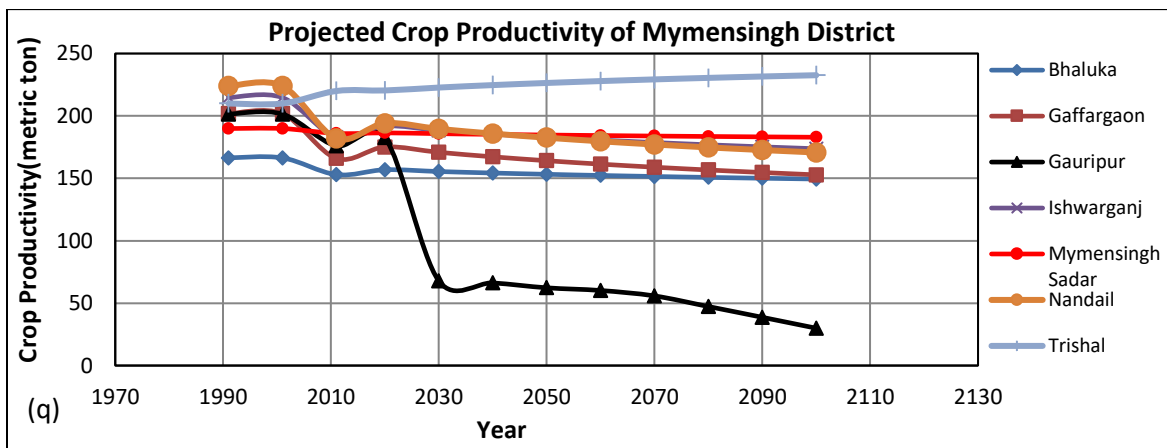
Figure 4.36 (q): Future trend of "Crop Productivity" for all the upazilla of Mymensingh district

Trend analysis of the poverty rate of Bangladesh for the last 30 years represents that the countries poverty is decreasing but in a lower rate as shown in Figure 4.21(r). To predict the variables "Poverty Rate" and "Literacy Rate" upazilla wise data of upper poverty and Literacy rate for the year 1981, 1991, 2001 and 2011 have been collected from the Population Census reports of the districts. Using the dataset of last four decades trend analysis have been performed in which polynomial distribution fit the data in both case with

acceptable correlation coefficient. The predicted decadal from 2008 to 2040, 2040 to 2070 and 2070-2100 were then averaged to get the mean poverty rate and Literacy Rate of each upazilla for early century (2020s) mid-century (2050s) and late century (2080s). Figure 4.21(s) and (t) show the predicted "Poverty Rate" and "Literacy Rate" of upazillas of Gazipur district.
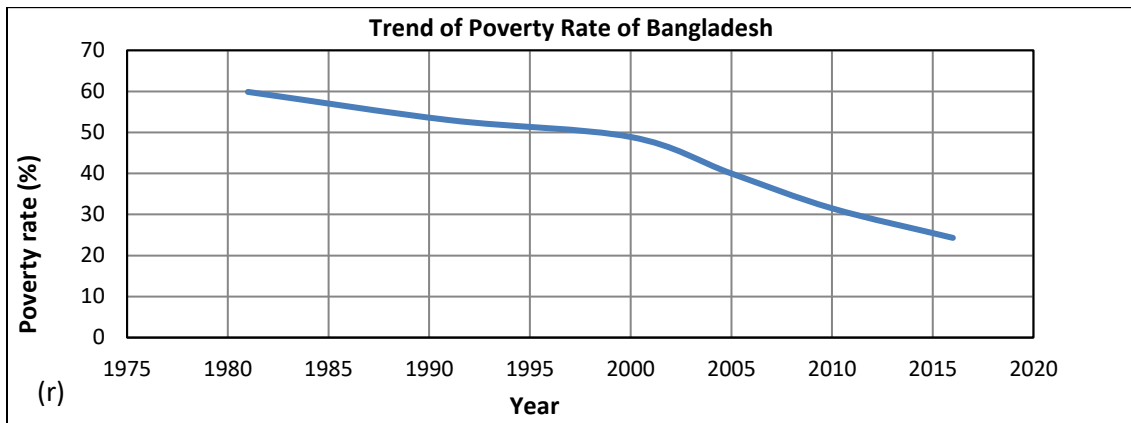
Figure 4.37 (r): "Poverty Rate" of Bangladesh (Source: UNDP, 2017)
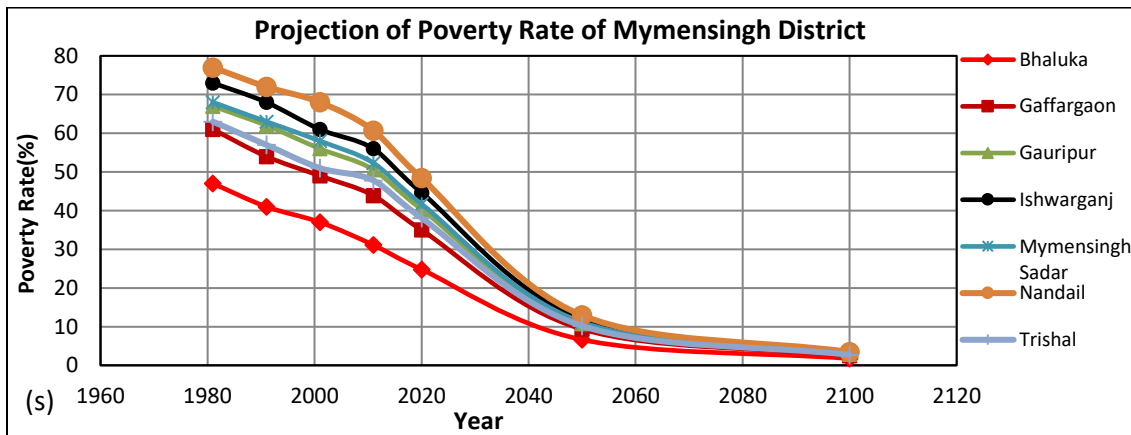
Figure 4.38 (s): Predicted "Poverty Rate" of upazillas of Mymensingh district
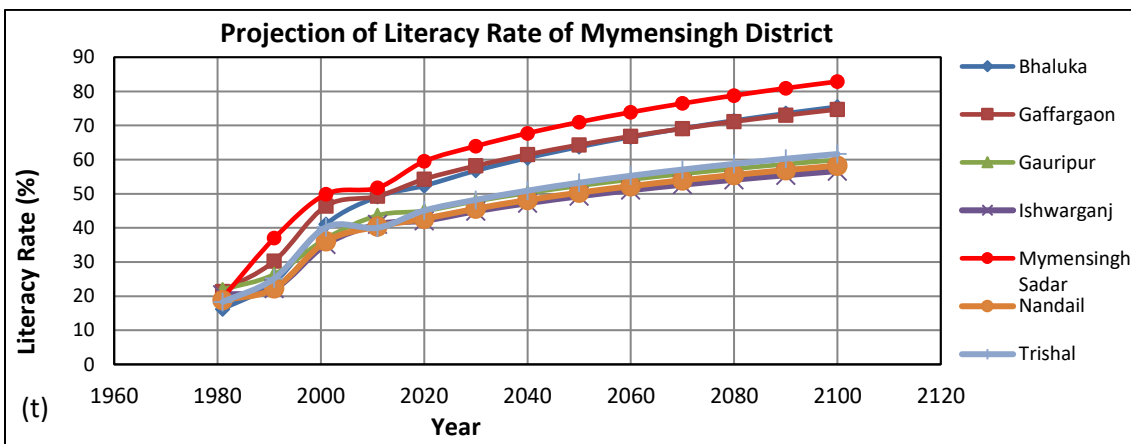
Figure 4.39 (t): Predicted "Literacy Rate" of upazillas of Mymensingh district

To project variables: total male population, total female population, people of age 10-60, people of age 0-10 and people of age >60, data of the variables for 1981, 1991, 2001 and 2011 were collected and the ratio of the variable to total population have been calculated. With the rates of previous decades for each of the variable, future rates are predicted by trend analysis. Using future rates and future total population of each upazilla the variable values are calculated.
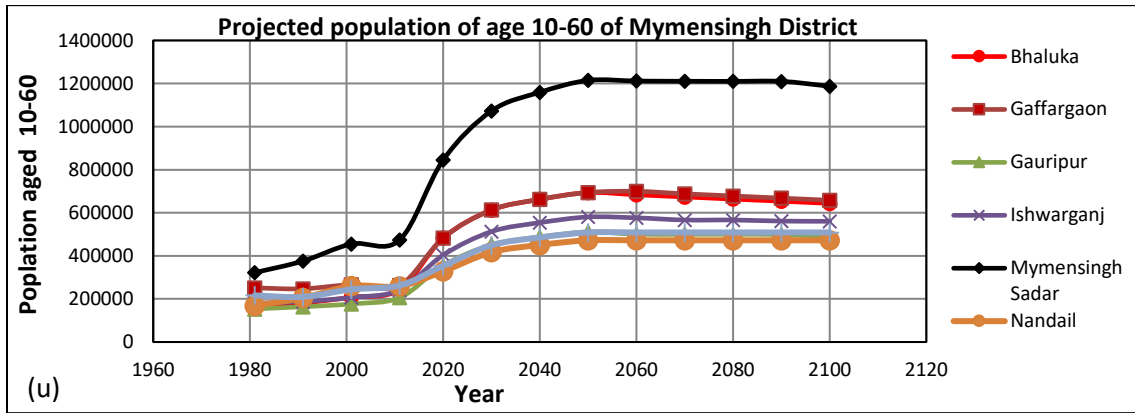
Figure 4.40 (u): Predicted "Population of age 10-60" of upazillas of Mymensingh district
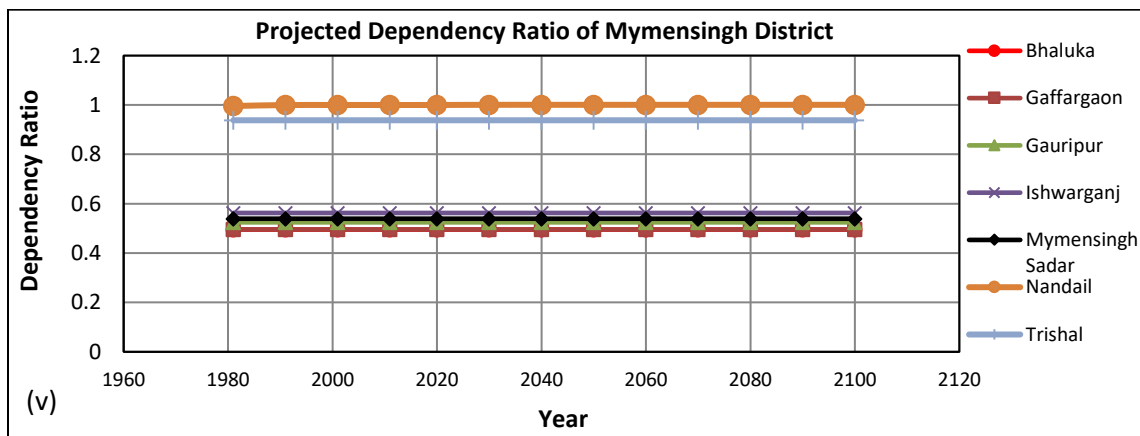
Figure 4.41 (v): Predicted "Dependency Ratio" of upazillas of Mymensingh district
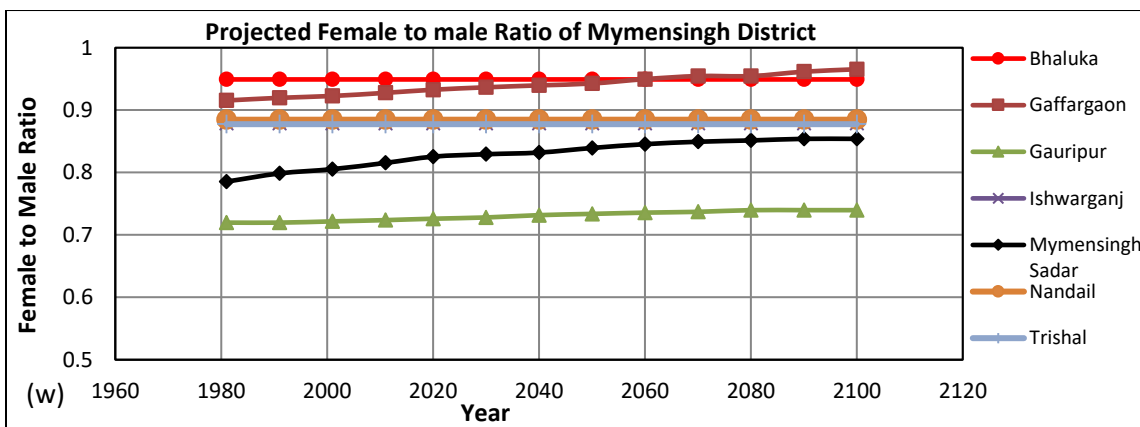
Figure 4.42 (w): Predicted "Female to Male Ratio" of upazillas of Mymensingh district

86

To calculate the dependency ratio for each of the decade the ratio of the sum of the population aged 0-10 and >60 to population aged 10-60. To calculate the indicator Female to Male ratio number of female to 100 male were obtained. Figure 4.21(u), (v), (w) show the future trend of the three indicators.

Few of the selected sensitivity, adaptive capacity and exposure like "Total Cropped Area", "% electricity connection", "Number of Hospitals and Clinics" "Length of Unpaved Road", "Percent Disabled People" values obtained from the latest census of 2001 have been kept constant for the future time regime as sequential data for past decade were not available and no definite trend was observed for the particular indicators.

Finally all the present and future projected sensitivity, adaptive capacity and exposure indicators of the year 2011, 2020s, 2050s and 2080s were then normalized into 1 – 100 scale. After weightage determination by using PCA, sensitivity, adaptive capacity, vulnerability and exposure were calculated by using weighted sum method as mentioned earlier. Vulnerability is viewed as the function of positive and negative relation with selected indicators which means the higher the value, higher the vulnerability and vice-versa.

4.13   Risk Assessment

Flood induced risk for the Old Brahmaputra river floodplain has been assessed following the IPCC concept of climate risk according to the 5th assessment report of IPCC where flood risk (R) is comprised of three parameters: Hazard, vulnerability and exposure and is calculated using the following equation. This approach of integrated flood risk assessment has been recently adopted by some recent studies like Rakib et. al., 2017, Allen, et al., 2016 and many others.

Risk = Hazard ×Vulnerability× Exposure (4.18)

Finally, hazard, sensitivity, adaptive capacity, vulnerability, exposure and risk have been classified into five categories, maintaining an equal interval for each case, 0-20, 20-40, 40-60, 60-80 and 80-100 for Very Low, Low, Medium, High and Very High respectively. On the basis of this categorization, Upazila-wise hazard, sensitivity, adaptive capacity, vulnerability, exposure and risk maps have been prepared in ArcGIS.

CHAPTER 5

RESULTS AND DISCUSSION

5.1   General

The chapter included the results and discussions relating to the flood inundation modeling, hazard, vulnerability and risk mapping. It contains calibration and validation of developed hydrodynamic model, analysis of historical flood events and simulation of future floods and hazard assessment for climate change scenario. It also discusses the assessment of socio-economic vulnerability of the study area It also combined the results obtained from hazard, vulnerability and exposure assessment to evaluate the risk by monsoon flood for the present and future climate change scenario of RCP8.5.

5.2   Calibration and Validation of HEC-RAS 1D-2D coupled Model of Old Brahmaputra River

Calibration and Validation of HEC-RAS 1D-2D coupled Model of Old Brahmaputra River include two phases, one is the calibration and validation of 1D river channel and calibration and validation of the surrounding flood plain of the river channel.

5.2.1   Calibration & Validation of 1D Model

In this study, the 1D model of Old Brahmaputra River has been calibrated and validated for the year 2017 and 2010 respectively. Flow hydrograph and stage hydrograph are used as the upstream and downstream boundary condition respectively. Mean daily water level data of the intermediate location named as Toke (SW 229) has been compared with the model simulated daily water level at the same location. The developed 1D model of Old Brahmaputra River has been simulated using the mean daily discharge and water level data from 1st January to 31st December of 2017 as the boundary conditions using the value of Manning's roughness n as tuning parameter. Several trial simulations with variable Manning's n ranging from n = 0.010-0.025 along the different cross sections were conducted. Initial simulation with the manning's roughness, n=0.025 fixed for all the cross sections overestimated the water level at the calibration location compared with the observed values of the water levels. As we know water surface elevation gets increased by higher value of Manning's roughness coefficient which retards the flow velocity, for the subsequent trials lower values of Manning's roughness from 0.010 to 0.025 have been

used. After several trials, Manning's roughness values ranging from 0.014-0.017 for different cross sections have been found to produce closer approximation of simulated water level with observed water levels.

Table 5.1 (a): Performance Evaluation of Developed 1D 2D coupled model of Old Brahmaputra River

Component	Calibration		Validation	
	Value	Remark	Value	Remark
R^2	0.924	Very Good	0.975	Very Good
NSE	0.976	Very Good	0.985	Very Good
PBIAS	-7.193	Very Good	-4.166	Very Good
RSR	0.1519	Very Good	0.122	Very Good
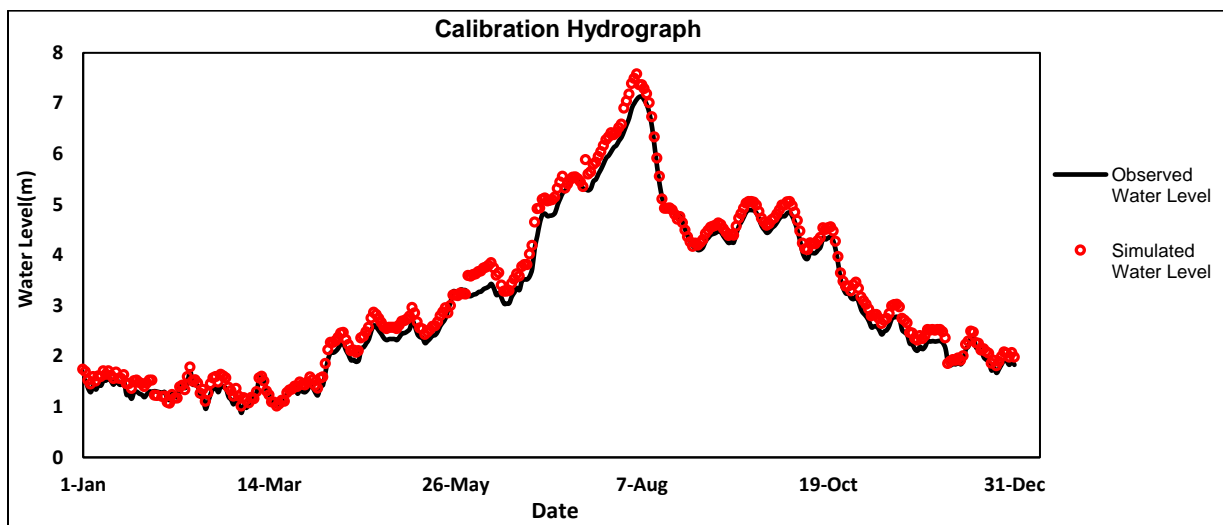
Figure 5.1: Comparison of Observed and simulated water level for 2017
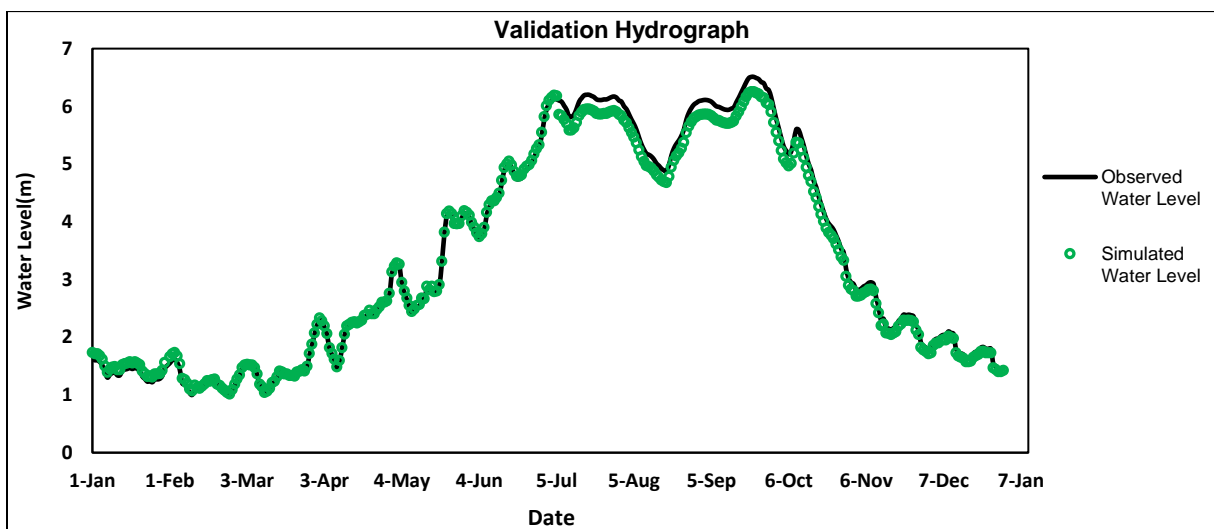
Figure 5.2: Comparison of Observed and simulated water level for 2010

89

The values of the model performance evaluation techniques of R^2, NSE, PBIAS and RSR for the finally accepted range of n= 0.014-0.017 are calculated as shown in Table 5.1 depicting satisfactory matching of the simulated and observed data. Using the calibrated Manning's roughness coefficient (n) value, validation for the model has been performed from 1st January to 31st December of the year 2010. The validation result shows good agreement of the simulated water level with the observed water level for the time span. The values of the model performance evaluation techniques of R^2, NSE, PBIAS and RSR for the finally accepted range of n= 0.016-0.018 depict satisfactory matching of the simulated and observed data as shown in Table 5.1(a). Figure 5.1 and Figure 5.2 show the graphical representation of observed and simulated water level for calibration and validation.

5.2.2   Calibration and Validation of 2D Flood Inundation Model

After calibration and validation of the 1D model, a 1D-2D coupled model is set up to simulate the flood inundation in the floodplain. Thus it is necessary to calibrate and validate the simulated 2D flood inundation as well. The approach hereby followed for calibration of 2D floodplain is to compare the flood inundation of the 2D flood flow areas of the study area with the flood inundation map prepared by FFWC and available satellite image of Sentinel-1. Firstly, qualitative comparison of the inundation extent is done between the simulation of 1D 2D coupled model and flood map of FFWC and observed available satellite image of Sentinel-1 for the date of 16th August of the year 2017. To replicate the actual flood inundation scenario, the manning's roughness value of the 2D floodplain and the values of the inflow and outflow boundaries of the 2D model domain have been used as the tuning parameters. For Manning's roughness value 0.074 for the 2D floodplain and specific percentages of the flows of Old Brahmaputra river, Meghna river and Lakhya river as inflow to and outflow from the 2D model domain, inundation extent of the Sentinel-1 image, inundation map of FFWC and simulated map are adequately alike for the day of 16th August of the year 2017. Figure 5.2 shows the comparison among the simulated and observed flood extents and the common places of the inundated area between model-simulated flood map and observed flood maps have been marked by a circle for better visualization.

To predict the flood indicators like depth, velocity and inundation area with better confidence, comparison on the flood depth obtained from simulation with the actual flood depth in the study area for any historical flood need to be done besides qualitative matching of the inundation area within the study area. To meet up the need, as a part of validation of 2D floodplain, upazilla wise mean inundation depth for the year 2017 obtained from the 1D 2D coupled model simulation have been compared with the upazilla wise

inundation depth obtained from inundation modeled by FFWC for the same year as the part of validation. To prepare the Upazilla specific average inundation depth, RASTER file of the inundation of the date 16th August for the study area has been collected from FFWC and processed in ArcGIS for the flood year 2017. Figure 5.3 shows the comparison. Figure 5.4 shows the correlation between the flood depths of FFWC and HEC-RAS 1D 2D coupled model. Figure 5.5 shows the correlation graph of the flood depth [produced by FFWC and the HEC-ARS 1D-2D coupled model simulation.
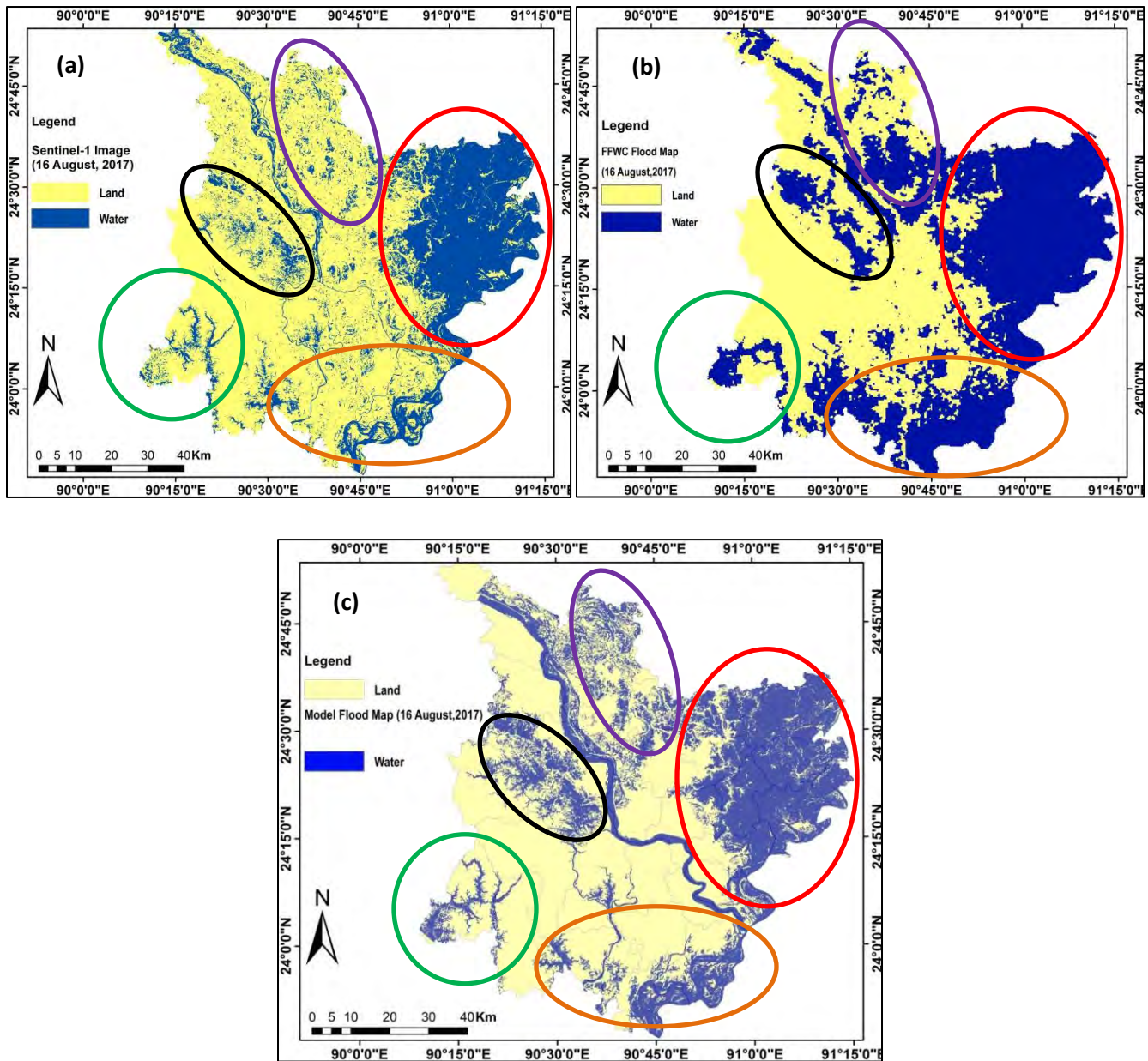
Figure 5.3: Qualitative comparison among the flood maps for 16th August, 2017 (a) Sentinel-1 Image (b) FFWC produced map (c) simulated flood map from HECRAS 1D2D coupled model
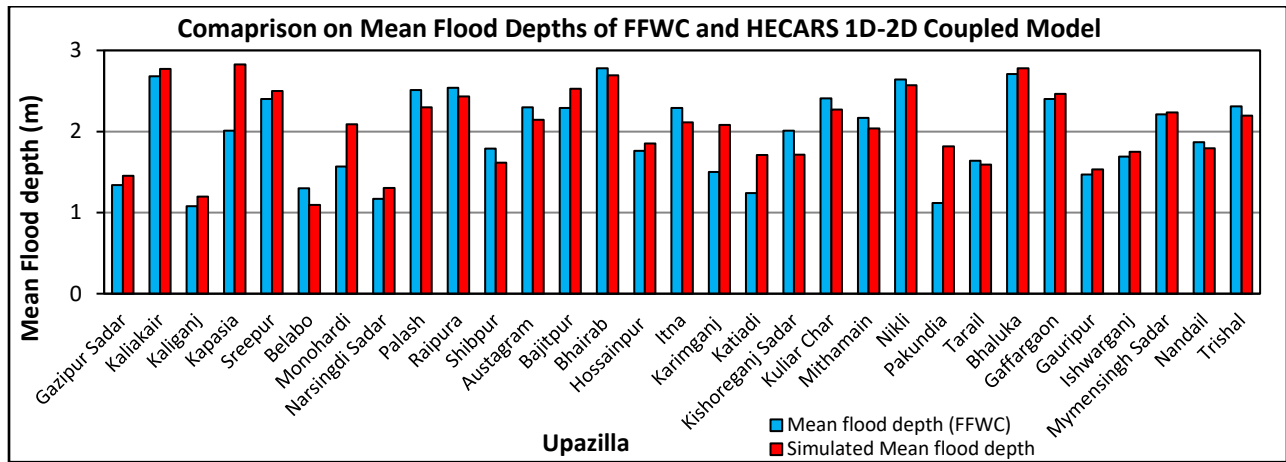
Figure 5.4: Comparison on Mean Flood depth of FFWC and HEC-RAS 1D 2D coupled model
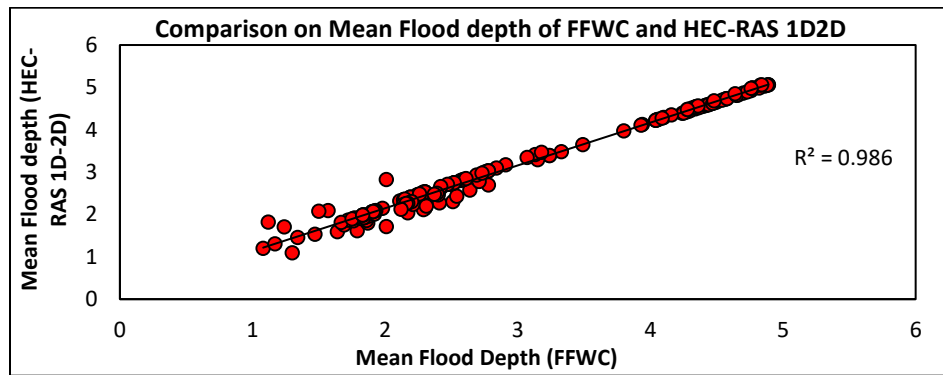
Figure 5.5: Correlation between Mean Flood depth of FFWC and HEC-RAS 1D 2D coupled model

The values of the model performance evaluation techniques of R^2, NSE, PBIAS and RSR have also been obtained and represented in Table 5.1(b) to evaluate the level of matching of the inundation depths of FFWC and HECARS 1D-2D coupled simulation.

Table 5.1 (b): Performance Evaluation of Developed flood map of Old Brahmaputra River

Component	Validation	
	Value	Remark
R^2	0.986	Very Good
NSE	0.703	Good
PBIAS	-3.687	Very Good
RSR	0.544	Good

5.3   Analysis of Historical Flood Events of Old Brahmaputra River

5.3.1   Analysis on Flood Inundation Depth of Historical Flood Events

The calibrated and validated 1D-2D coupled model of Old Brahmaputra River has been simulated for the flood events of few years including 1988, 1998, 2004, 2007, 2010, 2013, 2016 and 2017. Later, the

exported RASTER file of inundation depth of the study area for the historical flood years have been post-processed to prepare maps showing flood depths categorizing the depths into five classes. The classes were denoted as (F0), (F1), (F2), (F3) and (F4) with range of the flood depth of 0m-0.30m, 0.3m-0.9m , 0.9m-1.8m 1.8 m-3.6 m and more than 3.6 m respectively as prescribed by the National Water Management Plan (NWMP). Figure 5.6 (a) (b), (c), (d), (e), (f) and (g) shows the inundation depth maps of Old Brahmaputra river floodplain for the maximum inundation condition of the year 1988, 1998, 2004, 2007, 2010, 2013, 2016 and 2017 respectively.
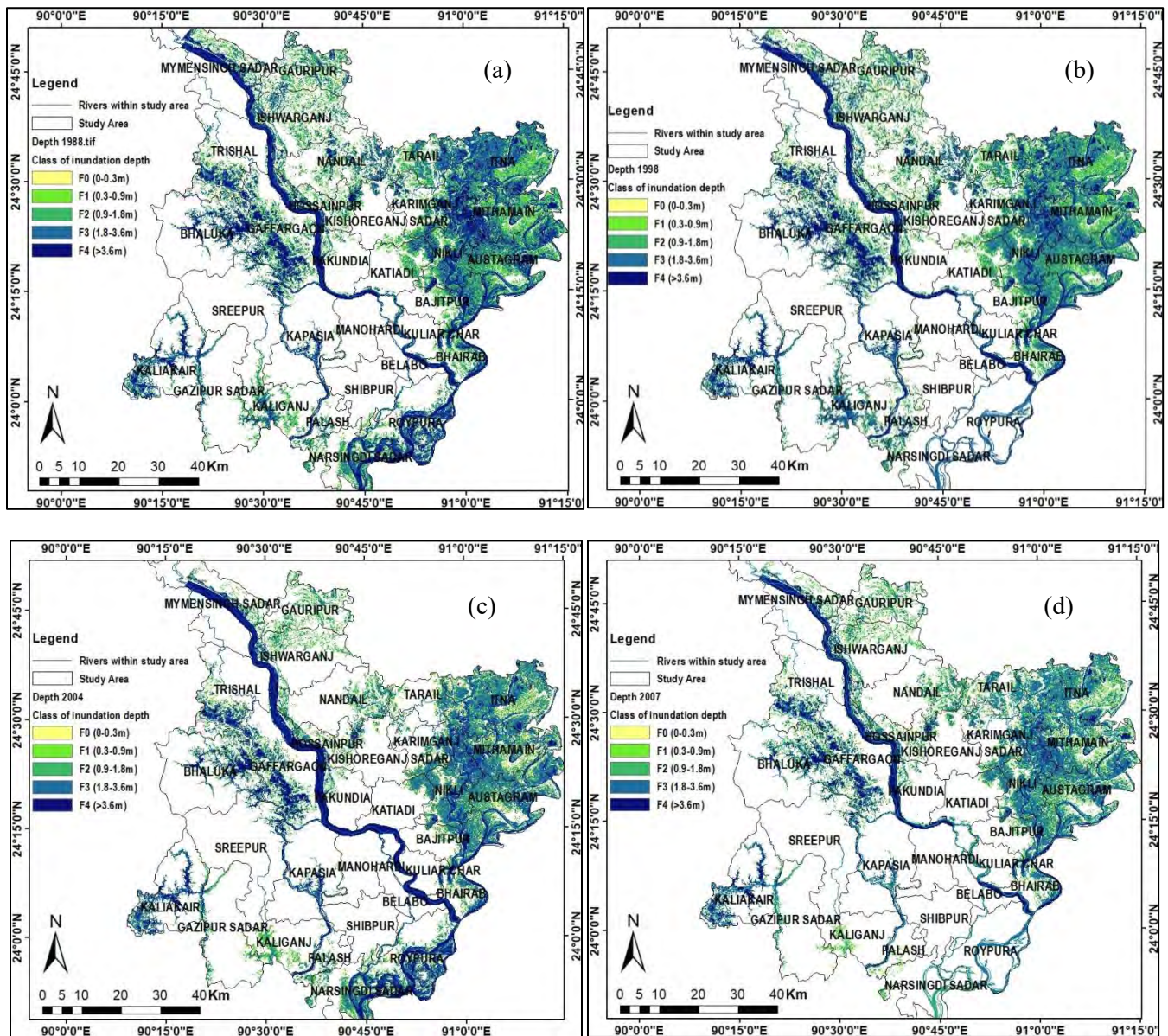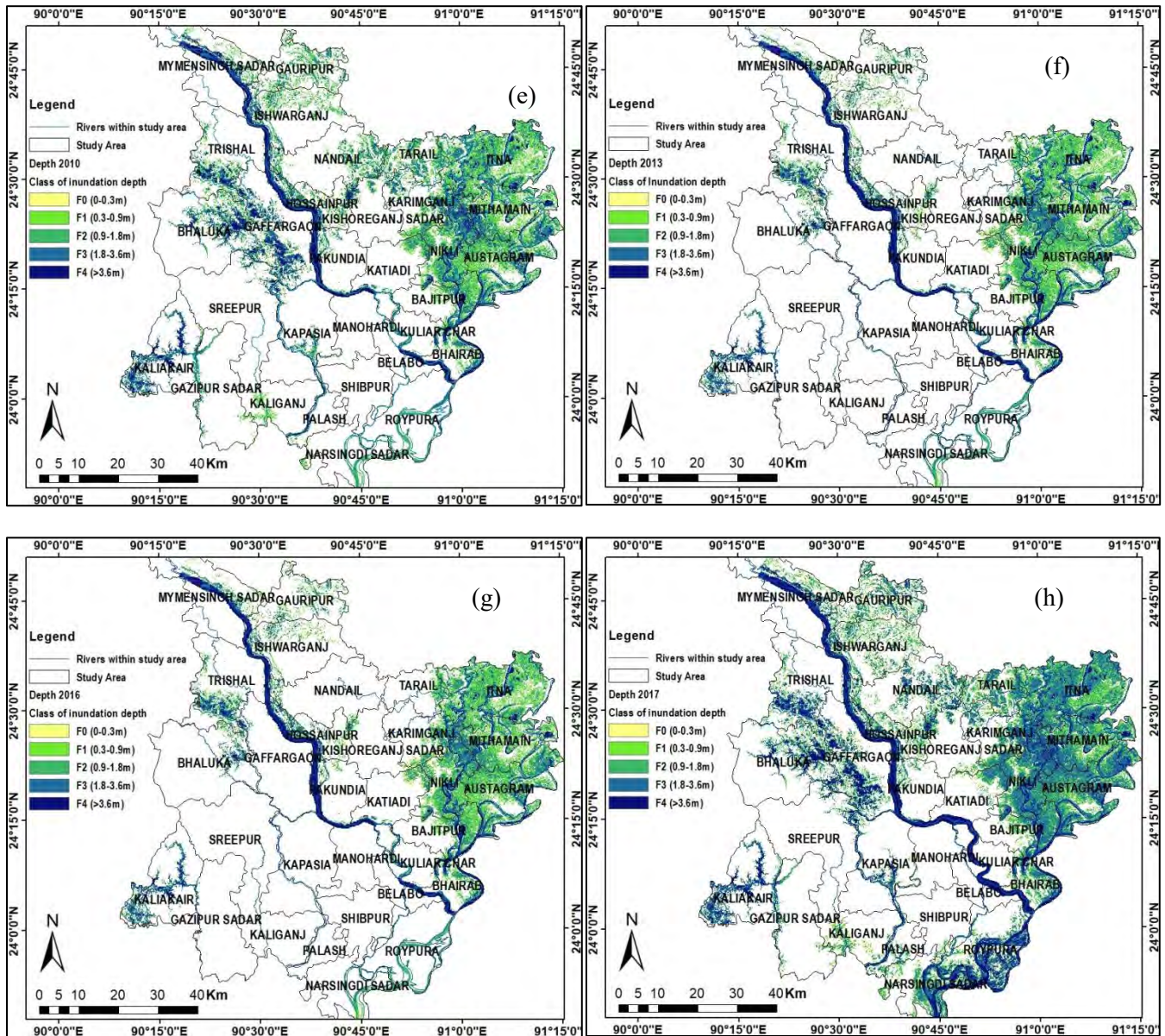
Figure 5.6: Maximum Inundation depth maps of Old Brahmaputra river floodplain (a) 1988 (b) 1998, (c) 2004, (d) 2007, (e) 2010, (f) 2013, (g) 2016 and (h) 2017

The mean flood depth observed in each Upazilla for the historical flood years have been presented in Table 5.2. Table 5.2 shows that, almost all the Upazilla experienced maximum flooding in the year 1988 and minimum flooding in the year 2013 among the years considered. Kaliakair, Kapasia, Raipura, Austagram, Itna, Kuliar Char, Trishal and Mymensingh upazilla experienced greater flood depth in most of the years comparing with other regions within the study area. The maximum mean flood depth experienced by Gaffargaon in 1998 and the minimum mean flood depth occurred in Belabo upazilla in the year 2013.For the flood year 1988, mean flood depth of the upazilla lied with the range of 1.51m to 3.16m

94

with maximum depth in Gaffargaon upazilla and minimum mean flood depth in Belabo Upazilla. In 1998, mean flood depth varied from 1.11m to 3m with maximum depth in Kaliakair upazilla and minimum mean flood depth in Shibpur Upazilla. For the flood event of 2004, maximum depth of 2.85 occurred in Kapasia and Pakundia Upazilla experienced the minimum mean flood depth of 1.18m. In 2007, maximum depth of 3m happened in Bhairab and Narsingdi Sadar had the minimum depth of 0.97m. In 2010, maximum depth of 3m occurred in Bhairab and Shibpur experienced the minimum depth of 1.02m. In 2013, maximum depth of 2.29m occurred in Bhairab and Belabo experienced the minimum mean flood depth of 0.54m. In 2016, maximum depth of 4.33m occurred in Manohardi and Belabo had the minimum depth of 0.69m. In 2017, maximum depth of 2.83m occurred in Kapasia and Belabo had the minimum depth of 1.1m.

Table 5.2: Mean flood depth observed for the historical flood years

District	Upazilla	Mean Flood Depth (m)							
		1988	1998	2004	2007	2010	2013	2016	2017
Gazipur	Gazipur Sadar	1.81	1.80	1.51	1.46	1.41	1.31	1.34	1.45
	Kaliakair	3.01	3.00	2.79	2.50	2.20	2.02	2.53	2.77
	Kaliganj	1.98	2.02	1.33	1.39	1.09	0.64	1.09	1.20
	Kapasia	2.86	2.79	2.85	2.56	2.56	2.23	2.62	2.83
	Sreepur	2.28	2.20	2.57	2.27	2.27	1.72	2.18	2.50
Narsingdi	Belabo	1.51	1.39	1.49	1.83	1.83	0.54	0.69	1.10
	Monohardi	2.06	2.11	2.04	2.16	2.16	0.92	4.33	2.09
	Narsingdi Sadar	2.17	2.20	1.41	0.97	1.31	0.89	0.80	1.31
	Palash	2.31	2.28	2.34	2.19	2.19	0.86	0.91	2.30
	Raipura	2.50	2.02	2.43	2.05	2.05	1.34	1.47	2.43
	Shibpur	1.62	1.11	1.62	1.90	1.02	0.78	1.84	1.61
Kishoreganj	Austagram	2.47	2.35	1.86	1.98	1.98	1.70	1.87	2.14
	Bajitpur	2.82	2.71	2.29	2.46	2.46	2.20	2.36	2.53
	Bhairab	3.09	2.90	2.64	3.00	3.00	2.79	2.93	2.69
	Hossainpur	2.11	1.89	2.06	1.72	1.72	1.76	1.79	1.85
	Itna	2.46	2.32	1.78	1.89	1.89	1.62	1.81	2.11
	Karimganj	2.36	2.25	1.88	1.97	1.97	1.78	1.89	2.08
	Katiadi	1.77	1.72	1.66	1.63	1.73	1.43	1.51	1.71
	Kishoreganj Sadar	1.84	1.82	1.49	1.71	1.71	1.36	1.50	1.72
	Kuliar Char	2.82	2.42	2.24	2.72	2.72	2.49	2.68	2.27
	Mithamain	2.37	2.25	1.74	1.94	1.94	1.66	1.83	2.04
	Nikli	2.88	2.76	2.26	2.31	2.31	2.02	2.19	2.57
	Pakundia	1.59	1.61	1.18	1.58	1.58	1.17	0.86	1.82
	Tarail	1.86	1.77	1.31	1.53	1.53	1.26	1.37	1.59
Mymensingh	Bhaluka	2.90	2.93	2.83	2.69	2.69	1.65	1.90	2.78
	Gaffargaon	3.16	2.69	2.80	2.24	2.24	0.90	0.83	2.46
	Gauripur	1.93	1.63	1.37	1.34	1.34	1.21	1.34	1.53
	Ishwarganj	1.80	1.60	1.88	1.62	1.62	1.39	1.61	1.75
	Mymensingh Sadar	2.44	2.30	2.78	2.30	2.30	1.85	2.27	2.24
	Nandail	1.79	1.75	1.75	1.72	1.72	1.75	1.73	1.79
	Trishal	2.44	2.10	2.21	2.26	2.26	1.97	2.19	2.19

5.3.2   Analysis on Flood Flow Velocity of Historical Flood Events

The exported RASTER file of flood flow velocity of the area for the historical flood years have been post-processed to prepare maps showing the spatial variation of flood flow velocity on the whole extent of area. Velocities are categorized into five classes that are denoted as (V0), (V1), (V2), (V3) and (V4) with range of the flood depth of 0m/s-0.15m/s, 0.15m/s-0.3m/s , 0.3m/s-0.45m/s 0.45 m/s-0.60 m/s and more than 0.6 m/s respectively. Figure 5.7 (a) (b), (c), (d), (e), (f) and (g) shows the maps showing spatial variation of flood flow velocities on the extent of 31 upazilla for the maximum inundation condition of the year 1988,   1998,   2004,   2007,   2010,   2013,   2016   and   2017   respectively.
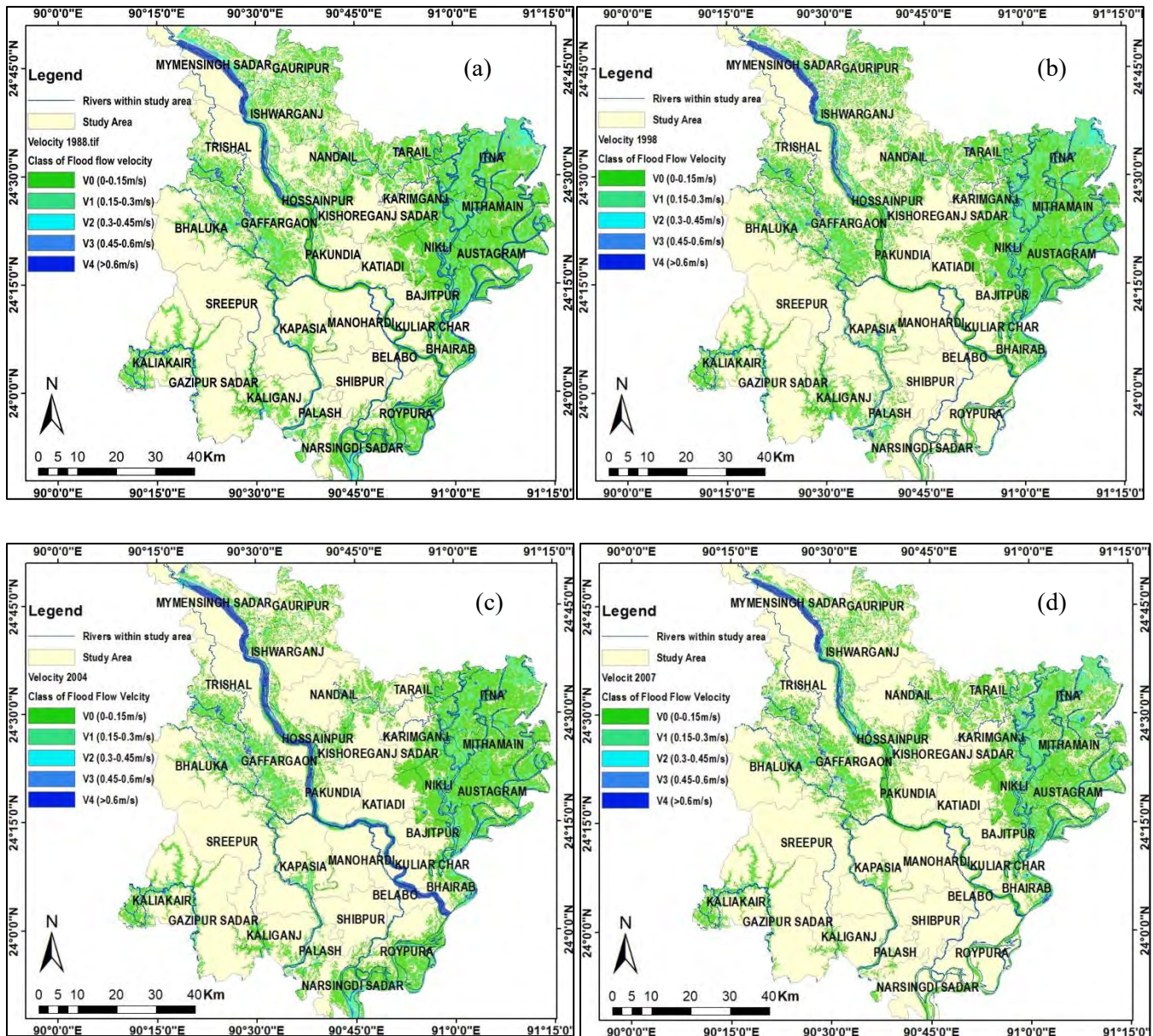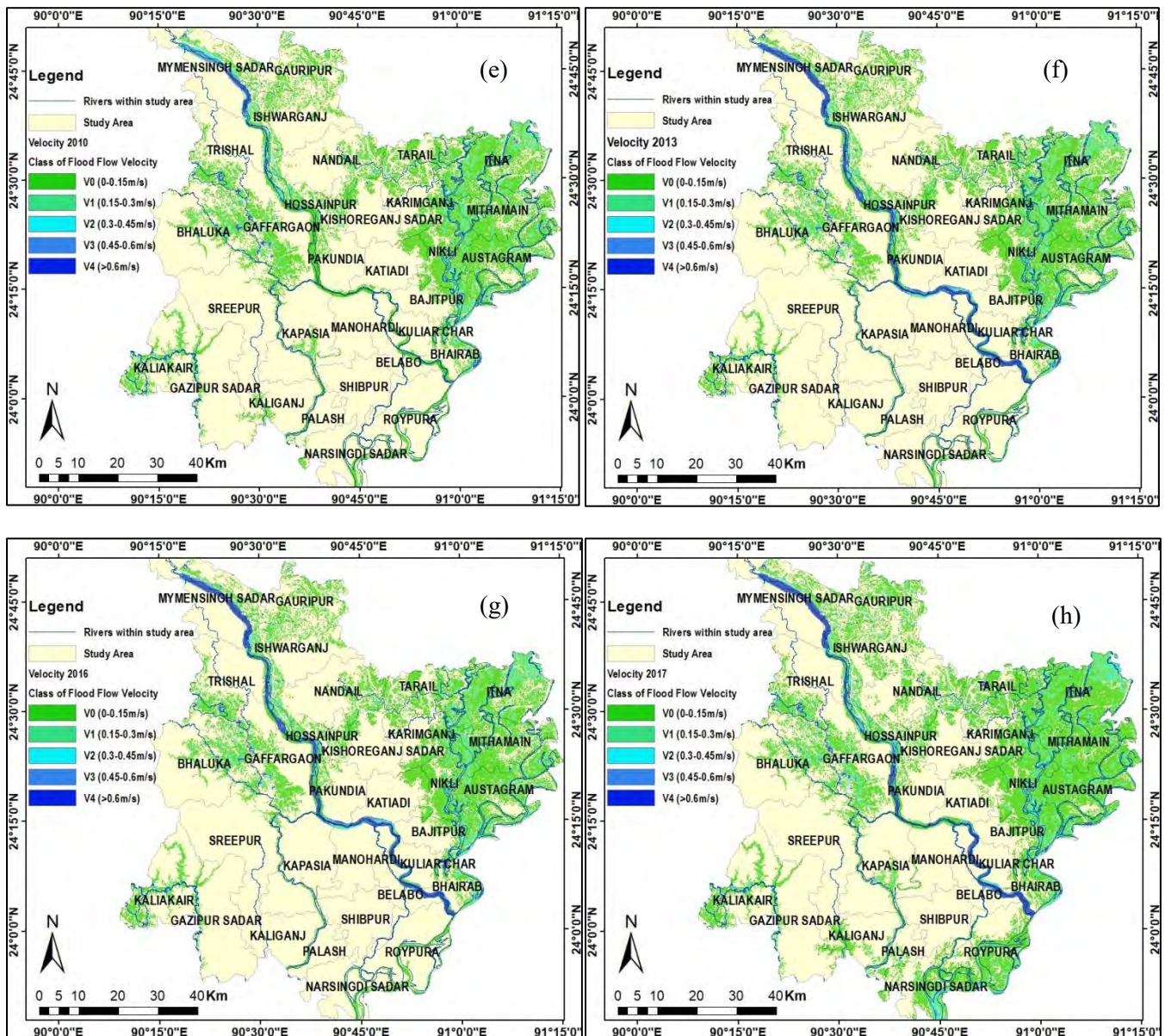
Figure 5.7: Maximum Flood flow velocity maps (a) 1988 (b) 1998, (c) 2004, (d) 2007, (e) 2010, (f) 2013, (g) 2016 and (h) 2017

The mean flood flow velocity observed in each Upazilla for the historical flood years have been presented in Table 5.3. Table 5.3 shows that, almost all the Upazilla experienced maximum flood flow velocity in 1988 and minimum velocity falls to 0 in 2013 among the years considered. Nikli, Pakundia, Kaliakair, Kapasia, Raipura, Austagram, Itna, Kuliar Char, Trishal and Mymensingh upazilla experienced greater flood flow velocity highlighting greater damage potential.

Table 5.3: Mean flood flow velocity observed for the historical flood years

District	Upazilla	Mean Flood Flow Velocity (m/s)							
		1988	1998	2004	2007	2010	2013	2016	2017
Gazipur	Gazipur Sadar	0.126	0.126	0.119	0.083	0.121	0.054	0.056	0.122
	Kaliakair	0.142	0.142	0.129	0.120	0.109	0.017	0.119	0.136
	Kaliganj	0.155	0.155	0.137	0.151	0.130	0.026	0.115	0.142
	Kapasia	0.140	0.140	0.169	0.130	0.138	0.052	0.054	0.145
	Sreepur	0.189	0.189	0.141	0.175	0.146	0.025	0.056	0.151
Narsingdi	Belabo	0.139	0.139	0.157	0.131	0.133	0.080	0.130	0.136
	Monohardi	0.126	0.126	0.096	0.109	0.088	0.004	0.099	0.114
	Narsingdi Sadar	0.155	0.155	0.257	0.143	0.142	0.018	0.138	0.165
	Palash	0.138	0.138	0.127	0.137	0.116	0.005	0.009	0.118
	Raipura	0.100	0.100	0.105	0.093	0.089	0.003	0.092	0.096
	Shibpur	0.132	0.132	0.104	0.100	0.096	0.005	0.106	0.146
Kishoregonj	Austagram	0.144	0.144	0.122	0.127	0.117	0.096	0.127	0.117
	Bajitpur	0.150	0.150	0.162	0.146	0.140	0.008	0.147	0.140
	Bhairab	0.170	0.170	0.149	0.158	0.141	0.009	0.145	0.149
	Hossainpur	0.147	0.147	0.133	0.133	0.133	0.006	0.134	0.145
	Itna	0.169	0.127	0.131	0.095	0.090	0.057	0.166	0.113
	Karimganj	0.176	0.168	0.139	0.105	0.086	0.055	0.064	0.121
	Katiadi	0.100	0.100	0.120	0.099	0.101	0.004	0.093	0.107
	Kishoreganj Sadar	0.156	0.156	0.172	0.165	0.163	0.029	0.183	0.176
	Kuliar Char	0.188	0.188	0.155	0.120	0.110	0.004	0.085	0.140
	Mithamain	0.130	0.130	0.139	0.127	0.135	0.010	0.135	0.132
	Nikli	0.105	0.105	0.118	0.118	0.103	0.006	0.164	0.218
	Pakundia	0.090	0.090	0.077	0.080	0.082	0.000	0.261	0.088
	Tarail	0.100	0.100	0.174	0.004	0.004	0.001	0.194	0.153
Mymensingh	Bhaluka	0.110	0.110	0.118	0.117	0.113	0.031	0.131	0.112
	Gaffargaon	0.178	0.178	0.196	0.233	0.198	0.025	0.149	0.166
	Gauripur	0.110	0.110	0.107	0.098	0.081	0.042	0.086	0.107
	Ishwarganj	0.139	0.139	0.118	0.064	0.064	0.072	0.086	0.119
	Mymensingh Sadar	0.144	0.141	0.117	0.104	0.110	0.090	0.078	0.126
	Nandail	0.273	0.273	0.181	0.146	0.159	0.099	0.086	0.206
	Trishal	0.149	0.149	0.161	0.068	0.054	0.035	0.081	0.158

5.3.3   Analysis on Flood Inundation Area of Historical Flood Events

The exported polygon vector file of flood inundation extent of 31 upazilla for the historical flood years have been post-processed to prepare maps. Figure 5.8 (a) (b), (c), (d), (e), (f) and (g) shows the maps showing flood inundation extent of Old Brahmaputra river floodplain for the maximum inundation condition of the year 198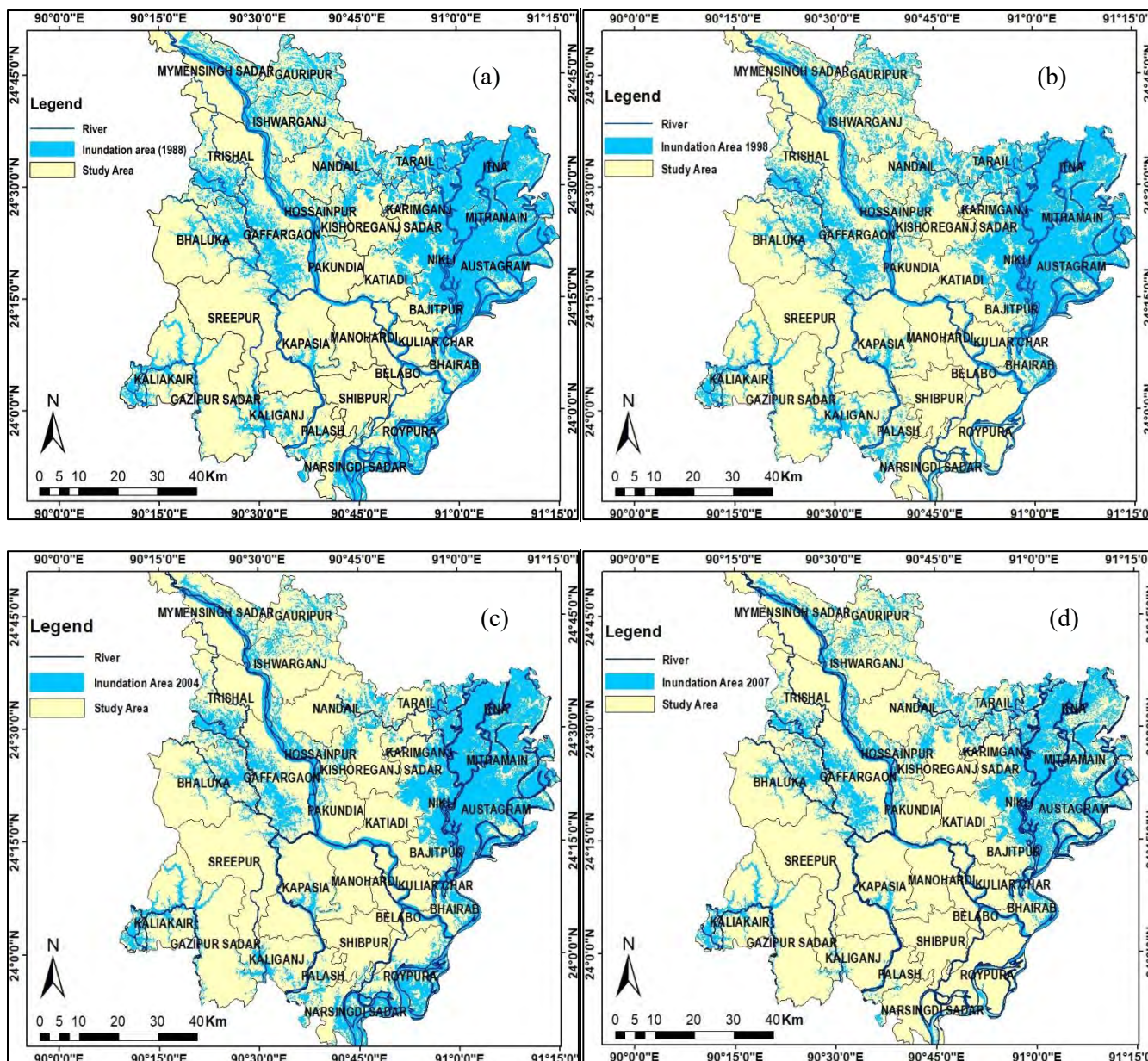8, 1998, 2004, 2007, 2010, 2013, 2016 and 2017 respectively. Comparison on variation of inundation area over the years in each Upazilla for the historical flood years have been presented in Table 5.4 and Table 5.5 represents the percentage area of an Upazilla inundated each year. The study area comprises an area of 8104 km^2. In 1988, total inundation area was 3144 km^2 which is about 39% of the study area. In 1988, total inundation area was 3144 km^2 which is about 39% of the study area. For the years 1998, 2004, 2007, 2010, 2013, 2016 and 2017 total inundation area were obtained as 2764

km², 2534 km², 2080 km², 2080 km², 1611 km², 1947 km² and 2738 km² which are 34, 31%, 26%, 26%, 20%, 24% and 34% respectively. Thus it can be concluded from the analysis on the flood depth, velocity and inundation area that flood induced hazard and related damage was higher for the flood of 1988, 1998 and 2016 and least for the year 2013. This result coincides with the real flood statistics of Bangladesh as well. The flood event of 1998 is considered as the biggest flood event of the twentieth century and the floods of 2007, 2010 and 2013 were not catastrophic.
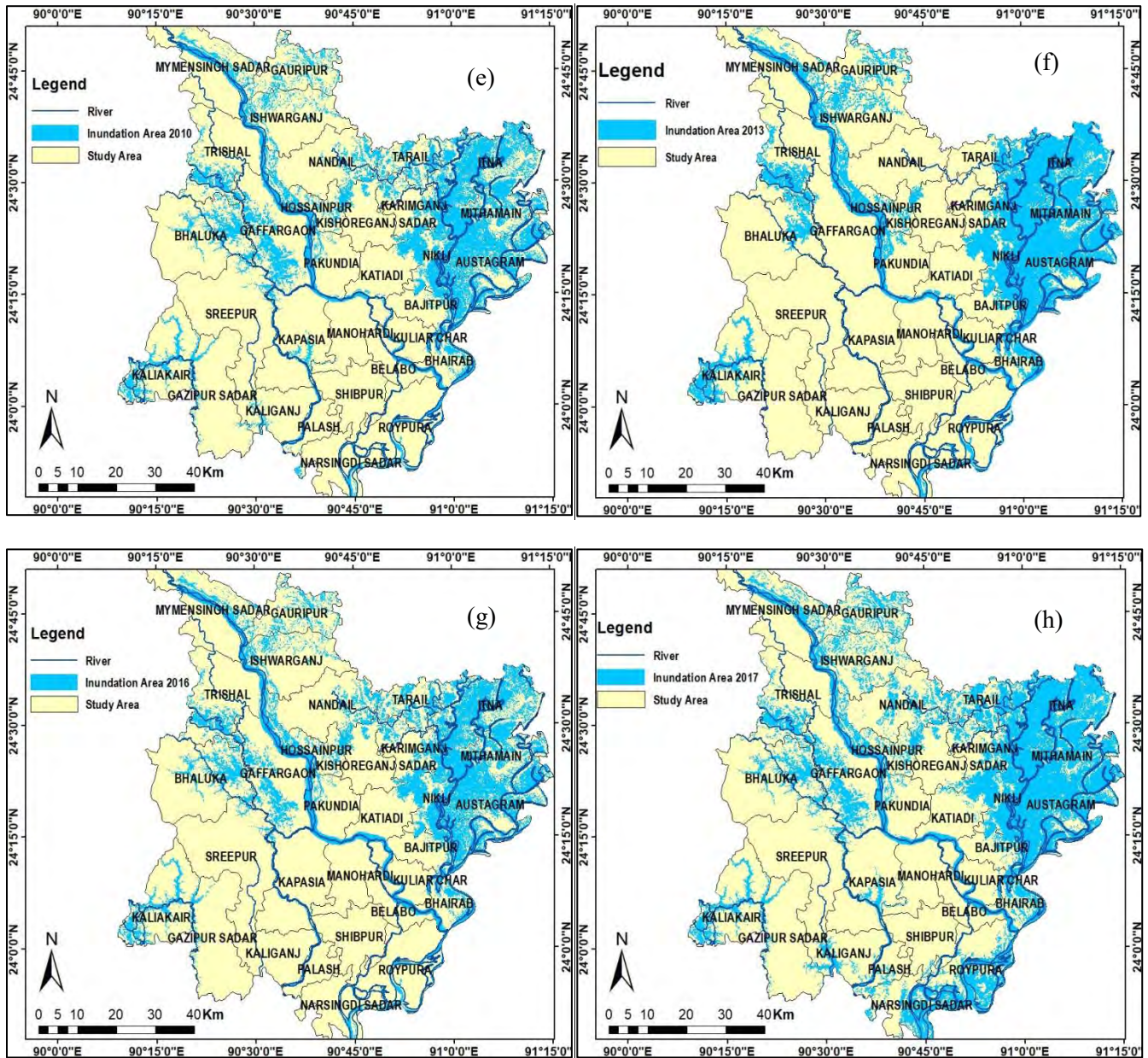
Figure 5.8: Flood inundation extent for the maximum inundation condition of the year (a)1988 (b)1998, (c)2004, (d)2007, (e)2010, (f)2013 (g)2016 and (h)

Table 5.4: Comparison on variation of inundation area over the years in each Upazilla for the historical flood years

District	Upazilla	Inundation Area (sq km)								
		Upazilla Area (sq km)	1988	1998	2004	2007	2010	2013	2016	2017
Gazipur	Gazipur Sadar	458	37.0	40.0	32.2	23.4	23.4	12.5	16.2	26.6
	Kaliakair	314	102.8	102.6	100.1	92.4	92.4	85.5	85.6	96.6
	Kaliganj	215	66.7	81.6	46.7	19.2	19.2	0.0	2.6	40.2
	Kapasia	357	49.1	57.8	44.6	34.3	34.3	0.0	11.9	40.4
	Sreepur	463	38.3	41.9	20.8	19.7	19.7	3.0	14.1	20.3
Narsingdi	Belabo	118	17.7	0.0	0.0	0.0	0.0	0.0	0.0	0.0
	Monohardi	194	10.5	5.5	4.0	2.3	2.3	0.1	0.5	3.7
	Narsingdi Sadar	213	125.4	47.6	123.4	30.8	30.8	22.7	22.9	120.6
	Palash	94	25.2	34.3	25.7	13.2	13.2	0.0	4.4	22.1
	Raipura	313	172.2	38.5	170.2	33.8	33.8	33.4	34.6	170.2
	Shibpur	218	7.8	4.0	7.9	0.2	0.2	0.2	0.1	7.8
Kishoreganj	Austagram	356	263.8	263.7	257.3	223.4	223.4	219.6	219.9	263.7
	Bajitpur	194	102.2	101.7	95.2	82.8	82.8	81.3	81.7	99.7
	Bhairab	139	76.0	65.8	57.9	48.1	48.1	46.2	47.0	65.8
	Hossainpur	121	54.2	51.5	46.3	46.7	46.7	39.2	46.4	51.0
	Itna	402	345.4	343.6	339.5	292.5	292.5	284.5	285.4	343.5
	Karimganj	201	103.9	103.7	83.1	84.3	84.3	64.3	83.8	101.7
	Katiadi	219	66.4	53.1	28.2	24.4	24.4	24.2	24.3	39.1
	Kishoreganj Sadar	194	29.1	28.4	17.7	19.7	19.7	9.0	19.5	27.2
	Kuliar Char	104	14.4	6.4	5.4	4.1	4.1	4.0	4.0	6.2
	Mithamain	223	192.7	192.7	189.0	155.7	155.7	153.5	153.8	192.7
	Nikli	214	174.6	174.6	169.9	155.7	155.7	154.5	154.7	171.9
	Pakundia	181	35.8	17.8	17.1	14.9	14.9	13.5	16.8	18.1
	Tarail	141	91.6	89.9	38.2	69.6	69.6	19.7	67.9	88.6
Mymensingh	Bhaluka	444	108.9	107.6	103.7	101.4	101.4	75.6	97.4	101.8
	Gaffargaon	401	228.8	189.3	151.9	141.0	141.0	19.2	111.2	145.0
	Gauripur	274	122.1	113.5	76.6	79.8	79.8	64.7	78.0	109.8
	Ishwarganj	286	137.6	119.8	69.5	71.0	71.0	60.0	70.8	111.8
	Mymensingh Sadar	388	103.3	61.9	47.2	43.1	43.1	36.9	43.3	58.2
	Nandail	326	137.9	132.5	73.6	78.3	78.3	19.8	76.8	112.5
	Trishal	339	103.0	92.0	91.6	74.2	74.2	63.7	70.6	80.9
Total inundated Area		8104	3144	2764	2534	2080	2080	1611	1947	2738

Table 5.5: Percentage area of an Upazilla inundated for the historical flood years

District	Upazilla	% of Upazilla Inundated							
		1988	1998	2004	2007	2010	2013	2016	2017
	Gazipur Sadar	8.1	8.7	7.0	5.1	5.1	2.7	3.5	5.8
	Kaliakair	32.7	32.7	31.9	29.4	29.4	27.2	27.3	30.7
	Kaliganj	31.1	38.0	21.8	9.0	9.0	0.0	1.2	18.8
	Kapasia	13.8	16.2	12.5	9.6	9.6	0.0	3.3	11.3
Gazipur	Sreepur	8.3	9.1	4.5	4.2	4.2	0.7	3.1	4.4
	Belabo	15.0	0.0	0.0	0.0	0.0	0.0	0.0	0.0
	Monohardi	5.4	2.9	2.1	1.2	1.2	0.1	0.2	1.9
	Narsingdi Sadar	58.7	22.3	57.8	14.4	14.4	10.6	10.7	56.5
	Palash	26.7	36.3	27.2	14.0	14.0	0.0	4.6	23.4
	Raipura	55.0	12.3	54.4	10.8	10.8	10.7	11.1	54.4
Narsingdi	Shibpur	3.6	1.8	3.6	0.1	0.1	0.1	0.1	3.6
	Austagram	74.2	74.2	72.4	62.8	62.8	61.8	61.8	74.2
	Bajitpur	52.7	52.5	49.1	42.7	42.7	41.9	42.2	51.4
	Bhairab	54.5	47.2	41.6	34.5	34.5	33.1	33.8	47.2
	Hossainpur	44.7	42.4	38.2	38.5	38.5	32.3	38.3	42.0
	Itna	85.9	85.5	84.5	72.8	72.8	70.8	71.0	85.5
	Karimganj	51.8	51.7	41.4	42.0	42.0	32.1	41.8	50.7
	Katiadi	30.3	24.2	12.9	11.1	11.1	11.0	11.1	17.8
	Kishoreganj Sadar	15.0	14.7	9.1	10.2	10.2	4.6	10.1	14.0
	Kuliar Char	13.9	6.2	5.2	3.9	3.9	3.8	3.8	6.0
	Mithamain	86.5	86.4	84.8	69.8	69.8	68.8	69.0	86.4
	Nikli	81.5	81.4	79.2	72.6	72.6	72.1	72.1	80.2
	Pakundia	19.8	9.9	9.5	8.3	8.3	7.5	9.3	10.0
Kishoreganj	Tarail	64.8	63.5	27.0	49.2	49.2	13.9	48.0	62.6
	Bhaluka	24.5	24.2	23.3	22.8	22.8	17.0	21.9	22.9
	Gaffargaon	57.0	47.2	37.9	35.1	35.1	4.8	27.7	36.1
	Gauripur	44.5	41.4	27.9	29.1	29.1	23.6	28.5	40.1
	Ishwarganj	48.1	41.8	24.3	24.8	24.8	21.0	24.7	39.1
	Mymensingh Sadar	26.6	15.9	12.1	11.1	11.1	9.5	11.2	15.0
	Nandail	42.3	40.6	22.6	24.0	24.0	6.1	23.6	34.5
Mymensingh	Trishal	30.4	27.2	27.0	21.9	21.9	18.8	20.8	23.9

5.4   Analysis on Future Flood Events

5.4.1   Analysis on Future Flood Inundation Depth under Climate Change Scenario of RCP 8.5

The flood inundation maps of base period, 2020s, 2050s and 2080s for RCP 8.5 scenario are shown in Figure. 5.8. In these inundation maps, flood depths are classified in 5 classes: F0 (0-0.3m), F1 (0.3m-0.9m), F3 (0.9m-1.8m), F4 (1.8m-3.6m) and F4 (>3.6m) as adapted for the historical flood depth mapping. Comparison on the classified flood maps of different time regime shows that, there is an increasing trend of flood depth from baseline to 2080s as the flood depth mapping turns more bluish as we move to future. Table 5.6 represents the mean flood depth for the baseline, 2020s, 2050s and 2080s respectively of RCP

8.5 climate change scenario. Table 5.6 shows that from baseline to 2080s, the mean flood depth that the upazilla might experience in future increases but the increment is less significant form baseline to 2020s but the increase of depth from baseline to 2050s and 2080s is prominent. According to the produced predicted mean flood depth flood depth can be as high as 4.16 that Itna Upazilla might experience in 2080s.
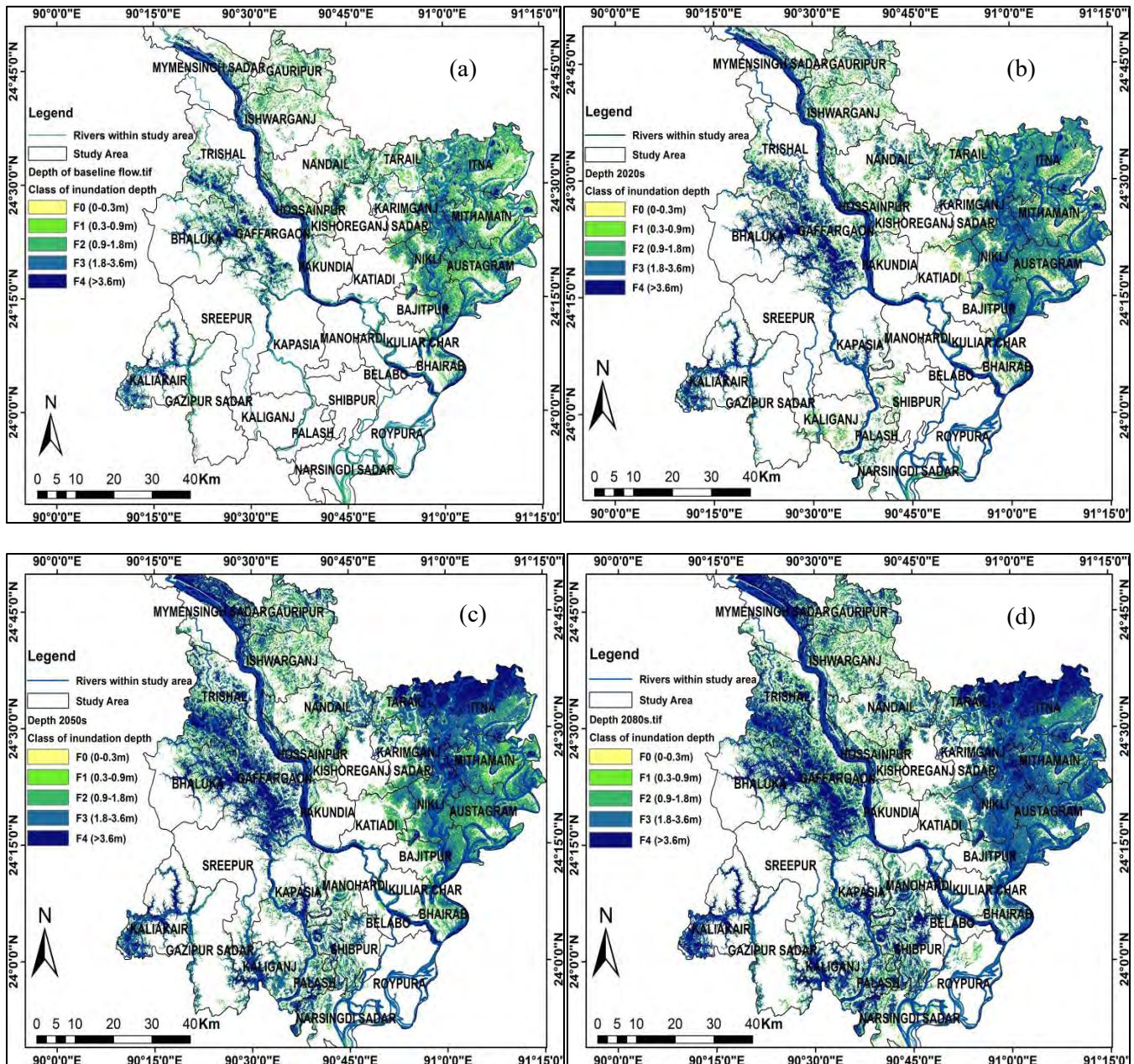

Figure 5.9: Flood inundation maps for RCP 8.5 scenario (a) baseline period (b) 2020s (c) 2050s and (d) 2080s

Table 5.6: Mean flood depth for the baseline, 2020s, 2050s and 2080s for climate change scenario of RCP 8.5

| District | Upazilla | Mean Flood Depth (m) for RCP 8.5 | | | |
		Base line Flow	2020s	2050s	2080s
Gazipur	Gazipur Sadar	1.10	1.45	2.19	2.49
	Kaliakair	2.01	2.63	3.12	3.83
	Kaliganj	0.89	1.16	2.62	2.94
	Kapasia	2.01	2.21	2.75	3.03
	Sreepur	2.17	2.31	2.67	2.69
Narsingdi	Belabo	1.40	1.75	1.87	3.53
	Monohardi	1.22	1.65	2.26	2.61
	Narsingdi Sadar	1.02	1.48	2.18	2.43
	Palash	1.85	1.88	2.35	2.76
	Raipura	1.91	1.91	2.72	2.96
	Shibpur	1.19	1.57	2.20	2.89
Kishoregonj	Austagram	1.64	2.00	2.34	2.67
	Bajitpur	2.02	2.38	2.73	3.00
	Bhairab	2.40	2.54	2.92	3.15
	Hossainpur	1.23	1.82	1.95	2.53
	Itna	1.56	1.94	3.95	4.16
	Karimganj	1.58	1.96	2.38	2.60
	Katiadi	1.18	1.38	1.79	2.30
	Kishoreganj Sadar	1.38	1.66	2.20	2.57
	Kuliar Char	2.71	2.80	3.44	4.00
	Mithamain	1.80	1.88	2.34	2.76
	Nikli	2.26	2.42	2.80	3.07
	Pakundia	1.42	1.62	1.64	1.68
	Tarail	1.27	1.55	3.01	3.20
Mymensingh	Bhaluka	2.56	2.76	3.21	3.43
	Gaffargaon	2.21	2.89	3.23	3.48
	Gauripur	1.38	1.52	1.94	2.18
	Ishwarganj	1.51	1.61	1.83	1.93
	Mymensingh Sadar	1.98	2.23	3.47	3.80
	Nandail	1.68	1.80	1.87	1.87
	Trishal	1.86	2.15	2.86	2.98

5.4.2   Analysis on Future Flow Velocity under Climate Scenario of RCP 8.5

The exported RASTER files of flood flow velocity of the study area for base period, 2020s, 2050s and 2080s for RCP 8.5 scenario have been post-processed to prepare maps showing the spatial variation of flood flow velocity on the floodplain. The maps are shown in Figure. 5.9. Velocities are categorized into five classes that are denoted as (V0), (V1), (V2), (V3) and (V4) with range of the flood depth of 0m/s-0.15m/s, 0.15m/s-0.3m/s , 0.3m/s-0.45m/s 0.45 m/s-0.60 m/s and more than 0.6 m/s respectively as adapted for the historical flood flow velocity mapping. Careful observation on the classified flood flow velocity maps of different time regime shows that, there is an increasing trend of flood velocity from baseline to 2080s.
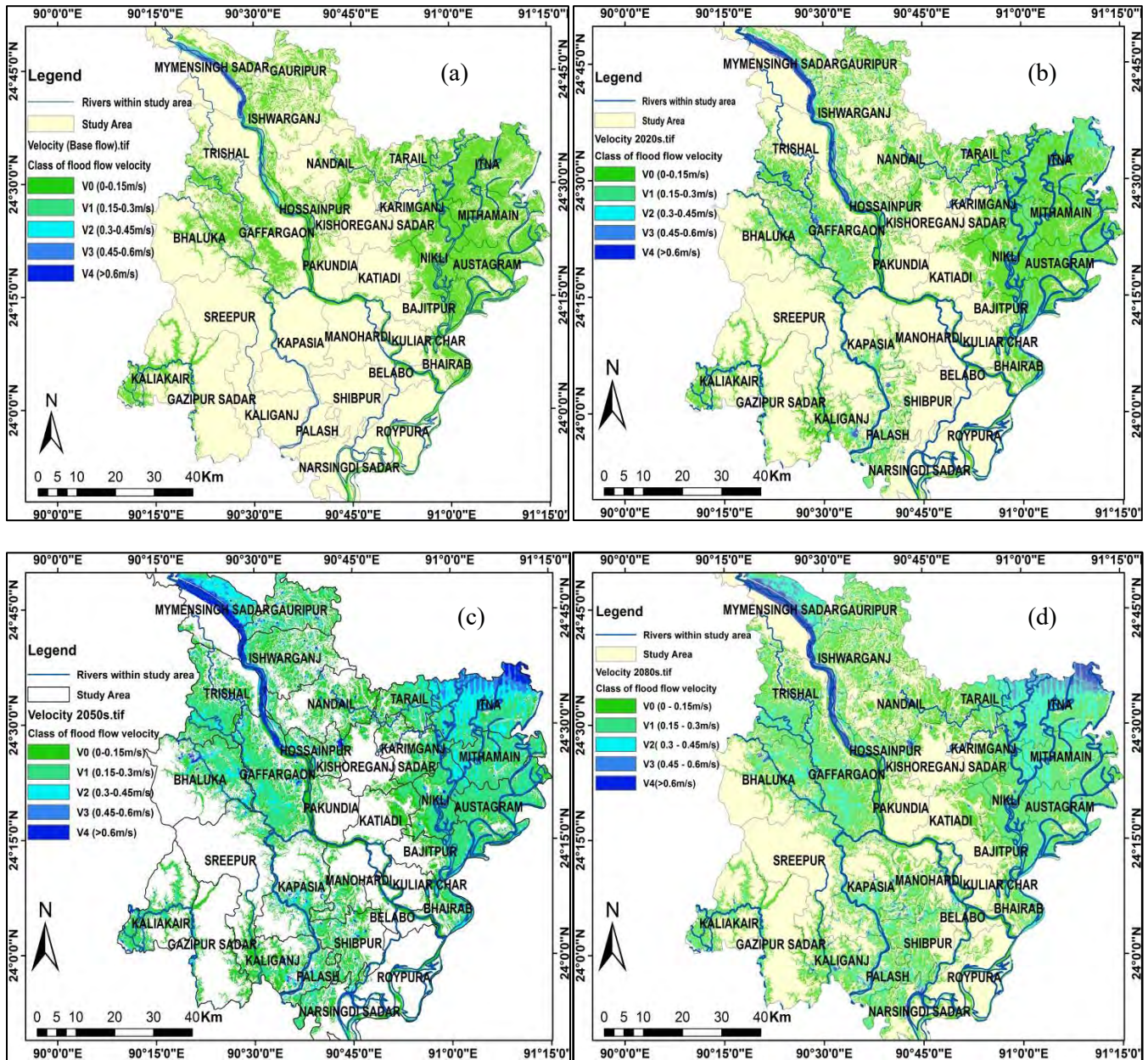
Figure 5.10: Flood flow velocity maps of base period, 2020s, 2050s and 2080s for RCP 8.5 scenario

Table 5.7 represents the mean flood flow velocity of the upazilla within study area for the baseline, 2020s, 2050s and 2080s respectively of RCP 8.5 climate change scenario. Table 5.7 shows that from baseline to 2080s, the mean flood flow velocity that the upazilla might experience in future increases but the increment is less significant form baseline to 2020s but the increase of flow velocity from baseline to 2050s and 2080s is prominent. According to the produced predicted mean flood flow velocity flood flow velocity can be as high as 0.493 that Mymensingh Sadar Upazilla might experience in 2080s depicting increased plausibility of damage potential for the infrastructures on the floodplain and erosion.

Table 5.7: Mean flood flow velocity for the baseline, 2020s, 2050s and 2080s for climate change scenario of RCP 8.5

District	Upazilla	Mean Flood Velocity(m/s) for RCP 8.5			
		Base flow	2020s	2050s	2080s
Gazipur	Gazipur Sadar	0.044	0.067	0.129	0.256
	Kaliakair	0.015	0.124	0.262	0.342
	Kaliganj	0.090	0.136	0.160	0.290
	Kapasia	0.070	0.145	0.205	0.272
	Sreepur	0.009	0.011	0.200	0.217
Narsingdi	Belabo	0.063	0.138	0.251	0.376
	Monohardi	0.004	0.098	0.138	0.205
	Narsingdi Sadar	0.056	0.093	0.205	0.255
	Palash	0.015	0.038	0.228	0.237
	Raipura	0.030	0.030	0.211	0.231
	Shibpur	0.030	0.080	0.118	0.215
Kishoreganj	Austagram	0.097	0.118	0.224	0.290
	Bajitpur	0.094	0.158	0.222	0.320
	Bhairab	0.009	0.100	0.225	0.243
	Hossainpur	0.027	0.132	0.235	0.234
	Itna	0.084	0.151	0.369	0.383
	Karimganj	0.087	0.110	0.179	0.229
	Katiadi	0.009	0.092	0.116	0.139
	Kishoreganj Sadar	0.046	0.115	0.168	0.186
	Kuliar Char	0.010	0.052	0.180	0.195
	Mithamain	0.093	0.018	0.247	0.256
	Nikli	0.065	0.111	0.227	0.290
	Pakundia	0.009	0.079	0.113	0.115
	Tarail	0.038	0.102	0.204	0.290
Mymensingh	Bhaluka	0.089	0.101	0.230	0.236
	Gaffargaon	0.092	0.102	0.219	0.294
	Gauripur	0.072	0.104	0.213	0.216
	Ishwarganj	0.043	0.090	0.119	0.199
	Mymensingh Sadar	0.117	0.177	0.459	0.493
	Nandail	0.094	0.140	0.161	0.266
	Trishal	0.088	0.103	0.203	0.244

5.4.3 Analysis on Future Flood Inundation Extent under Climate Change Scenario of RCP 8.5

The exported polygon vector file of flood inundation extent of 31 Upazilla for base period, 2020s and 2080s for RCP 8.5 scenario have been post-processed to prepare maps. Figure 5.10 (a) (b), (c), and (d) show the maps showing flood inundation extent for the base and future time regime. Comparison on variation of inundation area over the years in each Upazilla for the future time regime have been presented in Table 5.8 including the percentage area of an Upazilla inundated as well. Table 5.8 shows that from baseline to 2020s, the total inundation area extended from 1975 km^2 to 2595 km^2 which are 24% and 32% of the total study area. In 2050s and 2080s the inundation extend may extend to 3555 km^2 and 3923 km^2 that are around 44% and 48% of the total study area.
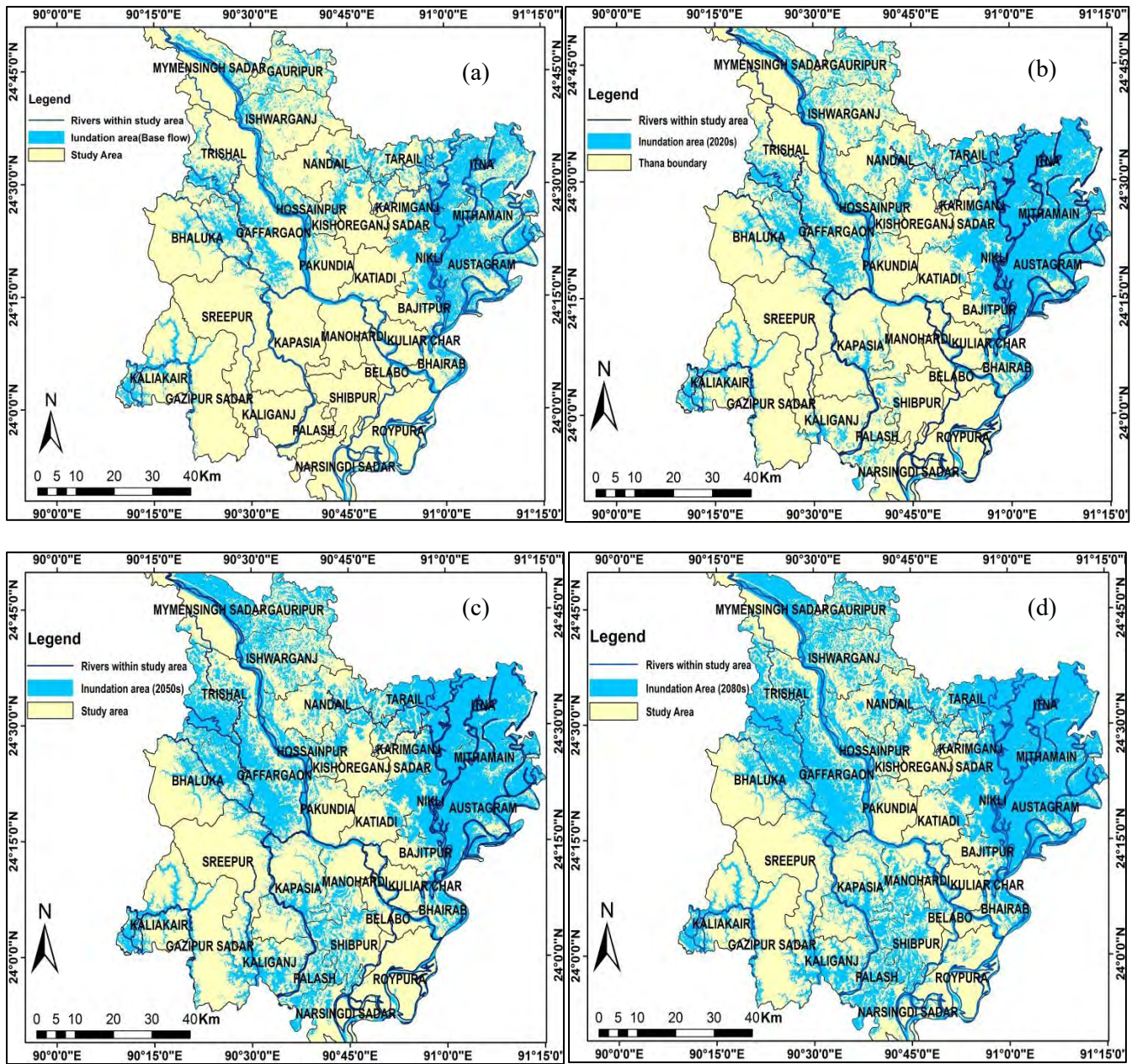
Figure 5.11: Flood inundation extent maps for baseline period, 2020s, 2050s and 2080s for RCP 8.5 scenario

Table 5.8: Comparison on variation of inundation extent area in each Upazilla for baseline period, 2020s, 2050s and 2080s for RCP 8.5 scenario

District	Upazilla	Base line Flow		2020s		2050		2080	
		Inundated Area (sq km)	% of Upazilla inundated	Inundation Area (sq km)	% of Upazilla inundated	Inundation Area (sq km)	% of Upazilla inundated	Inundation Area (sq km)	% of Upazilla inundated
Gazipur	Gazipur Sadar	19.9	4.4	27.0	5.9	57.3	12.5	61.9	13.5
	Kaliakair	80.0	25.5	93.8	29.8	117.9	37.5	122.4	39.0
	Kaliganj	0.1	0.1	46.3	21.6	107.3	50.0	118.6	55.3
	Kapasia	8.0	2.2	53.9	15.1	118.2	33.1	152.6	42.7
	Sreepur	15.6	3.4	18.9	4.1	66.1	14.3	78.4	16.9
Narsingdi	Belabo	0.1	0.1	0.1	0.1	9.0	7.6	28.7	24.3
	Monohardi	0.1	0.1	7.7	4.0	56.0	28.9	96.2	49.6
	Sadar	22.8	10.7	46.5	21.8	79.2	37.1	102.4	48.0
	Palash	0.1	0.1	28.9	30.6	58.3	61.7	65.8	69.7
	Raipura	34.1	10.9	34.1	10.9	42.6	13.6	69.5	22.2
	Shibpur	14.8	6.8	20.8	9.5	109.6	50.3	133.8	61.5
Kishoreganj	Austagram	221.1	62.2	243.6	68.5	263.7	74.2	266.8	75.0
	Bajitpur	76.0	39.2	99.3	51.2	101.8	52.5	103.2	53.3
	Bhairab	47.4	34.0	46.4	33.3	65.8	47.2	67.5	48.5
	Hossainpur	49.9	41.1	50.9	41.9	60.7	50.0	63.0	52.0
	Itna	287.0	71.4	343.3	85.4	362.5	90.2	367.0	91.3
	Karimganj	81.2	40.5	101.6	50.7	104.6	52.2	109.7	54.7
	Katiadi	24.2	11.0	43.9	20.0	52.9	24.1	66.4	30.3
	Kishoreganj Sadar	20.0	10.3	27.5	14.2	29.1	15.0	31.6	16.3
	Kuliar Char	4.0	3.8	6.1	5.9	6.4	6.2	7.1	6.8
	Mithamain	154.3	69.2	192.7	86.4	192.9	86.5	198.8	89.2
	Nikli	155.0	72.3	171.8	80.2	174.6	81.5	176.8	82.4
	Pakundia	15.3	8.5	16.7	9.2	17.9	9.9	18.2	10.1
	Tarail	57.0	40.3	88.3	62.4	108.2	76.5	111.8	79.0
Mymensingh	Bhaluka	101.4	22.8	120.1	27.0	168.1	37.8	178.6	40.2
	Gaffargaon	121.0	30.1	192.5	48.0	258.6	64.5	287.4	71.6
	Gauripur	85.7	31.3	99.6	36.4	139.1	50.8	145.2	53.0
	Ishwarganj	77.8	27.2	104.7	36.6	151.7	53.0	168.5	58.9
	Mymensingh Sadar	46.1	11.9	57.5	14.8	123.3	31.7	128.9	33.2
	Nandail	82.4	25.3	116.9	35.8	143.9	44.1	168.7	51.7
	Trishal	73.0	21.5	93.6	27.6	207.9	61.3	227.3	67.0
Total inundated Area		1975		2595		3555		3923	

5.4.4 Hazard and Risk Assessment of Old Brahmaputra River Floodplain under Climate Change Scenario of RCP 8.5

5.4.4.1 Flood Hazard Assessment for RCP 8.5 Scenario

In this study, the flood depth, flood flow velocity and percent of an upazilla inundated are considered as the flood hazard indicators. Mean flood depth, mean flood flow velocity and percentage of an Upazilla inundated are calculated for each of the Upazilla of the study area for baseline, 2020s, 2050s and 2080s.

The mean flood depth varies from 0.89m to 4.16m from the baseline flow to 2080s for RCP 8.5 climate change scenario. For the mean flood flow velocity the values varied from 0.004m/s to 0.383m/s. Values of the percent of Upazilla inundated varied from 0.1% to 91.3%. To assign weights to the three hazard indicators principal component analysis (PCA) has been conducted with the normalized values of the indicators. Hazard indicators are normalized in a range of 1 to 100 using Equation (4.5) as discussed earlier. Using the normalized values of the indicators and corresponding weights hazard for each upazilla calculated using Equation (4.6). Table 5.9 presents the indicators of flood hazard.

Table 5.9: Weights of the Hazard Indicators

Component	Name of the Indicator	Weight
Flood Hazard	Flood depth	0.44
	Flood flow velocity	0.20
	Percent of Upazilla Inundated	0.36

For preparing zone-wise flood hazard maps, the study area is categorized into five hazard zones – 0 to 20, 20 to 40, 40 to 60, 60 to 80 and 80 to 100 named as Very Low, Low, Medium, High and Very High hazard zones. The spatio-temporal change of different hazard zones of 31 selected upazilla for RCP 8.5 scenario is shown in Appendix B. Analyses on the flood hazard show that in baseline period, Gazipur Sadar, Kaliganj, Shibpur, Belabo, Katiadi, Pakundia, Kishoreganj Sadar, Narsigdi Sadar, Manohardi were in the very low hazard zone. Gauripur, Trishal, Ishwarganj, Nandail, Tarail, Karimganj, Sreepur, Kapasia, Hossainpur, Palash and Raipura fall into the low hazard zone initially. Mymensingh Sadar, Bhaluka, Gaffargaon, Kaliakair, Itna, Mithamain, Austagram, Bajitpur, Kuliar Char and Bhiarab are within the medium hazard zone in baseline period. Only Nikli upazilla lies within the high hazard zone and there is no administrative unit within the very high hazard zone in baseline period. In 2020s, Narsingdi Sadar jumps to the low hazard category from very low hazard type, Trishal and Karimganj upazilla jump into the medium hazard zone from the low hazard type and Gaffargaon and Itna jumps into the high hazard category from the medium hazard zone. There is still no administrative unit in the very high hazard class in 2020s. As we move to the 2050s, we see from the hazard map that, Mymensingh Sadar and Tarail upazilla devolve to the high hazard zone from medium and low hazard zone respectively. Itna upazilla further degrades to the very high hazard zone from the high hazard zone in 2050s.Ultimately in 2080s, only the Kishoreganj Sadar and Pakundia upazilla are within the very low hazard zone. Gauripur, Ishwarganj, Nandail, Hossainpur, Katiadi, Sreepur, Manohardi, Kuliar Char, Raipura, Narsingdi Sadar and Gazipur Sadar lie within the low hazard zone. Trishal, Bhaluka, Kaliakair, Kapasia, Kaliganj, Palash,

Shibpur, Belabo, Bhiarab, Bajitpur, Austagram, Mithamain and Karimganj lie within the medium hazard class. Mymensingh, Gaffargaon, Tarail and Nikli are in the high hazard class and only Itna upazilla comprises the very high hazard category. The finding indicates that, most of the administrative units have been degrading to 1 or 2 categories in the 2020s, 2050s and 2080s for the RCP 8.5 climate change scenario. Figure 5.12 shows the hazard maps for the Old Brahmaputra floodplain for RCP 8.5 scenario.
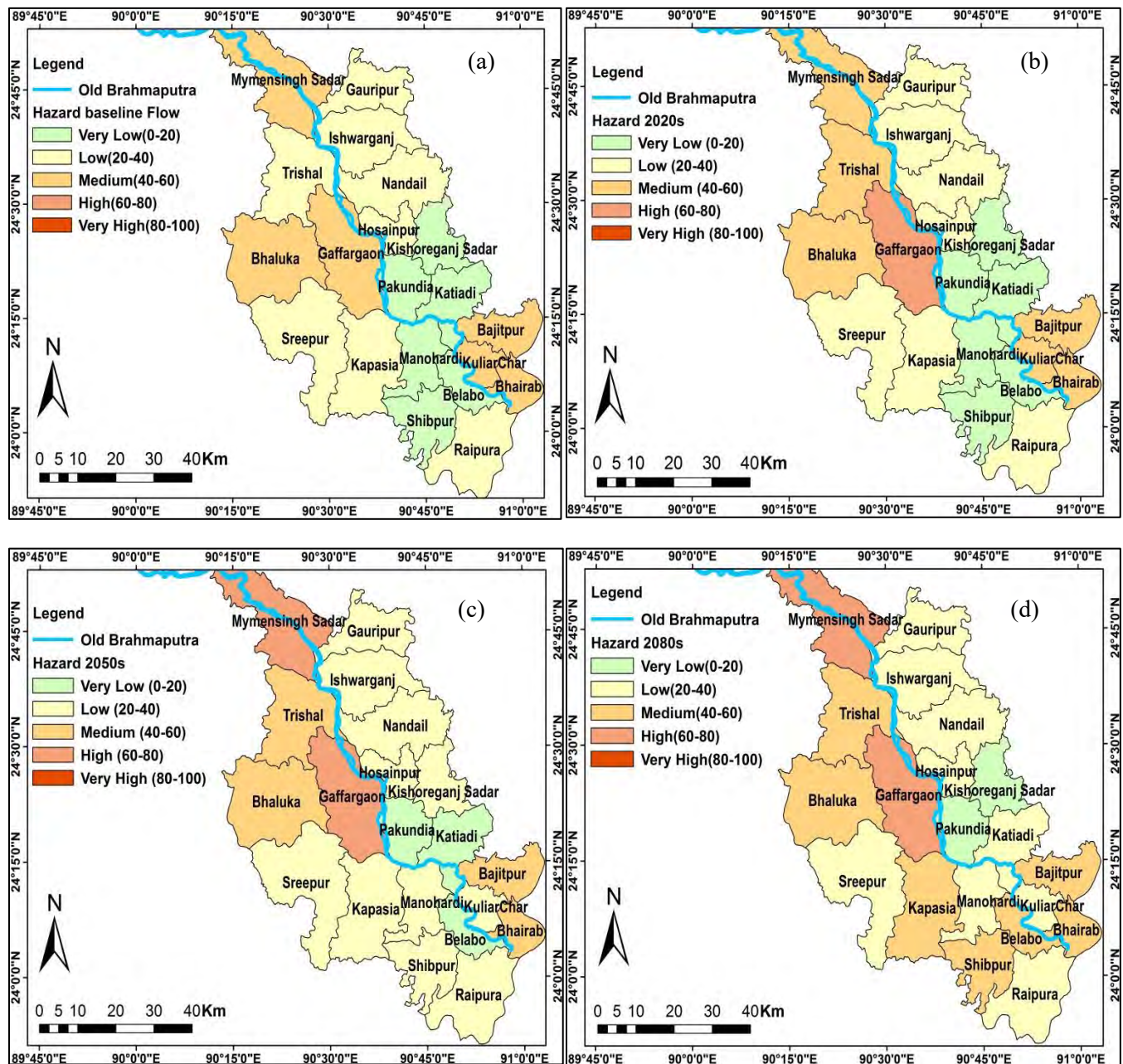

Figure 5.12: Flood hazard maps of Old Brahmaputra river floodplain for RCP 8.5 Climate Scenario (a) Baseline period (b) 2020s (c) 2050s and (d) 2080s

In baseline period, among the 19 districts within the Old Brahmaputra floodplain, there is no high and very high hazard zone. Gaffargaon, Bhaluka, Mymensingh Sadar, Bajitpur and Bhairab are comparatively higher in hazard magnitude relative to others. In 2020s, Gaffargaon degraded to high hazard zone and remained into this category for the late century. Mymensingh Sadar degraded to the high hazard zone in 2050s and remained in high hazard class for the late of the century.

The percentage area under different hazard zones for RCP 8.5 Scenario has been presented in Table 5.10. Table 5.10 shows that at baseline flow condition 25%, 36%, 36% and 3% area lie in the very low, low, medium and high hazard zone respectively. For the baseline condition there is no area under very high hazard category. However, in 2020s, the very low, low and medium hazard zone got reduced to 22%, 32% and 33% respectively whereas the high hazard zone rises to 13%. There is still no area under very high hazard category for the 2020s. In 2050s, the percent area within very low hazard zone gets reduced to 12% comparing with the value of 2020s and the percent area in low hazard zone gets increased to 38% representing shifting of few Upazilla from very low category to low category of hazard. Percent area within medium hazard zone gets reduced to 31% whereas percent area within high hazard zone gets increased to 14%. In 2050s, 5% of total study area underlies within very high flood hazard zone. In 2080s, both the values of percent area in very low and low hazard zone get reduced leading to a significant increase in percent area of medium hazard zone. High and very high hazard zones remain stable comparing to the 2050s. Results interpret the fact that in late century, climate change will decrease the very low and low hazard zone drastically and medium, high and very high hazard zone will experience significant rise due to climate change induced increased inflow compared to the baseline flow.

Table 5.10: Percentage of Area under different hazard zones for different projections of RCP 8.5

Component	Time period	Categorization									
		Very Low		Low		Medium		High		Very High	
		Area (sq km)	% Area	Area (sq km)	% Area	Area (sq km)	% Area	Area (sq km)	% Area	Area (sq km)	% Area
Hazard	Base Line	2008.72	25	2915.73	36	2965.30	36	214.39	3	0.00	0
	2020s	1795.28	22	2589.69	32	2701.67	33	1017.50	13	0.00	0
	2050s	791.94	12	3063.15	38	2701.67	31	1145.44	14	401.93	5
	2080s	374.26	5	2971.61	36	3210.89	40	1145.44	14	401.93	5

5.5   Assessment of Vulnerability for Present and Future Projected Socio-Economic Regime

5.5.1   Assessment of Sensitivity for Present and Future Projected Socio-Economic Regime

The Upazila-wise data of the 14 selected indicators of sensitivity from the available population and agricultural census reports of 2011, 2001, 1991, 1981 and others have been collected, processed and analyzed to obtain the value of all the sensitivity indicators for 2011, 2020s, 2050s and 2080s. The indicator values are then normalized in a range of 1 to 100 by the early mentioned Equation 4.5. Using the weights of the particular indicators and domain weights sensitivity value of each upazilla for 2011, 2020s, 2050s and 2080s have been calculated from Equation 4.7 and Equation 4.8.

Figure 5.13 (a), (b), (c) and (d) show the relative sensitivity of the upazillas of Gazipur, Narsingdi, Kishoreganj and Mymensingh district respectively. Figure 5.13 (a) shows that among the five upazilla of Gazipur district Gazipur Sadar is the most sensitive upazilla and Kaliganj is the least sensitive for present and future time regime. Figure 5.13 (b) shows that among the six upazilla of Narsingdi district Narsingdi Sadar is the most sensitive upazilla and Palash is the least sensitive. Figure 5.13 (c) shows among the thirteen upazilla of Kishoreganj district Austagram has been found as the most sensitive and Mithamain was the least sensitive upazilla for the present and future projected socio-economic scenario. According to the Figure 5.13 (d) shows among the upazilla of Mymensingh district, Gaffargaon is the highest sensitive upazilla and Tarail is the least sensitive.

Sensitivity maps were generated for the study area for present and future projected socio-economic condition using five categories and an equal interval for the normalized sensitivity values. The specified five categories are Very Low, Low, Medium, High and Very High sensitive zones for the normalized value range 0-20, 20-40, 40-60, 60-80 and 80-100 respectively. Figure 5.14 shows the sensitivity maps for socio-economic regime of present, 2020s, 2050s and 2080s. The maps were then compared and analyzed for identification of administrative units under different sensitivity categories as shown in Table 5.11.
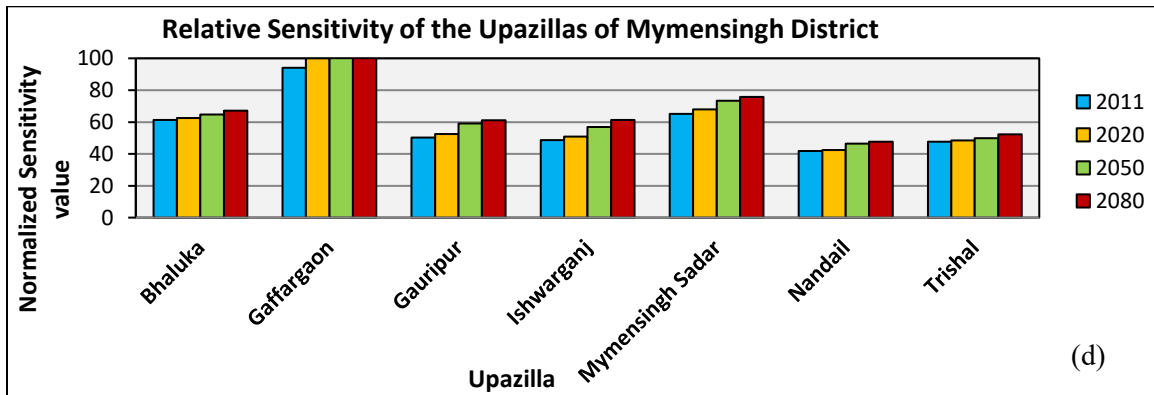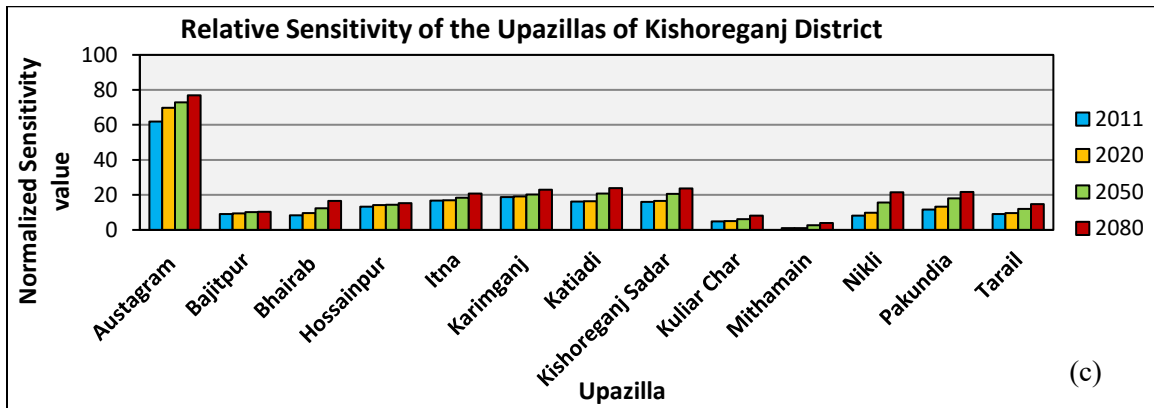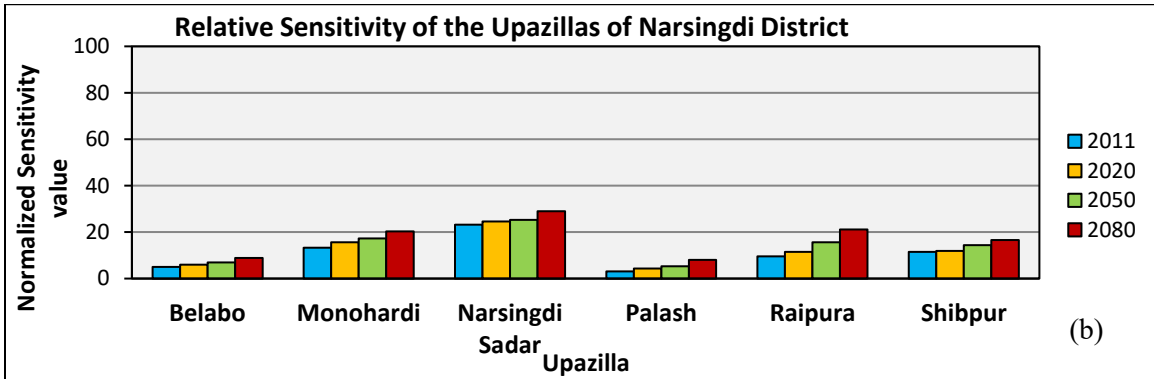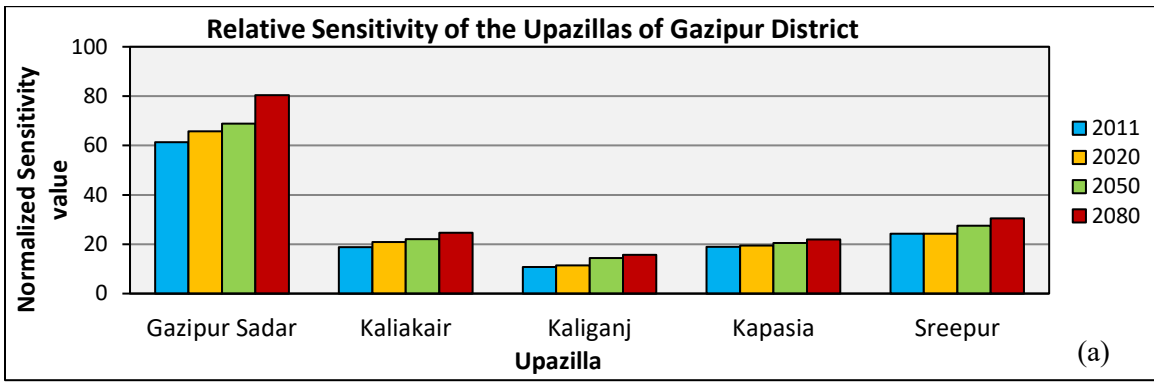
Figure 5.13: Relative sensitivity of the upazillas of (a) Gazipur (b) Narsingdi (c) Kishoreganj and (d) Mymensingh district

113
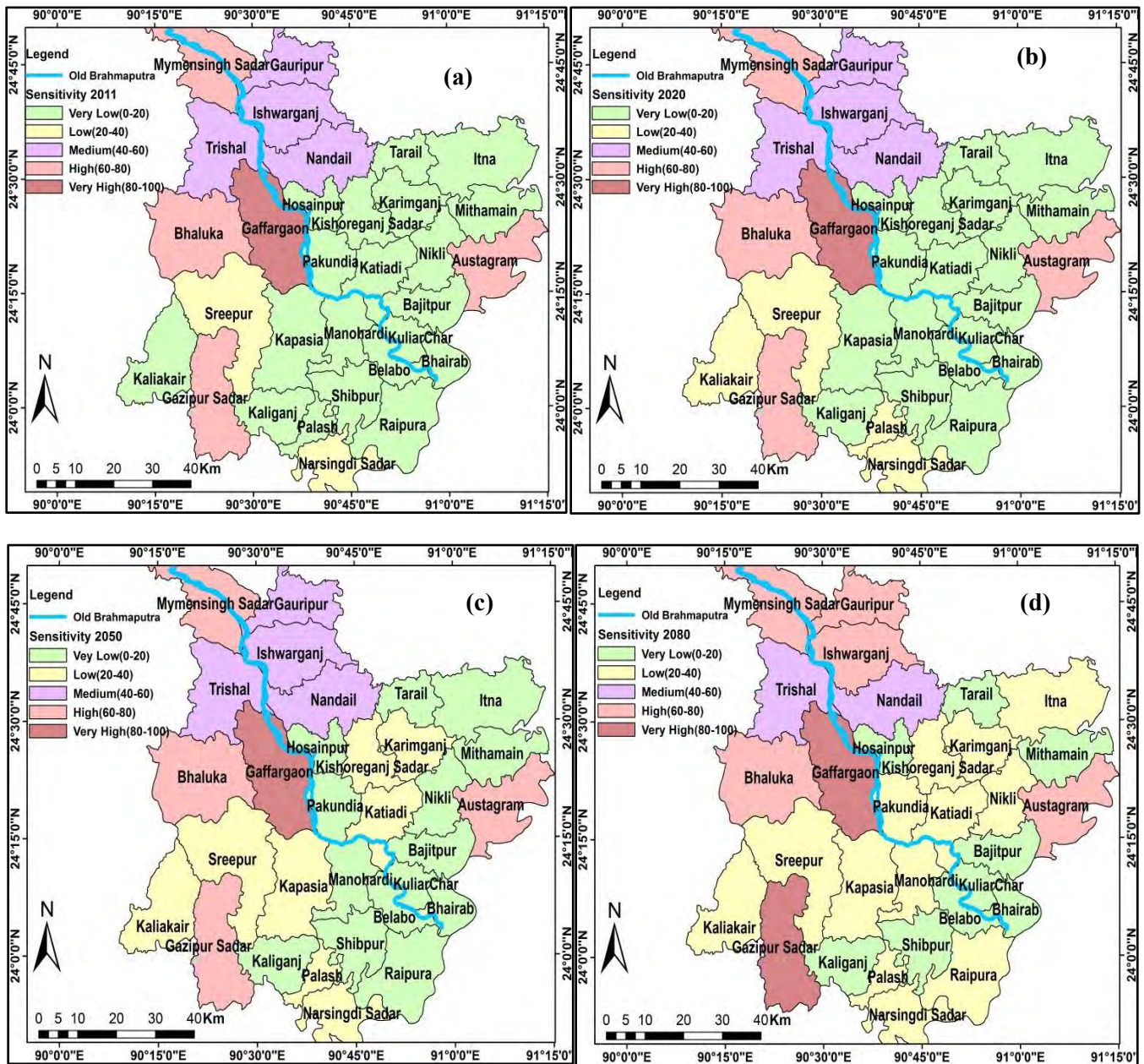
Figure 5.14: Sensitivity map for present and future socio-economic regime (a) Present (b) 2020s (c) 2050s (d) 2080s

The numbers of administrative units (Upazilla) under different sensitivity categories are 20, 2, 4, 4, 1 for 2011 and the percentage areas are 51%, 8%, 15%, 20% and 5% for Very Low, Low, Medium, High and Very High sensitive zones respectively. The numbers of administrative units under different categories have been found as 18, 4, 4, 4, 1 for 2020s and the percentage areas are 46%, 13%, 15%, 20% and 5% for Very Low, Low, Medium, High and Very High sensitive zones respectively implying the fact that comparing with 2011, in 2020s a part of the study area shifts from very low sensitive zone to the low sensitive zone indicating overall increase in the sensitivity in those particular Upazilla. The numbers of

114

land units under different sensitivity categories have been found as 14, 8, 4, 4, 1 for 2050s and the percentage areas are 34%, 25%, 15%, 20% and 5% for Very Low, Low, Medium, High and Very High sensitive zones respectively. During 2080s the numbers of Upazilla under different categories were 9, 13, 2, 5, 2 and the percentage areas are 18%, 41%, 8%, 22% and 11% for Very Low, Low, Medium, High and Very High sensitive zones respectively indicating a significant shift of the areas from previous category to the next category depicting overall increase in sensitivity from 2050s to 2080s. Gaffargaon, Gazipur Sadar, Mymensingh Sadar, Bhaluka and Austagram were much more sensitive comparing with other upazilla within the study area. Higher sensitivity accounted for higher social dependency ratio, greater poverty rate, higher unemployment rate, poor household structure and limited sanitation facility. Sensitivity analysis of all the upazilla of the study area shows that in 2020s, 2050s and 2080s sensitivity increases for all the upazilla. The reason behind the increased sensitivity is the increased social dependency ratio, floating population, unemployment rate and the thriving condition of Aman crop production in some of the upazilla.

Table 5.11: Percentage of Area under different sensitivity zones for different socio-economic regime

Components	Time period	Categorization									
		Very Low		Low		Medium		High		Very High	
		Area (sq km)	% Area	Area (sq km)	% Area	Area (sq km)	% Area	Area (sq km)	% Area	Area (sq km)	% Area
Sensitivity	2011	4156	51	676	8	1225	15	1646	20	401	5
	2020s	3747	46	1085	13	1225	15	1646	20	401	5
	2050s	2154	34	2055	25	1225	15	1646	20	401	5
	2080s	1874	18	3359	41	665	8	1748	22	458	11

5.5.2 Assessment of Adaptive Capacity for Present and Future Projected Socio-Economic Regime

The Upazila-wise data of the 11 selected indicators of adaptive capacity from the available population and agricultural census reports of 2011, 2001, 1991, 1981 and others have been collected, processed and analyzed to obtain the value of all the adaptive capacity indicators for 2011, 2020s, 2050s and 2080s. The indicator values are then normalized in a range of 1 to 100 by the early mentioned Equation 4.5. Using the weights of the particular indicators and domain weights sensitivity value of each upazilla for 2011, 2020s, 2050s and 2080s have been calculated from Equation 4.9 and Equation 4.10. Figure 5.15 (a), (b), (c) and (d) show the relative adaptive capacity of the upazillas of Gazipur, Narsingdi, Kishoreganj and Mymensingh district respectively.
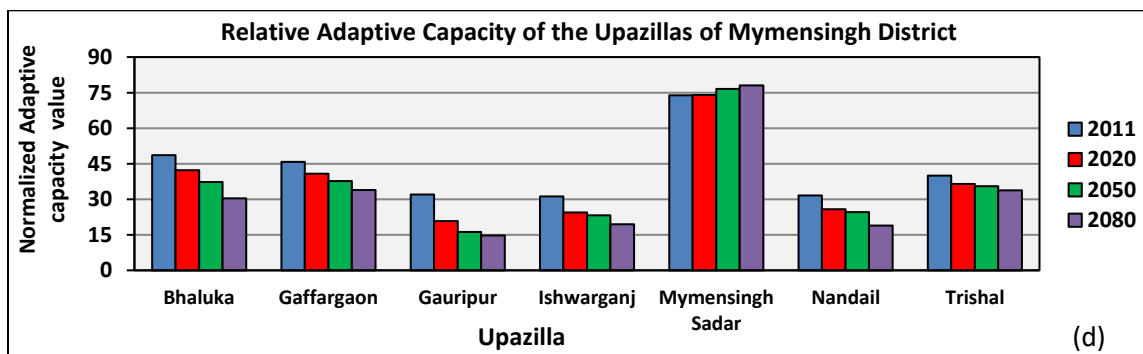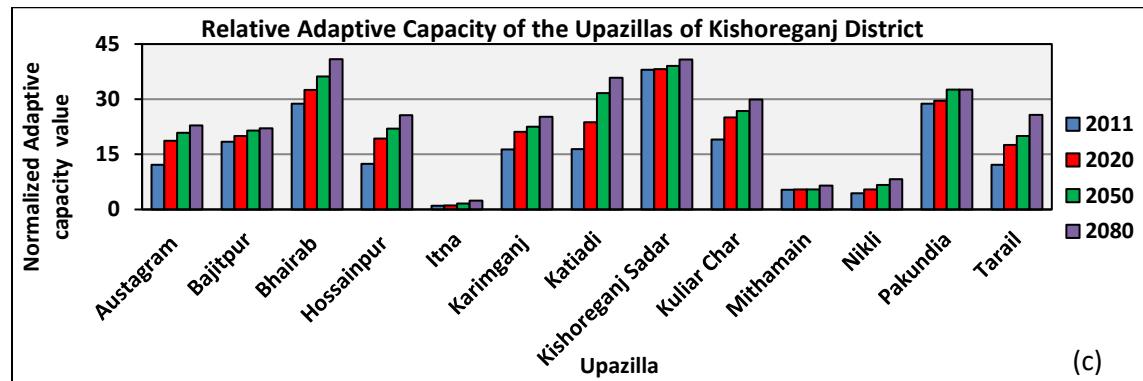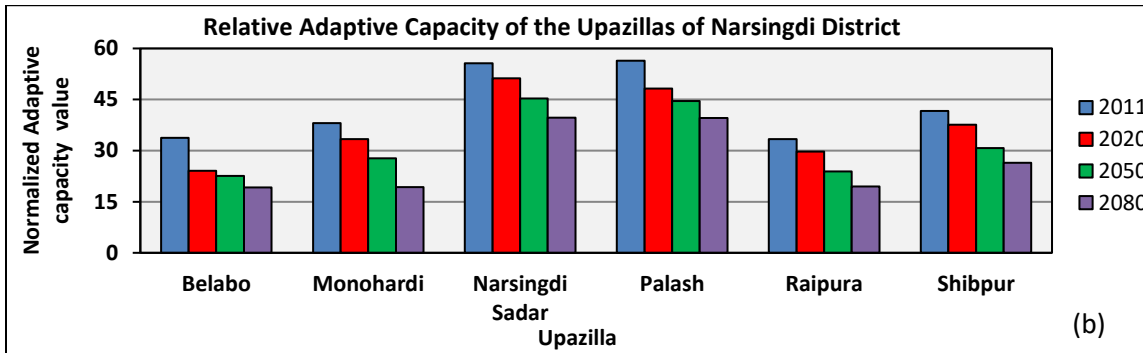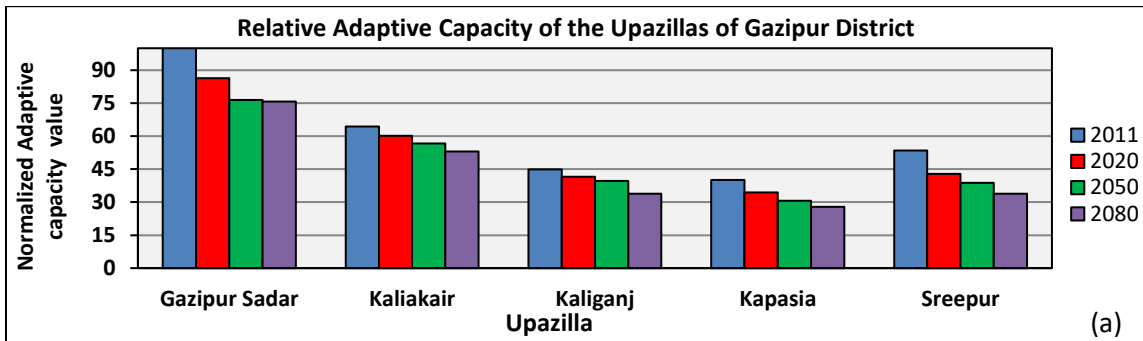
Figure 5.15: Relative adaptive capacity of upazilla of (a) Gazipur (b) Narsingdi(c) Kishoreganj (d) Mymensingh

Figure 5.15 (a) shows that among the five upazilla of Gazipur district Gazipur Sadar is the strongest upazilla in respect of adaptive capacity and Kapasia possesses the least adaptive capacity. All the upazilla

of Gazipur district losses their adaptive capacity as we go forward in time. Figure 5.15 (b) shows that among the six upazilla of Narsingdi district Narsingdi Sadar and Palash are more adaptive comparing with other upazilla. For all the upazillas of Narsingdi district, adaptive capacity decreases from present to 2080s significantly. Figure 5.15 (c) shows among the thirteen upazilla of Kishoreganj district Bhairab and Kishoreganj Sadar have been found more adaptive and Itna was the least adaptive upazilla for the present and future projected socio-economic scenario. Figure 5.15 (d) shows among the selected upazillas of Mymensingh district, Mymensingh Sadar possess the maximum adaptive capacity and Gauripur, Ishwarganj and Nandail were comparatively lower in adaptive capacity.

Lower adaptive capacity accounted for low literacy rate and decreasing trend of crop productivity, low percentage of people engaged in industry and service and lack of sanitation facility. Adaptive capacity analysis of all the upazilla of Gazipur, Narsingdi districts and selected upazilla of Mymensingh districts except Mymensingh Sadar. But in case of the upazilla of Kishoreganj districts, adaptive capacity showed an increasing trend for the 2020s, 2050s and 2080s. The reason behind the increased adaptive capacity of the upazilla of Kishoreganj district is the increased percentage of the people in engaged in industry and service, high school attendance rate of the people of the upazilla, increased percentage of household having electricity connection and the increased percentage of household having Sanitation Facility.

Adaptive capacity maps were generated for the study area for present and future projected socio-economic condition using five categories and an equal interval for the normalized adaptive capacity values as shown in Figure 5.16. The specified five categories are Very Low, Low, Medium, High and Very High adaptive capacity zones for the normalized value range 0-20, 20-40, 40-60, 60-80 and 80-100 respectively. The maps were then compared and analyzed for identification of land units under different categories as shown in Table 5.12. The numbers of upazilla under different adaptive capacity categories are 9, 12, 7, 2, 1 for 2011 and the percentage areas are 24%, 35%, 26%, 9% and 6% for Very Low, Low, Medium, High and Very High adaptive capacity zones respectively. The numbers of upazilla under different adaptive capacity have been found as 7, 15, 6, 2, 1 for 2020s and the percentage areas are 20%, 43%, 23%, 9% and 6% for Very Low, Low, Medium, High and Very High sensitive zones respectively implying the fact that comparing with 2011, in 2020s a part of the study area shifts from medium to low adaptive capacity zones. The numbers of administrative units under different categories have been found as 4, 21, 3, 2 and 0 for 2050s and the percentage areas are 14%, 68%, 8%, 10% and 0% for Very Low, Low, Medium, High and Very High sensitive zones respectively. During 2080s the numbers of land units under different categories were 9, 17, 3, 2, 0 and the percentage areas are 29%, 53%, 8%, 10% and 0% for Very Low, Low, Medium,

High and Very High sensitive zones respectively indicating a significant shift of the areas from low adaptive zone to very low adaptive capacity zones from 2050s to 2080s.As we move from present to 2020s,2050s and 2080s the adaptive capacity of the upazillas decreases and in 2080s, there seem to be no upazilla in very high adaptive capacity category and only two upazilla named Gazipur Sadar and Mymensingh Sadar in high adaptive capacity zone.
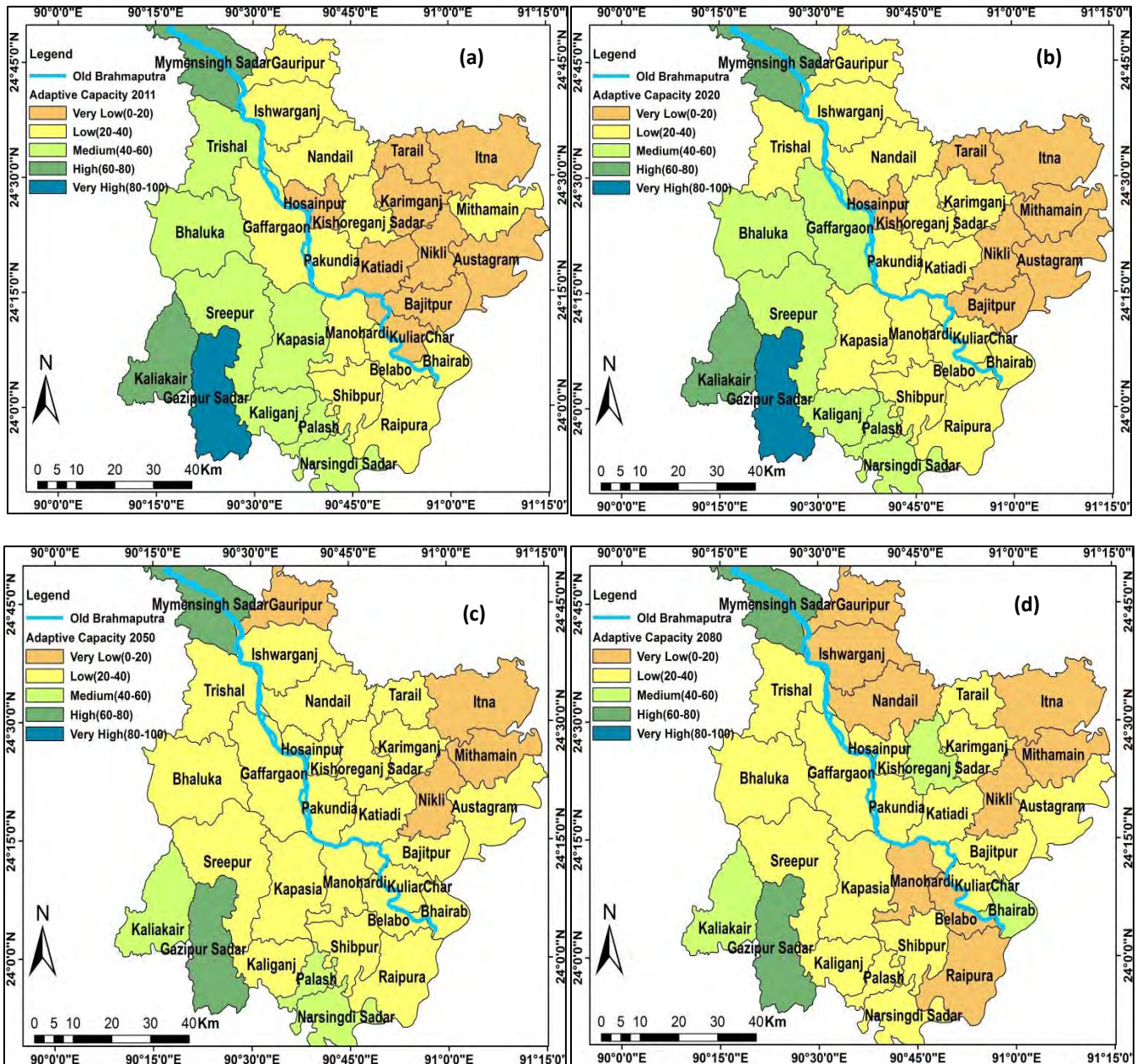

Figure 5.16: Adaptive Capacity maps for present and future socio-economic regime (a) Present (b) 2020s (c) 2050s (d) 2080s

Table 5.12: Percentage of Area under different adaptive capacity zones for Present and future socio-economic regime

Components	Time period	Very Low		Low		Medium		High		Very High	
		Area (sq km)	% Area	Area (sq km)	% Area	Area (sq km)	% Area	Area (sq km)	% Area	Area (sq km)	% Area
Adaptive Capacity	2011	1952	24	2866	35	2125	26	703	9	458	6
	2020s	1651	20	3462	43	1831	23	703	9	458	6
	2050s	1113	14	5523	68	622	8	846	10	0	0
	2080s	2350	29	4261	53	647	8	846	10	0	0

5.5.3 Assessment of Vulnerability of Old Brahmaputra Floodplain for Present and Future Projected Socio-Economic Regime

Vulnerability of each upazilla within the study area for present, 2020s, 2050s and 2080s have been calculated using the total sensitivity and adaptive capacity value of each upazilla from Equation 4.11. Figure 5.17 (a), (b), (c), (d) shows that the relative vulnerability of the upazilla of Gazipur, Narsingdi, Kishoreganj and Mymensingh district respectively. Figure 5.17 (a) shows that among the five upazilla of Gazipur district Gazipur Sadar is the most vulnerable upazilla for all the considered time span and Kaliakair and Kaliganj possess the least vulnerability. Figure 5.17 (b) shows that among the six upazilla of Narsingdi district Manohardi and Narsingdi Sadar are more vulnerable upazilla comparing with other upazilla. Figure 5.17 (c) shows among the thirteen upazilla of Kishoreganj district Austagram have been found as the most vulnerable zone for 2011, 2020s, 2050s and 2080s comparing with other upazilla within this district.

Figure 5.17 (d) shows among the selected upazilla of Mymensingh district Gaffargaon has been found the most vulnerable upazilla for 2011, 2020s, 2050s and 2080s. For all the upazilla except Hossainpur, vulnerability increases with time as we move forward in time. Lower vulnerability values in upazilla like Kaliakair, Kaliganj, Belabo, Palash, Shibpur, Kuliar Char, Mithamain, Bajitpur and Bhairab accounted for low disable and dependent population, lower poverty rate, better household and infrastructural condition and facilities and increased number of flood shelter and growth center.
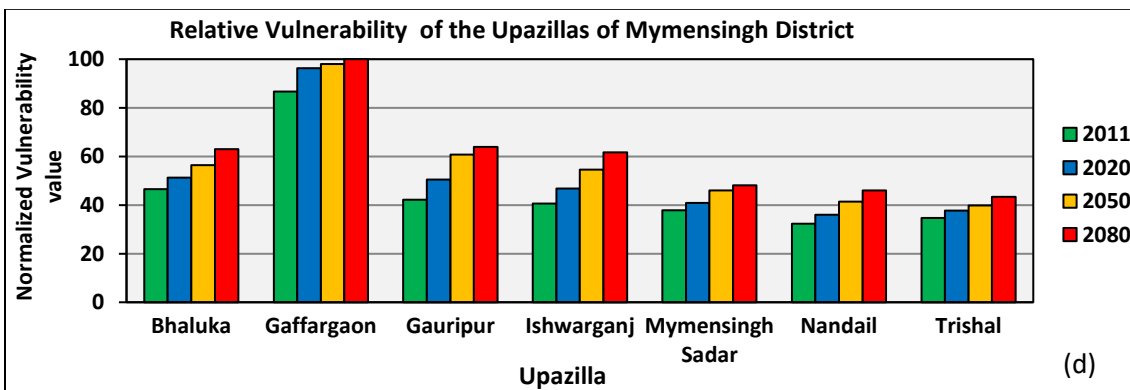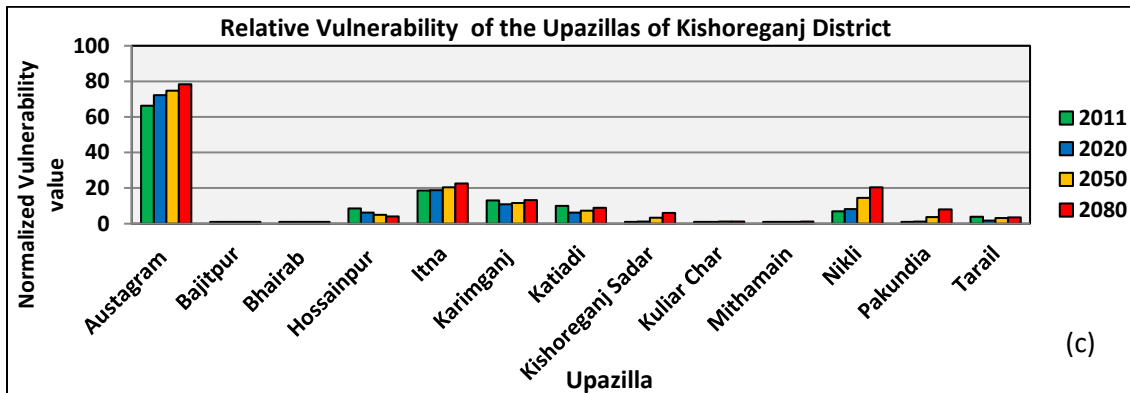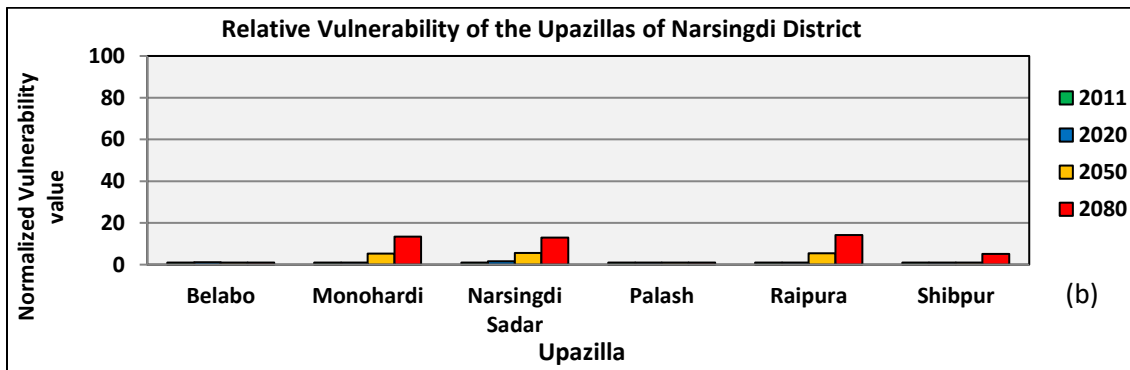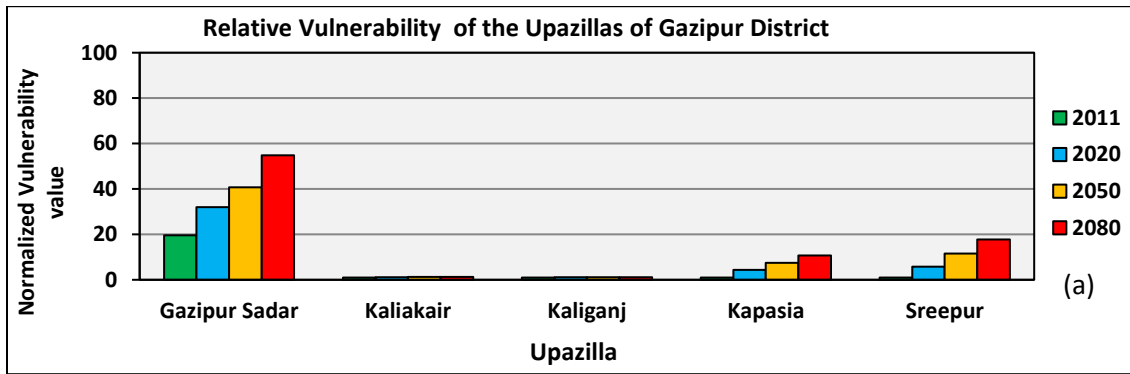
Figure 5.17: Relative vulnerability of the upazillas of (a) Gazipur (b) Narsingdi (c) Kishoreganj and (d) Mymensingh

Then the vulnerability maps were generated for the selected area for present and future projected socio-economic condition using five categories and an equal interval for the normalized vulnerability values as shown in Appendix B. The specified five categories are Very Low, Low, Medium, High and Very High vulnerability zones for the normalized value range 0-20, 20-40, 40-60, 60-80 and 80-100 respectively. Analyses on the generated maps show that Gaffargaon, Bhaluka, Austagram, Mymensingh Sadar and Ishwarganj have greater vulnerability comparing with other upazilla within the study extend comprising of 31 upazilla. Figure 5.18 shows the vulnerability of the Old Brahmaputra river floodplain consisting of 19 upazilla among the 31 upazilla. Gaffargaon, Bhaluka, Ishwarganj, Gauripur possess higher vulnerability comparing with others. Bhaluka upazilla lied within the medium vulnerable category for present, 2020s and 2050s but shifts to the high vulnerable zone in 2080s. Gauripur initially lied within medium vulnerable zone and jumped into the high vulnerability in 2050s. Mymensingh Sadar initially lied in the low vulnerability category but devolved into and persisted in the medium vulnerable zone for the rest of the time of 2020s, 2050s and 2080s.

The maps of the whole study extent were then compared and analyzed for identification of land units under different categories as shown in Table 5.13. The numbers of upazilla under different vulnerability categories are 3, 5, 4, 14, 5 for 2011 and the percentage areas are 11%, 13%, 12%, 45% and 20% for Very Low, Low, Medium, High and Very High vulnerability zones respectively in 2011. The numbers of upazilla under different categories have been found as 0, 7, 7, 14, 3 for 2020s and the percentage areas are 0%, 21%, 22%, 44% and 13% for Very Low, Low, Medium, High and Very High vulnerability zones respectively implying the fact that comparing with 2011, in 2020s a part of the study area shifts from very low to medium and from medium to high vulnerability zones. The numbers of upazilla under different categories have been found as 0, 3, 9, 14, 5 for 2050s and the percentage areas are 0%, 8%, 26%, 50% and 16% for Very Low, Low, Medium, High and Very High vulnerability zones respectively. During 2080s the numbers of administrative units under different categories were 0, 2, 8, 15, 6 and the percentage areas are 0%, 11%, 25%, 44% and 20% for Very Low, Low, Medium, High and Very High vulnerability zones respectively indicating a significant shift of the areas from high to very high vulnerability zones from 2050s to 2080s. For all the time frame considered, very high vulnerable zone comprises of Gaffargaon upazilla only. Austagram upazilla was in the high vulnerable zone for present, 2020s, 2050s and 2080s. Gazipur Sadar moves from the very low vulnerable zone to the medium vulnerable zone gradually from baseline period to 2080s. Bhaluka upazilla lied within the medium vulnerable category for present, 2020s and 2050s but shifts to the high vulnerable zone in 2080s. Mymensingh Sadar initially lied in the low vulnerability category but devolved into and persisted in the medium vulnerable zone for the

rest of the time of 2020s, 2050s and 2080s. Trishal upazilla lies within the low vulnerable category for present, 2020s and 2050s but might go down to the medium vulnerable zone in 2080s. Nandail upazilla is under the low vulnerable region for present and 2020s but may degrade to the medium vulnerable category in 2050s and 2080s.Other upazilla remained within the very low to low vulnerability for present, 2020s, 2050s and 2080s.
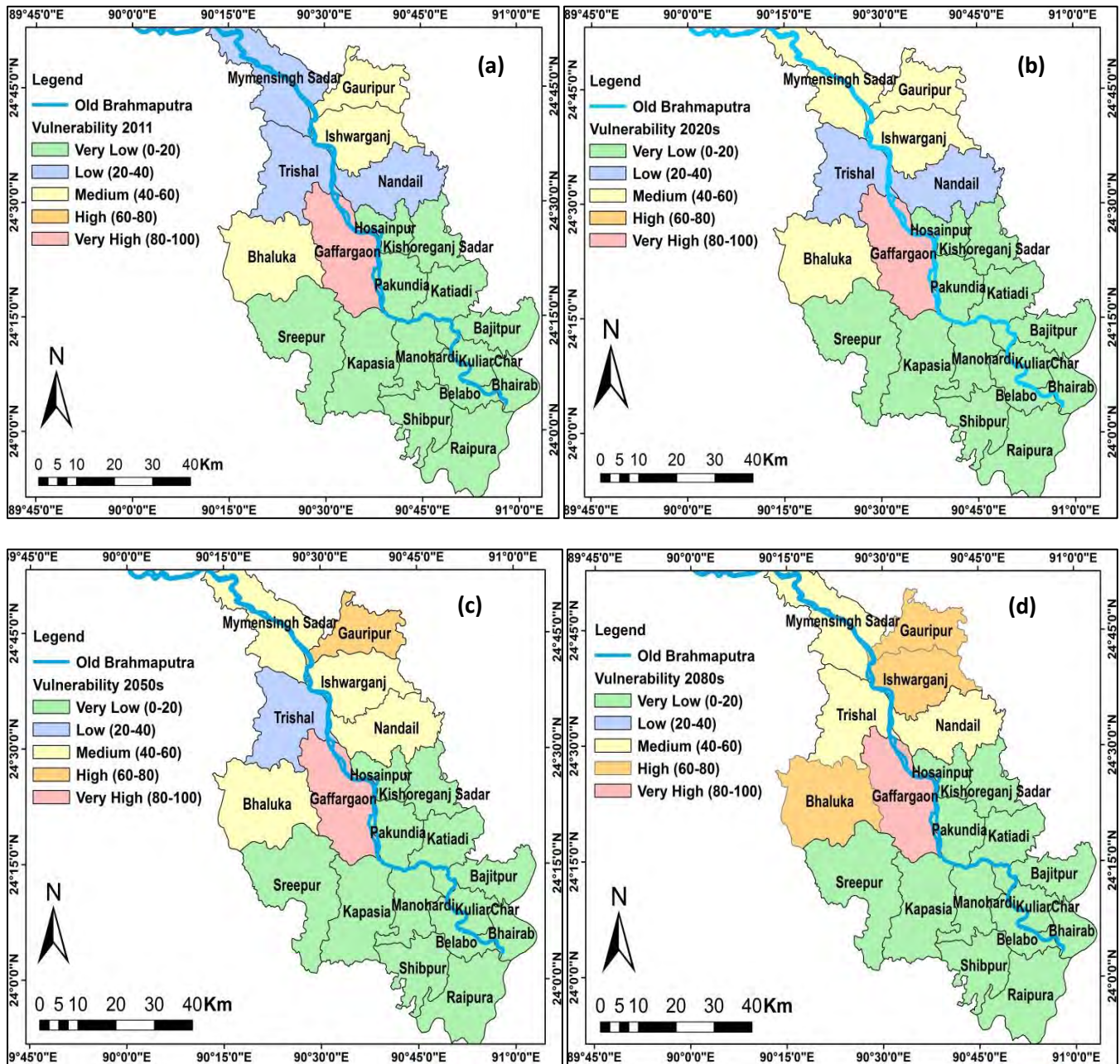

Figure 5.18: Vulnerability Map of Old Brahmaputra River Floodplain for the year (a) 2011 (b) 2020s (c) 2050s (d) 2080s

Table 5.13: Percentage of Area under different vulnerability zones for present and future socio-economic regime

Components	Time period	Very Low		Low		Medium		High		Very High	
		Area (sq km)	% Area	Area (sq km)	% Area	Area (sq km)	% Area	Area (sq km)	% Area	Area (sq km)	% Area
Vulnerability	2011	5290	65	1054	13	1004	12	356	4	401	5
	2020s	4832	60	1123	14	1393	17	356	4	401	5
	2050s	4430	55	741	9	1902	23	630	8	401	5
	2080s	4216	52	616	8	1511	19	1360	17	401	5

The results of vulnerability indicate that upazilla high in vulnerability are mostly areas with high concentration of development activities and densely populated region, limited medical facilities, and livelihood standard with large and poor infrastructure existence. The results of vulnerability indicate that upazilla high in vulnerability are mostly areas with high concentration of development activities and densely populated region, limited medical facilities, greater length of unpaved roads and livelihood standard with large and poor household and sanitation facility.

5.6 Assessment of Exposure for Present and Future Projected Socio-Economic Regime

The Upazila-wise data of the 3 selected indicators of exposure from the available population and agricultural census reports of 2011, 2001, 1991, 1981 and others have been collected, processed and analyzed to obtain the value of all the exposure indicators for 2011, 2020s, 2050s and 2080s. The indicator values are then normalized in a range of 1 to 100 by the early mentioned Equation 4.5. Using the weights of the particular indicators and domain weights sensitivity value of each upazilla for 2011, 2020s, 2050s and 2080s have been calculated from Equation 4.12. Figure 5.18 (a), (b), (c), (d) shows that the relative exposure of the upazilla of Gazipur, Narsingdi, Kishoreganj and Mymensingh district respectively. Figure 5.18 (a) shows that among the five upazilla of Gazipur district Gazipur Sadar is the most exposed upazilla for all the considered time span and Kaliganj possesses the least exposure. Figure 5.18 (b) shows that among the six upazilla of Narsingdi district Narsingdi Sadar is the most exposed upazilla comparing with other upazilla and Palash is the least exposed upazilla. Figure 5.18 (c) shows among the thirteen upazilla of Kishoreganj district Austagram have been found as the most exposed for 2011, 2020s, 2050s and 2080s and Mithamain was the least exposed upazilla for the present and future projected socio-economic scenario. Figure 5.18 (d) shows among the selected upazilla of Mymensingh district Gaffargaon have been found as the most exposed for 2011, 2020s, 2050s and 2080s and Nandail was the least exposed upazilla

for the present and future projected socio-economic scenario. For all the upazilla exposure values increase gradually from present to 2080s.
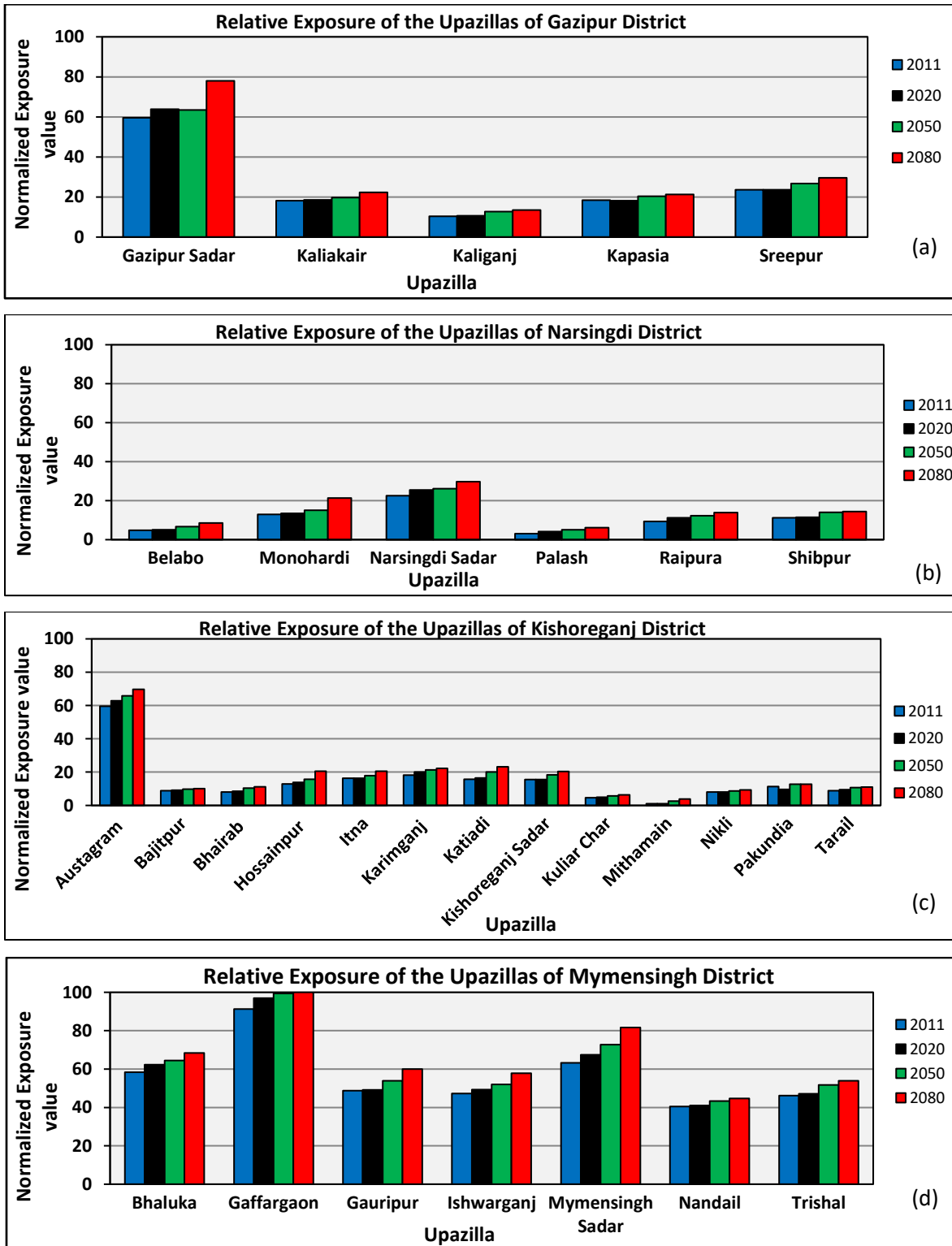
Figure 5.19: Relative Exposure of the upazillas of (a) Gazipur (b) Narsingdi (c) Kishoreganj and (d) Mymensingh district

As we know, population can be viewed as an immensely important "socio-economic variable" (DILLEY and RASID, 1990). In densely populated areas, natural calamities like flood incur major economic lose to the houses, land, possessions and infrastructure as greater people possess greater resources and liabilities (DEVOY, 1992; RIVAS and CENDRERO, 1994). Areas with few people may not suffer the same pressure on the environment or have the same resources for protection. Thus higher exposure accounted for high population density and increased cropped area in the upazilla. The reason behind low exposure is the low population density. As there are few populations in these areas, they are less exposed to any hazard and climate change impacts. On the other hand, the higher population density is more or less aligned with the higher number of household thus make an upazilla highly exposed to the hazard considered. Presence of the greater cropped land area make an area more exposed to the hazard making it more vulnerable.

Exposure maps were generated of 31 upazilla for present and future projected socio-economic condition using five categories and an equal interval for the normalized exposure values. The specified five categories are Very Low, Low, Medium, High and Very High exposure zones for the normalized value range 0-20, 20-40, 40-60, 60-80 and 80-100 respectively as shown in Appendix B. Figure 5.20 shows the exposure map of the Old Brahmaputra river floodplain including 19 districts among the 31 upazilla. Gaffargaon, Mymensingh Sadar, Bhaluka, Gauripur are more exposed comparing with other upazilla.

The maps were then compared and analyzed for identification of land units under different categories as shown in Table 5.14. The numbers of upazillas under different categories are 20, 2, 7, 1, 1 for 2011 and the percentage areas are 51%, 8%, 31%, 5% and 5% for Very Low, Low, Medium, High and Very High exposure zones respectively for the present condition. The numbers of land units under different categories have been found as 19, 3, 4, 4, 1 for 2020s and the percentage areas are 49%, 11%, 15%, 20% and 5% for Very Low, Low, Medium, High and Very High exposure zones respectively implying the fact that comparing with 2011, in 2020s a part of the study area shifts from very low to medium and from medium to high exposed zones. The numbers of land units under different categories have been found as 17, 5, 4, 4, 1 for 2050s and the percentage areas are 42%, 18%, 15%, 20% and 5% for Very Low, Low, Medium, High and Very High exposed zones respectively in 2050s. During 2080s the numbers of land units under different categories were 12, 10, 3, 4, 2 and the percentage areas are 27%, 33%, 12%, 20% and 9% for Very Low, Low, Medium, High and Very High vulnerability zones respectively indicating a significant shift of the areas from high to very high exposure zones from 2050s to 2080s. Mymensingh Sadar lies in the high exposure category up to 2050s but devolved into in the very high exposure zone in 2080s. Gaffargaon upazilla is under the very high exposure zone for present, 2020s, 2050s and 2080s. Gazipur

Sadar, Austagram and Bhaluka move from the medium exposure zone to the high exposure zone from baseline period to 2020s and persisted in the zone for the rest of the century. Gauripur upazilla lies within the medium exposure category for present, 2020s and 2050s but shifts to the high exposure zone in 2080s. Other upazilla remained within the very low to low vulnerability for present, 2020s, 2050s and 2080s.
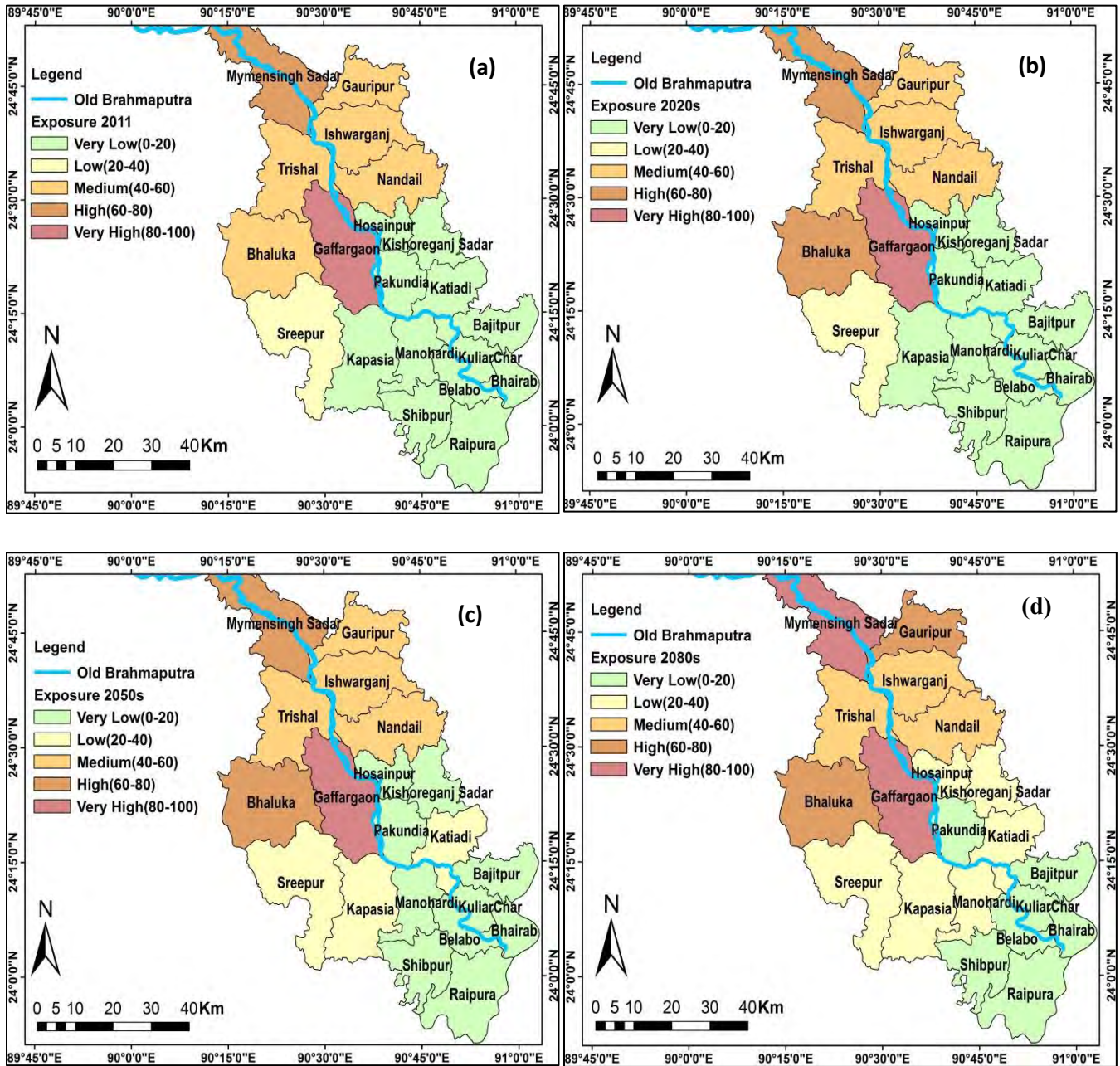

Figure 5.20: Exposure Map of Old Brahmaputra River Floodplain for the year (a) 2011 (b) 2020s (c) 2050s (d) 2080s

Table 5.14: Percentage of Area under Exposure zones for present and future socio-economic regime

Component		Categorization

	Time period	Very Low		Low		Medium		High		Very High	
		Area (sq km)	% Area	Area (sq km)	% Area	Area (sq km)	% Area	Area (sq km)	% Area	Area (sq km)	% Area
Exposure	2011	4156	51	676	8	2483	31	388	5	401	5
	2020s	3955	49	877	11	1225	15	1646	20	401	5
	2050s	3379	42	1453	18	1225	15	1646	20	40	5
	2080s	2154	27	2678	33	951	12	1531	20	790	9

5.7   Flood Risk Assessment for RCP 8.5 Scenario

This study targeted to evaluate the monsoon flood induced risk which has been expressed as a function of hazard, exposure and vulnerability and calculated using Equation 4.16.

Table 5.15: Risk on the administrative unit for RCP 8.5 Scenario

District	Upazilla	Risk Values for RCP 8.5			
		Baseline flow	2020s	2050s	2080s
Gazipur	Gazipur Sadar	5523	9837	15292	26561
	Kaliakair	54	82	119	145
	Kaliganj	2	14	67	83
	Kapasia	45	875	1864	2919
	Sreepur	55	1272	2915	3760
Narsingdi	Belabo	6	11	1	39
	Manohardi	9	15	491	3406
	Narsingdi Sadar	29	145	1410	4351
	Palash	9	14	22	26
	Roypura	25	23	508	1675
	Shibpur	14	15	39	1039
Kishoreganj	Austagram	63121	73996	80838	90595
	Bajitpur	33	37	36	38
	Bhairab	35	33	38	38
	Hossainpur	1222	1021	862	876
	Itna	5886	6348	10901	13008
	Karimganj	3002	2985	3231	3800
	Katiadi	695	469	782	1353
	Kishoreganj Sadar	20	37	346	706
	Kuliar Char	20	26	31	38
	Mithamain	12	14	25	34
	Nikli	1363	1595	2871	4353
	Pakundia	16	25	127	79
	Tarail	344	131	568	682
Mymensingh	Bhaluka	45417	53342	56330	60903
	Gaffargaon	125018	192169	182984	195104
	Gauripur	20749	22757	37516	38254
	Ishwarganj	21974	24479	30980	33482
	Mymensingh Sadar	38889	45918	77629	91382
	Nandail	14972	16232	16855	16630
	Trishal	19222	22699	34355	37743

Flood hazard of each of the Upazilla for baseline, 2020s, 2050s and 2080s has been multiplied with the exposure and vulnerability of that particular upazilla for present, 2020s, 2050s and 2080s respectively to

obtain the risk value for that upazilla for present, 2020s, 2050s and 2080s respectively. Table 5.15 shows the risk values of each of the Upazillas. The risk values among the administrative units were found to vary from 1 to 195104 for present and future projection RCP 8.5. Thereafter the risk values were normalized from 1 to 100 as shown in Table 5.16.

Table 5.16: Normalized Risk values on the administrative unit for RCP 8.5 Scenario

District	Upazilla	Normalized Risk Values for RCP 8.5			
		Base line flow	2020s	2050s	2080s
	Gazipur Sadar	3.8	6.0	8.8	14.5
	Kaliakair	1.0	1.0	1.1	1.1
	Kaliganj	1.0	1.0	1.0	1.0
	Kapasia	1.0	1.4	1.9	2.5
Gazipur	Sreepur	1.0	1.6	2.5	2.9
	Belabo	1.0	1.0	1.0	1.0
	Manohardi	1.0	1.0	1.2	2.7
	Narsingdi Sadar	1.0	1.1	1.7	3.2
	Palash	1.0	1.0	1.0	1.0
	Roypura	1.0	1.0	1.3	1.8
Narsingdi	Shibpur	1.0	1.0	1.0	1.5
	Austagram	33.0	38.5	42.0	47.0
	Bajitpur	1.0	1.0	1.0	1.0
	Bhairab	1.0	1.0	1.0	1.0
	Hossainpur	1.6	1.5	1.4	1.4
	Itna	4.0	4.2	6.5	7.6
	Karimganj	2.5	2.5	2.6	2.9
	Katiadi	1.4	1.2	1.4	1.7
	Kishoreganj Sadar	1.0	1.0	1.2	1.4
	Kuliar Char	1.0	1.0	1.0	1.0
	Mithamain	1.0	1.0	1.0	1.0
	Nikli	1.7	1.8	2.5	3.2
	Pakundia	1.0	1.0	1.1	1.0
Kishoregonj	Tarail	1.2	1.1	1.3	1.3
	Bhaluka	24.0	28.1	29.6	31.9
	Gaffargaon	64.4	98.5	93.9	100.0
	Gauripur	11.5	12.5	20.0	20.4
	Ishwarganj	12.1	13.4	16.7	18.0
	Mymensingh Sadar	20.7	24.3	40.4	47.4
	Nandail	8.6	9.2	9.6	9.4
Mymensingh	Trishal	10.8	12.5	18.4	20.2

Risk maps were then generated for 31 Upazilla for present and future condition using five categories and an equal interval for the normalized risk values as adopted in the case of hazard, sensitivity, adaptive capacity, exposure and vulnerability. The specified five categories are Very Low, Low, Medium, High and Very High exposure zones for the normalized value range 0-20, 20-40, 40-60, 60-80 and 80-100 respectively as shown in Appendix B. Figure 5.21 shows the flood risk map of the Old Brahmaputra river

floodplain including 19 upazilla among 31 upazilla of the study extent. Gaffargaon is the most risky upazilla among all the upazilla within the Old Brahmaputra river floodplain.
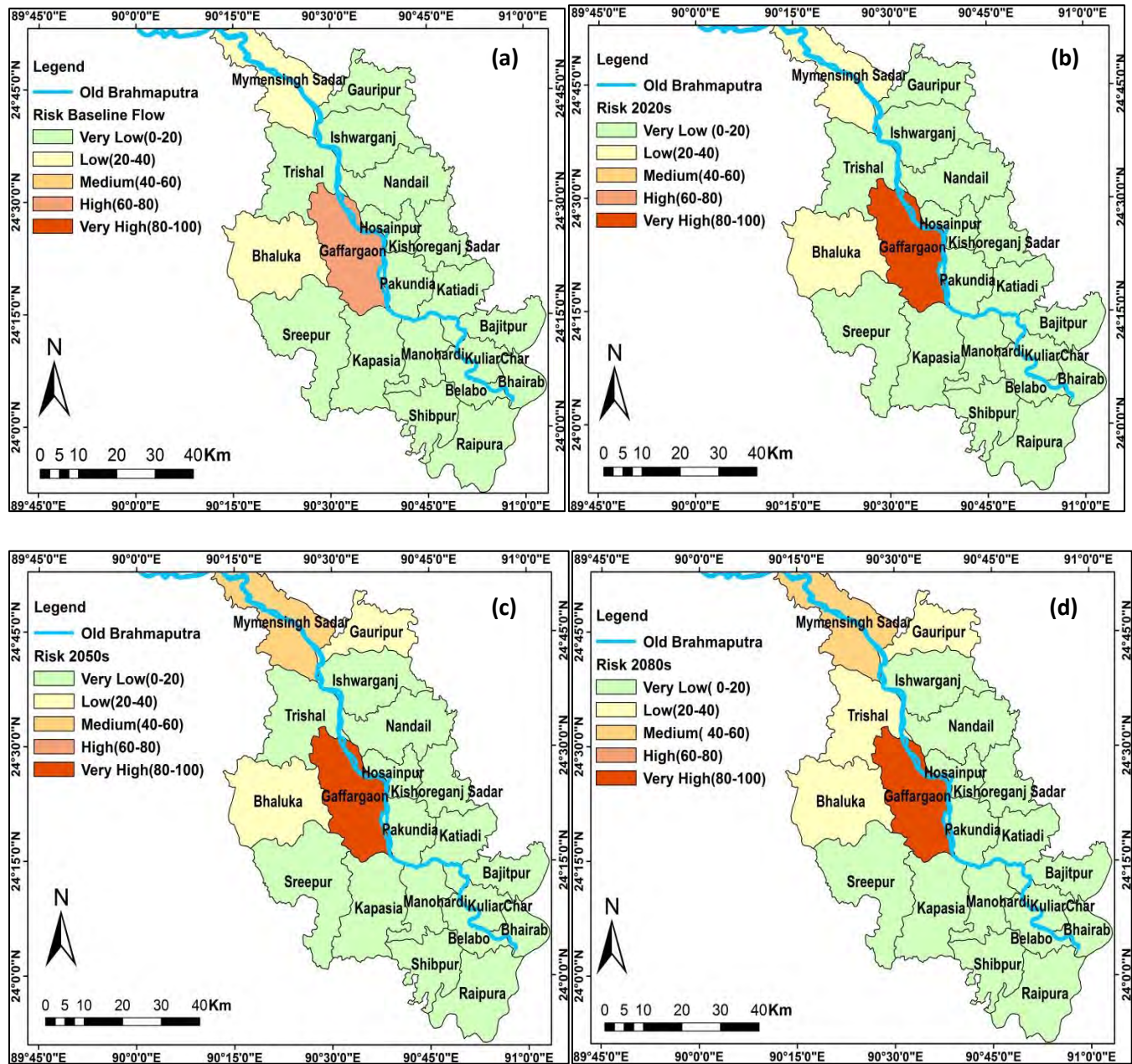
Figure 5.21: Risk Map of Old Brahmaputra River Floodplain for (a) Baseline flow (b) 2020s (c) 2050s (d) 2080s

The maps on the risk of whole study extent were then compared and analyzed for identification of administrative units under different risk categories as shown in Table 5.17. The numbers of upazillas under different categories are 27, 3, 0, 1, 0 for baseline flow and the percentage areas are 80%, 15%, 0%, 5% and 0% for Very Low, Low, Medium, High and Very High risk zones respectively for the present

condition. The numbers of upazilla under different categories are 27, 3, 0, 0, 1 for baseline flow and the percentage areas are 80%, 15%, 0%, 0% and 5% for Very Low, Low, Medium, High and Very High risk zones respectively for 2020s. The numbers of upazilla under different categories are 26, 2, 2, 0, 1 for baseline flow and the percentage areas are 77%, 9%, 9%, 0% and 5% for Very Low, Low, Medium, High and Very High risk zones respectively for 2050s. The numbers of upazilla under different categories are 25, 3, 2, 0, 1 for baseline flow and the percentage areas are 73%, 13%, 9%, 0% and 5% for Very Low, Low, Medium, High and Very High risk zones respectively for 2080s.

Table 5.17: Percentage of Area under different Risk zones for present and future

Components	Time period	Categorization									
		Very Low		Low		Medium		High		Very High	
		Area (sq km)	% Area	Area (sq km)	% Area	Area (sq km)	% Area	Area (sq km)	% Area	Area (sq km)	% Area
Risk	Base Line	6514.9	80	1188	15	0	0	401	5	0	0
	2020s	6514.9	80	1188	15	0	0	0	0	401	5
	2050s	6240.8	77	718	9	743.98	9	0	0	401	5
	2080s	5901.8	73	1057	13	743.98	9	0	0	401	5

In the base period, there was no administrative unit in medium and very high risk zone. All the upazillas are in the very low to low risk zone except Gaffargaon. The scenario remained almost same for 2020s as well excluding the fact that Gaffargaon shifts to the very high risk zone. During 2050s to 2080s risk of two upazilla named Mymensingh Sadar and Austagram increased to some extent. Major part of the total study area is under the very low to low risk zone throughout the century. High and very high risk magnitude reflects the impact of climate change compared to the base period. So, it can be interpreted that future climate change is going to have moderate impact on the flood situation of major portion of the old Brahmaputra River floodplain even if the wettest climate change scenario of RCP 8.5 is considered.

Risk maps depict the spatio-temporal variation of risk aggregating the hazard, vulnerability, and exposure in which the intensity of risk depends on the contribution of the hazard, vulnerability, and exposure. Higher contribution of hazard, vulnerability, and exposure certainly produces greatest risk whereas moderate hazard can also cause higher risk due to greater contribution of vulnerability and exposure. Sometimes a community having significantly high hazard can also possess moderate to low risk due to having low exposure and vulnerability to the particular hazard. In this study, among the Upazillas, Gaffargaon is in the high risk zone at baseline condition and degrades to the very high risk zone in 2020s remaining in the very high category for rest of the century. Careful observation on the hazard, sensitivity,

exposure and vulnerability maps highlights the fact that higher contribution of hazard, vulnerability, and exposure certainly produces greatest risk. A reverse case occurred in case of Itna Upazilla. In hazard assessment, Itna was within the medium to high hazard category for up to 2020s and relegated to the very high hazard category for rest of the century. But the risk map shows that Itna lies within the low risk zone throughout the century. This occurred due to fact that though the contribution of hazard is greater for the particular Upazilla, associated contribution of exposure and vulnerability is quite low. The result necessitates the incorporation of vulnerability and exposure along with the hazard assessment to evaluate the risk and risk assessment is required together with hazard assessment to quantify the actual climate change impact and to incorporate any disaster mitigation and management strategy.

CHAPTER 6

CONCLUSION AND RECOMMENDATION

6.1 Conclusion of the Study

Brahmaputra-Jamuna River is one of the largest rivers in the Ganges-Brahmaputra-Meghna river basin carrying enormous volume of water from upstream in monsoon. Climate change and economic development of ever-growing population are expected to intensify both the magnitude and frequency of extreme precipitation events increasing the monsoon flow and leading to more frequent river flooding. Thus the floodplain of Old Brahmaputra River, a major distributary of Brahmaputra-Jamuna River is certainly vulnerable to monsoon flooding. Hence, this study is formulated to assess the monsoon flood hazard, vulnerability and risk of Old-Brahmaputra River and its surrounding floodplain for future climate change scenario of RCP 8.5 using numerical modeling approach understanding the predicament of the river in particular. Around 130 km reach of Old-Brahmaputra River across the 31 upazilla of Mymensingh, Kishoreganj, Narsingdi and Gazipur district has been proposed as the study area for analyzing flood variables for past and future and hazard, vulnerability and risk have been reported for both the study area having 31 upazilla and Old Brahmaputra river floodplain with 19 upazilla in particular. To go with the numerical modeling approach of flood inundation, data on DEM, cross section, discharge, water level data of Old-Brahmaputra river floodplain have been collected from primary and secondary sources. To conduct the vulnerability and exposure of the study area, data on various socio-economic indicators were obtained from previous population and agricultural census reports.

Firstly, an already calibrated and validated hydrologic model of Brahmaputra river catchment in HEC-HMS was used to obtain the future flow magnitudes at Bahadurabad transit of Brahmaputra river basin using predicted rainfall of the selected model representing the wettest scenario of RCP 8.5. Correlation of flow at the Bahadurabad transit of Brahmaputra River and at Mymensingh Sadar of Old Brahmaputra River was established to achieve the future flow at the Mymensingh Sadar of Old Brahmaputra River for applying the concept of linear regression analysis the corresponding wettest climate condition of RCP 8.5 scenario. Then a HEC-RAS 1D-2D coupled model of Old Brahmaputra River has been set up for assessing the flood inundation and hazard Old Brahmaputra River floodplain for RCP 8.5 scenario. Calibration and validation of the developed model have been performed for the year of 2017 at an intermediate location

of the study reach, where Manning's roughness coefficient 'n' for the main river channel acted as the tuning parameter. Manning's roughness coefficient 'n' of 0.016-0.018 provided acceptable matching between the observed and simulated water level data with satisfactory output of the model performance evaluation techniques like R^2, NSE, RMSE and PBIAS. To calibrate the inundation extent on the floodplain considered, flood inundation extent obtained from simulation of 1D 2D coupled model has been compared with the Sentinel satellite image and flood map produced by FFWC on the maximum flooding condition of the year 2017 which produced satisfactory results. To produce the representative flood depth for future climate change condition, flood depth and related parameters need also to be validated to some extent. In this regard, mean flood depth obtained in each upazilla under the study area has been compared with the mean flood depth for the upazilla within the study area recommended by FFWC for the maximum inundation context of year 2017. After developing the 1D-2D calibrated model of Old-Brahmaputra River, the model has been simulated for the historical flood events and flood hazard, vulnerability and risk have been assessed for future climate change scenario. Findings of the analyses are concluded below:

- Analysis on the mean flood depth, flood flow velocity, flood inundation area and percent of an Upazilla inundated for each of the upazilla within the study area of 1988, 1998, 2004, 2007, 2010, 2013, 2016 and 2017 depict that among the historical flood years, flood event of 1988 and 1998 were of devastating consequences and events of 2010 and 2013 were less influential among all the all events.

- Simulation of flow of Old Brahmaputra River for baseline period (1976-2010), 2020s (2010-2039), 2050s (2040-2069) and 2080s (2070-2099) for the wettest scenario of RCP 8.5 show that, there is an increasing trend of flood area from baseline to 2080s. From baseline to 2080s, the total inundation area extended from 1975 km^2 which is 24% of total study area to 3923 km^2 which is about 48% of study area. Additionally, the mean flood depth and mean flood flow velocity are found to be increased as well. According to the produced predicted mean flood depth flood depth can be as high as 4.16 that Itna Upazilla might experience in 2080s. According to the produced predicted mean flood flow velocity flood flow velocity can be as high as 0.493 that Mymensingh Sadar Upazilla might experience in 2080s.

- The percentage area under different hazard zones for RCP 8.5 Scenario has been analyzed which shows that at baseline flow condition 25%, 36%, 36% and 3% area lie in the very low, low, medium and high hazard zone respectively having no area under very high hazard class. However, in 2020s, the very low, low and medium hazard zone got reduced to 22%, 32% and 33% respectively whereas

the high hazard zone rises to 13%. In 2050s, the percent area within very low hazard zone gets reduced to 12% comparing with the value of 2020s and the percent area in low hazard zone gets increased to 38% Percent area within medium hazard zone gets reduced to 31% whereas percent area within high hazard zone gets increased to 14%. In 2050s, 5% of total study area underlies within very high flood hazard zone. In 2080s, both the values of percent area in very low and low hazard zone get reduced leading to a significant increase in percent area of medium hazard zone. High and very high hazard zones remain stable comparing to the 2050s.

- The study considered the socio-economic vulnerability and exposure of the communities to be incorporated with hazard for the risk assessment. Socio-economic vulnerability and exposure have been estimated for the present and future using the data of Population and Agricultural Census of available previous years. Future population of each Upazilla was estimated using the logistic growth method. Future data of the selected indicators have been obtained observing the trend of the indicators of previous 4 decades expressing the indicators as a function of population. For all the time frame considered including present, early, mid and late century, very high vulnerable zone comprises of Gaffargaon upazilla only. Austagram upazilla was in the high vulnerable zone for present, 2020s, 2050s and 2080s. Bhaluka upazilla lied within the medium vulnerable category for present, 2020s and 2050s but shifts to the high vulnerable zone in 2080s. Most of the upazillas are under the low to moderate vulnerability for present, 2020s, 2050s and 2080s. Assessment of exposure for present and future time regime highlights significant shift of few of the upazillas from high to very high exposure zones from in 2080s. For example, Mymensingh Sadar lies in the high exposure category up to 2050s but devolved into in the very high exposure zone in 2080s. Gaffargaon upazilla is under the very high exposure zone for present, 2020s, 2050s and 2080s. Other upazilla remained within the very low to medium vulnerability for the time frame.

- Risk assessment shows that in the base period, there was no administrative unit in medium and very high risk zone. All the upazillas are in the very low to low risk zone except Gaffargaon. The scenario remained almost same for 2020s as well excluding the fact that Gaffargaon shifts to the very high risk zone. During 2050s to 2080s risk of two upazilla named Mymensingh Sadar and Austagram increased to some extent. Major part of the total study area is under the very low to low risk zone throughout the century. High and very high risk magnitude reflects the impact of climate change compared to the base period.

So, it can be interpreted that future climate change is going to have moderate impact on the flood situation of major portion of the old Brahmaputra River floodplain even if the wettest climate change scenario of RCP 8.5 is considered. But overall, there is an increasing trend of the flood from baseline to 2080s RCP 8.5 and the increment is significant after 2020s. Analysis of future hazard and risk maps show that some high hazard zones have a moderate risk of flood damage and vice versa. This happens when the land units with important land use and infrastructure have more unprotected areas or the socio-economic vulnerability is high in those land units. Hence, for a proper flood management scheme or plan, both hazard and risk assessment is required. The results found in this study provide useful information about the flood hazard and flood risk areas in the Old Brahmaputra River floodplain. The hazard and risk maps can be useful for the concerned authorities and planners and policy makers in identifying the hazard and risk zones of the particular river and thereby incorporating and planning a more suitable, economical and sustainable flood management strategies along the River.

6.2   Recommendations for Further Study

In this study, flood hazard, vulnerability and risk assessment are conducted for Old Brahmaputra River floodplain under future climate change scenario of RCP 8.5. To achieve the goal, a HEC-RAS 1D-2D coupled model of the river Old-Brahmaputra has been set up and calibrated and validated. The validated hydrodynamic model has been sued to develop the flood inundation scenario for future climate change scenario incorporated as the boundary conditions. From the inundation scenario of the study area, flood hazard map were prepared. Sequentially, socio economic vulnerability has also been assessment for selected indicators using weighted sum method. Later, risk maps were prepared for present and future flood flow condition and projected socio-economic condition. Based on the results and the experience gained during the study, some actions can be recommended for the improvement of this study as stated below.

➢ Digital elevation model plays vital role to enhance the capability and accuracy of model. It is recommended to use high resolution digital spatial database for real replication of topography for the better performance of the model.

➢ To establish the correlation of the flow between the Bahadurabad transit of Brahmaputra-Jamuna River and at Mymensingh of Old-Brahmaputra River, the concept of simple linear regression has been utilized considering only the effect of discharge of Bahadurabad transit on the flow at Mymensingh of

Old-Brahmaputra River. Consideration of other statistical approach such as non-linear or multiple regression technique considering the impact of sediment flow and other morphometric property of the two specific rivers would provide better estimation of the future flow at Mymensingh of old Brahmaputra river.

➢ In this study, flood depth, flood flow velocity and flood inundation area were used as the hazard parameters. However, more hazard parameters such as flooding duration, recession of the flood water, product of flood depth & velocity and shear stress can be used for the more comprehensive estimation of hazard.

➢ To assign weight to the indicators of flood hazard, sensitivity, adaptive capacity and exposure indicators, the concept of Principal Component Analysis (PRA) have been utilized in this study. The performance of the PCA has been verified by comparing the obtained weights with the weights suggested in available secondary literatures like journals, conference papers and theses and book chapters. Conducting analysis using Participatory Rural Appraisal (PRA) tools like Focus Group Discussion (FGD) or Analytical Hierarchy Process (AHP) would provide more reasonable weight incorporating the local people's perception.

➢ To estimate the level of vulnerability of the study area to flood, only the social and economic indicators have been used in this study. Incorporation of the indicators related to the "natural vulnerability", "physical vulnerability" and "institutional vulnerability" would provide the more rational assessment of sensitivity, adaptive capacity and exposure of the study area.

➢ Incorporation of local rainfall may validate the simulated flood inundation more accurately.

LIST OF REFERENCES

[1] Ahmed, A.U. 2006, Bangladesh, "Climate Change Impacts and Vulnerability.A Synthesis", Climate Change Cell, Department of Environment, Dhaka

[2] Ashley, R.M., Balmforth, D.J., Saul, A.J., Blanskby, J.D., 2005, "Flooding in the future–predicting climate change, risks and responses in urban areas", Water Science Technology.: J. Int. Assoc. Water Pollut. Res. 5, 265–273

[3] Alauddin K., 2010, "A report on Flood Situation Report of Sirajganj District -2010," Flood Situation Report-2010, NDP, Sirajgonj

[4] Afrose S. and Ahmed N., 2016, "Assessment of Fish Biodiversity and Fishing Practices of the Old Brahmaputra River, Bangladesh", Global Veterinaria, Volume: 17(3), Pages: 199-203

[5] Anh, T. N., Kha, D. D., Duc, D. D. and Son, N. T., 2016, "Hydraulic modeling for flood vulnerability assessment, case study in river basins in North Central Vietnam", Procedia Engineering, ELSEVIER, Volume 65, pp. 23-30

[6] Ahmed M.S., and Navera U.K., 2018, "Planform Observation of De-Connectivity of Old Brahmaputra Offtake in Lean Period Using Satellite Images", Journal of Modern Science and Technology Vol. 6. No.1, Pp.1-9

[7] Ali, 2010, "A Study on Siltation at the Intake Reach of the Old Brahmaputra River", MSc Thesis, Department of Water Resources Engineering, Bangladesh University of Engineering and Technology, BUET, Bangladesh

[8] Aulong, S., and Kast, R. (2011), "A conceptual framework to assess vulnerability", Application to global change stressors on South Indian farmers

[9] Agard, J., and Schipper, L. (2015), IPCC WGII AR5 glossary

[10] Azmeri, Hadihardaja I.K., Vadiya R., 2016, "Identification of flash flood hazard zones in mountainous small watershed of Aceh Besar Regency, Aceh Province, Indonesia", The Egyptian Journal of Remote Sensing and Space Sciences (2016) 19, 143–160

[11] Amrhein, M., Srinivasan, B., Bonvin, D., et al., 1996, "On the rank deficiency and rankaugmentation of the spectral measurement matrix", Chemometrics and Intelligent Laboratory Systems 33 (1), pages: 17–33

[12] Abson D.J., DougillA.J. and Stringer L.C.,2012, Using Principal Component Analysis for information-rich socio-ecological vulnerability mapping in Southern Africa, Applied Geography (2012) 1-10

[13] Akoglu H., 2018, "User's guide to correlation coefficients", Turkish Journal of Emergency Medicine, 18(3): 91–93

[14] Brunner, G. W., 2016b. Combined 1D and 2D Modeling with HEC-RAS..s.l.: US Army Corps of Engineers, Institute for Water Resources, Hydrologic Engineering Center.

[15] Brunner, G. W., 2016. HEC-RAS River Analysis System : Hydraulic Reference Manual.s.l.:U.S. Army Corps of Engineers, Institute for Water Resources, Hydrologic Engineering Center, 609 Second Street, Davis, CA 95616

[16] Brunner, G., Piper, S., Jensen, M. & Chacon, B., 2015.Combined 1D and 2D Hydraulic Modeling within HEC-RAS.s.l., s.n., pp. 1432-1443.

[17] Beaumont. R., (2012) An introduction to Principal Component Analysis & Factor Analysis Using SPSS 19 and R, http://www.floppybunny.org/robin/web/virtualclassroom/stats/statistics2/pca1.pdf [accessed 2/12/2013]

[18] Bangladesh Bureau of Statistics (BBS),2015, "Population Density and Vulnerability:A Challenge for Sustainable Development of Bangladesh", Population Monograph of Bangladesh,ISBN- 978-984-33-9952-6

[19] Biswas R.N.,, Mia M. J., Islam M.N., 2018, "Hydro-Morphometric Modeling for Flood Hazard Vulnerability Assessment of Old Brahmaputra River Basin in Bangladesh", Engineering Technology, Open access journal, Volume 1 Issue 4 - April 2018

[20] Brenkert A., and Malone E., 2005, "Modeling vulnerability and resilience to climate change: a case study of India and Indian states", Climate Change. 72:57–102.

[21] Brooks N. 2003, "Vulnerability, risk and adaptation: a conceptual framework", Tyndall Working Paper 38. Norwich: Tyndall Centre for Climate Change Research

[22] Birkmann J., 2006b, "Indicators and criteria for measuring vulnerability: theoretical bases and requirements. In: Birkmann J, editor. Measuring vulnerability to natural hazards–towards disaster resilient societies, New York: United Nations University; p. 55–77

[23] Birkmann, J. (2006), "Measuring vulnerability to promote disaster-resilient societies: Conceptual frameworks and definitions", Measuring Vulnerability to Natural Hazards: Towards Disaster Resilient Societies, 1, 9–54

[24] Bhuiyan M.S.R, 2014 "Flood Hazard and Vulnerability Assessment in a Riverine Flood Prone Area: ACase Study", MSc. Thesis, Institute of Water and Flood Management, Bangladesh University of Engineering and Technology

[25] BWDB, 2010, "Annual flood report, flood forecasting and warning centre", Bangladesh Water Development Board

[26] Bankoff, G., Frerks G., and D. Hilhorst D., 2004, "Mapping Vulnerability: Disasters, Development and People", Earthscan, London, ISBN-10: 1849771928, pp: 256

[27] Booij, M.J., 2005. Impact of climate change on river flooding assessed with different spatial model resolutions. J. Hydrol. 303, 176–198. http://dx.doi.org/10.1016/j.jhydrol.2004.07.013

[28] Basak S.R., Basak A.C., Rahman M.A., 2015, "Impacts of floods on forest trees and their coping strategies in Bangladesh", Weather and Climate Extremes 7 (2015) 43–48

[29] Bronstert A., 2003, "Floods and climate change: interactions and impacts", Risk Analysis, volume 23, issue 3, page: 545-557

[30] Brammer, H., Asaduzzaman, M., &Sultana., P. (1993). *Effects of climate and sea level changes on the natural resources of Bangladesh* Dhaka: Bangladesh Unnayan Parishad

[31] Cardona, et.al., 2012, "Determinants of risk: exposure and vulnerability. Managing the Risks of Extreme Events and Disasters to Advance Climate Change Adaptation", A Special Report of Working Groups I and II of the Intergovernmental Panel on Climate Change (IPCC) [Field, C.B., et al. (eds)]. (Cambridge, UK, and New York, NY, USA: Cambridge University Press), 65–108

[32] CDMP, IWM, "Comprehensive Disaster Management Programme & Institute of water Modeling. Climate Change Prediction Modeling Impact Assessment of Climate Change and Sea Level Raise on Monsoon Flooding," 2008

[33] Chowdhury J.U., Karim M. F., 1996, *A risk based zoning of storm surge prone area of the Ganges tidal plain*, Journal of Civil Engineering, The Institution of Engineers, Bangladesh, Vol. CE 24, No. 2, 1996

[34] Cutter, S. L., Carolina, S., Boruff, B. J., Carolina, S., Shirley, W. L., and Carolina, S. (2003). Social Vulnerability to Environmental Hazards n. *Social Science Quarterly*, *84*(2), 242–261

[35] Cutter, S. &Finch, C., 2008, "Temporal and spatial changes in social vulnerability to natural hazards", *Proc. Natl. Acad. Sci.,* Volume 105, p. 2301–2306

[36] Devoy, R. J. N. 1992, "Questions of coastal protection and the human response to sea-level rise in Ireland and Britain", *Irish Geography*, 25, (1), 1-22

[37] Dilley, R. S. and Rasid, H. 1990, "Human response to coastal erosion: Thunder Bay, Lake Superior", *Journal of Coastal Research*, 6, (4), 779-788

[38] Deressa T., Hassan R.M. and Ringler, C., (2008) Measuring Ethiopian Farmers' Vulnerability to Climate Change Across Regional States, Environment and Production Technology Division, IFPRI Discussion Paper, 00806

[39] Dulal Chandra Roy & Thomas Blaschke, 2015, "Spatial vulnerability assessment of floods in the coastal regions of Bangladesh", Geomatics, Natural Hazards and Risk, 6:1, 21-44, DOI: 10.1080/19475705.2013.816785

[40] Disaster Management Bureau, 2010, "National Plan for Disaster Management 2010-2015", Government of the People's Republic of Bangladesh, Disaster Management & Relief Division

[41] Dottori F., Salamon P., Bianchi A., Alfieri L., Hirpa F. A., Feyen L., 2016, "Development and evaluation of a framework for global flood hazard mapping", Advances in Water Resources, ELSEVIER, Volume 94, Pages 87-102

[42] European Commission, 2007, "Directive 2007/60/EC of the European Parliament and of the Council of 23 October 2007 on the assessment and management of flood risks", Official Journal of European Union L 288,page: 27–34

[43] Elisabeth Angel, Knut BjonStokke, "Vulnerability and adaptive capacity in Hammerfest, Norway", Ocean & Coastal Management (ELSEVIER), Volume 94, June 2014, Pages 56-65

[44] Everitt B S and Hothorn T. (2011) An introduction to applied multivariate analysis with R., Springer

[45] Eakin, H., and Tapia B., (2008), Insights into the composition of household vulnerability from multicriteria decision analysis. Global Environmental Change 18(1): 112–127

[46] Ebi, K.L., Hess, J.J., Isaksen, T.B, (2016), "Using uncertain climate and development information in health adaptation planning", Curr. Environ. Health Rep.2016,3, 99–105. [CrossRef] [PubMed]

[47] Flanagan, B. E., Gregory, E. W., Hallisey, E. J., Heitgerd, J. L., and Lewis, B. (2011), "A social vulnerability index for disaster management", Journal of Homeland Security and Emergency Management, 8(1)

[48] Fung, C. F., Farquharson, F., and Chowdhury, J. (2006), Exploring the impacts of climate change on water resources-regional impacts at a regional scale: Bangladesh. *IAHS PUBLICATION*, *308*, 389

[49] Flax, Lisa K., Jackson, Russell W., and Stein, David N. (2002), 'Community's Vulnerability Assessment Tool Methodology', Natural Hazards Review, ASCE,3(4), 163-176

[50] Flood Forecasting and Warning Center (FFWC), (2014), Annual Flood Report 2014, Bangladesh Water Development Board, Dhaka.

[51] Forkuo E.K., (2011), "Flood Hazard Mapping using Aster Image data with GIS", International Journal of Geomatics and Geosciences, Volume 1, No 4, 2011

[52]   Gemenne, F., Brücker, P. and Ionesco, D. (Eds.) 2012, The State of Environmental Migration 2011, Institute for Sustainable Development and International Relations (IDDRI) / International Organization for Migration (IOM)

[53]   Gain, A., Apel, H., Renaud, F., Giupponi, C., 2013, "Thresholds of hydrologic flow regime of a river and investigation of climate change impact—the case of the Lower Brahmaputra river Basin" Climate Change 120, 463–475. http://dx.doi.org/10.1007/s10584-013-0800-x

[54]   Geoscience, 2014.http://www.ga.gov.au/scientifictopics/hazards/risk-impact/vulnerability

[55]   George M. V., Smith S.K., Swanson D.A., and Tayman J.,2004, "Population Projections," chapter 21 in Jacob Siegel and David Swanson (eds.), The Methods and Materials of Demography. San Diego: Elsevier Academic Press

[56]   Gawatre D.W, Mahesh H. Kandgule M.H., Kharat S.D., 2016, "Comparative Study of Population Forecasting Methods", IOSR Journal of Mechanical and Civil Engineering (IOSR-JMCE), Volume 13, Issue 4, pages: 16-19

[57]   Hasan, S.M.I., 2006, "Application of Geoinformatics for Flood Study at Tarapur Union of Gaibandha", M.Sc. Thesis, IWFM, Bangladesh University of Engineering and Technology (BUET)

[58]   Haque, M.M. Khan,M.S.A., Islam,T., Salehin,M., Mondal, M.S., and Islam,A.S., "Development of Flood Hazard and Risk Maps with Effect of Climate Change Scenario," Climate Change Cell, Institute of Water and Flood Management, BUET, Dhaka, 2013

[59]   Hossain M.S., 2013, "Flood Damage and Risk Assessment Model in the Haor Basin of Bangladesh", MSc in Water Resources Development, Institute of Water and Flood Management, Bangladesh University of Engineering & Technology

[60]   HEC-RAS, 2016, "HEC-RAS River Analysis System: 2D Modeling User's Mannual", 5th edition

[61]   Hall, J., Arheimer, B., Borga, M., Brázdil, R., Claps, P., Kiss, A., Kjeldsen, T.R., Kriaučiūnienė, J., Kundzewicz, Z.W., Lang, M., et al., 2014, "Understanding flood regime changes in Europe: a state-of-the-art assessment", Hydrology and Earth System Sciences 18, 2735–2772, http://dx.doi.org/10.5194/hess-18-2735-2014

[62]   IPCC, 2001. Climate change 2001: synthesis report, a contribution of working groups I, II, and III to the Third Assessment Report of the intergovernmental panel on climate change. In: *The Third Assessment Report (TAR).* s.l.:Cambridge: Cambridge University Press, 398

[63]   IPCC 2014, Climate Change 2014: Synthesis Report. Contribution of Working Groups I, II and III to the Fifth Assessment Report of the Intergovernmental Panel on Climate Change [Core Writing Team, R.K. Pachauri and L.A. Meyer (eds.)], IPCC, Geneva, Switzerland

[64]   International Displacement Monitoring Center (IDMC) 2015, "Bangladesh: comprehensive response required to complex displacement crisis", accessed 28 February 2015, http://www.internal-displacement.org/south-and-south-east-asia/bangladesh/2015/bangladesh-comprehensive-response required-to-complex-displacement-crisis

[65] Islam, A., Bala, S. & Haque, M., 2010, "Flood inundation map of Bangladesh using MODIS time-series images", Journal of Flood Risk Management, Volume 3, p. 210–222

[66] International Sava River Basin Commission (ISRBC), 2014, "Preliminary Flood Risk Assessment in the Sava River Basin", page1-3

[67] IWM, 2014, *"Policy Brief : Local Level Policy Hazard Maps for Flood, Storm Surge & Salinity",* s.l.: Ministry of Disaster Management and Relief

[68] Islam, M. M., and Sado, K., "Development of flood hazard maps of Bangladesh using NOAA-AVHRR images with GIS," Hydrologic Sciences, Jl, 45(3), 337-355, 2000

[69] Ibrahim et.al., 2017, "Identification of vulnerable areas to floods in Kelantan River sub-basins by using flood

[70] Islam M.S., 2014, "Flood Risk Assessment in Bangladesh and People`s Adjustment Scenarios: A Case Study in Brahmaputra-Jamuna Floodplain", Ph. D. Thesis Department of Geography and Environment, University of Dhaka

[71] IPCC, 2012, "Managing the Risks of Extreme Events and Disasters to advance Climate Change Adaptation:, A Special Report of Working Groups I and II of the Intergovernmental Panel on Climate Change; Cambridge University Press: Cambridge, UK; New York, NY, USA, 2012.

[72] Jain S., Mishra N., Bokade S., Chaturvedi S., 2013, "A Review Paper on Forecasting of Demographic Features using Statistical and Data Mining Methods", International Journal of Science and Research (IJSR), National Conference on Knowledge, Innovation in Technology and Engineering (NCKITE), 10-11 April 2015 Kruti Institute of Technology & Engineering (KITE), Raipur, Chhattisgarh, India

[73] Jurgilevich, A.; Räsänen, A.; Groundstroem, F.; Juhola, S.A, "systematic review of dynamics in climate risk and vulnerability assessments"

[74] Jahan M., 2018, "Multi-Scale Assessment of Risks to Environmental Hazards in Coast Area of Bangladesh", M.Sc. Thesis, Institute of Water and Flood Management, BUET, Dhaka -1000

[75] Jeb, D. N and Aggarwal, S.P (2008), "Flood inundation hazard modeling of the River Kaduna using Remote Sensing and Geographic Information Systems", Journal of Applied Sciences Research, 4 (12)

[76] Kasperson J, Kasperson R, Turner BL, Hsieh W, Schiller A. 2005, "Vulnerability to globalenvironmental change", In: Kasperson J, Kasperson R, editors. The social contours ofrisk, volume II: risk analysis, corporations & the globalization of risk. London: Earthscan; p. 245–285

[77] Kasperson RE, Dow K. 2005,"Vulnerable people and places", In: Hassan R, Scholes R, Ash N. editors. Ecosystems and human well-being: current state and trends. Washington (DC): Island Press; p. 143–164

[78] Bishaw K., 2012, "Application of GIS and Remote Sensing Techniques for Flood Hazard and Risk Assessment", The Case of Dugeda Bora Woreda of Oromiya Regional State, Ethiopia, Berlin Conference on the Human Dimensions of Global Environmental Change

[79] Khatun M. A., Rashid M. B., Hygen H.O., 2016, Climate of Bangladesh, MET Report, no. 08/2016, ISSN 2387-4201, Climatess

[80] Kreibichet.al., 2009, "Is flow velocity a significant parameter in flood damage modelling?", Natural Hazards, Earth System Sciences, vol:9, pages: 1679–1692.

[81] Li-Na Wang, Xiao-Hong Chen, Quan-Xi Shao, Yan Li,2015, "Flood indicators and their clustering features in Wujiang River, South China", Ecological Engineering, ELSEVIER, 76 , pages: 66–74

[82] Laila F., 2013, "Assessment on social vulnerabilities to climate change–A study on southwestern coastal region of Bangladesh", Uppsala University

[83] Lorraine R., Maksym G., 2014, "Drought and Flood Risk Assessment on Manyame River Basin, Zimbabwe under Climate Change", International Center for Water Hazard and Risk Management (ICHARM)

[84] Malik M. I., and Ahmad F., 2014, "Flood Inundation Mapping and Risk Zoning of the Swat River Pakistan using HEC-RAS Model", Lasbela University Journal of Science and Technology, volume: 3, pages:45-52.

[85] Mirza M. M. Q., 2002 "Global warming and changes in the probability of occurrence of floods in Bangladesh and implications", Global environmental change, 12(2), pp. 127-138.

[86] Mujiburrehman k., 2015, "Preparation of Flood Inundation Map in Ganga River at Farakka Bridge, Malda, West Bengal, India", International Journal of Research in Geography (IJRG), Volume 1, Issue 1, June 2015, PP 1-7

[87] Merz et al, 2010, "Assessment of economic flood damage", Natural Hazards Earth System Science, 10, 1697–1724, Review article, doi: 10.5194/nhess-10-1697-2010, Copernicus Publications, European Geosciences Union

[88] MPO, 1986, Master Plan Organization, National Water Plan Phase-I, Technical Report, Ministry of Irrigation, Water Development and Flood Control, Dhaka

[89] Messner, F., 2007, Evaluating flood damages: guidance and recommendations on principles and methods, FLOODsite project Consortium, European Community

[90] Mirza, M. M. Q. (1997). "Modelling the effects of climate change on floodingin Bangladesh." Unpublished D.Phil Thesis, *International Global ChangeInstitute* (IGCI), University of Waikato, Hamilton, New Zealand

[91] Mirza M. M. Q. (2002), "Global warming and changes in the probability of occurrence of floods in Bangladesh and implication", Global environmental change, 12(2), 127-138

[92] Mirza, M. M. Q., 2003, "Climate change and extreme weather events: can developing countries adapt?", Climate policy, 3(3), 233-248

[93] Masood, M., 2006, "Flood Hazard and Risk Assessment in Mid-eastern Part of Dhaka, Bangladesh", Halcrow Group Limited, UK.

[94] Mondal M.S., Islam M.R., and Biswas S., "Simulation of Flood Risk due to Climate Change in Major Rivers of Bangladesh using a Hydrodynamic Model", Proceedings, International Conference on Disaster Risk Mitigation, Dhaka, Bangladesh, September 23 - 24, 2017

[95] Nasiri, H. and Shahram, S.K. "Flood vulnerability index as a knowledge base for flood risk assessment in urban area" Journal of Novel Applied Sciences, 2, 2013, pp. 269-272

[96] Noor, F., 2013, "Morphological Study of Old Brahmaputra Offtake Using Two Dimensional Mathematical Model", M. Sc. Thesis, Bangladesh University of Engineering and Technology (BUET), Dhaka, Bangladesh

[97] Nugraha A.L., Santosa P.B., Aditya T., 2015, "Dissemination of tidal flood risk map using online map in Semarang", Procedia Environmental Sciences 23, Pages: 64 – 71

[98] Ntajal J., Lamptey B.L., Mahamadou I.B., Benjamin K. Nyarko B.K., 2017, "Flood disaster risk mapping in the Lower Mono River Basin in Togo, West Africa", International Journal of Disaster Risk Reduction, Volume 23, Page: 93-103

[99] Nandargi, S., Dhar, O. N., Sheikh, M. M., Enright, B., and Mirza, M. M. Q. (2010), Hydrometeorology of Floods and Droughts in South Asia–A Brief Appraisal.In *Global Environmental Changes in South Asia* (pp. 244-257).Springer Netherlands

[100] Nishat, U., 2017. Flood Inundation Mapping of Jamuna River Floodplain Using HECRAS 2D Model. B.Sc. Thesis. Department of Water Resources Engineering, Bangladesh University of Engineering & Technology, Dhaka-1000

[101] Nur I. and Shrestha K.K., 2017, "An Integrative Perspective on Community Vulnerability to Flooding in Cities of Developing Countries ", Urban Traulnerability nsitions Conference, Shanghai, September 2016, Procedia Engineering, ELSEVIER, volume 198 (2017) Page: 958 – 967

[102] Nash, J. & Sutcliffe, J., 1970, "River flow forecasting through conceptual models part I — A discussion of principles", Journal of Hydrology , 10(3), pp. 282-290

[103] Preston, B.L.; Yuen, E.J.; West away, R.M., 2011, "Putting vulnerability to climate change on the map: A review of approaches, benefits, and risks", Sustain. Sci.,6, 177–202. [CrossRef]

[104] Piya L., Maharjan, K. L. and Joshi N.P., 2012, "Vulnerability of rural households to climate change and extremes: Analysis of Chepang households in the Mid-Hills of Nepal", Selected Paper prepared for presentation at the International Association of Agricultural Economists (IAAE) Triennial Conference, Foz do Iguaçu, Brazil, 18-24 August, 2012.

[105] Potsdam Institute for Climate Impact Research and Climate Analytics (PIK), 2013, "Turn Down the Heat: Climate Extremes, Regional Impacts, and the Case for Resilience", World Bank, Washington DC

[106] Rohat, G.; Flacke, J.; Dao, H.; Van M., 2018, "Co-use of existing scenario sets to extend and quantify the shared socioeconomic pathways", Climate Change (under review)

[107] Rakib M. R., Islam M.N., and Islam M.N., 2017, "Flood Vulnerability Mapping to Riverine Floods: A Study on the Old Brahmaputra River", Current Research in Geosciences, 2017, 7 (2): 47.58

[108] Roy D.C., and Blaschke T., 2015, "Spatial vulnerability assessment of floods in the coastal regions of Bangladesh", Geomatics, Natural Hazards and Risk, 6:1, 21-44.

[109] Rahman M. M., Hossain M. A., & Bhattacharya A. K., 2007, "Flood Management in the Flood Plain of Bangladesh", *CENeM.* Kolkata: International Conference on Civil Engineering in the New Millennium: Opportunities and Challenges.

[110] Rakib M. R., Islam M.N., and Islam M.N., 2017, "Flood Vulnerability Mapping to Riverine Floods: A Study on the Old Brahmaputra River", Current Research in Geosciences, 2017, 7 (2): 47.58 DOI: 10.3844/ajgsp.2017.47.58

[111] Raff, D.A., Pruitt, T., Brekke, L.D., 2009, "A framework for assessing flood frequency based on climate projection information", Hydrol. Earth Syst. Sci. 13, 2119–2136. http://dx.doi.org/10.5194/hess-13-2119-2009

[112] Rouf T., 2015, "Flood Inundation Map of Sirajganj District using Mathematical Model", MSc Engineering Thesis, Department of Water Resources Engineering, Bangladesh University of Engineering and Technology

[113] Samarasinghea S.M.J.S., Nandalalb H.K, Weliwitiyac D.P, Fowzed J.S.M, Hazarikad M.K, Samarakoond K., 2010, "Application of Remote Sensing and GIS for Flood Risk Analysis: A Case Study at Kalu-Ganga River, SRILANKA", International Archives of the Photogrammetry, Remote Sensing and Spatial Information Science, Volume XXXVIII, Part 8, Kyoto Japan 2010, page:110-115

[114] Sarker, A.A., and Rashid, A.K.M.M., 2013, "Landslide and Flashflood in Bangladesh. In: Disaster Risk Reduction Approaches in Bangladesh, Disaster Risk Reduction", Springer, Japan.

[115] Smith, K. and Ward, R, 1998, "Floods Physical Processes and Human Impact", WestSussex, England.

[116] Silva G.D., SB W., Herath S., 2016 "Event Based Flood Inundation Mapping Under the Impact of Climate Change: A Case Study in Lower Kelani River Basin, Sri Lanka", Hydrology Current Res 2016, Volume 7: Issue 1

[117] Satta, A., Venturini, S., Puddu, M., Firth, J., and Lafitte, A. (2015), "Strengthening the knowledge base on regional climate variability and change: application of a multi-scale coastal risk index at regional and local scale in the Mediterranean. Plan Bleu Report.

[118] Shrestha, M.S., Heggen, R., Thapa, K.B., Ghimire, M., and Shakya, N., 2004, "Flood Risk and Vulnerability Mapping using GIS: A Nepal case study," Proceedings of the 2nd International Conference of Asia-Pacific Association of Hydrology and Water Resources, Singapore, Volume I, pp. 180-190.

[119] Singh, A., & Sharma, A., "GIS and a remote sensing based approach for urban flood-plain mapping for the Tapi catchment, India," Hydroinformatics in Hydrology, Hydrogeology and Water Resources, Hyderabed, India. pp. 389-394, 2009

[120] S. McLaughlin, J.McKenna, J.A.G. Cooper, (2002), "Socio-economic data in coastal vulnerability indices: constraints and opportunities", Journal of Coastal Research, pages: 487-497

[121] Sarker, 2016, "Swept away? Mapping Flood Vulnerability in Bangladesh", poster, Class: DHP207: GIS for International Applications, The fletcher school , Tufts University

[122] Adhikary S., Bala S.K, Islam A. K. M. S., L. C. Shutradhar, Fahad M.G.R., 2015, "An Assessment of Climate Change Vulnerability Index at District Level of Bangladesh in Context of Extreme Temperature and Precipitation", International Conference on Recent Innovation in Civil Engineering for Sustainable Development(IICSD-2015), Department of Civil Engineering, DUET, Bangladesh

[123] Timbadiya, P., Patel, P. & Porey, P., 2011, "Calibration of HEC-RAS model on predictionof flood for lower Tapi River, India", Journal of Water Resource and Protection, 3(11), p. 805

[124] Akhter T., Hossain J., Jahan S., 2018, "Population Projection of the Districts Noakhali, Feni, Lakhshmipur and Comilla, Bangladesh by Using Logistic Growth Model", Pure and Applied Mathematics Journal2017; 6(6): 164-176

[125] Tran L. T., O'Neill R. V, and Smith E. R., 2010, "Spatial pattern of environmental vulnerability in the Mid-Atlantic region, USA", Applied Geography, 30(2), 191–202

[126] Tu V.T., Tingsanchali T., 2009, "Flood Inundation, Damage and Risk Assessment in Hoang Long Basin, Vietnam,", Thesis, Asian Institute of Technology, Thailand

[127] Tingsanchali T. &Karim M.F., 2005, Flood hazard and risk analysis in the southwest region of Bangladesh, Hydrol. Process, 19, 2055–2069, John Wiley and Sons Ltd

[128] Tazin T., 2018, "Flood Hazard Mapping of Dharala Floodplain using HEC-RAS 1D/2D Coupled Model", M. Sc. Thesis, Bangladesh University of Engineering and Technology (BUET), Dhaka, Bangladesh

[129] Tirpak D, Bernstein L, Bosch P, Canziani O, Chen Z, et al. (2007), "Synthesis Report Climate Change", Fourth Assessment Report of IPCC

[130] Tingsanchali T. & Karim M.F., 2005, "Flood hazard and risk analysis in the southwest region of Bangladesh", Hydrologic Process, 19, 2055–2069, John Wiley and Sons Ltd

[131] Toda L.L., Yokingco J.C.E., Paringit E.C., Lasco R.D., 2017, "A LiDAR-based flood modelling approach for mapping rice cultivation areas in Apalit, Pampanga", Applied Geography, ELSEVIER, Volume 80,page: 34-47, March, 2017.

[132] Uddin et.al., 2017, "Flood and Flood Management in Bangladesh", term paper, Course: DSMHT 403:Climate Modelling and Adaptation, Dept. of Disaster Science and Management Faculty of Earth and Environmental Sciences, University of Dhaka

[133] UNDRO, 1991, Mitigating natural disasters: phenomena, effects and options, A manual forpolicy makers and planners, United Nations Disaster Relief Organization, New York.

[134] UNISDR 2009, "UNISDR terminology on disaster risk reduction", Available from: http://www.unisdr.org/eng/terminology/terminology-2009-eng.html

[135] UNDP, 2004, "Reducing disaster risk: a challenge for development", A global report, Bureau for Crisis Prevention and Recovery (BRCP), New York: UNDP

[136] Uddin M., Talukder S., Hossen M.S., and Hossain M.T., 2017, "Physicochemical Analysis of Mymensingh Municipality Sewage Water and Old Brahmaputra River water", Journal of Environmental Science& Natural Resources, 10(2): 105-108

[137] UKCIP. Socioeconomic Scenarios for Climate Change Impact Assessment: A Guide to Their Use in the UK ClimateImpacts Programme; UKCIP: Oxford, UK, 2000.

[138] Wheater, H., Evans, E., 2009, "Land use, water management and future flood risk", Land Use Policy 26 (Suppl. 1), 251–264.http://dx.doi.org/10.1016/j.landusepol. 2009.08.019

[139] WARPO, (. R. P. O., 2004. *National Water Management Plan,* s.l.: s.n. Weedon, G. et al., 2014. The WFDEI meteorological forcing data set: WATCH Forcing

[140] Eigege, 2014, "Assessment of the 2012 Flooding in MararabaKaru Local Governemnt Area of Nasarawa State, Nigeria", MSc Thesis, Department of Geography, Ahmadu Bello University, Nigeria

APPENDICES

Appendix A

Population Growth and Projection of Gazipur District

(a)

Population Growth and Projection of Kishoreganj District

(b)

Population Growth and Projection of Narsingdi District

(c)
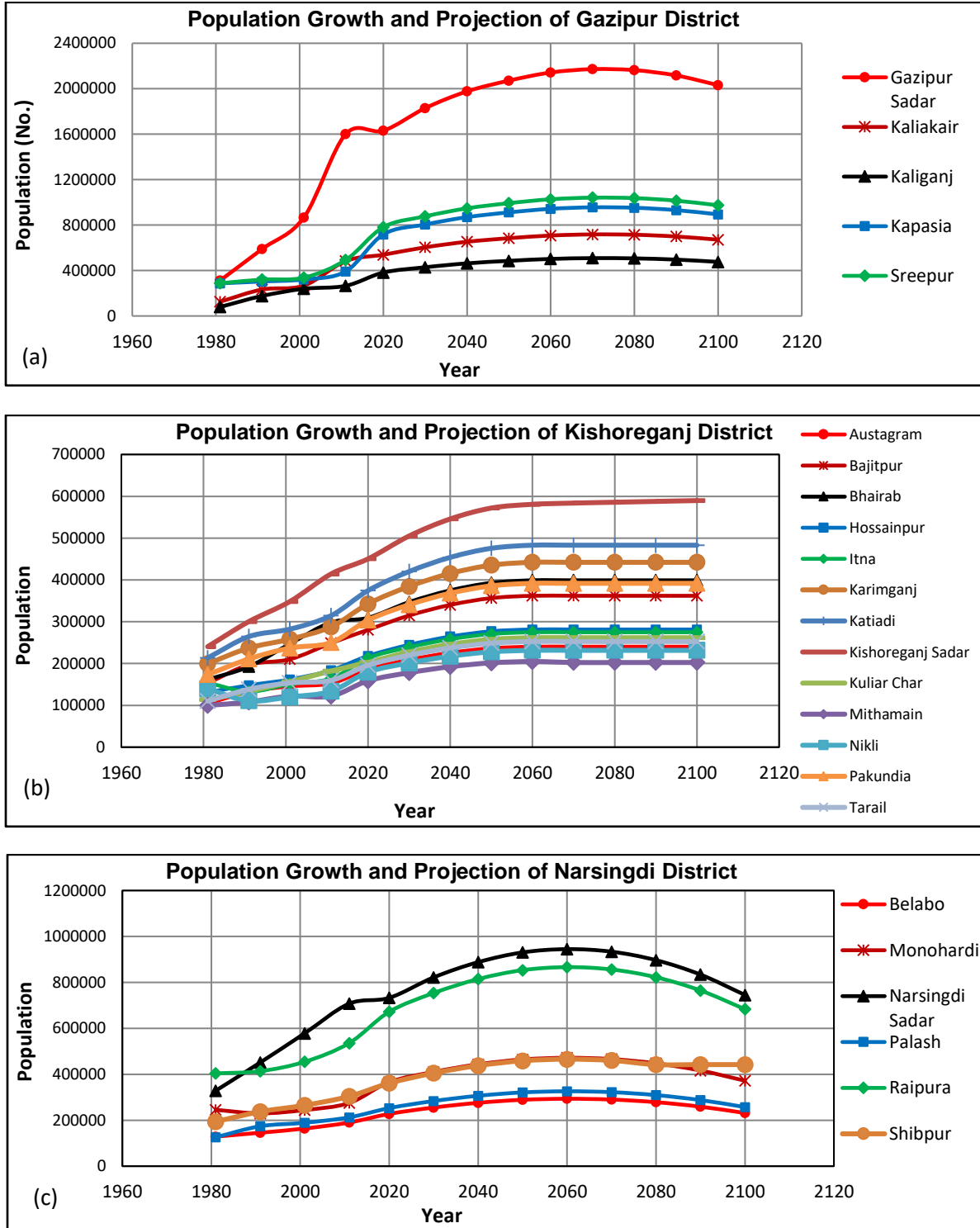
Figure A.1: Population Growth and Projection (a) Gazipur (b) Kishoreganj (c) Narsingdi

148
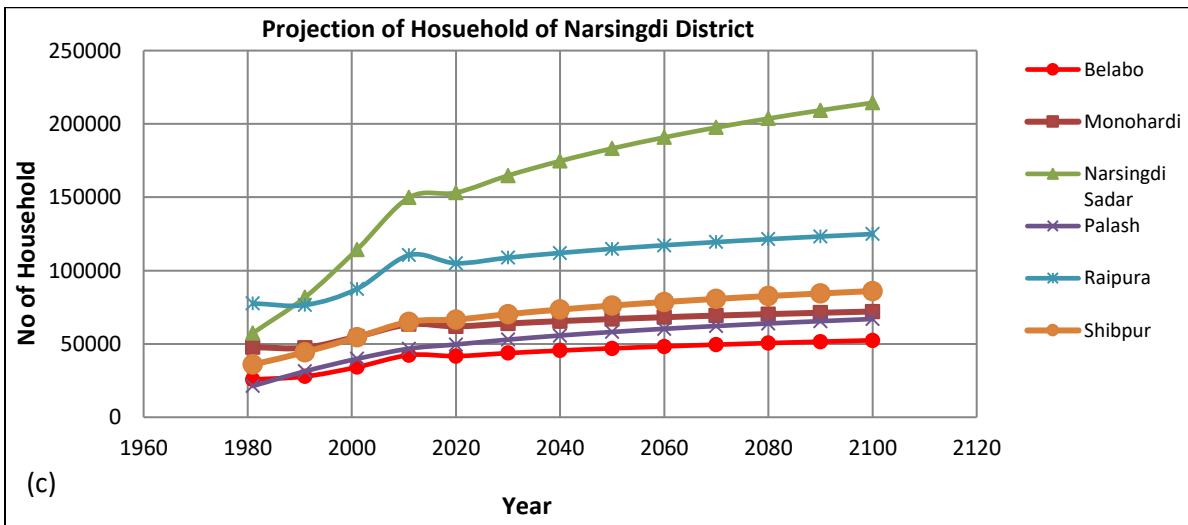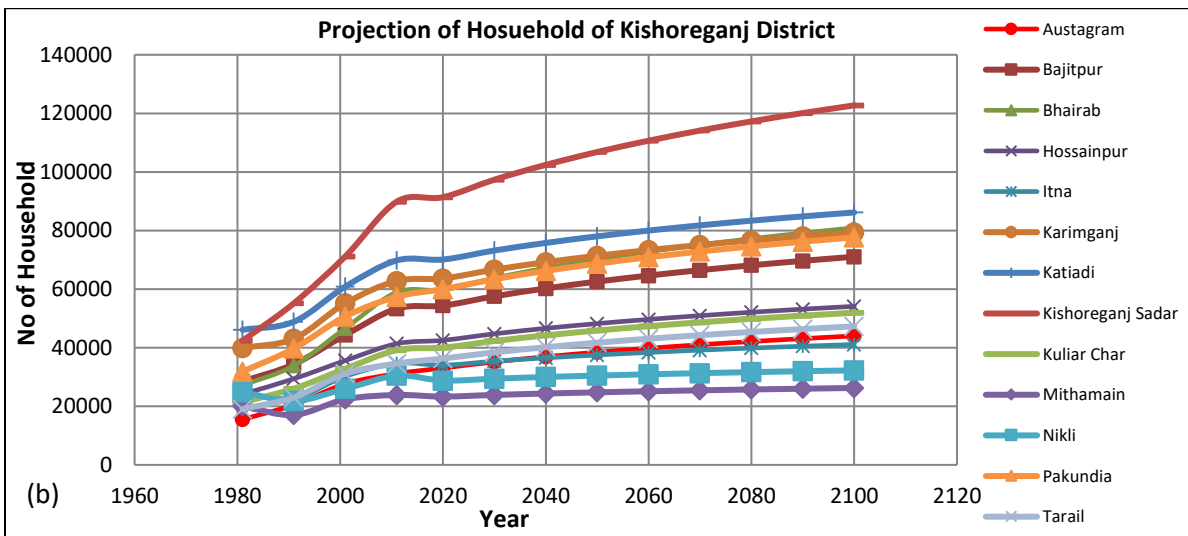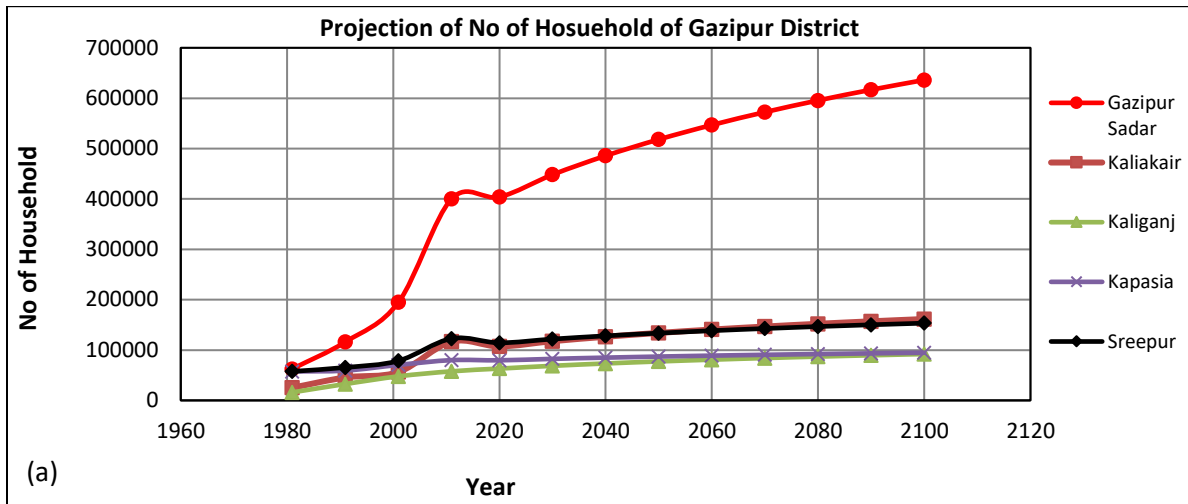
Figure A.2: Projection of Household (a) Gazipur (b) Kishoreganj (c) Narsingdi
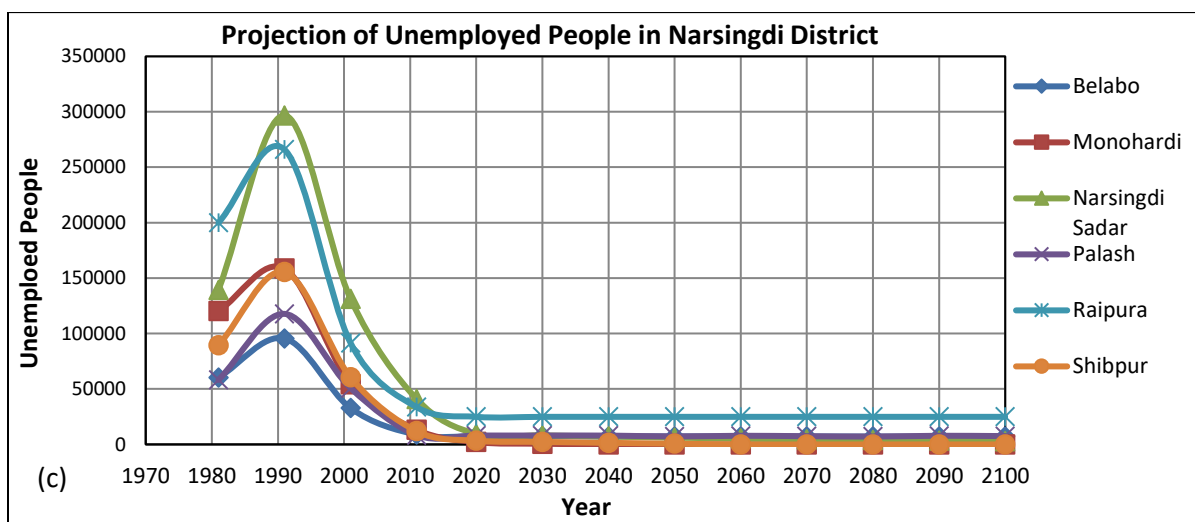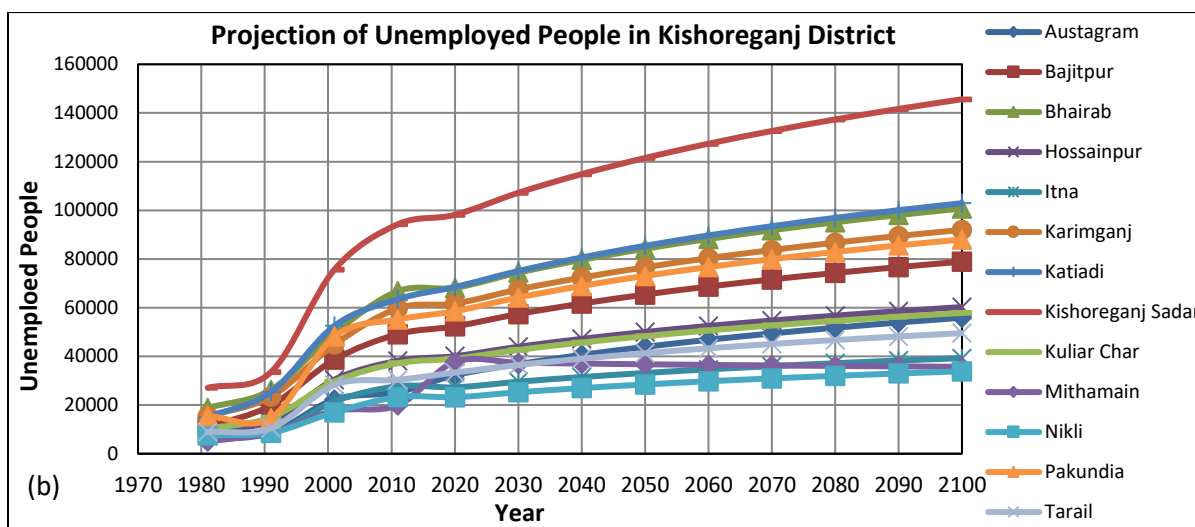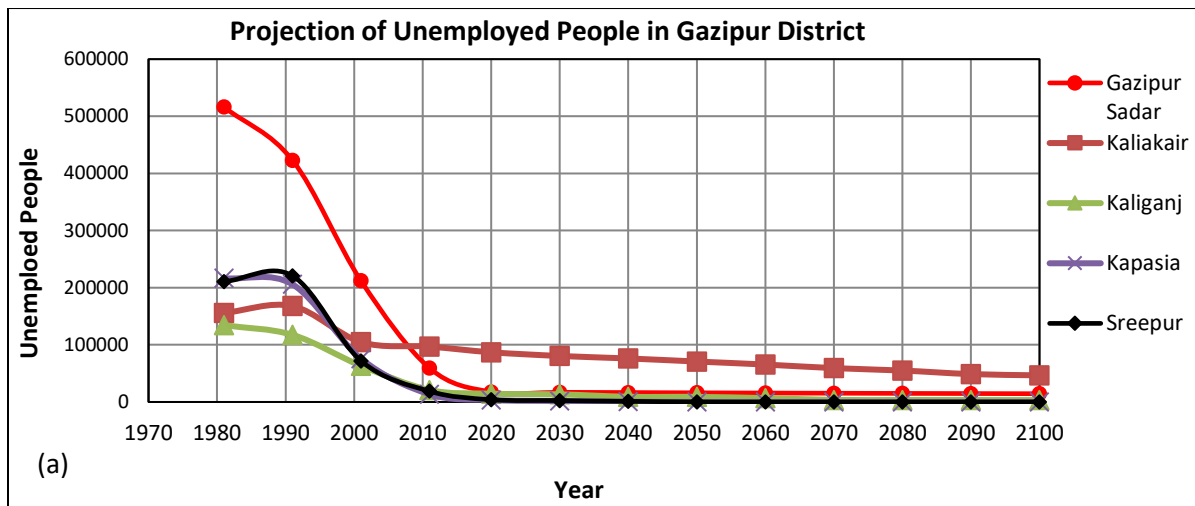
Figure A.3: Projection of Unemployed People (a) Gazipur (b) Kishoreganj (c) Narsingdi

Projection of Floating Population of Gazipur District

Projection of Floating Population of Kishoreganj District

Projection of Floating Population of Narsingdi District
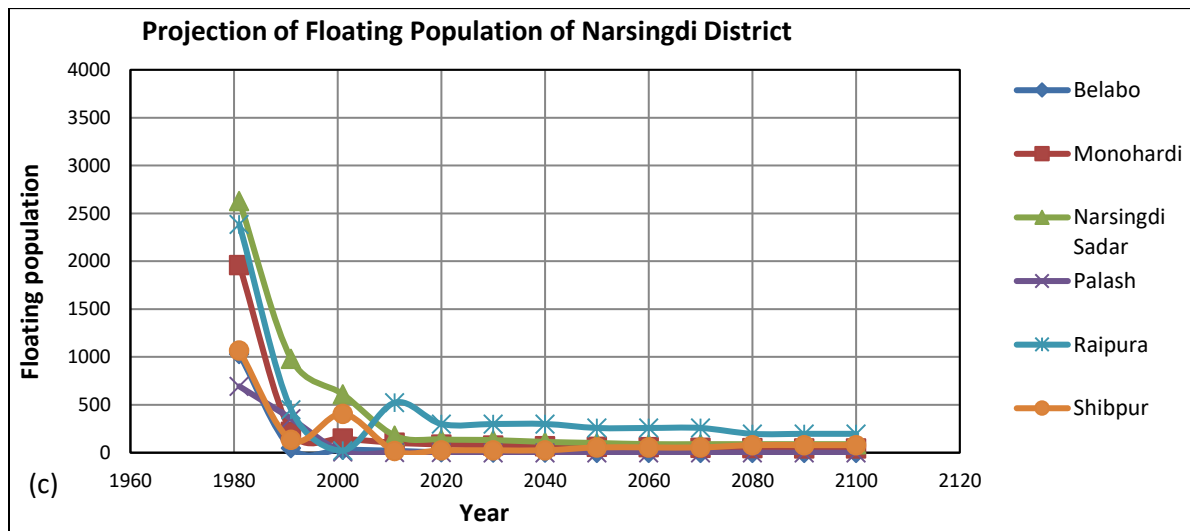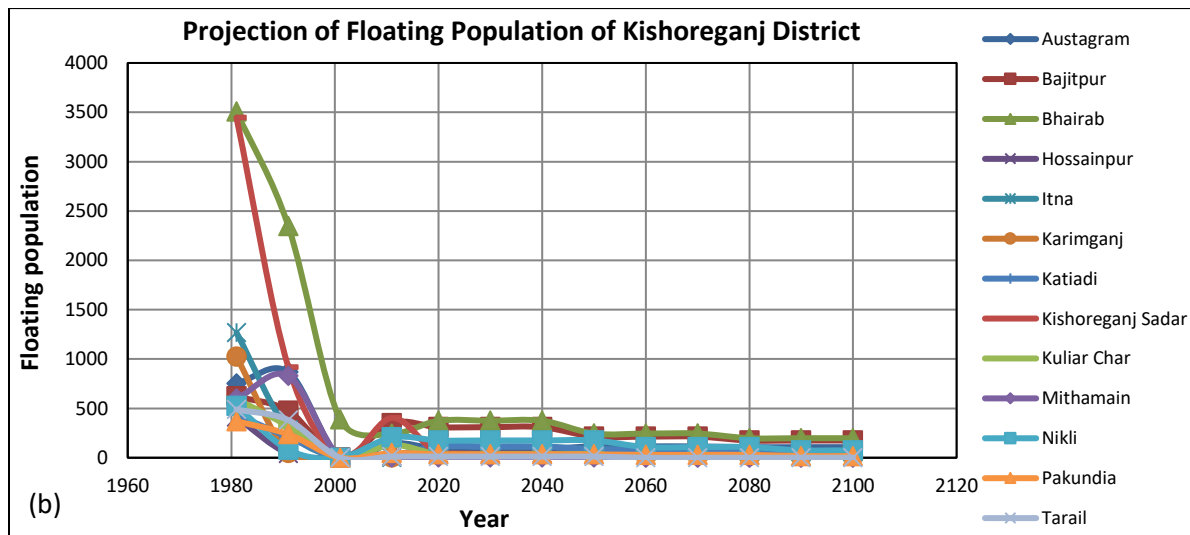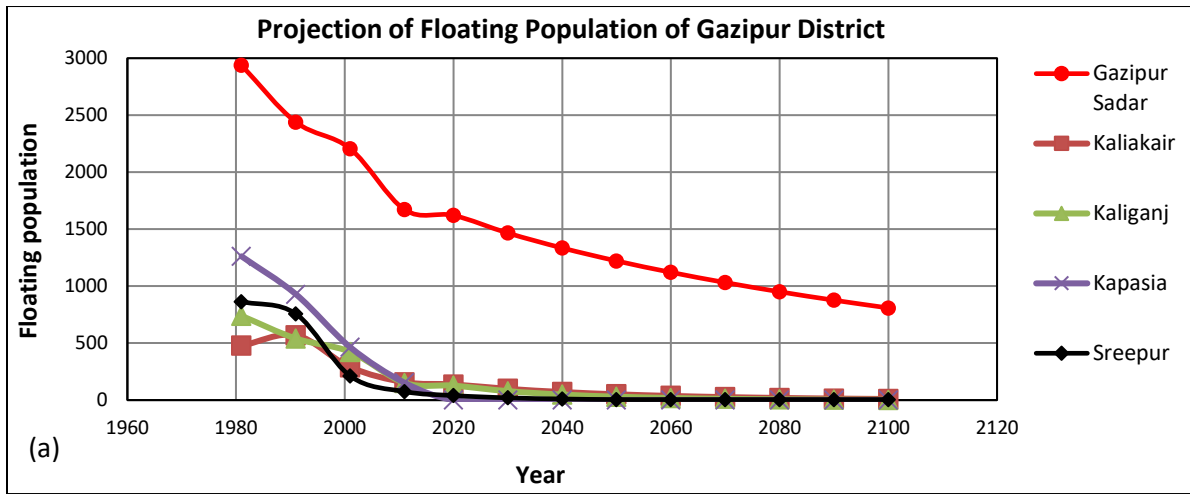
Figure A.4: Projection of Floating Population (a) Gazipur (b) Kishoreganj (c) Narsingdi

151
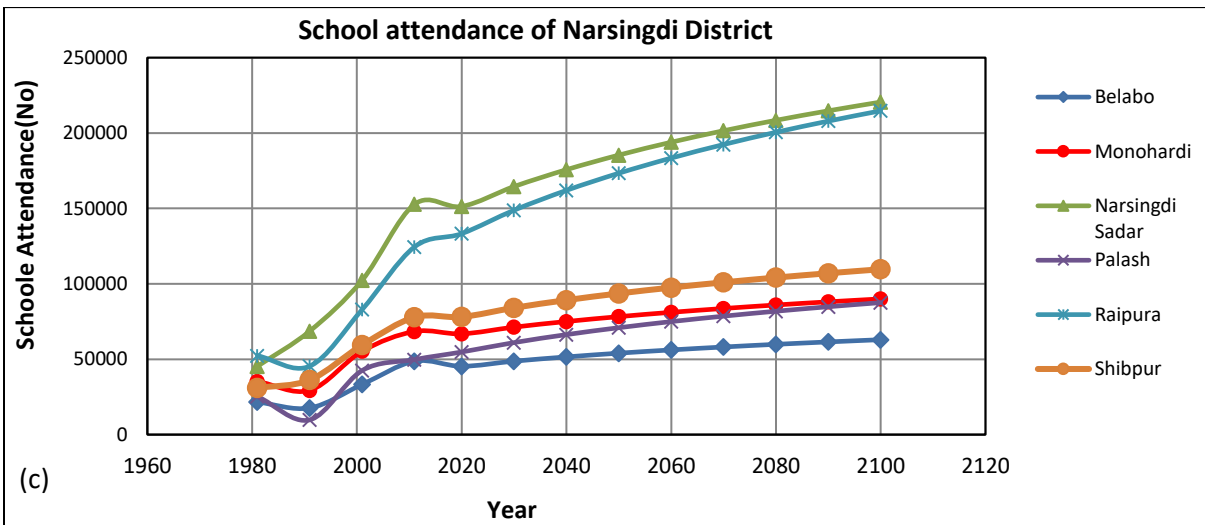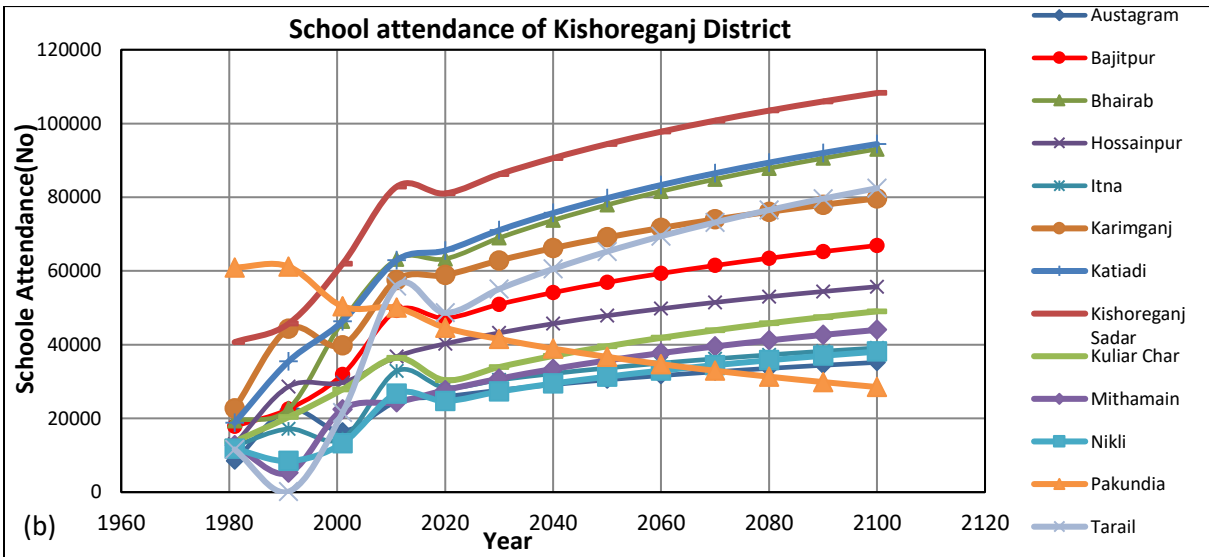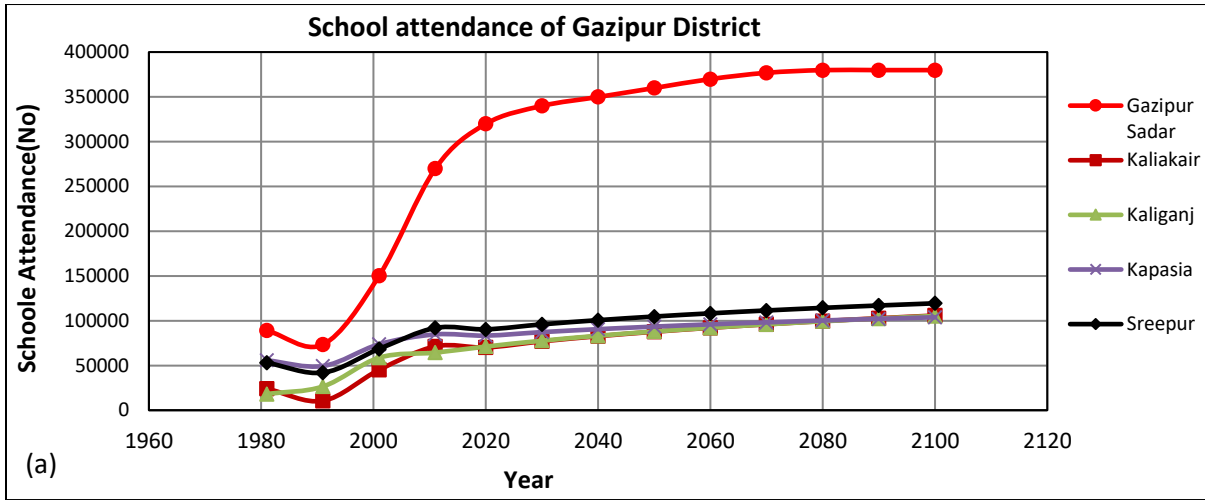
Figure A.5: Projection of School Attendance (a) Gazipur (b) Kishoreganj (c) Narsingdi
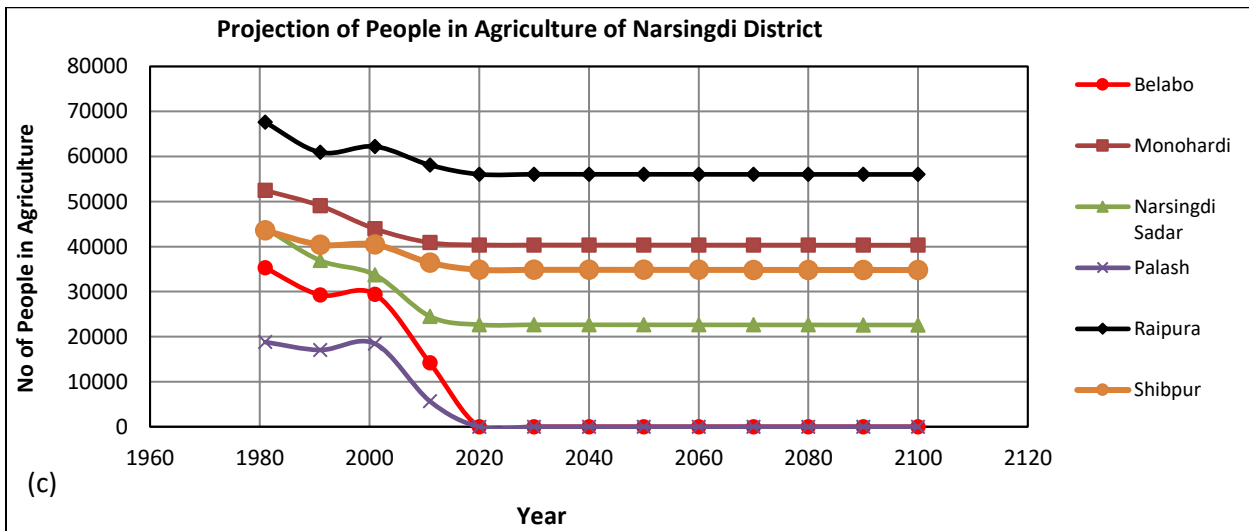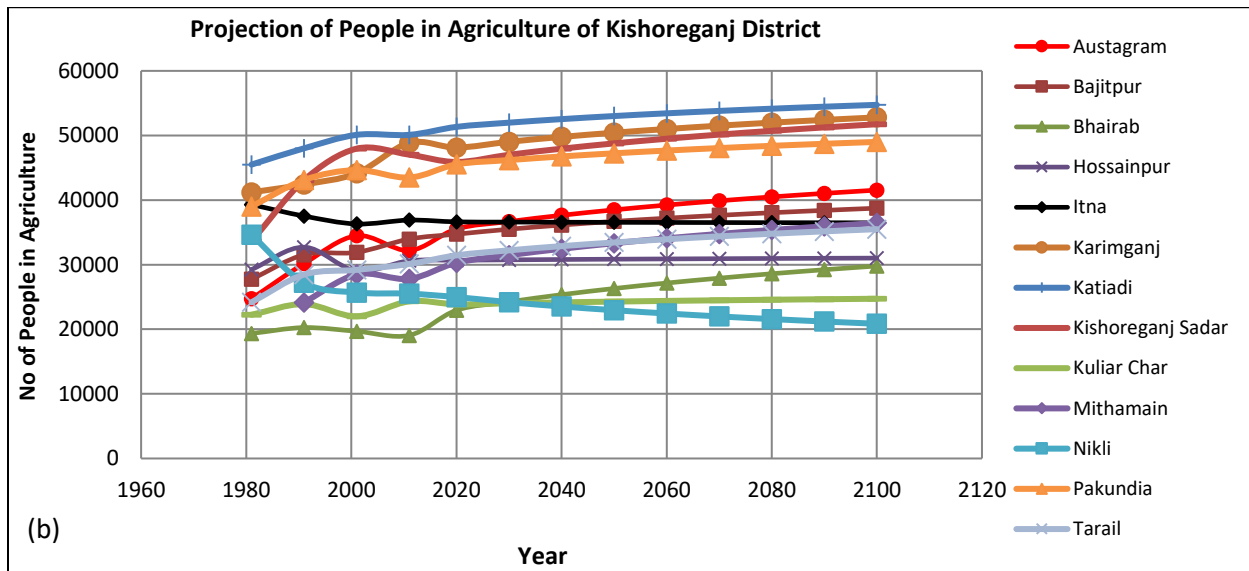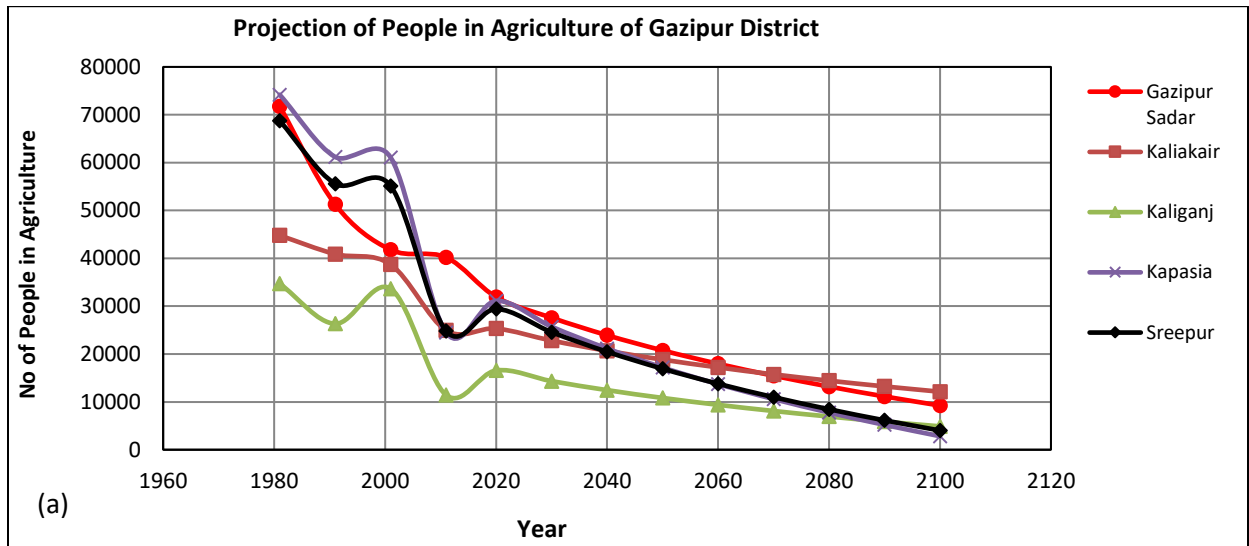
Figure A.6: Projection of People in Agriculture (a) Gazipur (b) Kishoreganj (c) Narsingdi
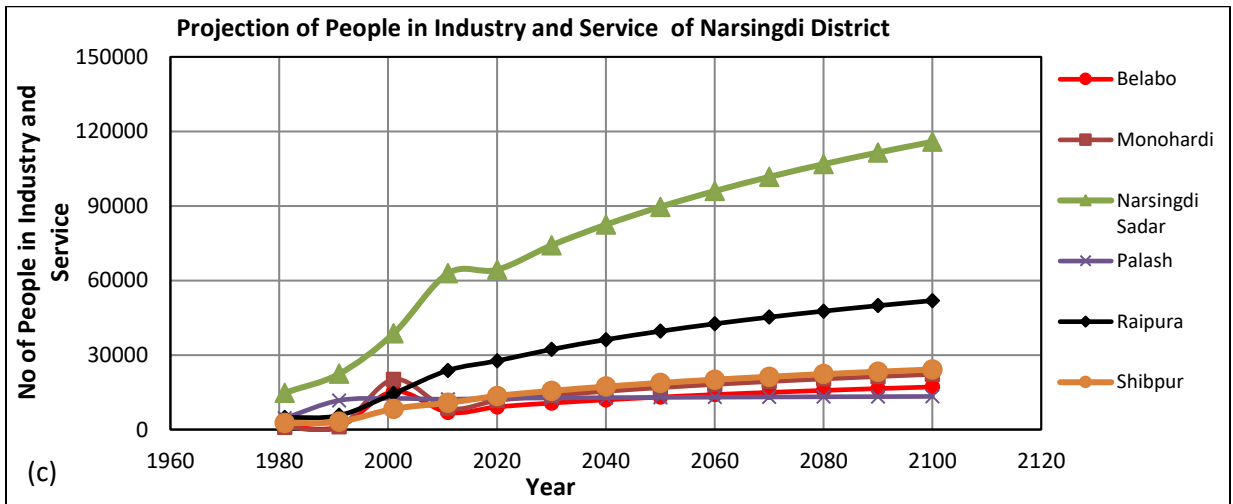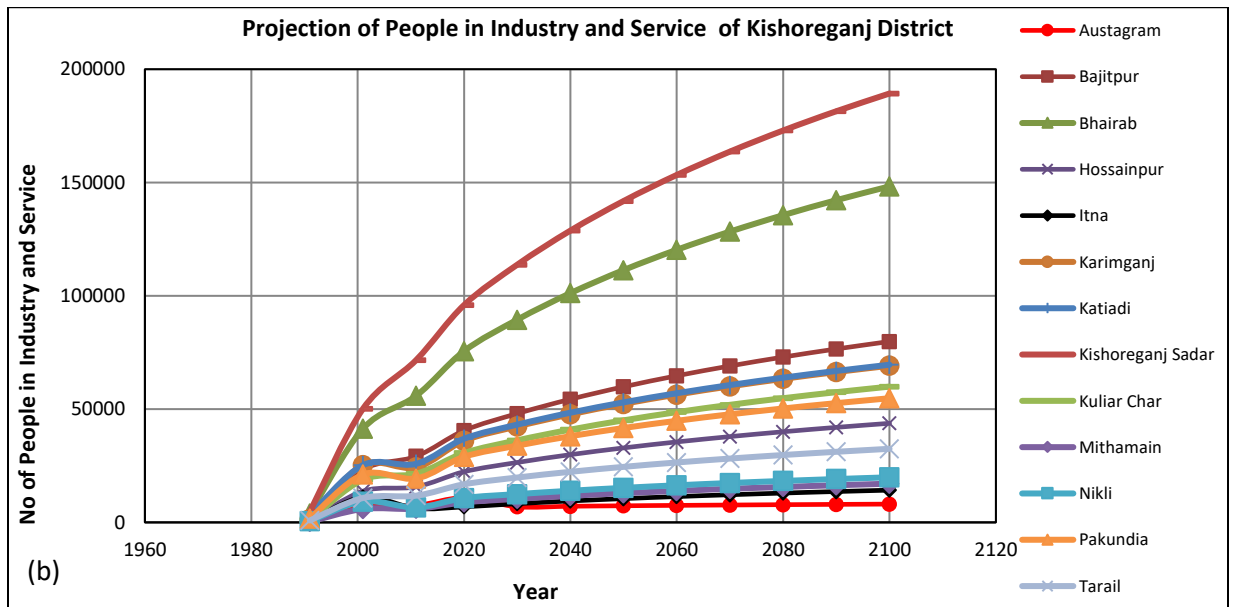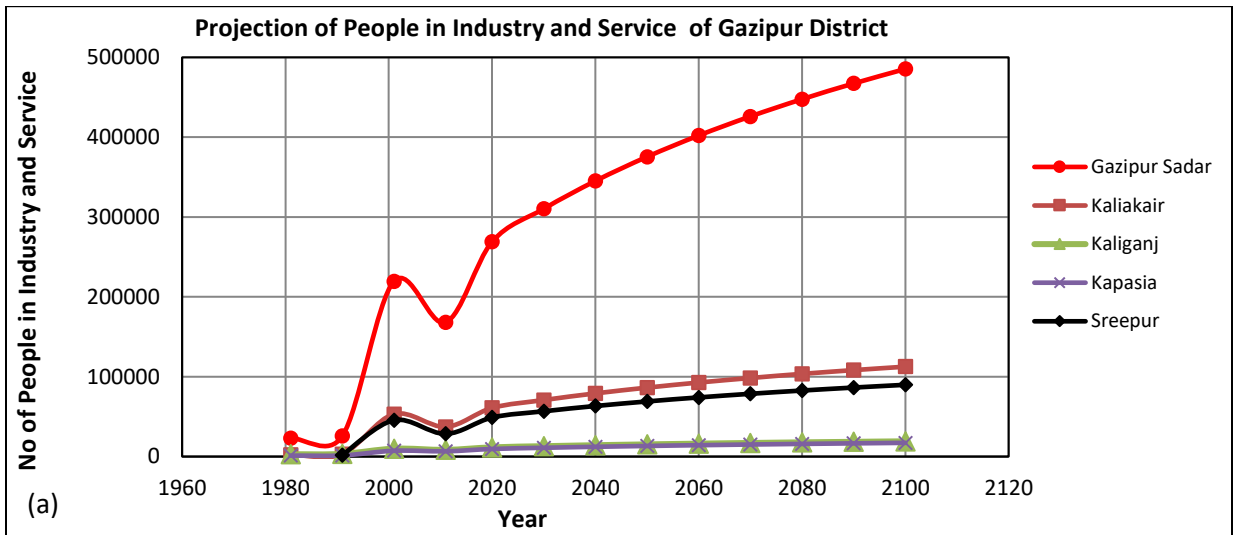
Figure A.7: Projection of People in Industry+Service (a) Gazipur (b) Kishoreganj (c) Narsingdi
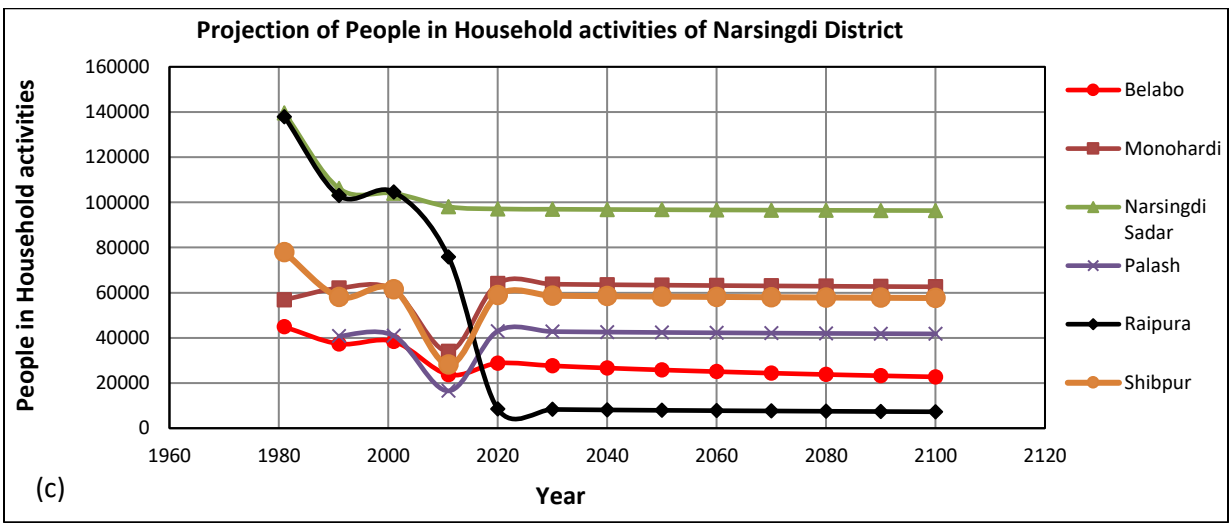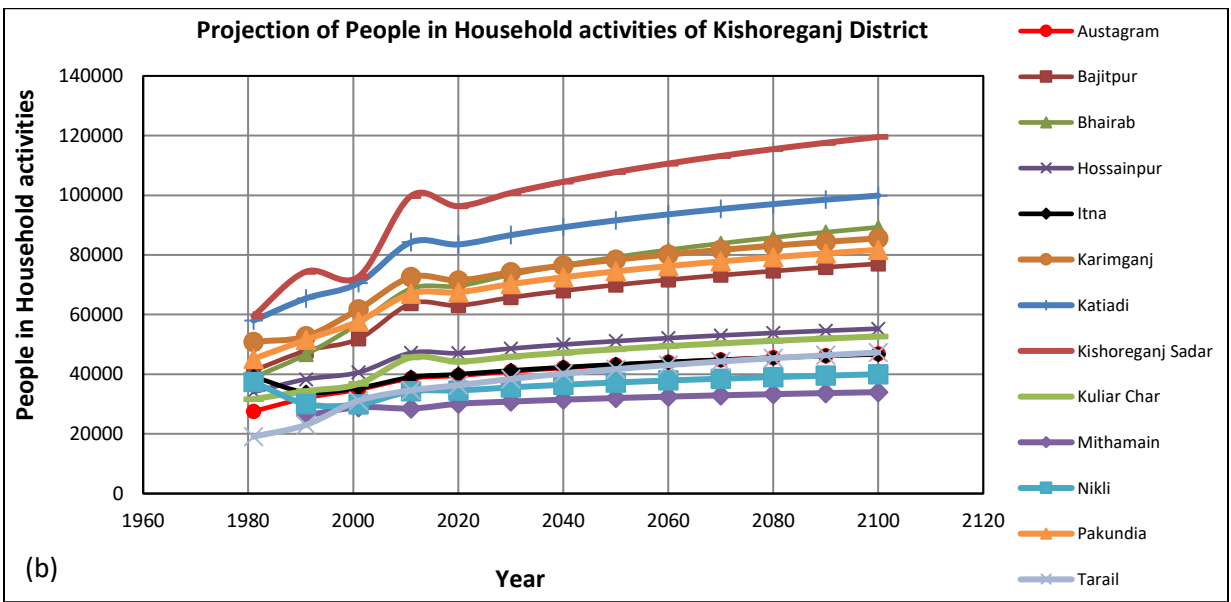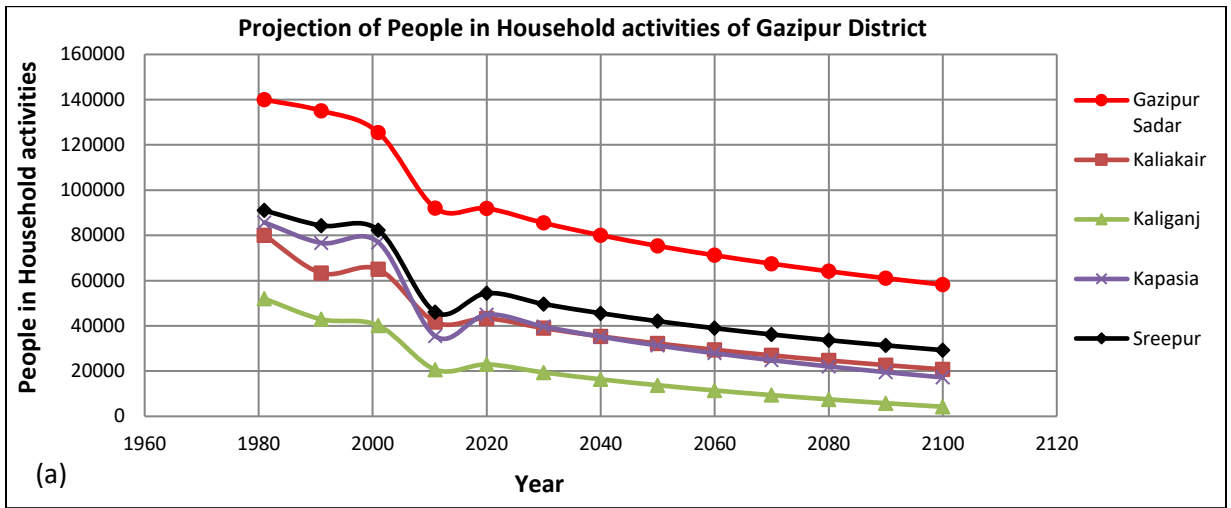
Figure A.8: Projection of People in Household (a) Gazipur (b) Kishoreganj (c) Narsingdi

155
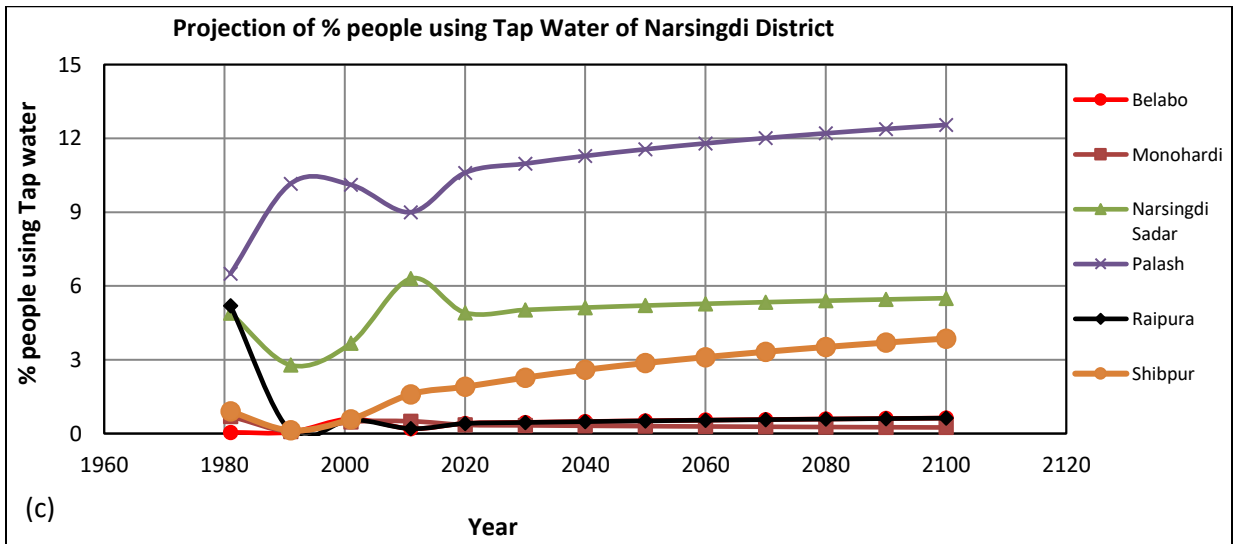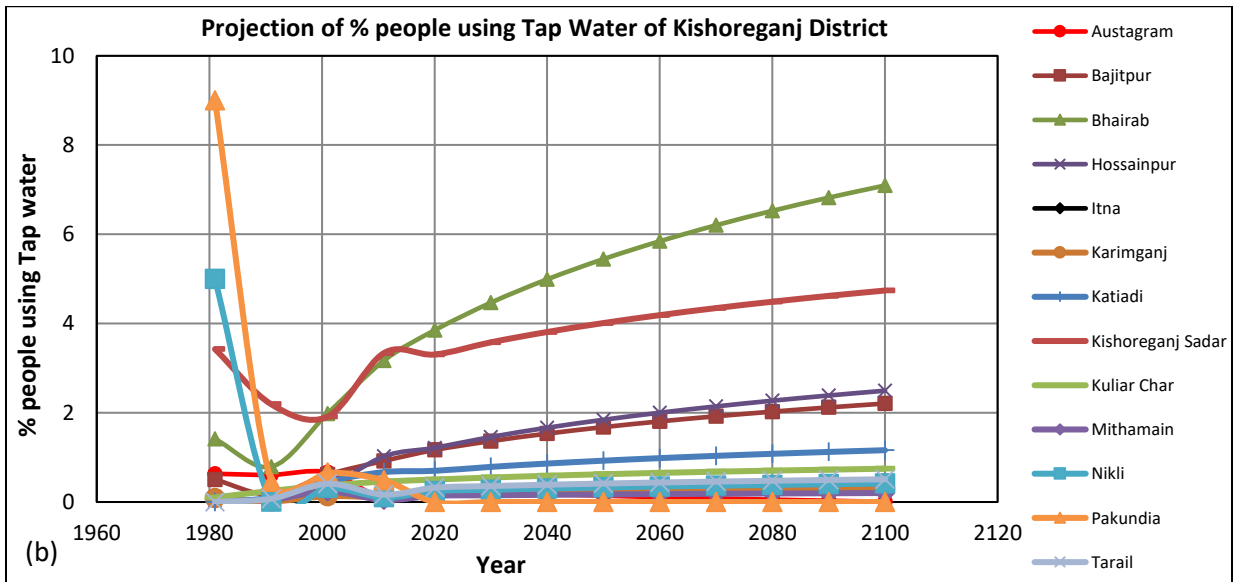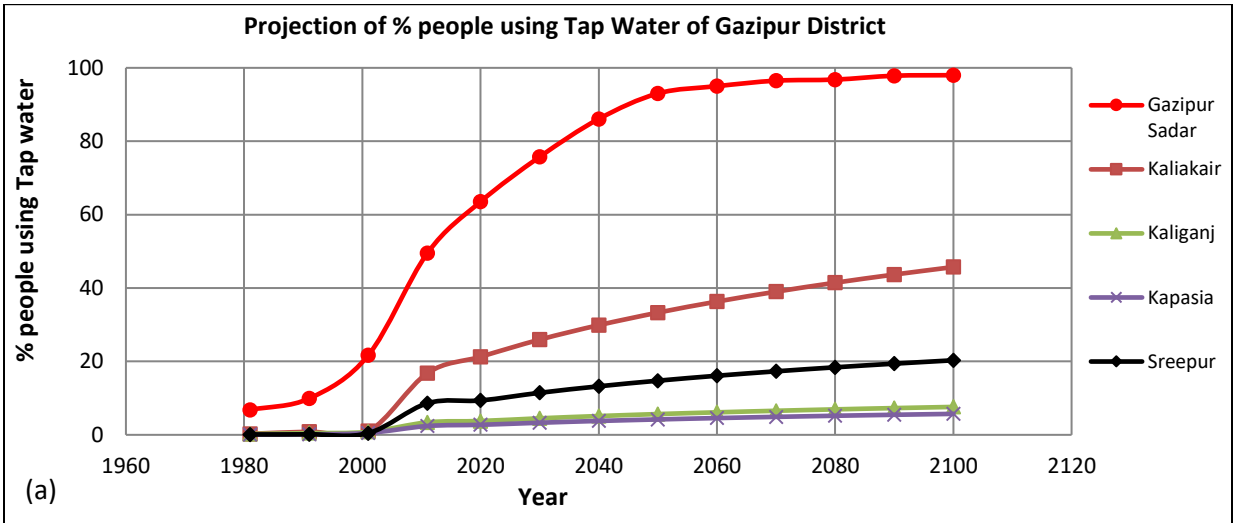
Figure A.9: Projection of People in Household (a) Gazipur (b) Kishoreganj (c) Narsingdi

156
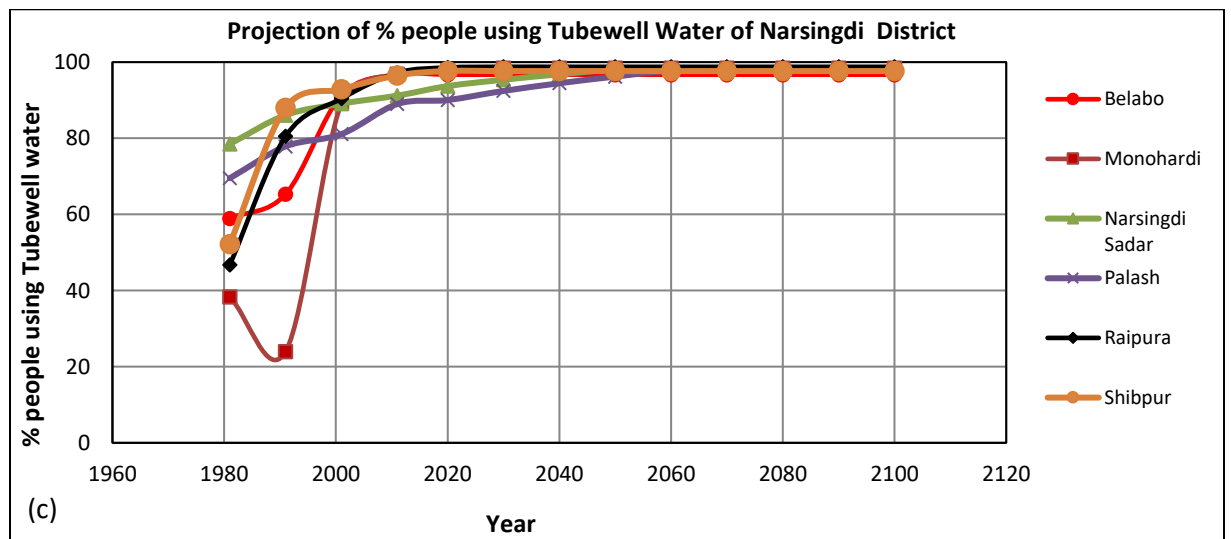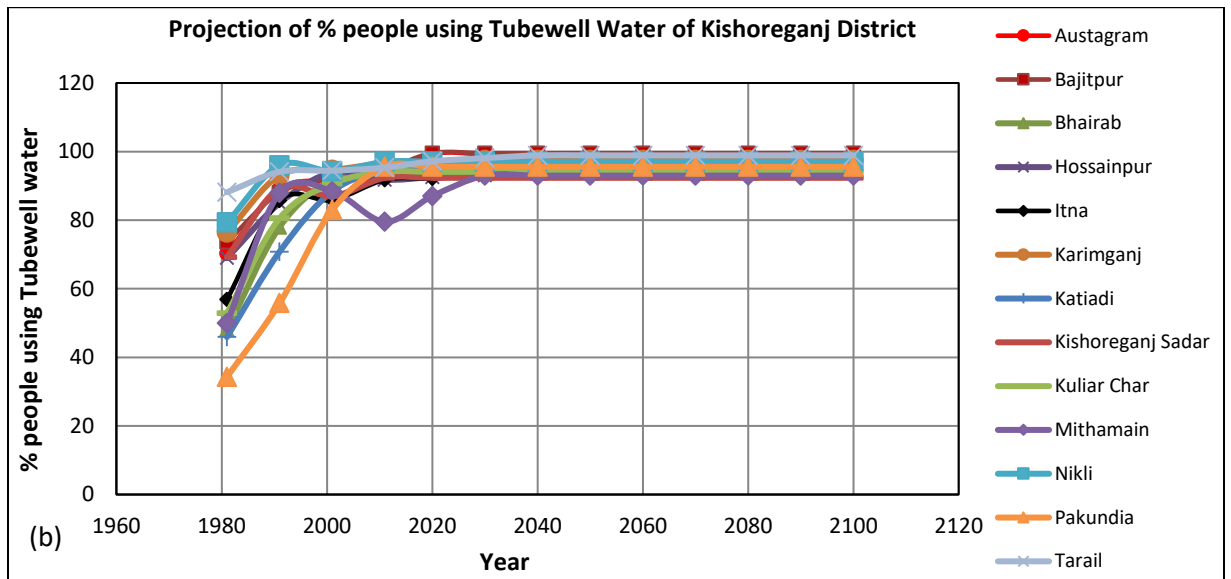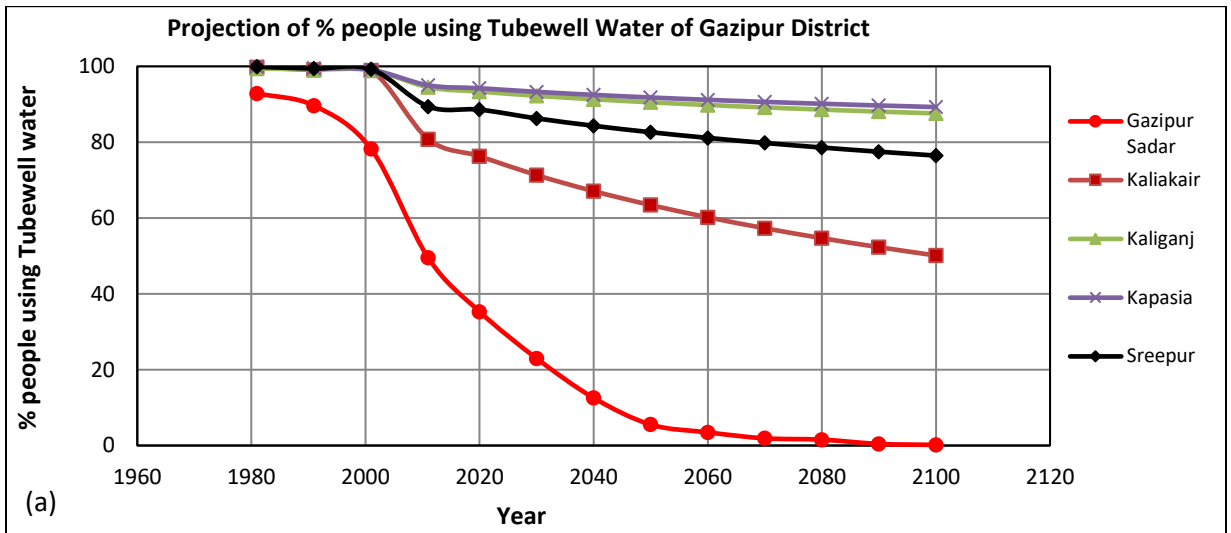
Figure A.10: Projection of People in Household (a) Gazipur (b) Kishoreganj (c) Narsingdi

157
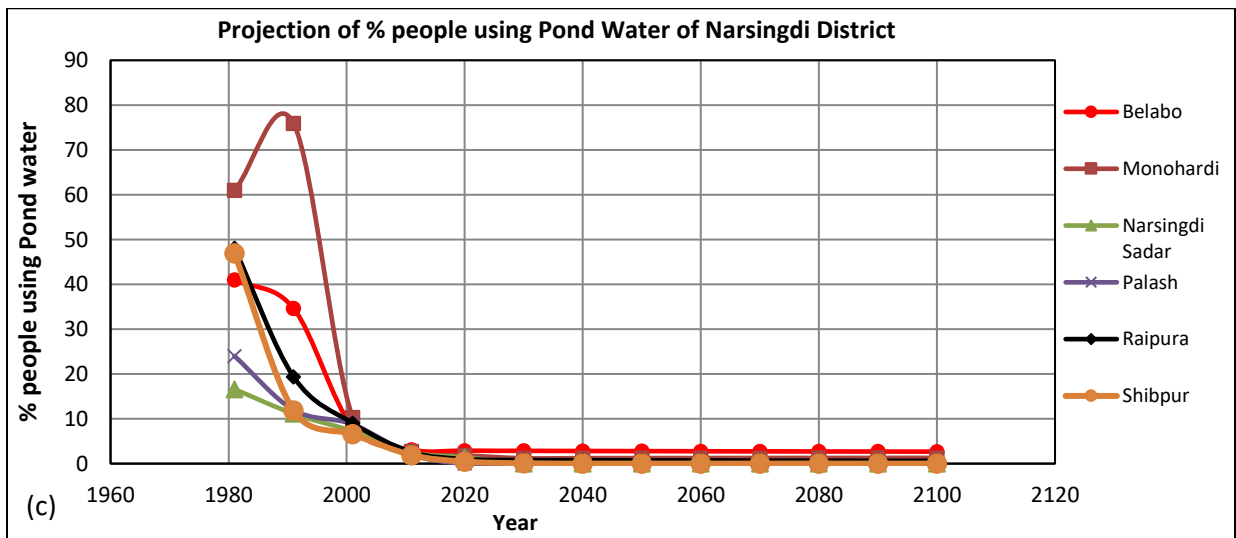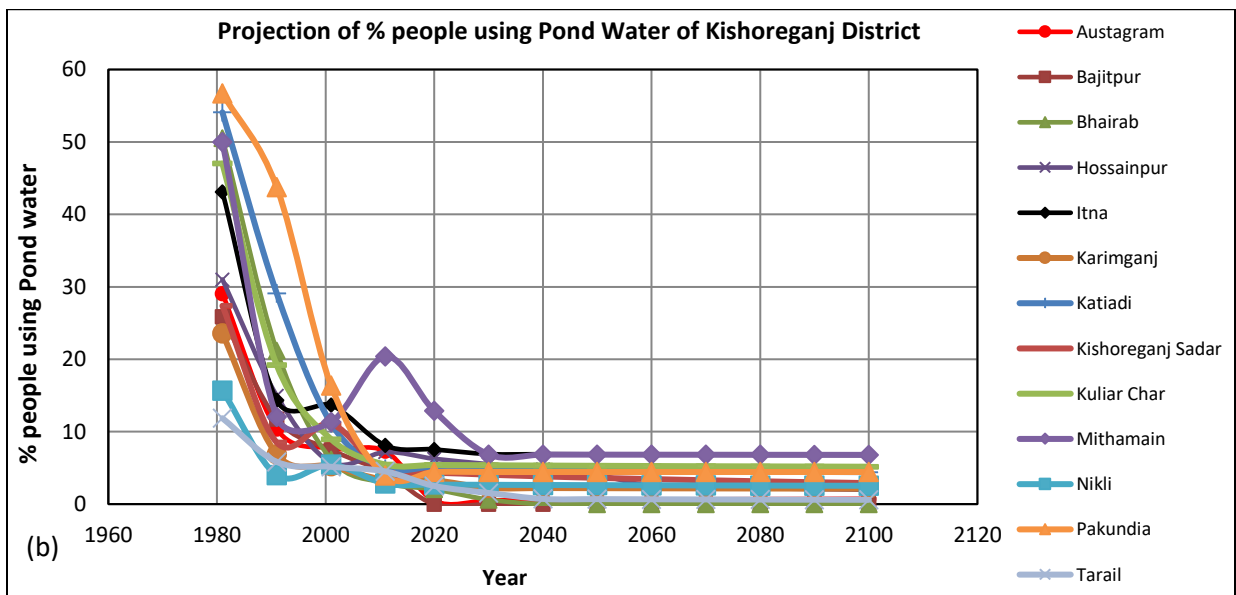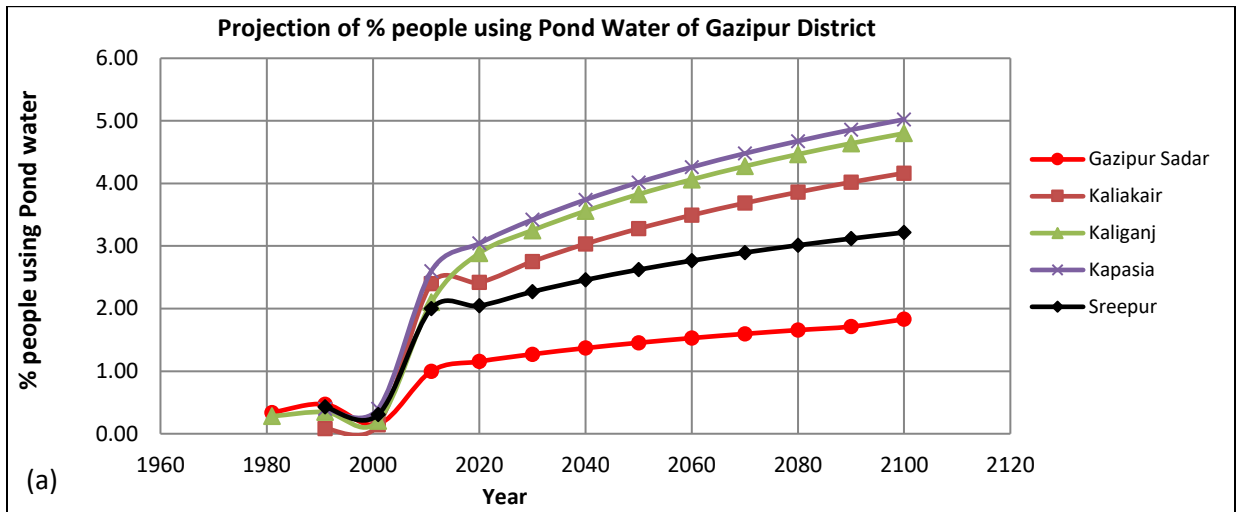
Figure A.11: Projection of People in Household (a) Gazipur (b) Kishoreganj (c) Narsingdi
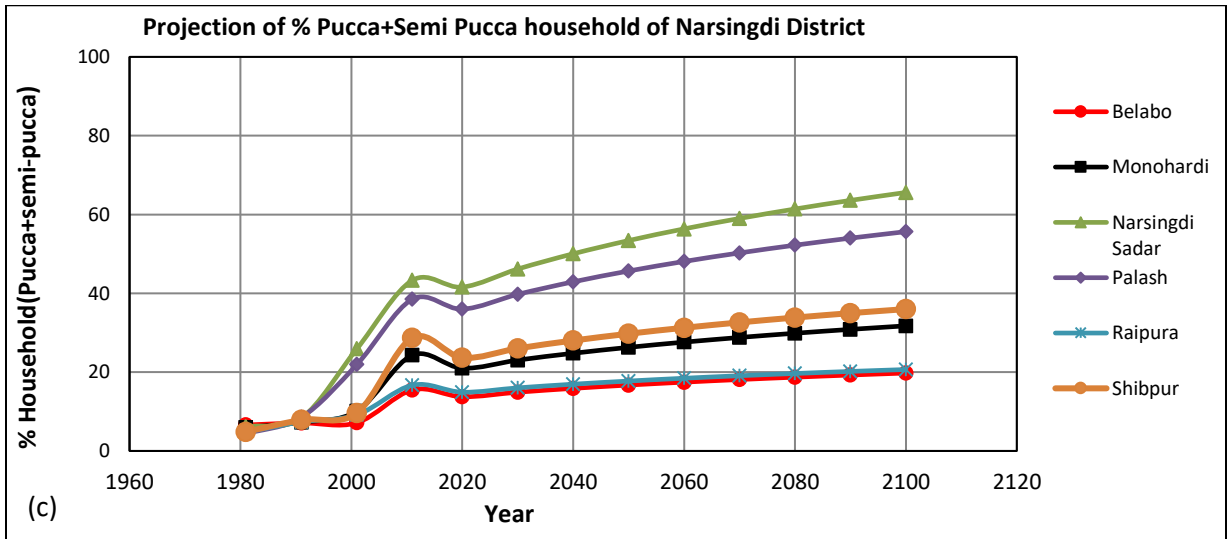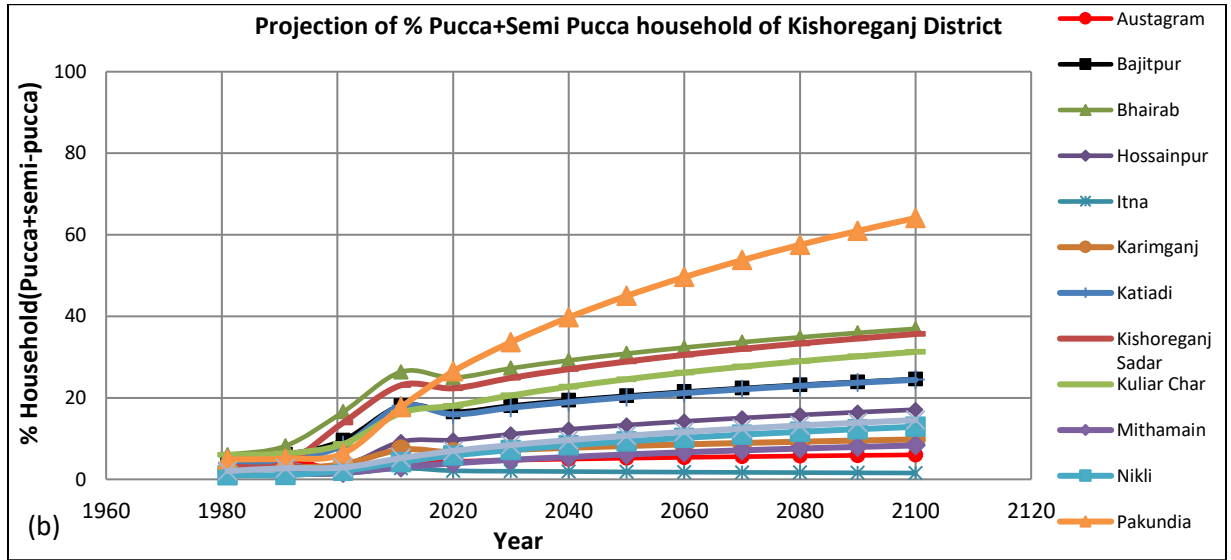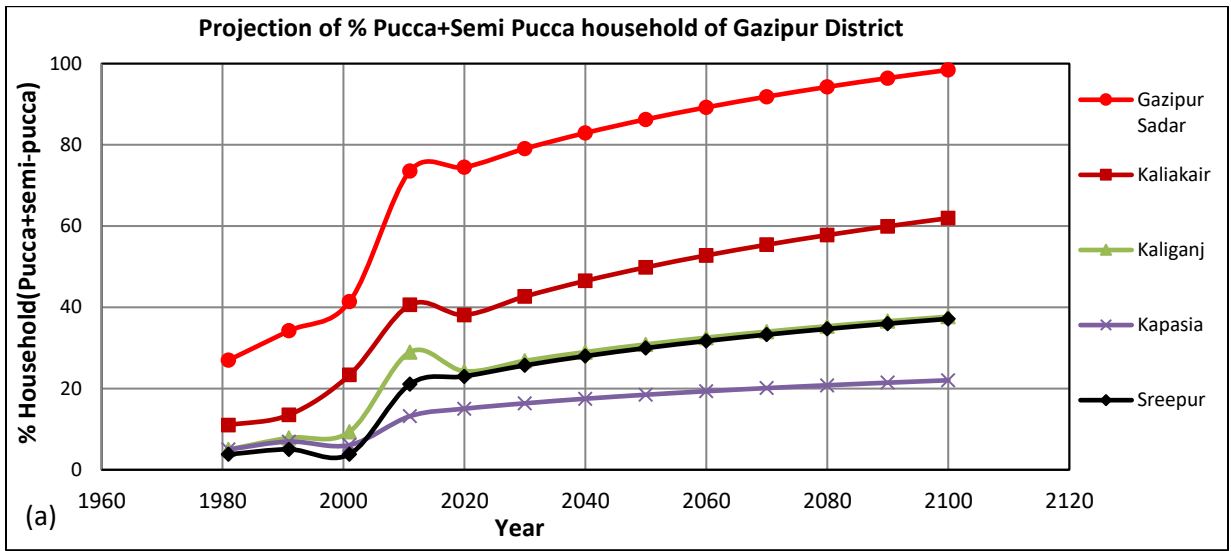
Figure A.12: Projection of People in Household (a) Gazipur (b) Kishoreganj (c) Narsingdi
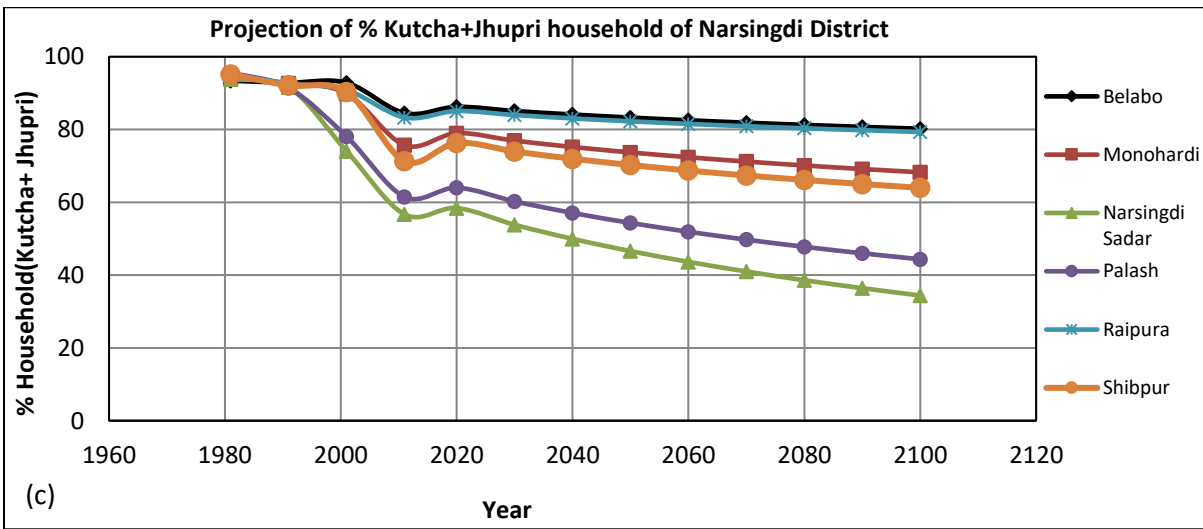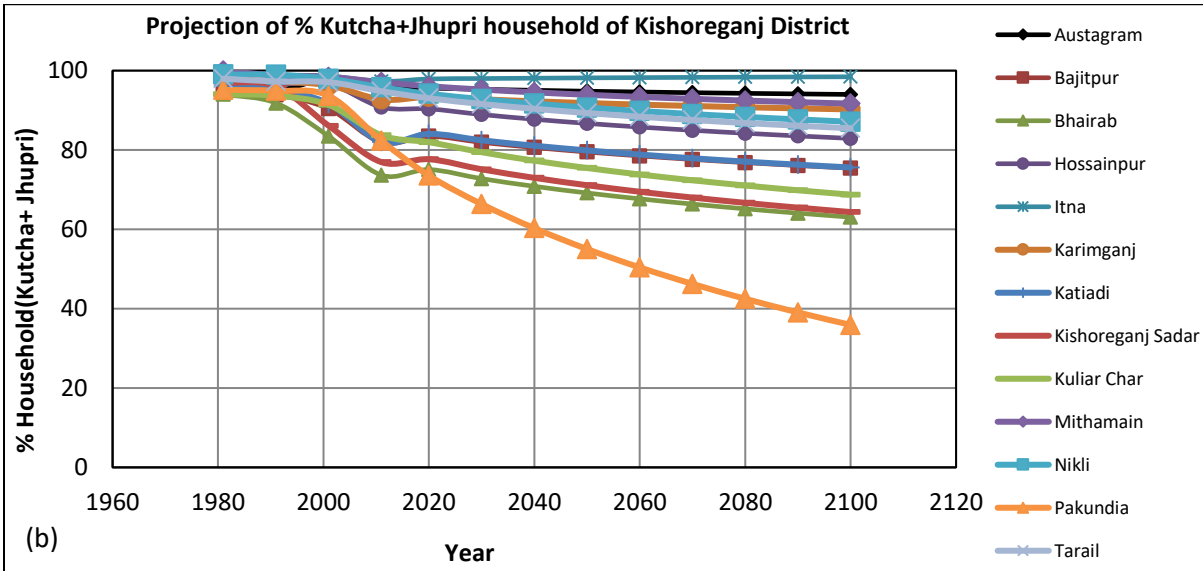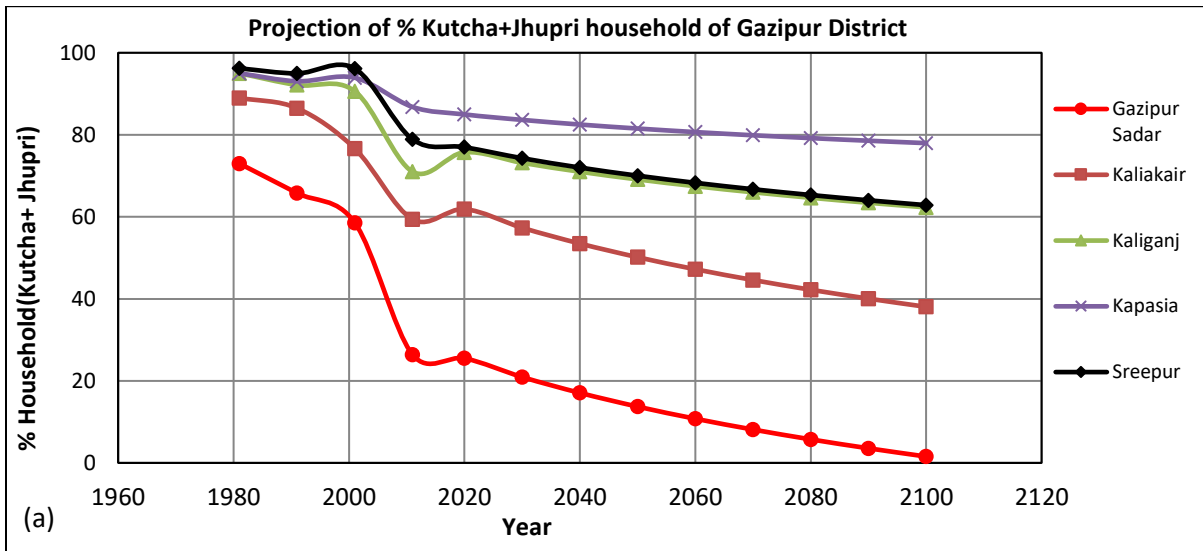
Figure A.13: Projection of % Kutcha+Jhupri in (a) Gazipur (b) Kishoreganj (c) Narsingdi
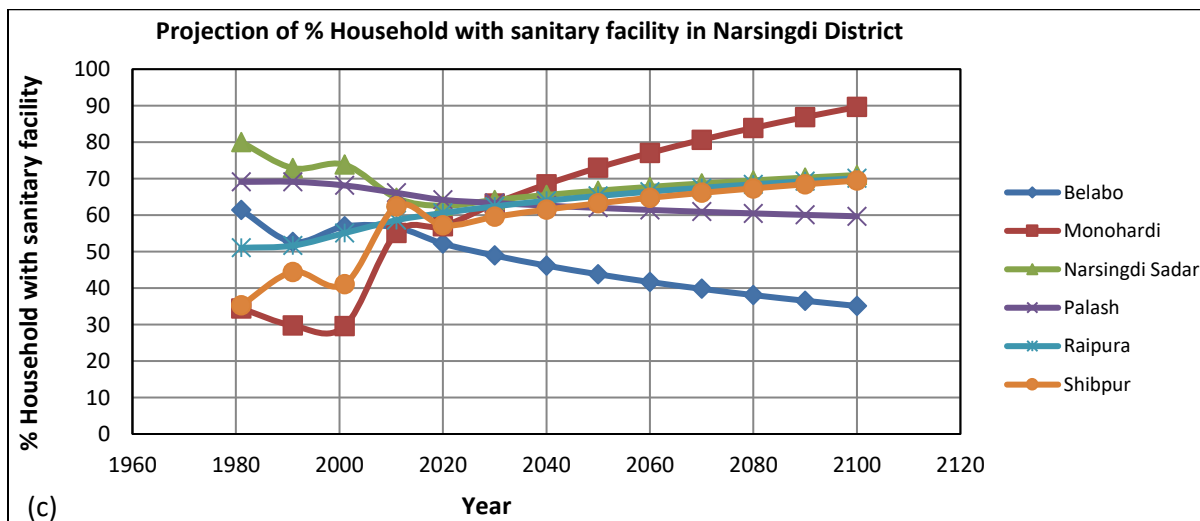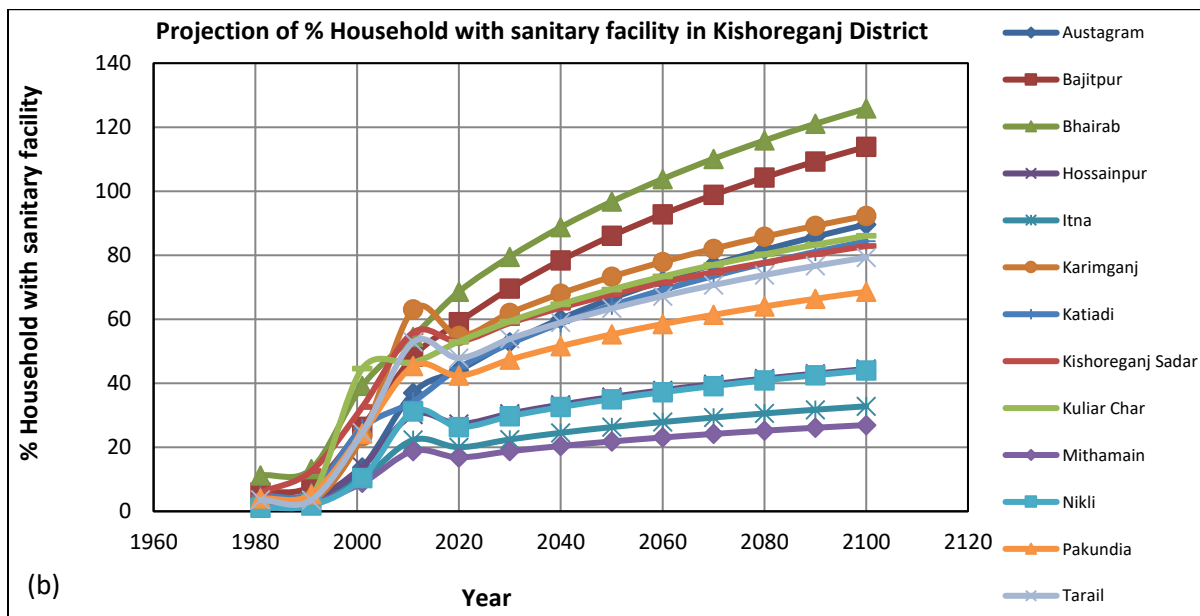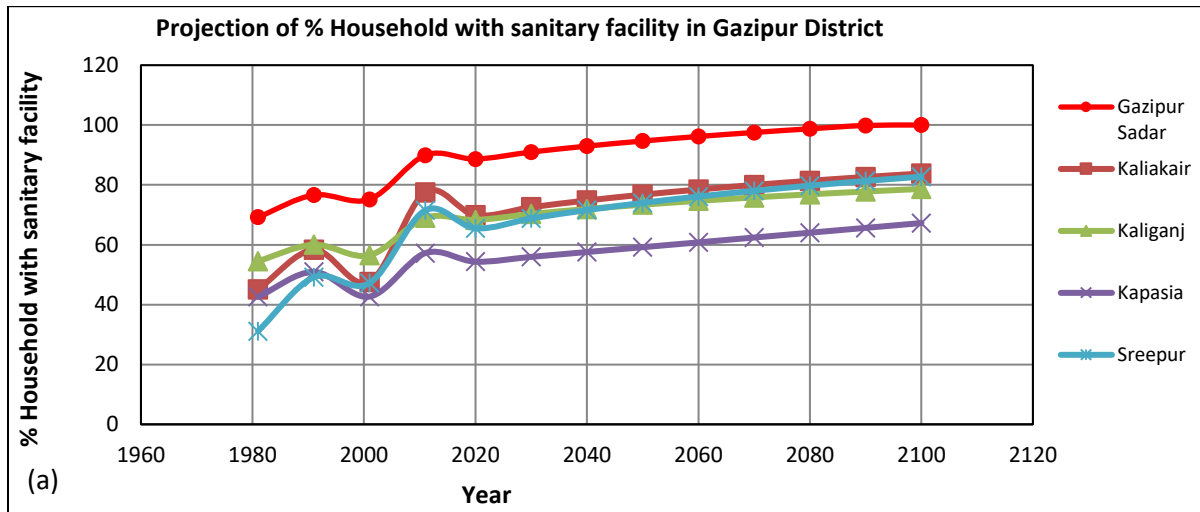
Figure A.14: Projection of % Kutcha+Jhupri in (a) Gazipur (b) Kishoreganj (c) Narsingdi
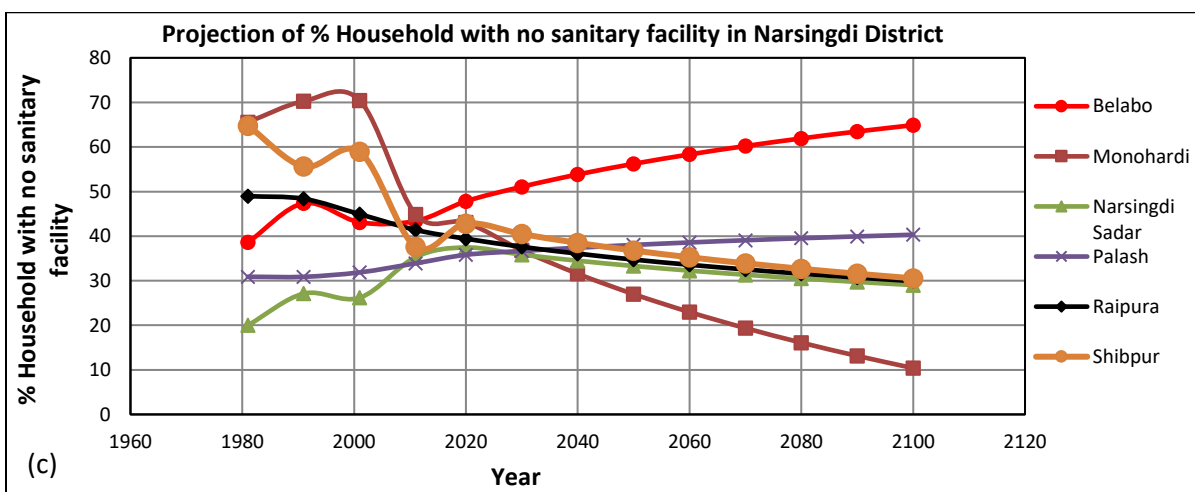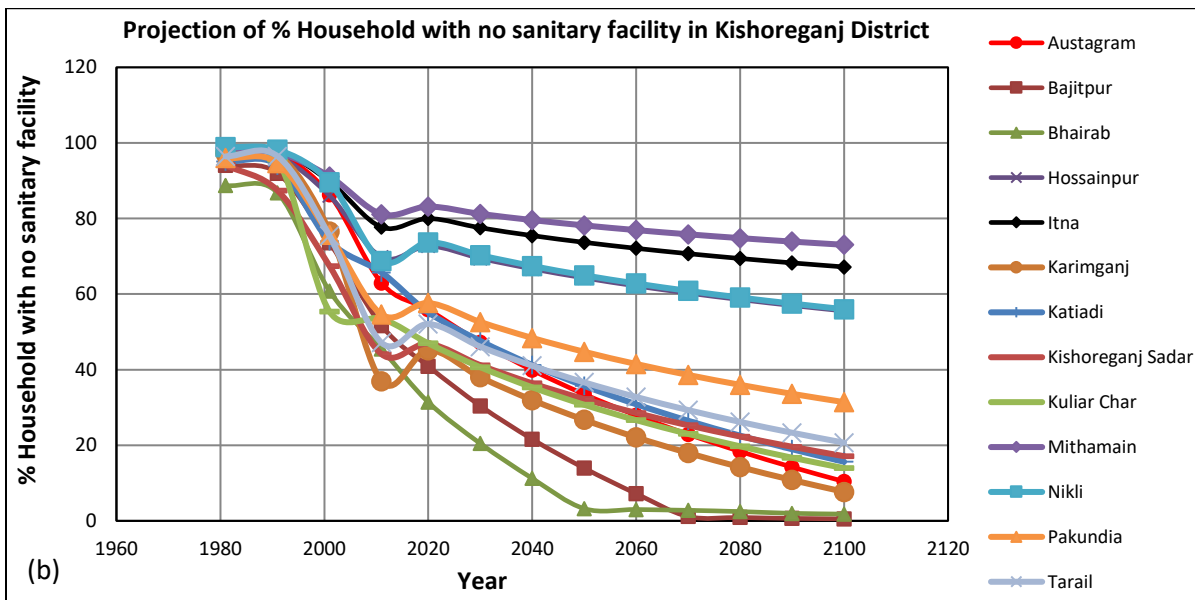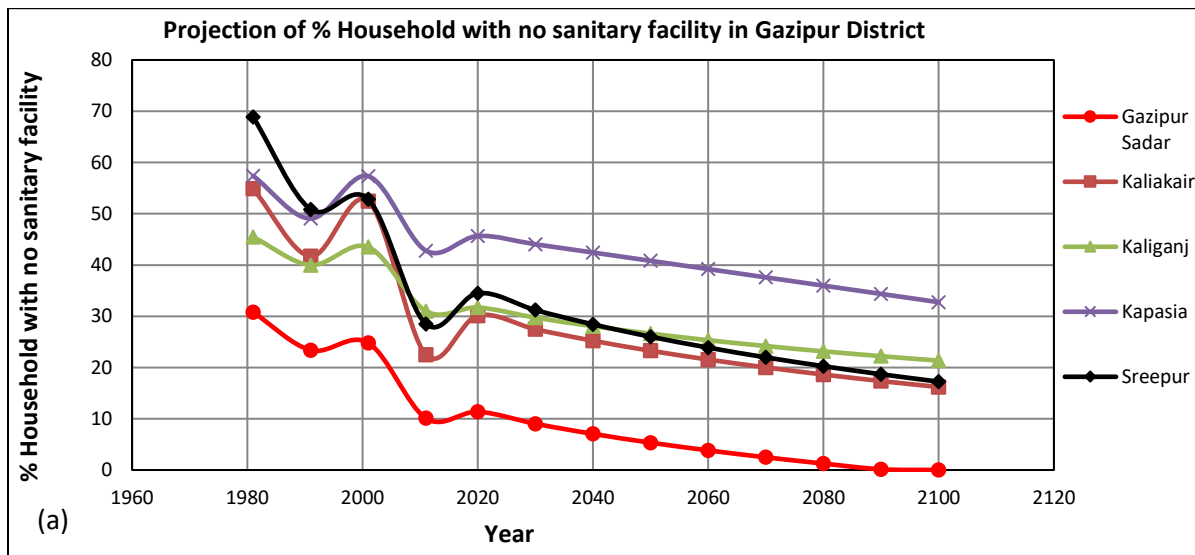
Figure A.15: Projection of % household with no Sanitary in (a) Gazipur (b) Kishoreganj (c) Narsingdi
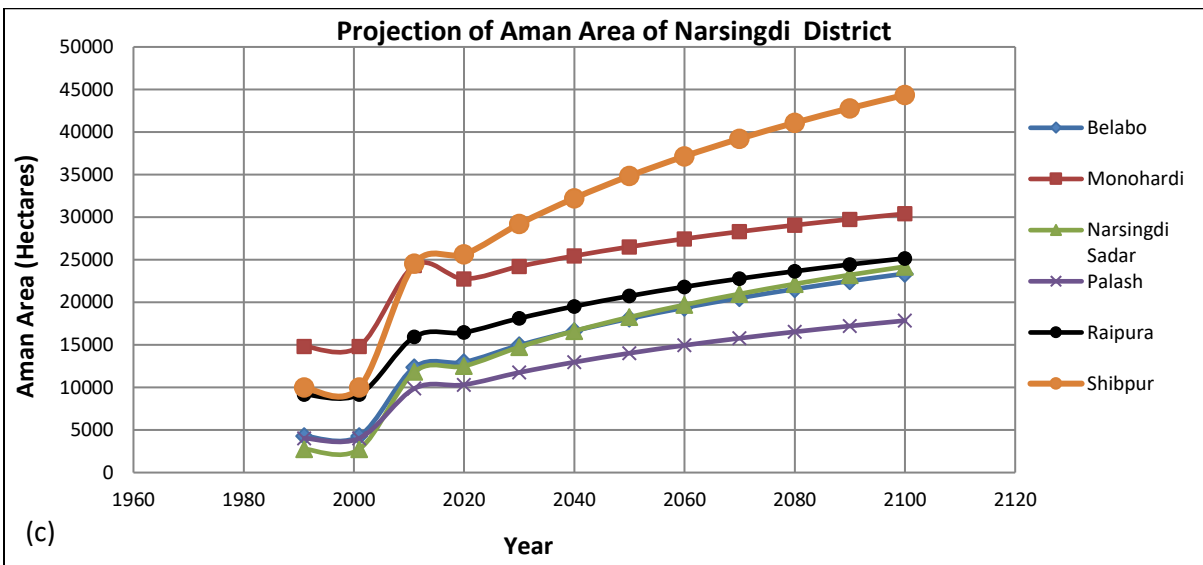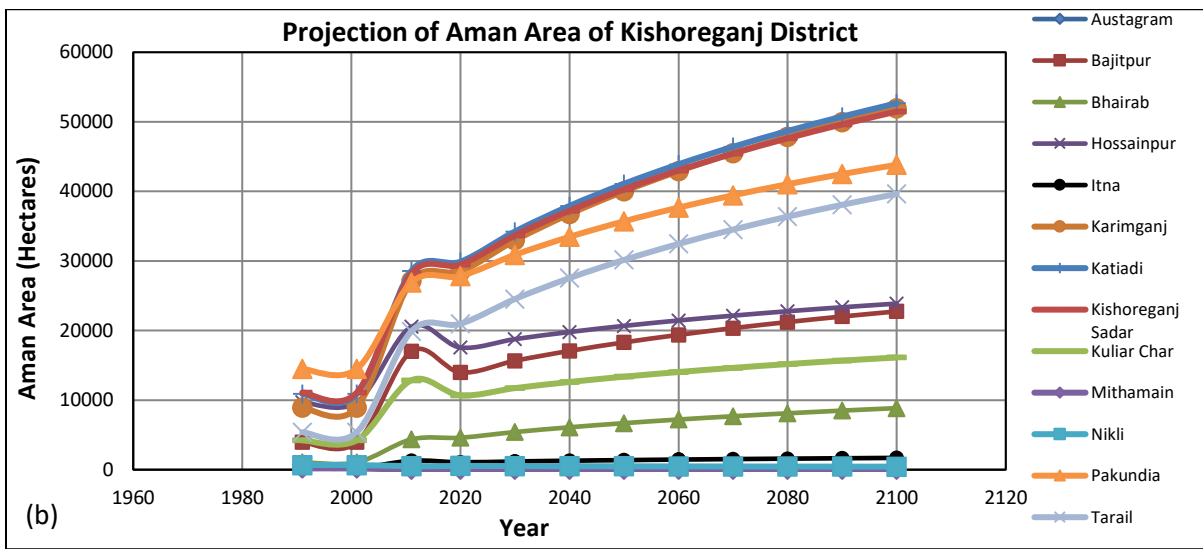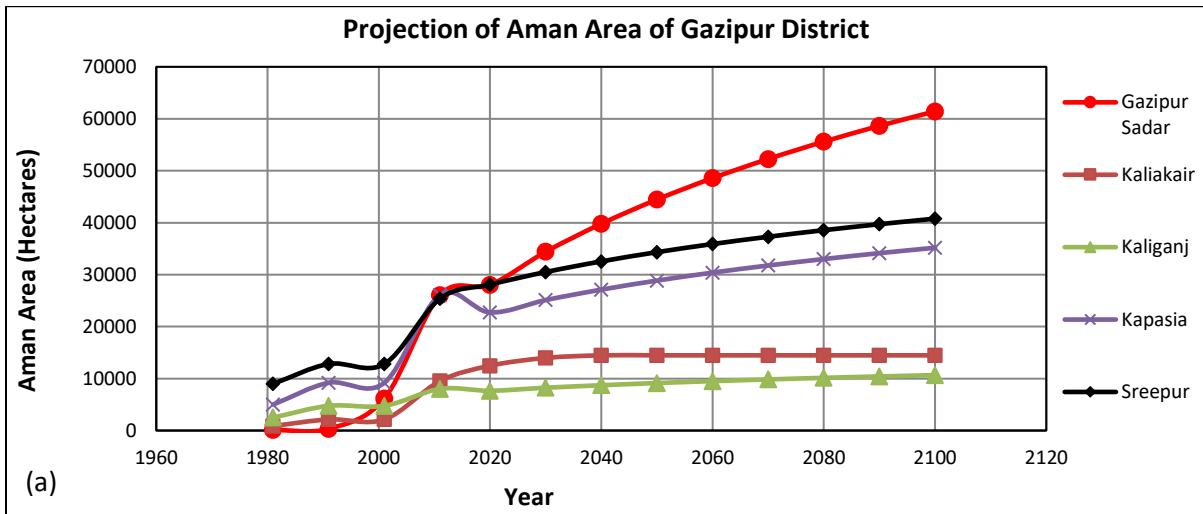
Figure A.16: Projection of % Kutcha+Jhupri in (a) Gazipur (b) Kishoreganj (c) Narsingdi
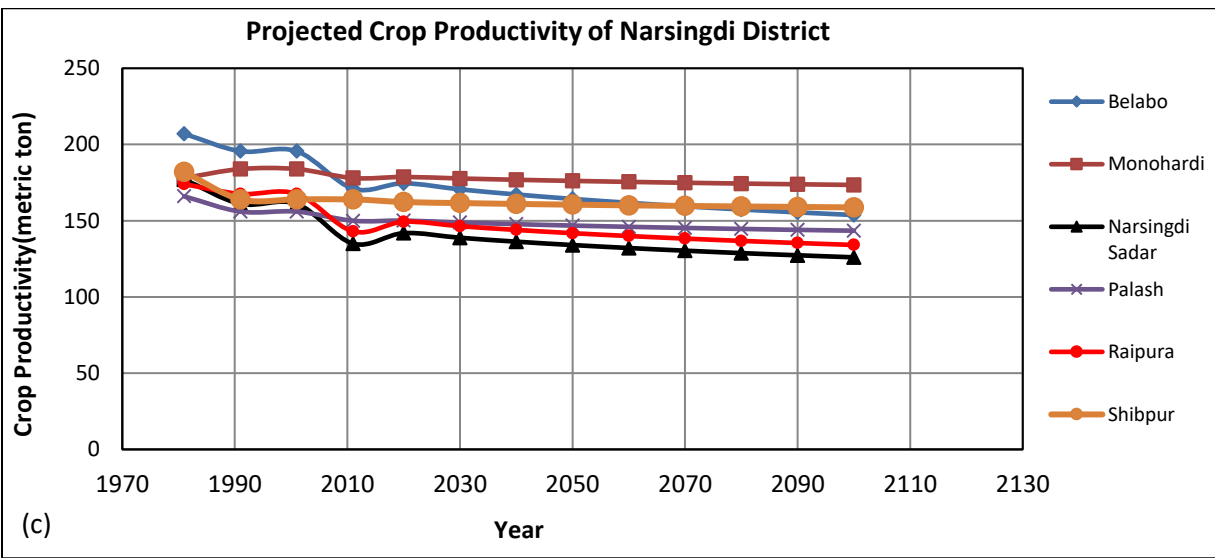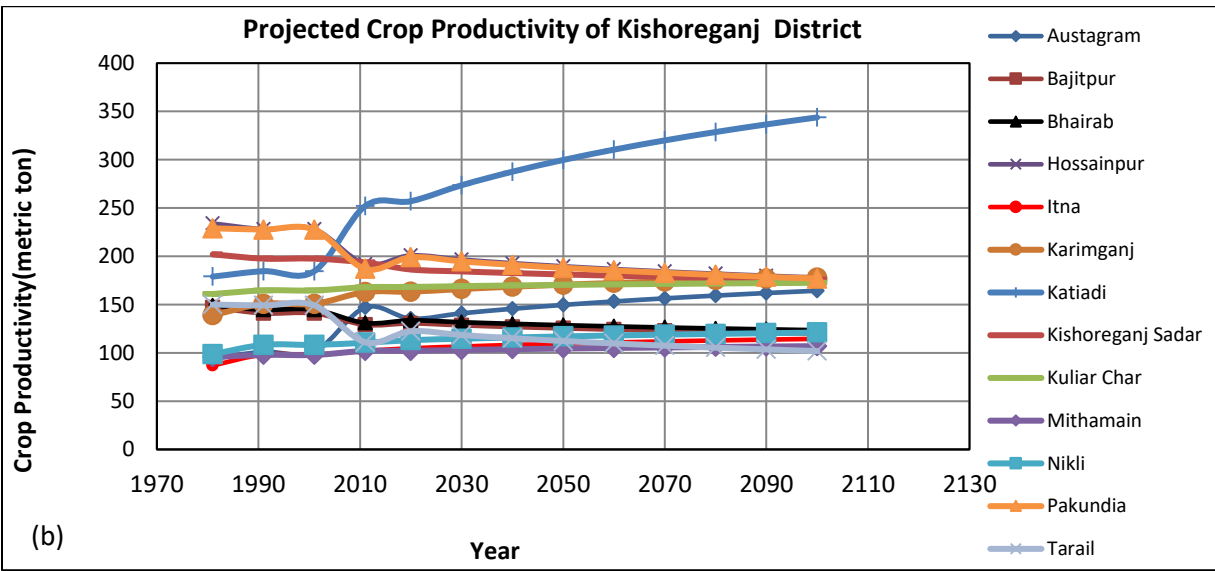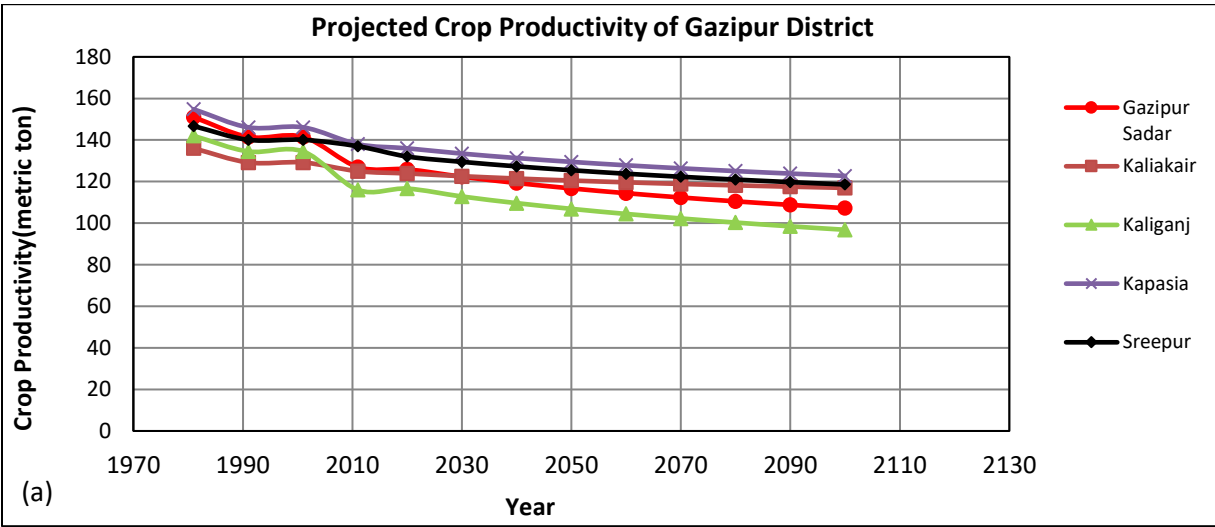
Figure A.17: Projection of Crop Productivity in (a) Gazipur (b) Kishoreganj (c) Narsingdi
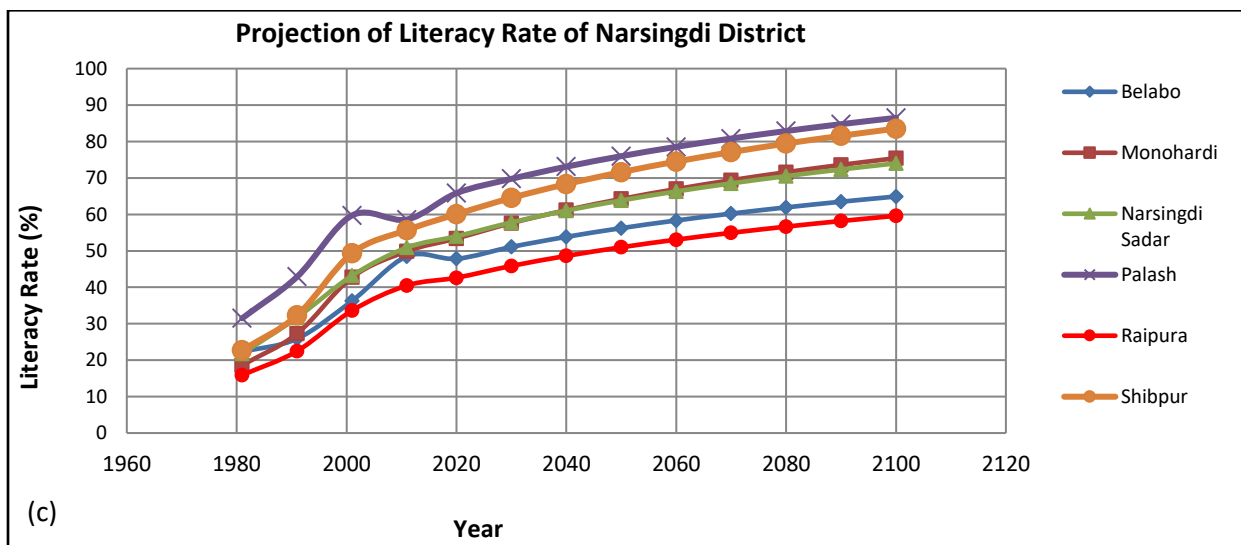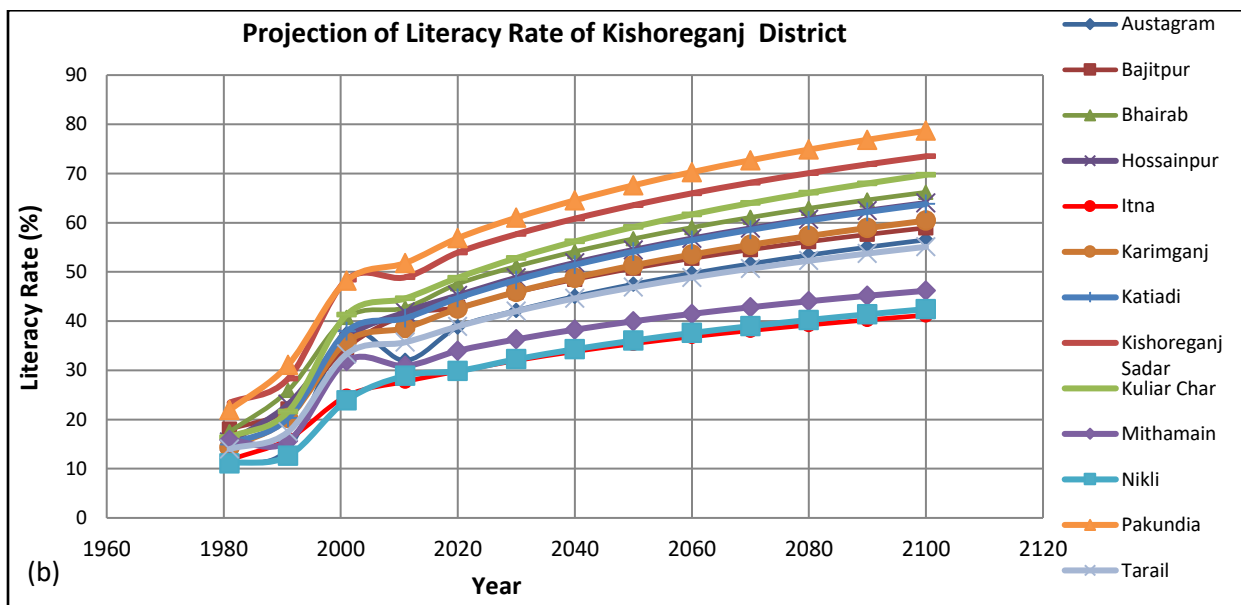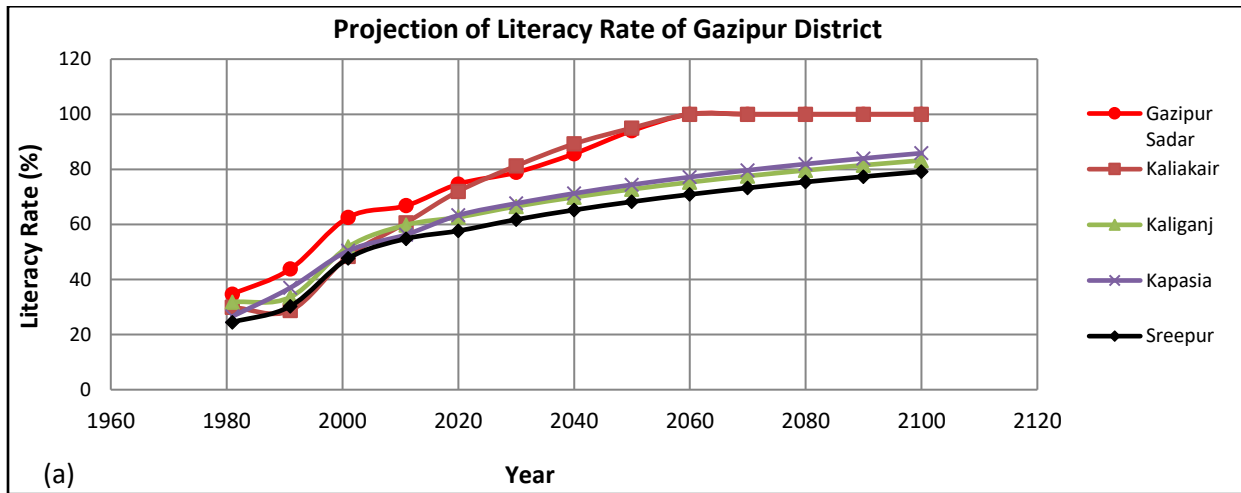
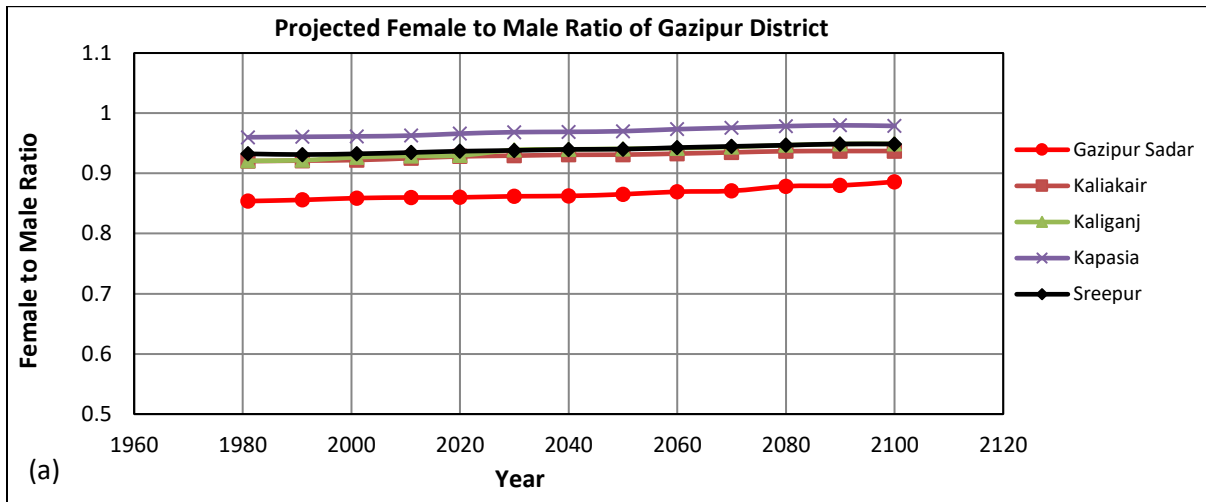Figure A.18: Projection of Literacy Rate in (a) Gazipur (b) Kishoreganj (c) Narsingdi
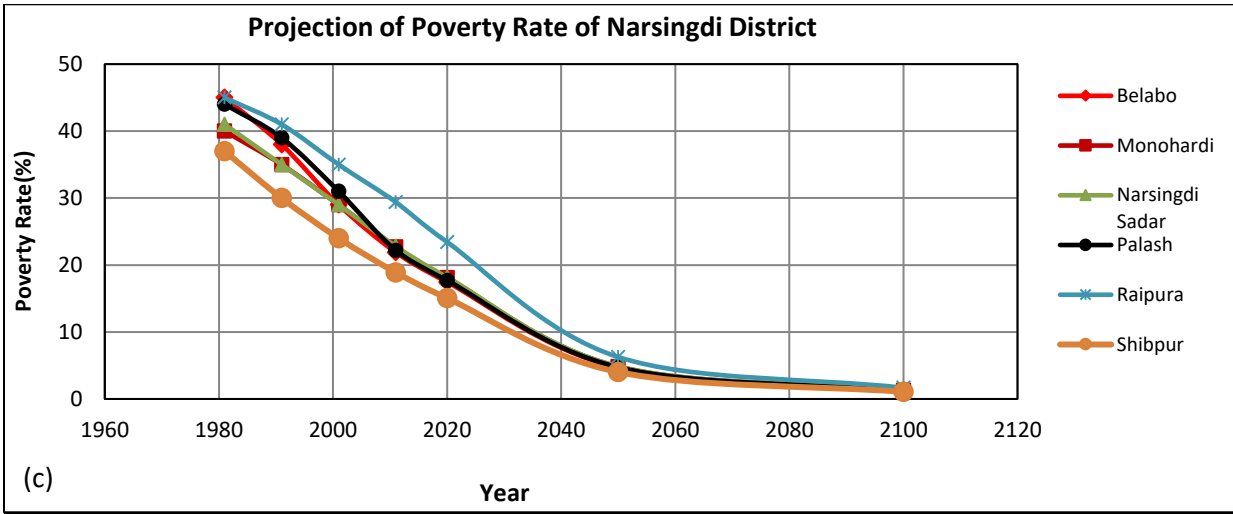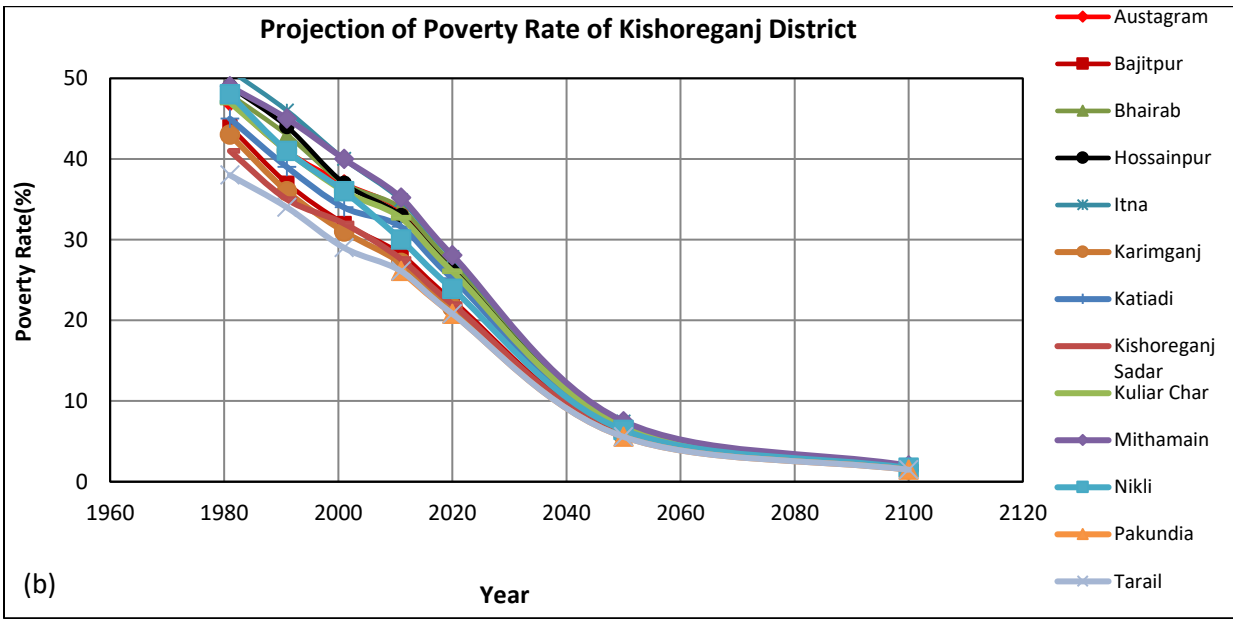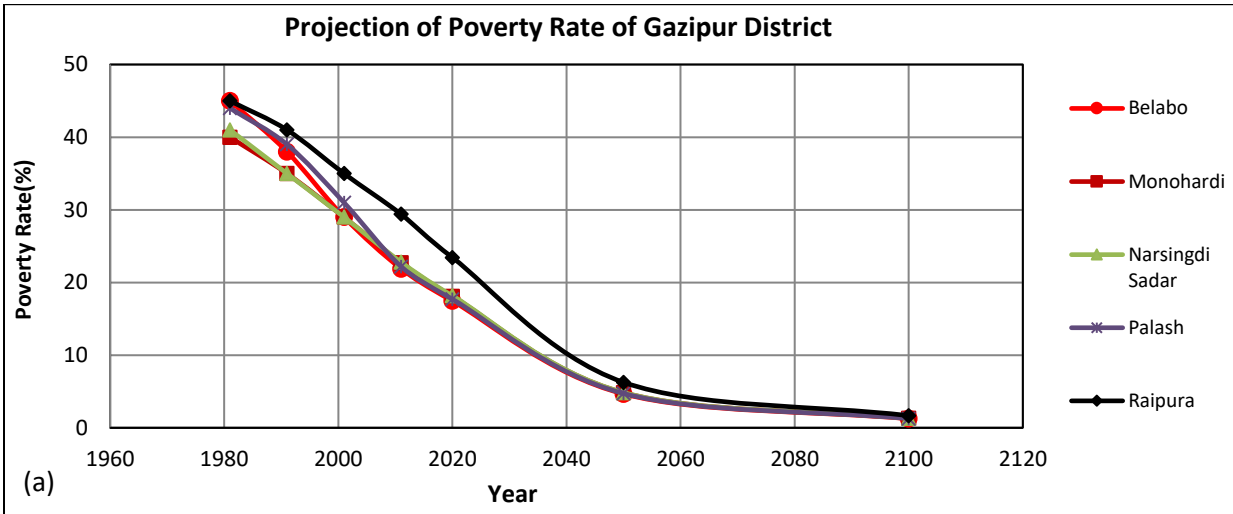
Figure A.19: Projection of Literacy Rate in (a) Gazipur (b) Kishoreganj (c) Narsingdi
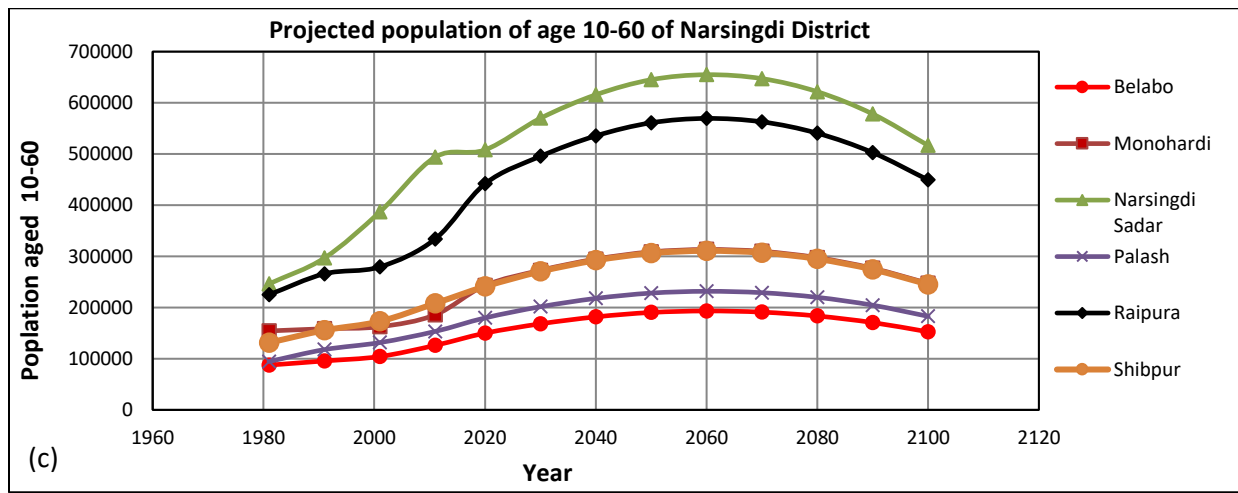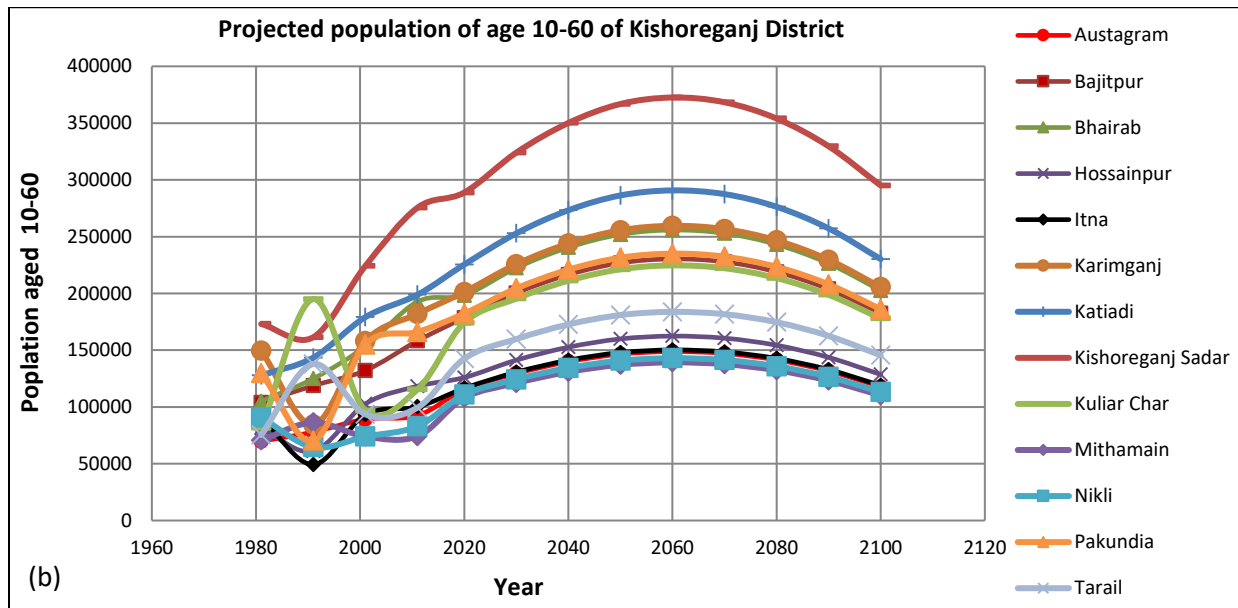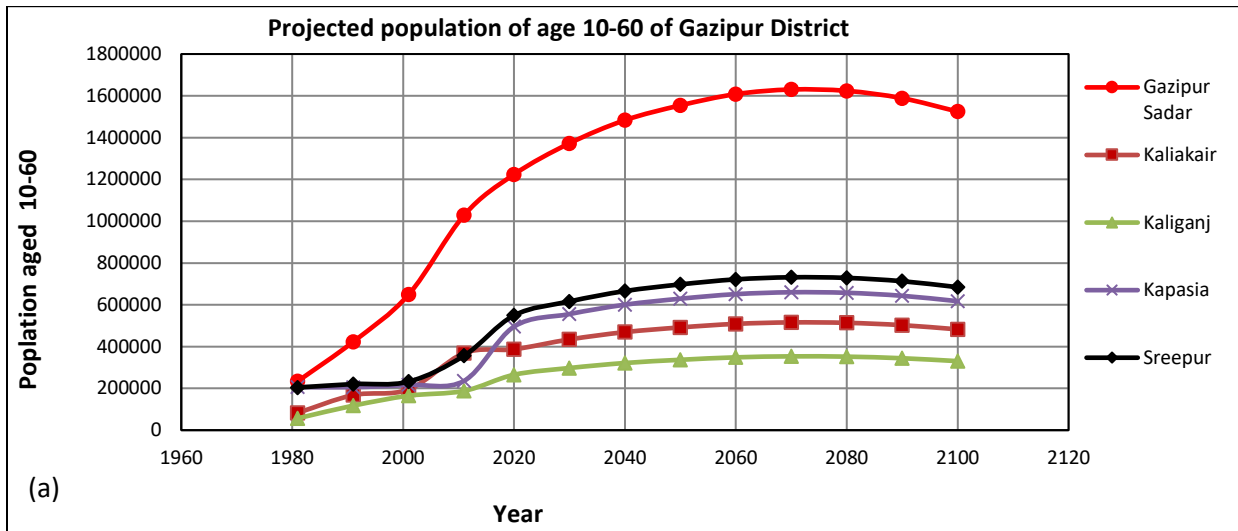
Figure A.20: Projection of Population of age 10-60 in (a) Gazipur (b) Kishoreganj (c) Narsingdi

167
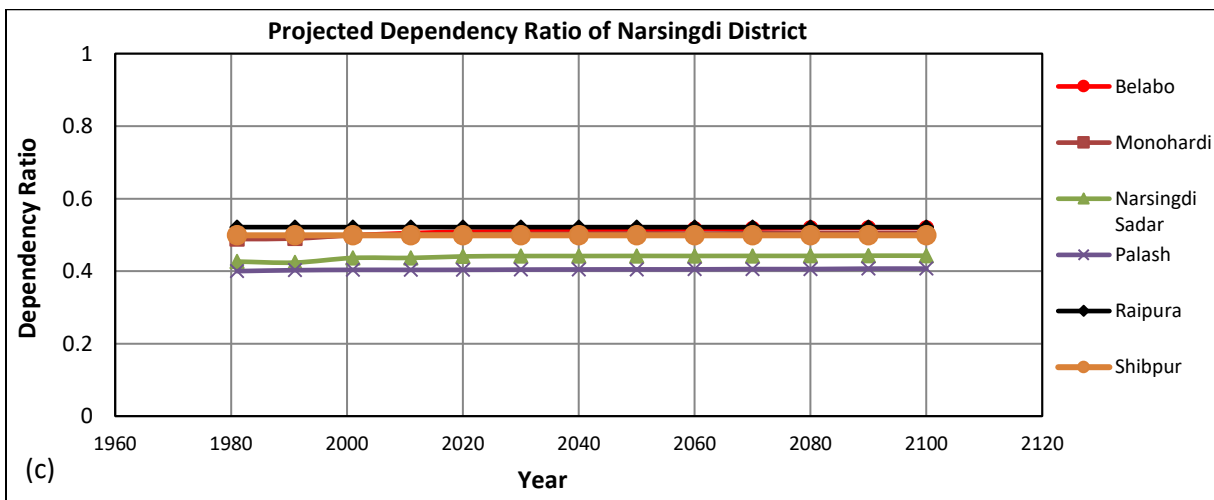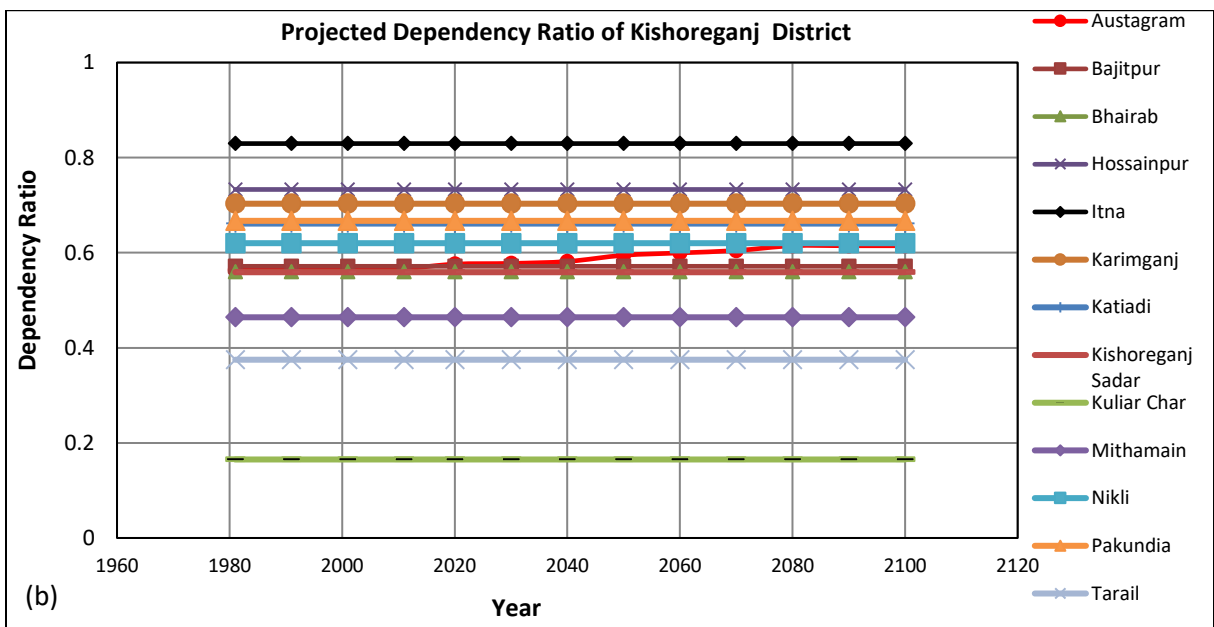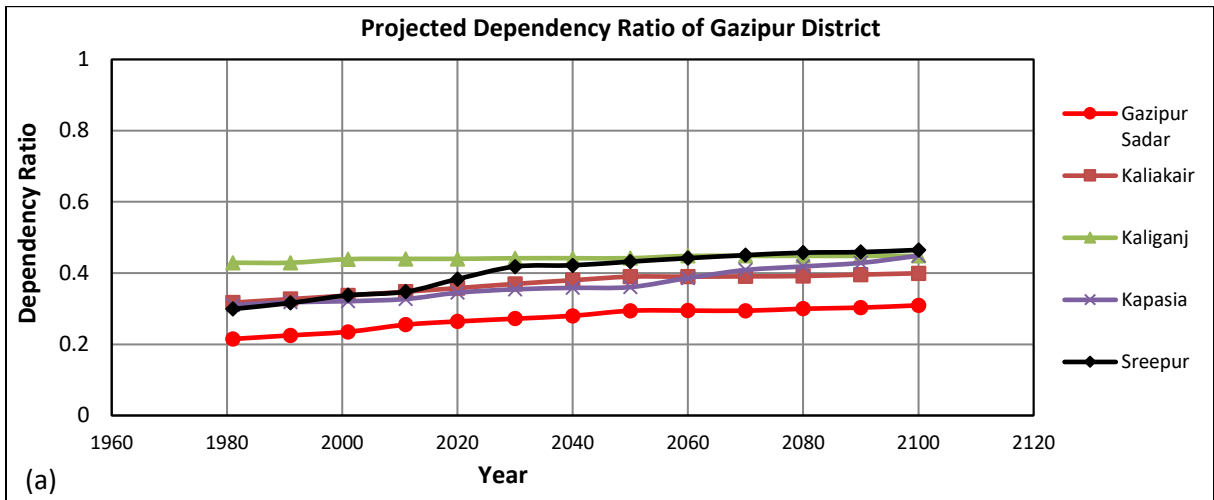
Figure A.21: Projection of Dependency ratio in (a) Gazipur (b) Kishoreganj (c) Narsingdi
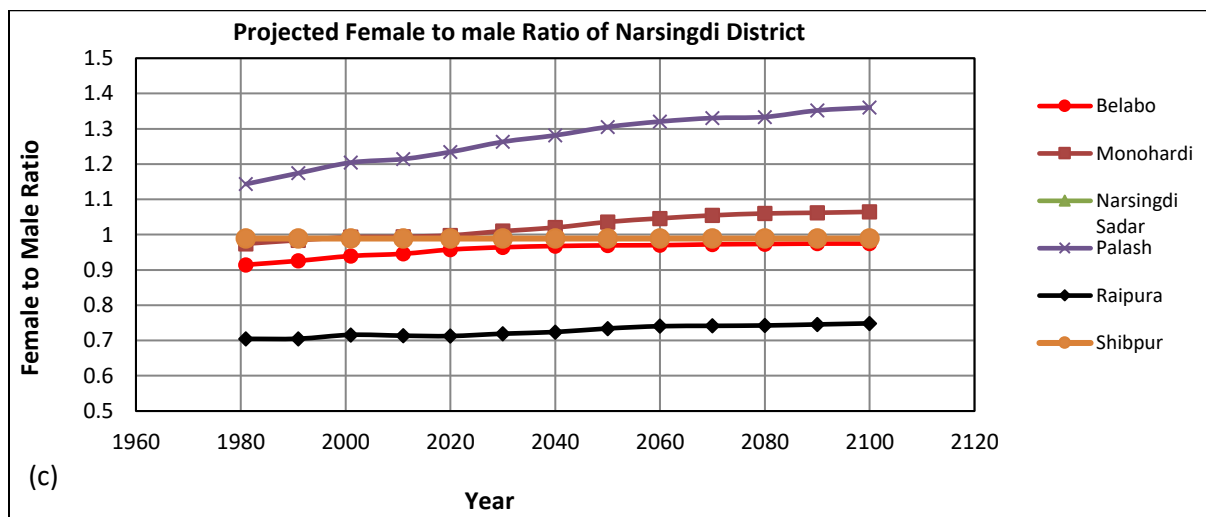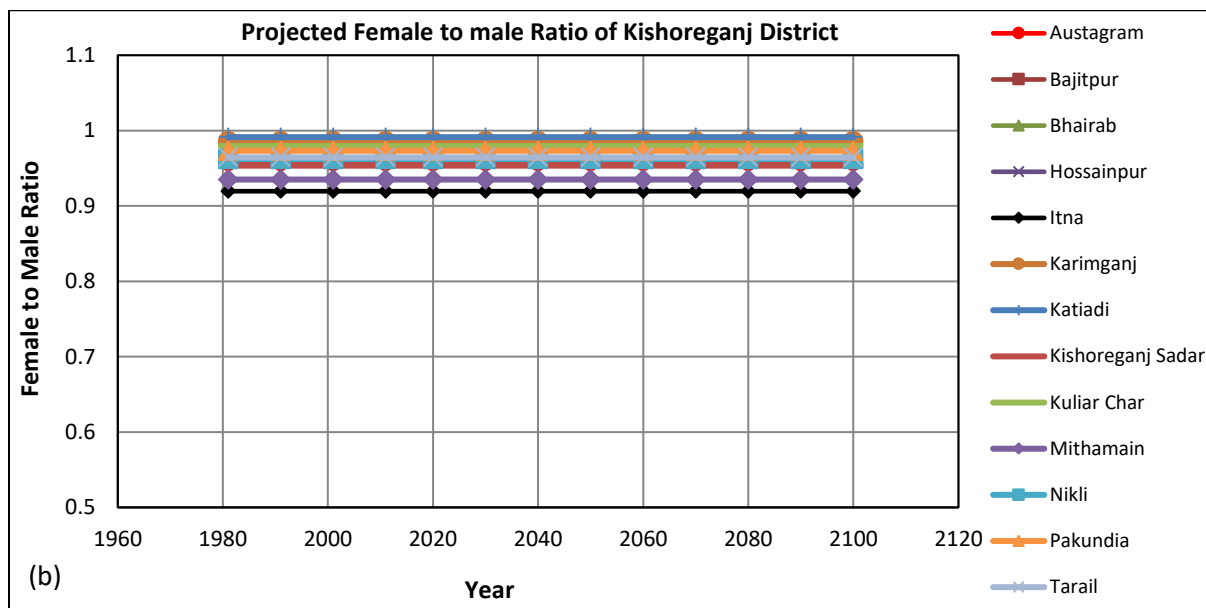
Figure A.22: Projection of Female to Male ratio in (a) Gazipur (b) Kishoreganj (c) Narsingdi

Appendix B
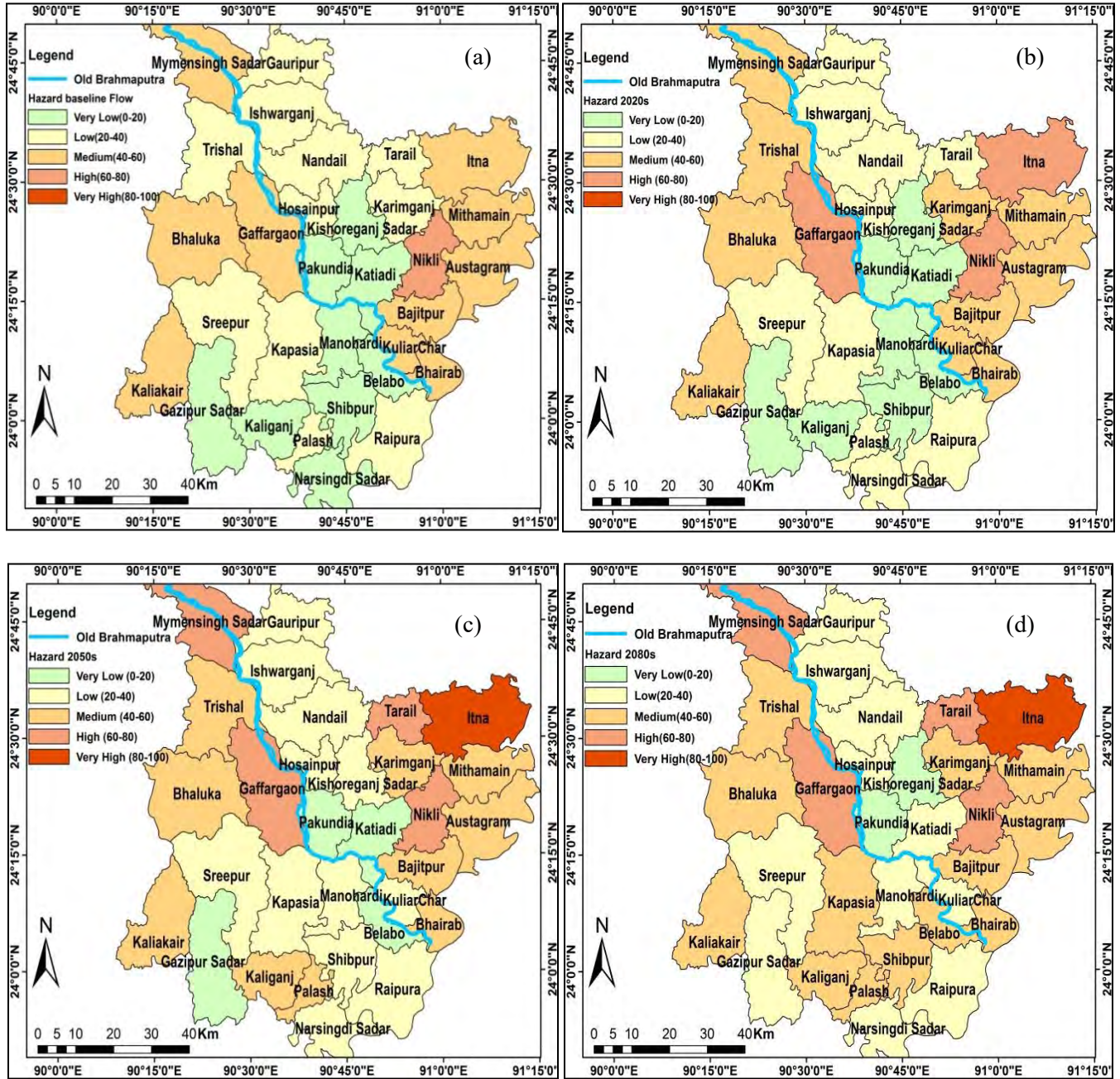
Figure B.1: Flood hazard maps of 31 Selected Upazilla for RCP 8.5 Climate Scenario (a) Baseline period (b) 2020s (c) 2050s and (d) 2080s
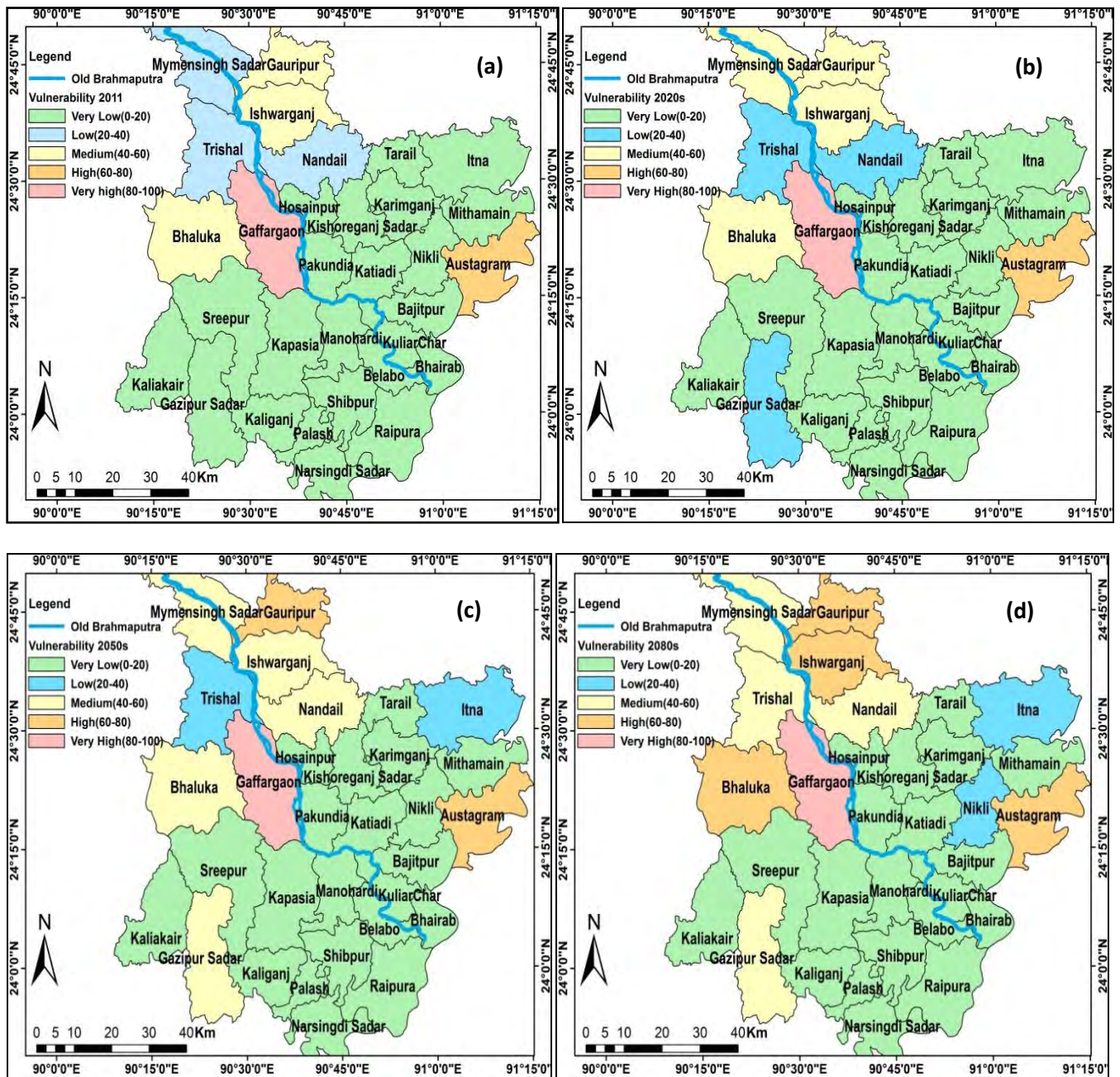
Figure B.2: Vulnerability Map of 31 Selected Upazilla for the year (a) 2011 (b) 2020s (c) 2050s (d) 2080s
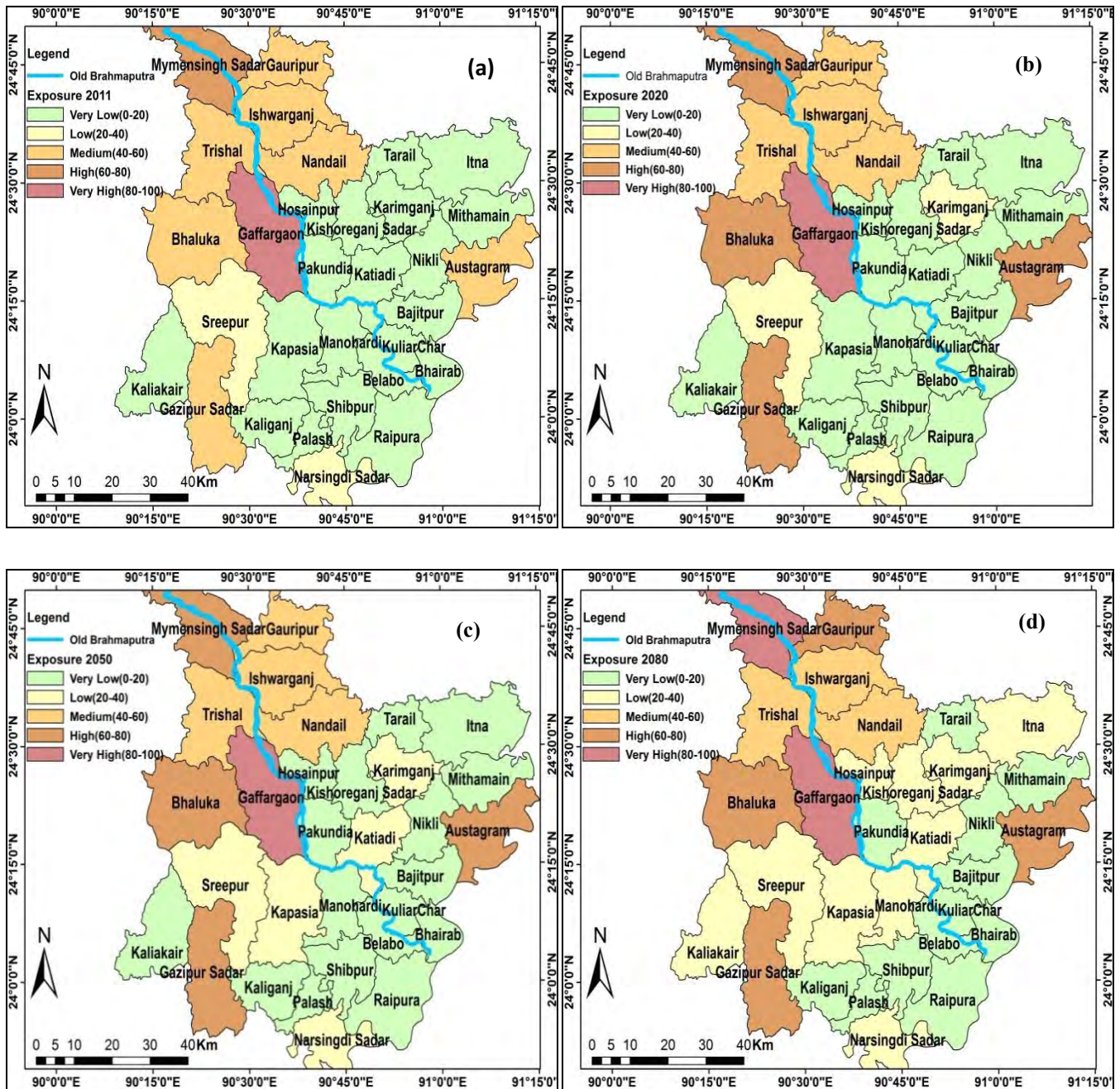
Figure B.3: Exposure Map of 31 Selected Upazilla for the year (a) 2011 (b) 2020s (c) 2050s (d) 2080s
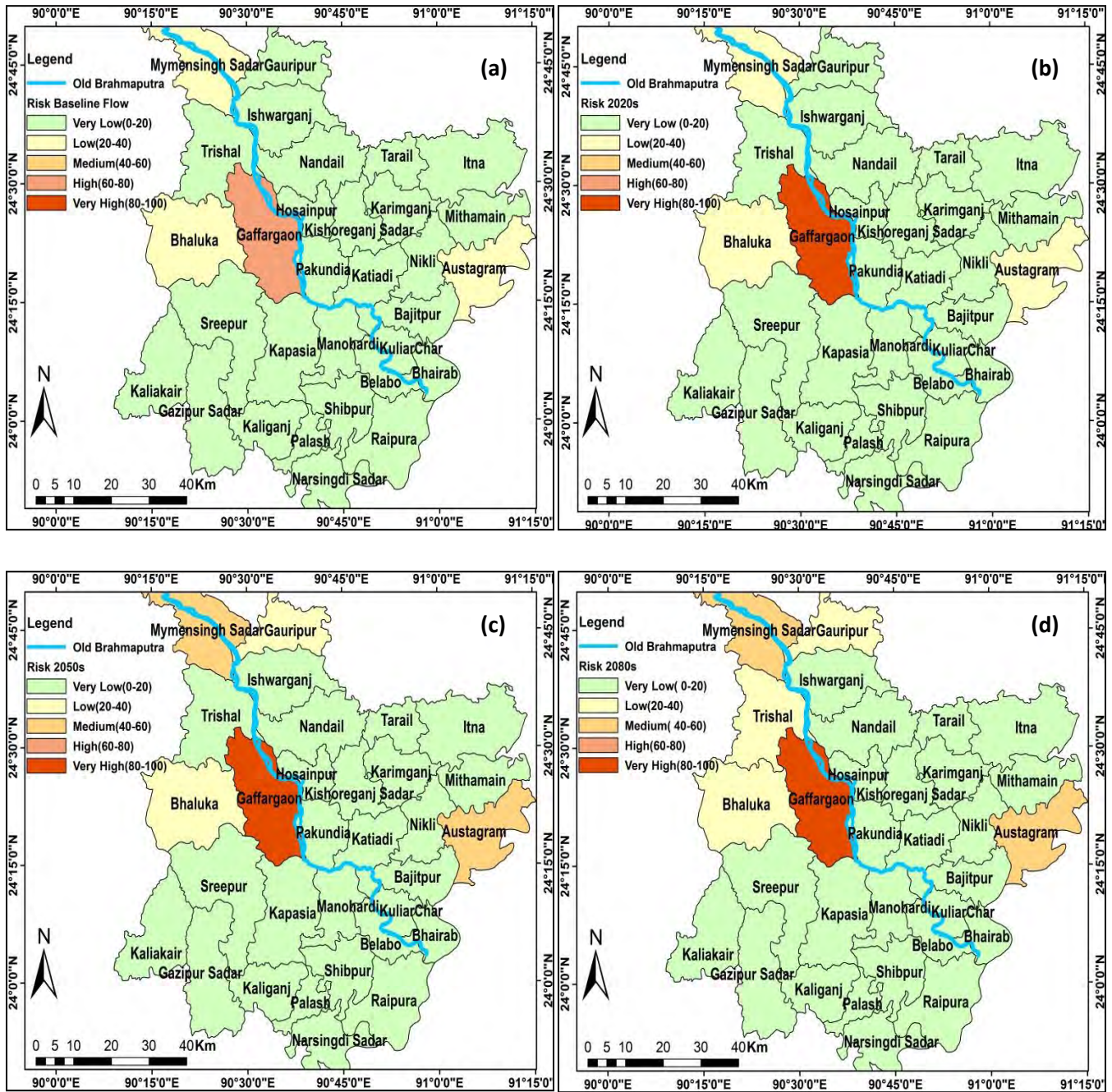
Figure B.4: Risk Map of 31 Selected Upazilla for (a) Baseline flow (b) 2020s (c) 2050s (d) 2080s